Universität Potsdam

Arbeitsgruppe Prof. A. Laschewsky

---

# Design, Synthesis and Characterisation of Amphiphilic Symmetrical Triblock Copolymers by the RAFT Process: Their Self-Organisation in Dilute and Concentrated Aqueous Solutions

**Dissertation**

**zur Erlangung des akademischen Grades**

**"doctor rerum naturalium"**

**(Dr. rer. nat.)**

**in der Wissenschaftsdisziplin Kolloid- und Polymerchemie**

**eingereicht an der Mathematisch-Naturwissenschaftlichen Fakultät**

**der Universität Potsdam**

**von**

**Achille Mayelle BIVIGOU KOUMBA**

**Potsdam, im Juli 2009**

Published online at the
Institutional Repository of the University of Potsdam:
URL http://opus.kobv.de/ubp/volltexte/2009/3954/
URN urn:nbn:de:kobv:517-opus-39549
http://nbn-resolving.org/urn:nbn:de:kobv:517-opus-39549

# DECLARATION

I, THE UNDERSIGNED, HEREBY DECLARE THAT THE WORK CONTAINED IN THIS THESIS IS MY OWN ORIGINAL WORK AND THAT I HAVE NOT PREVIOUSLY IN ITS ENTIRITY OR IN PART SUBMITTED IT AT ANY UNIVERSITY FOR A DEGREE.

_____ July 2009

A. M. BIVIGOU KOUMBA Potsdam

# Abstract

This work presents the synthesis and the self-assembly of symmetrical amphiphilic **ABA** and **BAB** triblock copolymers in dilute, semi-concentrated and highly concentrated aqueous solution. A series of new bifunctional bistrithiocarbonates as RAFT agents was used to synthesise these triblock copolymers, which are characterised by a long hydrophilic middle block and relatively small, but strongly hydrophobic end blocks. As hydrophilic **A** blocks, poly(N-isopropylacrylamide) (**PNIPAM**) and poly(methoxy diethylene glycol acrylate) (**PMDEGA**) were employed, while as hydrophobic **B** blocks, poly(4-*tert*-butyl styrene), polystyrene, poly(3,5-dibromo benzyl acrylate), poly(2-ethylhexyl acrylate), and poly(octadecyl acrylate) were explored as building blocks with different hydrophobicities and glass transition temperatures.

The five bifunctional trithiocarbonates synthesised belong to two classes: the first are RAFT agents, which position the active group of the growing polymer chain at the outer ends of the polymer (Z-C(=S)-S-R-S-C(=S)-Z, type I). The second class places the active groups in the middle of the growing polymer chain (R-S-C(=S)-Z-C(=S)-S-R, type II). These RAFT agents enable the straightforward synthesis of amphiphilic triblock copolymers in only two steps, allowing to vary the nature of the hydrophobic blocks as well as the length of the hydrophobic and hydrophilic blocks broadly with good molar mass control and narrow polydispersities. Specific side reactions were observed among some RAFT agents including the elimination of ethylenetrithiocarbonate in the early stage of the polymerisation of styrene mediated by certain agents of the type II, while the use of the RAFT agents of type I resulted in retardation of the chain extension of **PNIPAM** with styrene. These results underline the need of a careful choice of RAFT agents for a given task.

The various copolymers self-assemble in dilute and semi-concentrated aqueous solution into small flower-like micelles. No indication for the formation of micellar clusters was found, while only at high concentration, physical hydrogels are formed. The reversible thermoresponsive behaviour of the **ABA** and **BAB** type copolymer solutions in water with **A** made of **PNIPAM** was examined by turbidimetry and dynamic light scattering (DLS). The cloud point of the copolymers was nearly identical to the cloud point of the homopolymer and varied between 28-32 °C with concentrations from 0.01 to 50 wt%. This is attributed to the formation of micelles where the hydrophobic blocks are shielded from a direct contact with

water, so that the hydrophobic interactions of the copolymers are nearly the same as for pure **PNIPAM**.

Dynamic light scattering measurements showed the presence of small micelles at ambient temperature. The aggregate size dramatically increased above the cloud point, indicating a change of aggregate morphology into clusters due to the thermosensitivity of the **PNIPAM** block.

The rheological behaviour of the amphiphilic **BAB** triblock copolymers demonstrated the formation of hydrogels at high concentrations, typically above 30-35 wt%. The minimum concentration to induce hydrogels decreased with the increasing glass transition temperatures and increasing length of the end blocks. The weak tendency to form hydrogels was attributed to a small share of bridged micelles only, due to the strong segregation regime occurring.

In order to learn about the role of the nature of the thermoresponsive block for the aggregation, a new **BAB** triblock copolymer consisting of short polystyrene end blocks and **PMDEGA** as stimuli-responsive middle block was prepared and investigated. Contrary to **PNIPAM**, dilute aqueous solutions of **PMDEGA** and of its block copolymers showed reversible phase transition temperatures characterised by a strong dependence on the polymer composition. Moreover, the **PMDEGA** block copolymer allowed the formation of physical hydrogels at lower concentration, i.e. from 20 wt%. This result suggests that **PMDEGA** has a higher degree of water-swellability than **PNIPAM**.

# Zusammenfassung

Die Arbeit behandelt die Synthese und das Selbstorganisationsverhalten von neuen funktionellen symmetrischen "stimuli-responsiven" Triblockcopolymeren **ABA** und **BAB** in wässrigen verdünnten und höher konzentrierten Lösungen. Neue symmetrische, bifunktionelle Bistrithiocarbonate wurden als RAFT-Agentien benutzt, um Triblockcopolymere mit langen hydrophilen (**A**) Innen- und kurzen hydrophoben (**B**) Außenblöcken zu synthetisieren. Als hydrophile **A** Blöcke wurden Poly(N-isopropylacrylamid) **PNIPAM** und Poly(methoxy diethylene glykol acrylat) **PMDEGA** benutzt, während als hydrophobe Blöcke **B** Poly(4-*tert*-butyl styrol), Polystyrol, Poly(3,5-dibromo benzyl acrylat), Poly(2-ethylhexyl acrylat), und Poly(octadecyl acrylat) als Bausteine mit unterschiedlicher Glasübergangstemperatur untersucht wurden.

Die Selbstorganisation von **ABA** und **BAB** Copolymeren in Wasser mit **A** Blöcken aus **PNIPAM** wurde anhand von Trübungsphotometrie, dynamischer Lichtstreuung (DLS) und Rheologie untersucht. Die amphiphilen Blockcopolymere sind direkt wasserlöslich. Bei Konzentrationen von 0.01 bis 50 wt% zeigen Trübungsmessungen bei den Blockcopolymeren wie bei den Homopolymeren eine Übergangstemperatur bei 28-32 °C. Zurückzuführen ist dies auf die Bildung von Mizellen, bei der die hydrophoben Blöcke von einem direkten Kontakt mit Wasser abgeschirmt werden. DLS zeigt kleine Mizellen bei niedrigen Temperaturen und Aggregate mit großem hydrodynamischem Durchmesser bei Temperaturen oberhalb der Übergangstemperatur.

Die rheologische Untersuchung von **BAB** Polymeren zeigt die Bildung von Hydrogelen bei höheren Konzentrationen (über 30-35 wt%). Die minimal benötigte Konzentration, bei der die von Hydrogelen auftreten, nimmt mit wachsender Glasübergangstemperatur ab, und nimmt mit der Länge der hydrophoben Blöcke **B** zu. Im Unterschied zu **PNIPAM** zeigen wässrige Lösungen von **PMDEGA** und seinen Blockcopolymeren reversible Übergangstemperaturen abhängig von der chemischen Struktur. Außerdem bilden **PMDEGA** Blockcopolymere Hydrogele bei niedriger Konzentration (ab 20 wt%). Dieses Ergebnis deutet darauf hin, dass **PMDEGA** stärker Wasser bindet als **PNIPAM**.

# Acknowledgements

I will start to acknowledge the Deutscher Akademischer Austauschdienst (DAAD) for the financial support and the German course.

I am greatly indebted to Prof. Dr. André Laschewsky who has taught and provided me invaluable assistance in my work on normal working days as well as on weekends. He has also been a source of encouragement over the past three years. Many thanks also to his family for the warm hospitality.

My evaluation committees are thanked for the time and trouble that were required for the examination of my thesis.

Thank you very much Prof. Dr. Peter Müller-Buschbaum and Prof. Dr. Christine M. Papadakis (Technische Universität München) for your suggestions. Thanks also to Dr. Jean-François Lutz and Dr. Joachim Storsberg (both from Fraunhofer Institute for Applied Polymer Research Golm (IAP) for many fruitful discussions and advices.

The following individuals are acknowledged for analytical contributions to the work presented here: Prof. Dr. Sabine Beuermann and Eleonore Möller (University of Potsdam) and Dr. Helmut Schlaad and Marlies Gräwert (Max-Planck Institute, Golm (MPI-KG)) for access to SEC and their support with the measurements, Dr. Andreas Ebert (IAP) for NMR measurements, Dr. Hendrick Wetzel for elemental analysis (Fraunhofer Institute for Applied Polymer Research Golm). Dr. Eckhard Görnitz and Dr. Waltraud Vorwerg for Rheology measurements (IAP); Prof. Dr. Joachim Koetz and Mabya Fechner for DLS, Dr. Veronika Strehmel for DSC-TG (both from University of Potsdam), Dr. Klaus Tauer for IR (MPI-KG).

Particular thanks go to the following individuals who have done critical readings of chapters and the whole thesis: Isabel Haamel, Dr Nezha Badi and Jan Weiβ. I also extend my appreciation to Özgür Akdemir, Jean-Noël Marsat, Patrick Ott, Juliane Kristen, Zoya Zarafshani, Sascha Prentzel, Aleksandra Jelicic, Ulrike Schreiber, Rebekka Siegmann, Radovan Vukicevic and my football team of the Fraunhofer Institute. Everyone at this Institute and the University of Potsdam (Golm, Germany) who has made working here enjoyable during the three years of my PhD and everyone who I have forgotten to mention-thank you!

Loving thanks to my family, my mother Jeanne and her sister Luicie, my brothers Patrick and Cédrick, my sister Jessicka, and also Patrick N'goma, Jean-Aymard Nziegou, my grand mothers: Philomène and Henriette.

Finally, I owe individual gratitude to Isabel Haamel, the light of my nights and the strength of my soul for continuous and unconditional support that she has given to me since South Africa and here, in Germany. Thank you for helping me to find a PhD position and a scholarship in Germany. Thank you for being in my life, and for giving me this beautiful son, Christopher Achille. I am grateful to him for reminding me every day how beautiful life is.

# Index and lists

# List of Figures

# List of Appendix Figures

# List of Tables

# List of Schemes

# List of Symbols

| | |
|---|---|
| $\lambda$ | absorbance |
| $C_{tr}$ | chain transfer constant |
| $C_{-tr}$ | reverse chain transfer constant |
| $DP_n$ | average degree of polymerisation |
| $FW_m$ | molar mass of a monomer unit |
| $FW_{raft}$ | molar mass of a RAFT agent |
| G’ | storage modulus |
| G’’ | loss modulus |
| I | initiator |
| $k_{add}$ | addition rate coefficient |
| $k_{frag}$ | fragmentation rate coefficient |
| $k_d$ | dissociation constant |
| kj | reverse transfer constant |
| $k_{tr}$ | transfer rate coefficient |
| $k_p$ | propagation rate coefficient |
| M | monomer |
| $M_n$ | number average molar mass |
| $M_{n,exp}$ | experimental number average molar mass |
| $M_{n,th}$ | theoretically calculated number average molar mass |
| Mw | weight average molar mass |
| MWD | molecular weight distribution |
| $[M]_0$ | initial concentration of monomer |
| [Monomer] | monomer concentration |
| $Mw_{monomer}$ | molecular weight of monomer |

| | |
|---|---|
| $Mw_{raft}$ | molecular weight of RAFT agent |
| $Mt^n$/ligand | transition metal complex for atom transfer reaction, without the halide |
| P• | active species |
| $P_n$ | polymeric chain of n-degree of polymerisation |
| $P_n$• | propagating radical of n-degree of polymerisation |
| [P-X] | number of dithiobenzoate end-capped chains |
| P-X | dormant species |
| R | RAFT agent leaving group |
| R• | RAFT agent leaving group radical |
| $[RAFT]_0$ | initial concentration of RAFT agent |
| R-X | alkyl halide |
| X-$Mt^{n+1}$/ligand | transition metal complex for atom transfer reaction with the halide |
| Y• | intermediate RAFT radical |
| Z | RAFT agent stabilizing group |

# List of Acronyms

| | |
|---|---|
| AIBN | 2,2'-azobis(isobutyronitrile) |
| ATRA | atom transfer radical addition |
| ATRP | atom transfer radical polymerisation |
| $C_6H_5G$ | benzene derivatives |
| CTA | chain transfer agent |
| DBN | di-*tert*-butylnitroxide |
| DEPN | n-*tert*-butyl-N-(1-diethylphosphono-2,2-dimethylpropyl)nitroxide |
| DLS | dynamic light scattering |
| ESR | electron spin resonance |
| FRP | free radical polymerisation |
| GPC | gradient permeation chromatography |
| $^1$H-NMR | proton nuclear magnetic resonance |
| iniferter | initiator-transfer agent-terminator |
| IR | infrared |
| KOH | potassium hydroxide |
| LRP | living radical polymerisation |
| MDEGA | methoxydiethylene glycol acrylate |
| MMA | methylmethacrylate |
| NIPAM | N-isopropylacrylamide |
| NMR | nuclear magnetic resonance |
| NMP | nitroxide mediated polymerisation |
| PDI | polydispersity index |
| Ph | phenyl ring |
| PS | polystyrene |
| RAFT | reversible addition-fragmentation chain transfer |

| | |
|---|---|
| SEC | size exclusion chromatography |
| SFRP | stable free radical polymerisation |
| St | styrene |
| TEMPO | 2,2,6,6-tetramethyl-1-piperidinyloxyl radical |
| TIM | tube inversion method |
| THF | tetrahydrofuran |
| UV | ultraviolet |

*To my parents,*

*my mother,*

*my strength, Isabel*

*and my soul, Christopher Achille*

*"There is only one good, knowledge, and only one evil, ignorance." Socrates*

# *CHAPTER I: Introduction and objectives*

# 1.1 General introduction

Water-soluble polymers continue to fascinate engineers and polymer scientists because of their fundamental property to self-assemble into supramolecular systems. A major progress has come from the development of amphiphilic block copolymers. Most attention has been put in fields like detergents,[1, 2] separations,[3] cosmetic products[4] and surface modifiers so far. They have found numerous applications as thickeners in aqueous-media and additionally, amphiphilic block copolymers offer many possibilities to mimic biological behaviour.[5, 6]

# 1.2 Composition of amphiphilic block copolymers

Amphiphilic block copolymers consist at least of two incompatible polymer block chains that are covalently connected, one polar block chain which is soluble in water (the hydrophilic group) and one nonpolar block which is insoluble (the hydrophobic group). The hydrophilic group can be neutral or ionic. Typically, the hydrophobic group is characterised by either a hydrocarbon or, less frequently, a fluorocarbon chain. Depending on the block sequence, the architecture of linear block copolymers varies from simple topologies such as **AB** diblock copolymers,[7] **ABA**,[8] or **ABC**[9] triblock to complex structures including **ABCD** or **ABAC** multiblock copolymers. Possible molecular structures of amphiphilic block copolymers are shown in Figure 1.1.

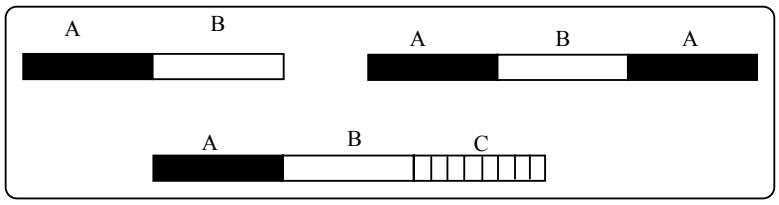


**Figure 1.1 Examples of block copolymer architectures.**

The following discussion is based on the behaviours of **AB**, **ABA**, and **BAB** amphiphilic block copolymers in contact with solvents that are thermodynamically good for one type of block (**A**), but poor for the other type of block (**B**). Regarding amphiphilic block copolymer architectures, the **AB** type represents the simplest copolymer architecture and has been extensively investigated. Depending on the miscibility character of **A** and **B** in the **AB** diblock copolymer, a vast array of unimolecular morphologies has been observed.[10] Actually, (I) if the **AB** segments are incompatible and the block copolymer is dissolved in a good solvent for the **A** block, that is however a poor one for the **B** block, the **A** block forms a swollen coil, while

the **B** block is collapsed to a globule or ball shape. (II) If the previous block copolymer is dissolved in a good solvent for both blocks **A** and **B**, two blobs resulting from **A** and **B** are formed.

Based on the situation (I), at a particular concentration (critical aggregation concentration, CAC) and temperature, unimers can self-assemble into regular complex structures including spherical micelles. The driving force for the micellization of **AB** amphiphilic block copolymers in water is the transfer free energy of the hydrophobic block from water into the core. By altering the ratio between the hydrophobic and the hydrophilic blocks, various microdomain structures can take place. In particular, spherical micelles are formed if the hydrophobic blocks are much shorter than the hydrophilic ones. Increasing the length of the hydrophobic blocks with respect to the hydrophilic blocks provide cylindrical microstructures. Finally, when the two blocks have approximately similar lengths, alternating hydrophobic and hydrophilic layers are obtained. Because of the rich structural variety, it is not surprising that the aggregation and properties of block copolymers have been thoroughly investigated in both academic and applied science.

Similarly to **AB**, **ABA** amphiphilic block copolymers can also self-assemble into classical morphologies.[11-13] For example, **ABA** triblock copolymers may form in selective solvents, which are good for the outer **A** blocks and poor for the middle **B** block, either ring or a dumbbell morphologies. A ring is formed when one **A** end blocks can join the other **A** group. The continuous formation of such structures leads to spherical "loop" micelles. The second type of geometry is created, if the **A** end blocks are sufficiently small so that the **B** block can push apart or isolate the two ends from each other to form a dumbbell-type unimer. Benchaim et al. noted that the two geometries are, however, not reciprocally exclusive.[10]

Whereas amphiphilic **AB** and **ABA** diblock copolymers have been much studied in the past years, the class of amphiphilic **BAB** triblock copolymers, in solvents which are thermodynamically good for the middle block, has been much neglected so far. Historically, the fundamental questions whether or not ordered structures could be formed from **BAB** triblock copolymers, has given rise to numerous discussions due to the limited number of experimental results available.[14, 15] While earlier researchers reported, for example, no experimental evidence for the formation of polymer micelles,[14] recent studies demonstrated that micelles can be experimentally observed.[15] Computer simulations on small symmetric triblock copolymers in dilute solution showed that an array of microstructures, including transitory aggregates, micelles with backfolding of the centre block, and branched assemblies,

might happen depending on the strength of net attractive interactions between the end blocks.[16, 17] It is currently accepted that **BAB** triblock copolymers tend to form flower-like micelles with the **B** insoluble blocks constituting the cores and the **A** soluble block forming the swollen corona.[16] Additionally, **BAB** triblock copolymers can also produce fringe structures.[18, 19] The latter type is possible if one end block **A** is placed in the core and the other **A** block in the dangling fringe.

A most promising achievement in amphiphilic block copolymers has been the incorporation of hydrophilic and/or the hydrophobic groups with stimuli-responsive moieties. This innovation allows to tune the micellar properties including changes in core or both core-shell shapes in response to specific stimuli. The challenge nowadays is to determine how these building blocks in molecular architecture operate. Thus, the following discussion focuses on the behaviour of stimuli-responsive polymers and its derivatives.

## 1.3 Stimuli-responsive polymers

The term "stimuli-responsive polymers" was invented to name a class of polymers that exhibit reversible changes in response to external stimuli.[20] The responses can be dissolution/precipitation, swelling/collapsing, hydrophilic/hydrophobic transition, sol-gel transitions and others.[20] The environmental triggers for these transitions can be either physical or chemical. The physical stimuli involve mostly changes in temperature and more recently, changes in electric and magnetic field,[20] increase in ionic strength, UV light or radiation forces.[20, 21] The chemical stimuli are based on changes for instance on acid/base reactions,[20] addition of an strongly interacting ion or polycation-polyanion complex formation.

Of these numerous stimuli, temperature is the most exploited one, because it is relatively easy to operate and to control. Moreover, there is no need to add or to remove any chemical reagent to induce reversible changes when temperature is used as stimulus. For these reasons, extensive research has been dedicated to polymers that exhibit reversible volume changes upon a change in temperature.[22, 23]

## 1.4 Phase separation of thermoresponsive polymers

Frequently, the term critical point is used to describe the properties of thermoresponsive polymers. The critical point is identified as the minimum or maximum observed in the temperature/concentration plot of a phase separation diagram (Figure 1.2).[24] It indicates the temperature for which a given polymer-solvent mixture changes from a one-phase system to a

two-phase system consisting of a polymer rich phase and a polymer poor phase. Polymers with minimum or maximum critical point can be classified as showing a lower critical solution temperature (LCST), and an upper critical solution temperature (UCST), respectively. The present work will focus on systems with a LCST.

When an aqueous solution of polymers with LCST is heated to a specific temperature ($T_s$), the solution becomes cloudy, indicating macroscopic phase separation. As a consequence, $T_s$ corresponds to phase separation temperature. The temperature at which phase separation occurs for a specific polymer concentration is referred to as the cloud point.

Phase transitions of aqueous solutions of thermoresponsive polymers have given rise to much debate. It has been suggested that the change from homogenous to heterogeneous phases (or vice versa) is linked to conformational transitions like coil to globule or globule to coil.[25] A possible approach for the clarification of this phenomenon comes from a thermodynamic viewpoint.[24]

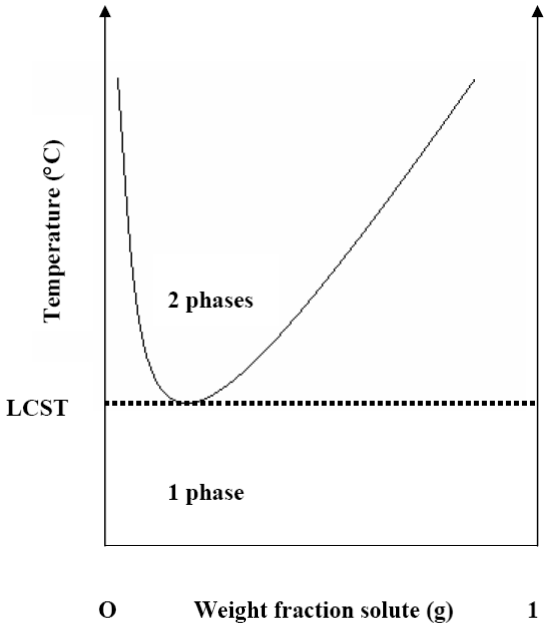


**Figure 1.2 Schematic phase diagram of a system exhibiting a lower critical solution temperature (LCST).**

## 1.5 Thermodynamic property for thermoresponsive polymers

Liquid water is known to form clusters of molecules that are stabilized by hydrogen bonding (also known as water-water interaction). When a thermoresponsive polymer exhibiting a

LCST is added into water, two types of interacting water molecules are created. The first one is involved in the so-called water cages, which surround the non-polar groups of the polymer. The second one corresponds to the bound water around the polar moieties of the polymer. The dependence of the solubility of thermoresponsive polymer with the temperature can be explained by the balance between the entropy and the enthalpy of mixing (Figure 1.3).

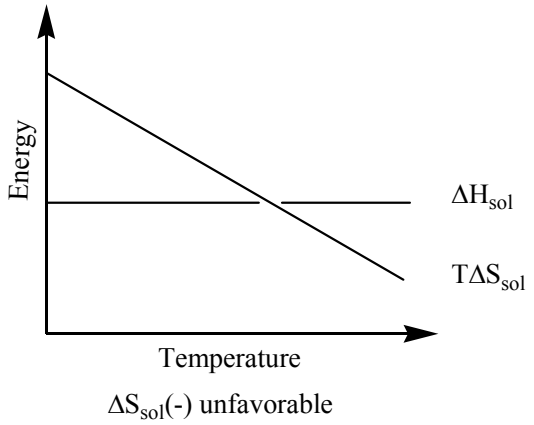


**Figure 1.3 Schematic energy diagram of PNIPAM exhibiting a LCST.**

These terms are given by the Gibbs' free energy on mixing in the equation below:

$$\Delta G_m = \Delta H_m - T\,\Delta S_m \qquad \text{Eq.1.1.}$$

where $\Delta G_m$, $T$, $\Delta H_m$, and $\Delta S_m$ are the change in Gibbs' free energy of mixing, the absolute temperature, the enthalpy, and the entropy of mixing, respectively.

Negative values of $\Delta G_m$ imply that the dissolution of polymers in water is spontaneous and thermodynamically favoured. Since the entropy of the dissolution is followed by small negative changes due to specific molecular orientations to favour hydrogen bonds between solutes and water, the enthalpy of mixing is the driving force responsible for the dissolution of uncharged polymers.

The enthalpy of mixing is exothermic and derives from difference between the intra- and intermolecular interactions (polymer-polymer association compared to polymer-solvent and solvent-solvent interactions).

As shown in Figure 1.3, when the temperature is increased, $T\,\Delta S_m$ decreases and becomes less than $\Delta H_m$. Near the LCST, $T\,\Delta S_m$ becomes more negative than $\Delta H_m$, at this moment $\Delta G_m$ becomes positive and the process of solvation becomes unfavourable leading to the precipitation of the polymer.

In other words, near the LCST, hydrogen bonds between the polymer and solvent decrease and water-polymer association becomes unfavourable compared to polymer-polymer and water-water interactions. Therefore, the polymer precipitates from the solution. This transition is often associated to a transition from a polymer coil to a globule.[25]

# 1.6 Thermoresponsive polymers

Many polymers that bear ether or amide moieties show a LCST in water. Typical polymers with LCST are displayed in Figure 1.4.

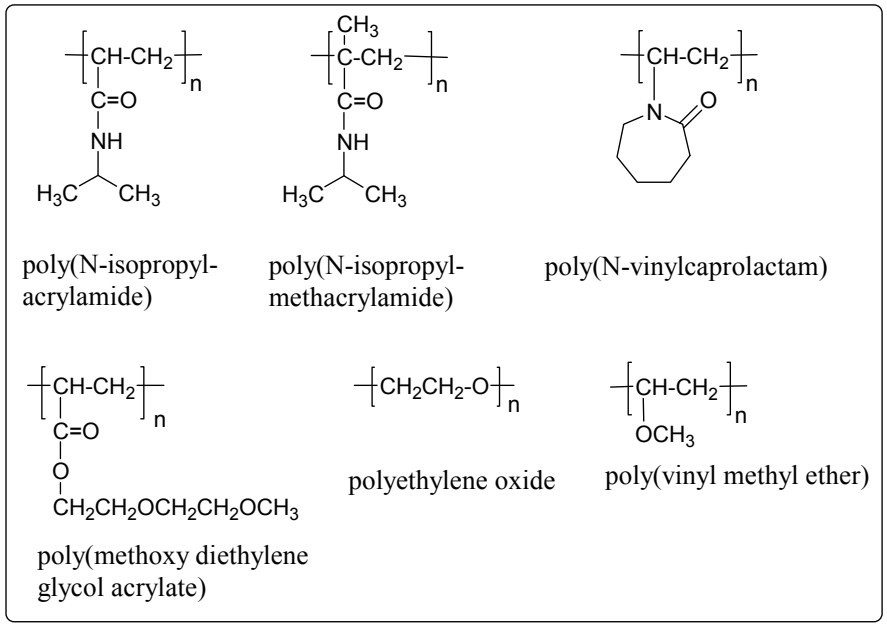


**Figure 1.4 Examples of thermoresponsive polymers showing a LCST in aqueous solution.**

## 1.6.1 Poly(N-isopropylacrylamide) (PNIPAM)

Poly(N-isopropylacrylamide) (**PNIPAM**) is the most prominent example of a thermoresponsive polymer. **PNIPAM** is characterised by both hydrophilic (amide) and hydrophobic (isopropyl) groups and has been described as a model system for understanding the properties of peptides and proteins.[25] **PNIPAM** owes its water solubility to the acrylamide moiety, which forms hydrogen bonds with water molecules at room temperature and a cage-like structure around the isopropyl group of the side chains of **PNIPAM**. The latter leads to entropically driven polymer-polymer interactions by the hydrophobic effect. Despite the unfavourable hydrophobic interaction of the side chains, **PNIPAM** is soluble in water at ambient temperature because of the strong attraction water-amide interactions (as discussed in

section 1.5). When the temperature of the solution is raised up to 32 °C, the solution however turns cloudy followed by the conformation change coil-globule (Figure 1.5).[24-28]

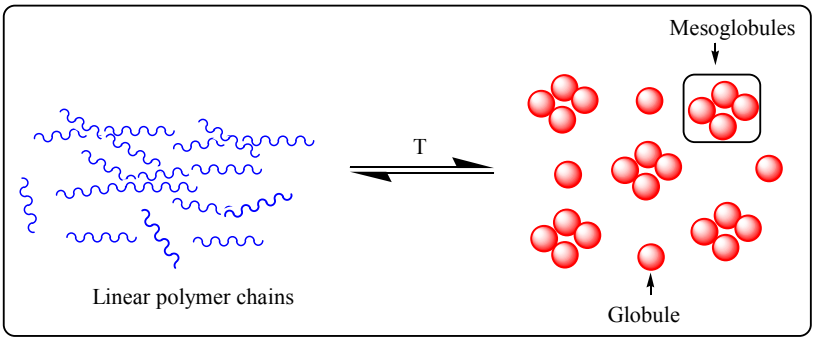


**Figure 1.5 Change in conformation from coil-globule in linear PNIPAM (T: temperature).**

The phase separation of the solution is attributed to a progressive release of water molecules oriented around the hydrophobic **PNIPAM** groups, and also from the formation of intermolecular hydrogen bonds between the amide groups (sites vacant where water molecules have been displaced). In this stage, water-polymer interactions become unfavourable compared to polymer-polymer interactions, which lead to a phase transition resulting in polymer precipitation. The critical temperature of **PNIPAM** is 32 °C.[28, 29] It should be pointed out that this explanation cannot justify the cloud point just by the hydrophilic and hydrophobic side-chain contributions to polymer solvation only. For example, poly(N-isopropylmethylacrylamide) (**PNIPMAM**) differs from **PNIPAM** by an additional single methyl group, and consequently should have a lower LCST compared to **PNIPAM**. However, this is not the case, as it has a higher cloud point in water (38-44 °C).[30] This implies that **PNIPMAM** behaves more hydrophilic despite a higher organic content. It seems that the increased in hydrophilicity results from a decrease in chain flexibility, which influences the entropic contribution to the free energy of mixing, and thus increases the cloud point.

Even if many different thermoresponsive polymers have been investigated, **PNIPAM** remains the most common polymer used in different investigations including hydrogels. A specific application of **PNIPAM** gels and its derivatives concern essentially they use in column packing materials for chromatography. For example, Kanzawa and co-workers have used the thermoresponsive properties of **PNIPAM** in chromatography to separate a variety of compounds, including peptides and proteins.[31-35]

### 1.6.2 Poly(methoxy diethylene glycol acrylate (PMDEGA))

Among the polymers that show LCST behaviour poly(methoxy diethylene glycol acrylate (**PMDEGA**)) is considered to be a new promising candidate as thermoresponsive polymer with a cloud point that lies in a temperature range of 35-38 °C.[36] It is therefore instructive to compare its aqueous behaviour to the one of **PNIPAM**. The controlled radical polymerisation of **MDEGA** is possible but only in bulk or in organic solvents because **MDEGA** is a water insoluble monomer. As derivative of linear poly(ethylene glycol) (**PEG**), **PMDEGA** side chains are expected to have similar advantages including beyond water-solubility and low toxicity.[37-39] This polymer should have therefore a great potential to find application in the fields of pharmaceutics, medical care or biotechnology.

## 1.7 Adjusting the LCST of PNIPAM

The LCST of a polymer can be tuned by varying several parameters including the effect of molar mass, end-group, tacticity, addition of salts, incorporation of block copolymers and or the addition of co-solvent.

### 1.7.1 Effect of molar mass and polymer concentration

The effect of molar mass on phase transition temperature of **PNIPAM** has given rise to numerous discussions. In general, the increase of the phase transition temperature is inversely proportional to the molar mass of linear **PNIPAM**.[11] This means that aqueous solutions of linear **PNIPAM** with higher molar mass exhibit a lower phase transition temperature whereas solutions composed of linear **PNIPAM** with low molar mass show higher phase transition temperature. Additionally, it was reported that an increase in the polymer concentration gradually reduced the LCST of **PNIPAM** and vice versa.[29] In this line, Schild et al.[40] examined the phase transition temperature of **PNIPAM** made with the molar mass of 5400 to 160 x $10^3$. They demonstrated that the LCST decreased with increasing molar mass and they argued that in particular at higher concentration, where the coil-to-globule transition is followed by globule aggregation through intermolecular associations, molar mass should have a significant influence on the LCST.[40] Furyk et al.[41] showed that molar mass and polydispersity have little effect on the LCST of **PNIPAM** as long as its molar mass is higher than 50,000 Da. For lower molar mass samples, small (about 1 °C) changes in LCST were observed and were correlated with changes in end-group structure and polarity.[41] Tong et al.[42]

demonstrated also a chain length effect on the phase transition in aqueous **PNIPAM** solutions.[42] They showed also that the cloud point monotonically decreases with increasing polymer concentration from 0.58 to 70 wt%. Other authors reported the influence of the polymer chain length on the phase transition temperature of **PNIPAM** at concentrations as low as 0.01-0.04 wt%.[25] In contrary, Fujishiege et al.[43] have demonstrated that the LCST is relatively independent of both the molar mass of the polymer and its concentration.[43] They studied **PNIPAM** with molar mass between 5 x $10^4$ and 8.4 x $10^6$ and polymer concentrations (from 0.01 to 1 wt%).[43] Furthermore, Tiktopulo et al.,[25] Takei et al.,[44] and Ding et al.[45] reported no appreciable change in LCST with changes in the molar mass of **PNIPAM**. The confusing variation in the LCST of **PNIPAM** with increasing molar mass has not yet been fully understood, but may be linked to the nature of the end-groups, as discussed in the following section.

## 1.7.2 Effect of end-group on LCST of thermoresponsive copolymers

The incorporation of specific end-groups during the polymerisation of **PNIPAM** may promote also a drastic change in the LCST. For example, Duan et al.[46] functionalized **PNIPAM** with the pyrenyl group through the ATRP of **NIPAM** using 1-pyrenyl 2-chloropropionate. They found that the pyrenyl group at the chain-end for **PNIPAM** induced huge **PNIPAM**-aggregates, and lowered their LCSTs to 21.7 °C.[46] It is noteworthy that the investigation of Duan and co-workers concern mainly **PNIPAM** solution with low molar masses.[46] Although there is still a lack of investigations addressing the effect of end-groups at high molar masses, it is believed that at high molar mass, the end-group effects will have no significant repercussion on the LCST of **PNIPAM**, because the effects of end-groups will be diluted by the increase of molar mass.[41]

In contrast to the findings of Duan et al.,[47] Winnik et al.[46] observed comparable values for the phase transition of **PNIPAM**, with and without a polyoctadecyl pyrene end-label. They reported that the cloud points were nearly the same as for the reference sample of **PNIPAM** homopolymer, 32 °C. They suggested that the hydrophobic groups were not exposed to water, but rather formed micellar structures protected from water by the **PNIPAM** chains. Therefore the hydrophobic groups were not effective to lower the LCST.[46]

A missing effect of the end-group was also noted by Ding et al.[45] and Baltes et al.[48] who prepared carboxyl-terminated **PNIPAM** oligomers with molecular weights ranging from 2 to 50 x $10^3$ g/mol and did not see any changes in LCST. It was even noted in the work of Freitag

et al.[49] that the ionization state of this carboxylic acid end-group did not affect the LCST of a polyacrylamide.

These contradictions may arise from insufficient information on the characterisation of polymer samples. It would be therefore instructive to re-examine these effects.

### 1.7.3 Effect of tacticity on LCST of PNIPAM

Recently, studies on the solubility and the cloud point of **PNIPAM** demonstrated that the stereoregularity of **PNIPAM** affect strongly its phase transition behaviour. For example, an increase in isotacticity of **PNIPAM** reduces its solubility[50, 51] and its cloud point compared to the atactic polymer,[52] while an increase in syndiotacticity increases the cloud point[53] and reduces the hysteresis between heating and cooling cycles.

### 1.7.4 Influence of co-monomers on LCST of PNIPAM

The solubility of **PNIPAM** systems can be easily altered by the chemical composition.[24] If the **NIPAM** monomer is statistically copolymerised with more hydrophilic monomers, the LCST generally increases. In contrast, if the **NIPAM** monomer is copolymerised with more hydrophobic monomers, LCST decreases.[54-56] For instance, polymerisation of **PNIPAM** with N,N-dimethylacrylamide (**DMAAM**) as hydrophilic monomer shifts the LCST of **PNIPAM** to higher values: **PNIPAM-co-DMAAM**: 80/20, LCST 43 °C.[54] As intuitively expected, the addition of hydrophilic monomer units increases the overall hydrophilicity of the copolymer and reduces the hydrophobic interactions, so that the LCST of the solution shifts to higher values.[56]

The situation is however different, when hydrophobic or hydrophilic monomers are sequentially added to **PNIPAM**. It seems that in such block copolymers the LCST is little changed, but systematic studies are still missing yet. For example, Chung et al.,[57, 58] showed that micelles formed by block copolymers of **PNIPAM-PBMA** or **PNIPAM-PS** showed the same LCST as that for the intact **PNIPAM**, irrespective of hydrophobic segment incorporation (**PBMA** (poly(butyl methacrylate)) or **PS** (polystyrene)).[57] They argued that the block copolymers form core-shell micellar structures with completely separated phases.[58]

## 1.7.5 Effect of co-solvent of PNIPAM

The addition of solvents to an aqueous solution of **PNIPAM** may induce a significant change in the LCST. For example, the phase transition temperature of an aqueous solution of **PNIPAM** decreases with increasing methanol concentration at about 55 % methanol. Beyond this concentration, the phase transition temperature of the mixture raises suddenly.[59-62] Similar phenomena for **PNIPAM** were also observed in the mixture of water with other water-miscible polar solvents, such as acetone, dioxane, dimethyl sulfoxide, tetrahydrofurane, and other alcohols (in all these solvents, **PNIPAM** is freely soluble). Freitas et al.[63] reported that the LCST of an aqueous solution of **PNIPAM** decreased when small amounts of ethanol are added then, a UCST behaviour arises from the addition of higher fractions of ethanol.[63] These observations were attributed to the formation of different water-solvent complexes which become poor solvents for **PNIPAM**.[26, 59, 64]

## 1.7.6 Effect of additives on LCST of thermoresponsive copolymers

The influence of salts on stimuli sensitive polymer solutions has been broadly investigated.[65] When a salt is added into a water-polymer solution, similar associations as those observed in case of alcohol-water mixture can occur including polymer-polymer, polymer-water, polymer-ion, water-water, and water-ion. In the case of **PNIPAM**, partial dehydration occurs if the interactions water-ion become dominant compared to polymer-water and polymer becomes more hydrophobic.[66] This effect reduces the phase transition temperature of the solution. For salts, this effect is correlated to the Hofmeister series,[66] according to which the precipitating efficiency of anions for proteins decreases in the following order: $SO_4^{2-} > Cl^- > Br^- > I^- > SCN^-$. The LCST of **PNIPAM** decreases when $SO_4^{2-}$ is used due to a strong salting-out effect, which has a high surface charge density and forms a complex of tightly bound water molecules.[29, 66, 67] In contrast, there is an increase of LCST when $SCN^-$ is used because of the strong salting-in effect of this ion.[68-71] Thus, the adjustment of the cloud point of **PNIPAM** depends on the amount as well as on the nature of the ion used.[72]

# 1.8 Thermoresponsive Core-Shell polymers

## 1.8.1 AB Diblock Core-Shell copolymers

In water, linear **AB** amphiphilic diblock copolymers made of hydrophilic **A** block and hydrophobic **B** block are known to form polymeric micelles.[7] These micelles consist of an inner core **B** that is surrounded by a swollen corona **A**. The core of the micelle is often used as a microphase for the incorporation of lipophilic drugs, while the corona is responsible for the stability of the micellar structure protecting the hydrophobic core from the external aqueous medium (Figure 1.6).

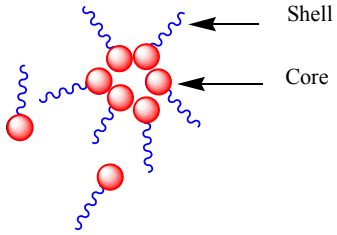


**Figure 1.6 Example of micellar structure.**

The functionalisation of polymeric micelles by the introduction of polymers with a lower critical solution temperature (LCST) enables to adjust the swelling propriety of these micelles.[20] Most work on such polymeric micelles has been conducted using hydrophilic-hydrophobic diblock copolymers or hydrophilic-hydrophilic diblocks in which one of the blocks becomes hydrophobic in response to change in temperature. For example, block copolymers of **PNIPAM-PSPP** (**PSPP** for 3-[N-(3-methacrylamidopropyl)-N,N-dimethyl]ammoniopropane sulfonate),[73] **PNIPAM-PEO** (**PEO** for polyethylene oxide),[74-78] and **PTEGMA-PTEGSt** (**PTEGMA** for poly[methoxytri(ethylene glycol) acrylate] and **PTEGSt** for poly[4-vinylbenzyl methoxytris(oxyethylene) ether][79]) have been synthesised. The micellization of the **AB** block copolymers depends strongly on the chemical composition of the amphiphilic block copolymers. The amphiphilic copolymers which contain a highly hydrophobic block have lower CMC values in water than those which include the less hydrophobic blocks.[80] For instance, Booth et al.[81] have studied the micellization of block copolymers **PEO-PBO**, **PEO-PPO** and **PEO-PSO**, (**EO** = oxyethylene oxide (**$OCH_2CH_2$**), **BO** = oxybutylene oxide (**$OCH_2CH(C_2H_5)$**, **PO**: oxypropylene oxide (**$OCH_2CH(CH_3)$**), **SO** = oxyphenylethylene oxide (**$OCH_2CH(C_5H_6)$**). They observed that micelles are formed in the following stability order: **PO < BO < SO**.[81]Additionally, micelles formed from

copolymers containing a hydrophobic block which has a high glass transition temperature will tend to disassemble more slowly than those with a low glass transition temperature.[80, 82]

## 1.8.2 ABA and BAB Triblock Core-Shell copolymers

After thermoresponsive diblock copolymers have been studied intensively, thermoresponsive **ABA** and **BAB** triblock copolymers have attracted the interest recently. They were predicted to self-assemble in contact of a selective solvent to form ordinary core-shell micelles at intermediate concentrations, but to show complex aggregation leading to transient networks (hydrogels) in the concentrated regime.[83, 84] Thus, the introduction of a third block is regarded as a powerful tool for achieving additional structural and functional features in polymeric micelles, with potential impact for instance in the biomedical field for separations or tissue engineering.

The micellization of **ABA** thermoresponsive triblock copolymers in a selective solvent for both **A** end-groups has been suggested to occur in the same way as for the corresponding **AB** diblocks. As discussed above (section 1.1). In dilute aqueous solutions, the copolymers **ABA** (with **A** as responsive block) form regular spherical loop-like micelles with the insoluble block **B** forming the core and the soluble end blocks **A** forming the swollen corona (Figures 1.6-1.7(**1**)).[85]

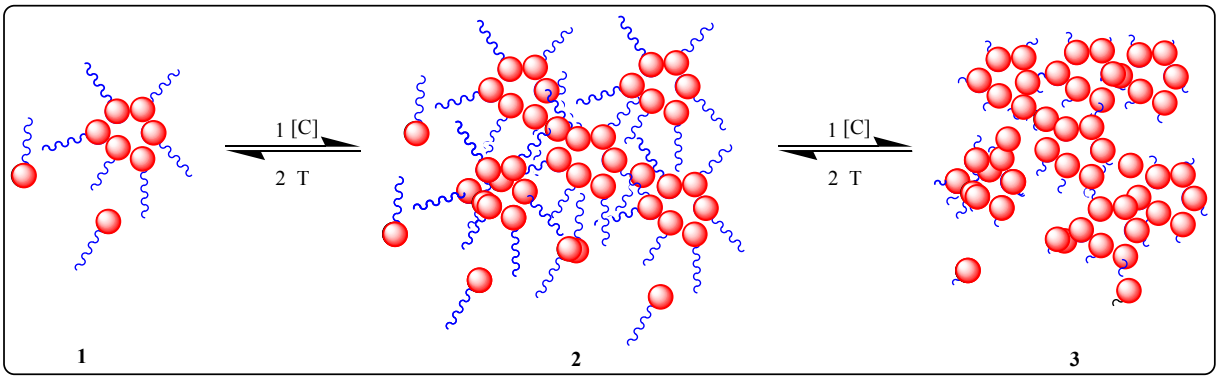


**Figure 1.7 Example of loop-like micelle (1) to transient physical networks (2) and collapsed states (3).**

As polymers concentration is increased a transient network is formed (Figure 1.7(**2**)). Even if the mechanism of gel formation remains uncertain, it is however postulated that in the concentration regime, the micelles pack together and occupy the entire free volume leading eventually to an immobile phase that is often qualified as "jamming" or gel phase.[82, 86]

Examples of such systems includes Pluronic ® poly(ethylene oxide-propylene oxide-ethylene oxide) (**$PEO_{27}$-$PPO_{39}$-$PEO_{27}$**).[87]

Taking advantage of the switch on-off character of the thermoresponsive polymer **A** blocks in **ABA** copolymers, gelation and morphological transitions can also be tuned by varying temperature (Figure 1.7).[88-91] It is suggested that the mechanism of packing micelles described above is also responsible for gel formation at high temperature.[92] Typical examples include poly(ethylene oxide-(DL-lactic acid-co-glycolic acid)-ethylene oxide) (**PEO-PLGA-PEO**)[92] and **$PEO_{58}$-$PBO_{17}$-$PEO_{58}$**.[84] At still higher temperature, the collapsed **A** blocks loose the residual bound water, this reduces the volume occupied by the clustered particles. Consequently, the physical networks previously formed break apart and the polymers precipitate. This phase is often referred as macroscopic phase separation (Figure 1.7(**3**)).

Although symmetrical thermoresponsive triblock copolymers **ABA** and **BAB** (with **A** as responsive block) are made of identical chemical blocks, they exhibit different association behaviours when they are in contact of water.[85] Unlike **ABA**, the self-assembly of **BAB** is less understood. It is supposed that once **BAB** triblock copolymers is dissolved in water, several states can be formed namely linear free chain, loop, dangling and bridge structures (Figures 1.8-1.9).[10, 16, 19, 85, 93]

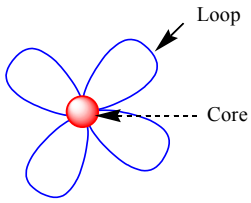


**Figure 1.8 Example of flower-like micelle.**

The loop geometry is induced by the additional loss of entropy needed for the hydrophilic **A** block to loop and keep the two end **B** block in the same micellar core.[19] As a consequence, the **A** block must be long enough so that both end blocks can come together. The growth of this process leads to core-shell micelles with a flower-like structure (Figure 1.8).[94] Typical example is observed for "reverse" Pluronic ® poly(propylene oxide-ethylene oxide-propylene oxide) (**PPO-15-PEO-156-PPO-15**) block copolymer. At ambient temperature, **PPO** blocks form the cores of the micelle while **PEO** forms the corona.[83] When a single block copolymer inserts one of its hydrophobic free end blocks **B** in the core of a flower-like micelle, a dangling **B** block structure is formed (Figure 1.9)

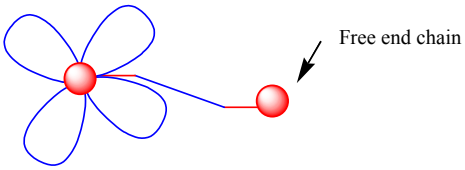


**Figure 1.9 Dangling end chain structure.**

As for **ABA** block copolymers, the sol-gel transition in **BAB** occurs by the packing of micelles, when the total volume fraction of micelles is larger than the maximum packing fraction. In addition to the packing mechanism described above, in the concentration regime, **BAB** block copolymers have the ability to form entanglements by bridges between micelles (Figure 1.10).

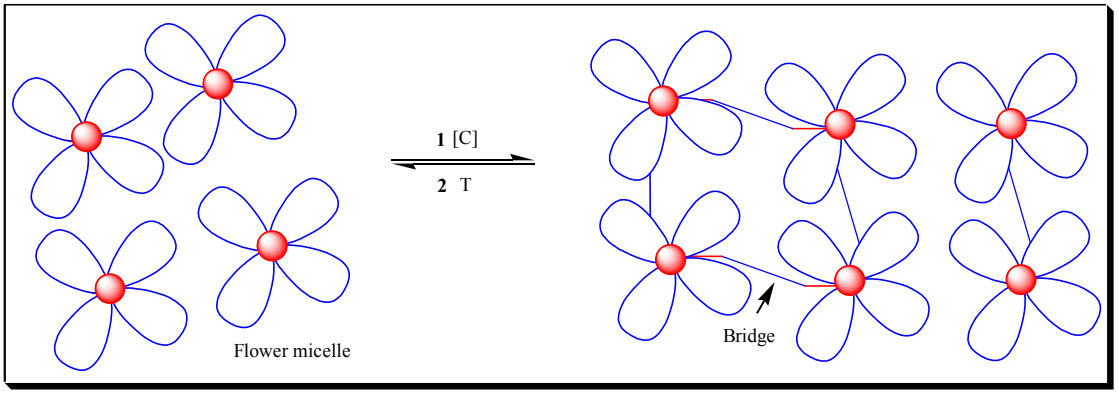


**Figure 1.10 Example of physical network formation using BAB triblock copolymers.**

These bridges result from the ability of linear polymer chains to diffuse both of their end blocks **B** into different micelles core.[83, 95] It should be mentioned that the bridge chains can be generated from the dangling chains as well.[19] Thus, physical networks originating from **BAB** copolymers can be formed through the bridging mechanism as well. Booth et al.[96] studied the aqueous solutions of **$PSO_5$-$PEO_{45}$-$PSO_5$** prepared at several concentrations 14, 20, 30, 50 and 60 w% (**SO**: styrene oxide and **EO**: ethylene oxide). Using the tube inversion method, they found that no gels were formed up to 20 wt%. They claimed the formation of a soft gel at 30 wt%. However, hard gels were observed from the concentration of 38-40 wt%. In addition, a sample with 60 wt% provided evidence of a hexagonal structure formed from packed cylindrical micelles. The formation of these gels was explained by the presence of transient molecular bridging between micelles.[88, 96] Liu et al.[97] recently reported that moderate network structures were formed at higher concentration for **$PBO_5$-$PEO_{91}$-$PBO_5$** (e.g., 25 wt%).[97] Other examples include aqueous solutions of poly(oxy alkylene) copolymers including

poly[(D,L-lactic acid)-co-(glycolic acid)]-poly(ethy1ene oxidel-poly[(D,L-lactic acid)-co-(glycolic acid)] (**PLGA-PEO-PLGA**).[98]

At a given polymer concentration and with increasing temperature, the transition from aqueous solutions of a flowing fluid to a non-flowing state is also observed in thermoresponsive **BAB** block copolymers.[98] In addition to the jamming of close-packed micelles (or overlapping between micelles), it is suggested that the sol-gel transition can also be associated with hydrophobic aggregation between micelles. In fact, as the temperature is increased, the dynamic equilibrium between micelles and clusters shifts in favour of cluster formation.[83] Thus, it becomes easier to find more transient networks comprising clusters linked by bridging chains. It should be mentioned that the intermicellar bridging of the **BAB**-type copolymer leads more easily to molecular clustering than **ABA**-type,[99] and consequently, a lower sol-to-gel transition temperature is formed in **BAB** than **ABA** type.[100] That is why the micellization behaviour of **BAB** triblock copolymers is of interest in this work.

When the temperature is further increased, the shell of micelles shrinks severely and water is expelled out. This dehydration is followed by a decrease of the number of micelles-micelles interaction. Gradually, a mobile or sol phase occurs (Figure 1.7(**3**)).[98] Typical examples include the triblock copolymer **PPO-PEO-PPO**,[83] **PLGA-PEO-PLGA**[98] and poly(caprolactone-ethylene oxide-caprolactone) (**PCL-PEO-PCL**) triblock copolymers. For instance, **PCL-PEG-PCL** aqueous solutions form sol-gel-sol transition with the increase of temperature.

### *1.8.2.1 Composition dependent of BAB on micelles formation*

Similar to **AB** diblock copolymers, the aggregation behaviour of the **BAB** block copolymers is strongly composition and molar mass dependent.[81] As expected, the hydrophobic **B** end blocks play a dominant role in the micellization of **BAB** block copolymers. For instance, their higher content in the copolymer lead to a decrease in the cmc[97, 101] and cloud point of the triblock copolymer.[102] For example, the hydrophobic **BO** end blocks induce faster micellization than **PO** end blocks in **PPO-PEO-PPO** (**EO** = ethylene oxide and **PO** = oxypropylene oxide and in **PBO-PEO-PBO** micellization (**EO** = ethylene oxide and **BO** = butylenes oxide).[102]

## 1.9 Interest of this work

Thermoresponsive polymers with a lower critical solution temperature (LCST) are currently under investigation for biomedical and pharmaceutical applications. One major advantage of **ABA** and **BAB** thermoresponsive triblock copolymers is their use in absence of organic solvents for the formation of hydrogels.

Since their discovery by Schmolka in 1967, amphiphilic block copolymers consisting of poly(ethylene oxide) (**PEO**) and poly(propylene oxide) (**PPO**) continue to attract much interest.[1-3, 103] Aqueous solutions of both **PEO** and **PPO** show lower critical solution temperature (LCST). The LCST of **PPO** is around 10 °C, whereas **PEO** has a LCST around 100 °C. The use of both polymers has allowed to synthesis two types of triblock copolymers with distinct properties. Typical examples include **PEO-PPO-PEO** and **PPO-PEO-PPO** copolymers. The latter type forms stable network compared to its analogous due to bridges between micelles. Although a number of applications are currently pursued as drug delivery carriers using both copolymers, they are some limitations. The difficulty to prepare these symmetrical triblock copolymers remains the first challenge to overcome. Even though living polymerisation techniques are suitable for the synthesis of such block copolymers, their preparation requires still stringent conditions (such as low temperature, inert atmosphere and high purity of solvents). Another drawback concerns the transfer reaction originating in hydrogen abstraction rather than addition. This cannot be excluded for the polymerisation of propylene oxide (**PPO**).[104]

The second limitation is the stability of the resulting micelles. As intuitively expected, the weakly hydrophilic **PPO** units fixed to **PEO** chain are not very effective to stabilize the micelles. This disadvantage weakens their potential utilization as drug carriers. The hydrogels show poor mechanical strength and limited stability with rapid dissolution. Although aqueous solutions of **PEO-PPO-PEO** and **PPO-PEO-PPO** block copolymers exhibit reversible sol-gel transitions when heated, their gelation mechanisms remain a controversial issue. Finally, aqueous solutions of pluronics and analogous block copolymers exhibit phase transition temperature, which depends on the amphiphile architectures and with many other factors including the length of both hydrophobic and hydrophilic blocks.[102, 105-107]

To better understand the basic molecular properties involved in their aqueous self-assembly, it is therefore important to study analogous block copolymers.

## 1.10 Objectives of the study

The overall objective of this work was therefore to study new amphiphilic triblock copolymers **ABA** or **BAB** carrying a hydrophilic thermoresponsive block "**A**" and a hydrophobic block "**B**" to improve the fundamental understanding of their self-assembly in aqueous solutions at moderate to high concentrations of polymers. As a means to achieve this, three specific areas were to be investigated: a) synthesis b) study aggregation in water and c) study thermoresponsiveness.

1) Because of its distinctiveness to be suited for the polymerisation of most common monomers, “Reversible Addition Fragmentation chain Transfer (RAFT)” was the method of choice for synthesising the block copolymers. With the aim of preparing **ABA** or **BAB** structures in only two steps, synthetic efforts were focused upon the synthesis of novel RAFT agents (trithiocarbonates), particularly, on the synthesis of new bifunctional RAFT agents. In this case, two types of RAFT agents were to be studied, those which place the active group of the growing polymer chain at the outer ends of the polymer (Z-C(=S)-S-R-S-C(=S)-Z, type I, and those which position the active groups in the middle of the growing polymer chain (R-S-C(=S)-Z-C(=S)-S-R, type II).

2) By the use of bifunctional RAFT agents, a series of amphiphilic triblock copolymers **ABA** and **BAB** should be prepared starting with the most widely studied stimuli-responsive (**PNIPAM**) as **A** block and polystyrene as standard hydrophobic end blocks **B**. **PNIPAM** is advantageously characterised by a weak dependence of the transition temperature ("cloud point" around 30-35°C) on concentration and molar mass, while polystyrene is the most common polymer used in different polymerisation systems. Noteworthy, it confers the frozen state to amphiphilic micelles due to its high glass transition temperature.

3) Next the nature and the lengths of the hydrophobic **B** blocks should be varied in order to learn about the role of the hydrophobic block in the triblock copolymers, while keeping the chemical nature of the hydrophilic block **A** constant by using always **PNIPAM**. For this purpose poly(4-*tert*-butyl styrene) **pM1**, polystyrene **pM2**, poly(3,5-dibromo benzyl acrylate) **pM3**, poly(2-ethylhexyl acrylate) **pM4**, and poly(octadecyl acrylate) **pM5** were used as the **B**

blocks. The strongly hydrophobic blocks show a high glass transition temperature in the decreasing order **pM1** (130 °C) > **pM2** (100 °C) > **pM3** (38 °C) > **pM4** (-70 °C). The glass transition of **pM5** is reported to occur in the intermediate temperature range, with a $T_g$ of about 57 °C. Moreover, due to the long alkyl side chains that confer extreme hydrophobicity to the polymer, **pM5** is semi-crystalline with a melting point of the side chains of ca. 48 °C.

4) While **ABA** block copolymers tend to form core-shell micelles in aqueous solution, **BAB** copolymers are expected to aggregate into structures such as flower-like micelles in dilute solution, and interconnected micelles and networks at higher concentrations. Special attention was therefore focussed on the aqueous solutions of **BAB** block copolymers. Hence the effect of the different hydrophobic **B** blocks on the thermo-sensitive self-organization of these **BAB** block copolymers into micelles and micellar hydrogels in dilute and concentrated aqueous solution, respectively, was to be investigated.

5) Finally, in order to learn on the importance of the nature of the thermoresponsive block in the "bridged micelles" mechanism, analogous triblock copolymers **BAB** were envisaged, which differ from the main series by replacing **PNIPAM** as middle block by the little studied poly(methoxy diethylene glycol acrylate) (**PMDEGA**), which is expected to exhibited a thermal transition in the same temperature range as **PNIPAM**. Thus, a new **BAB** triblock copolymer consisting of short polystyrene end-groups and poly(methoxy diethylene glycol acrylate) as stimuli-responsive block should be synthesised and studied with respect to the thermoresponsive aggregation behaviour in aqueous solution.

*"Doubt is the father of invention." Galileo Galilei*

# *CHAPTER 2: Controlled/"Living" radical polymerisation*

Chapter 2 deals with the background to controlled radical polymerisation and provides a comparison of the three main controlled radical polymerisation techniques, which are: nitroxide mediated polymerisation (NMP), atom transfer radical polymerisation (ATRP) and reversible addition fragmentation chain transfer polymerisation (RAFT). The relative advantages and limitations of each technique are described. It also demonstrates how crucial the choice of different R and Z groups is in designing RAFT agents with good efficiencies. Finally, the choice of initiator and the reasons for choosing bifunctional trithiocarbonates as chain transfer agents are discussed in detail in this Chapter.

# 2.1 Introduction

Living polymerisation and controlled polymerisation are two concepts, which have given rise to much debate in polymer science. Some researchers suggest, for example, that the concept of controlled radical polymerisation can be used "when chain-breaking reactions undoubtedly occur, like in radical polymerisation".[108] Other groups stipulate that the characteristics of living polymerisation occur "whenever propagation and reversible termination are significantly faster than any process for irreversible termination". To avoid any confusion, the author will consider both "living" and controlled radical polymerisation as processes "which allow polymers to grow whenever monomer is supplied, and such polymers can grow to a desired maximum size while their degree of termination or chain transfer is still negligible".[109, 110]

Since about the 1940s, vinyl polymerisation has seen the emergence of several techniques aimed at a common objective: to improve the architectural quality of polymers.[111] Among these polymerisation techniques can be found: living ionic (anionic and cationic) polymerisations, and free radical polymerisations which include controlled techniques such as stable free radical polymerisation (SFRP), atom transfer radical polymerisation (ATRP) and reversible addition fragmentation chain transfer (RAFT).

# 2.2 Background of living polymerisation techniques

## 2.2.1 Living ionic polymerisation

Living ionic polymerisation techniques were developed more than half a century ago, in the 1950s, by researchers such as M. Szwarc[112] and G.V. Schulz.[113] This class of polymerisation is widely employed to prepare polymers with narrow molar mass distribution and controlled architectures such as block and star copolymers. Those techniques are mediated by anionic or cationic agents. In such polymerisation systems, chain ends stay active unless terminating agents are added. A typical example is shown in Scheme 2.1.

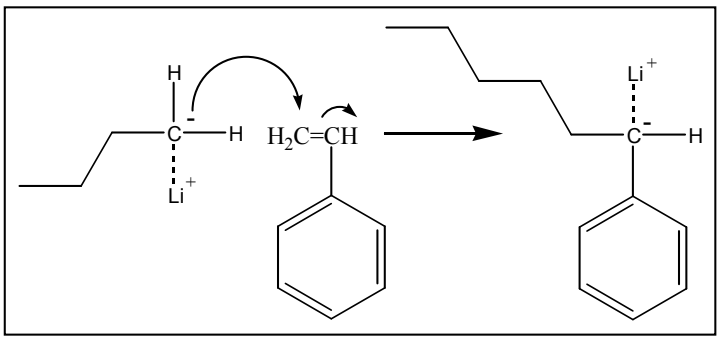


**Scheme 2.1 Example of anionic polymerisation: BuLi initiated polymerisation of styrene.**

In this reaction, there is no termination unless terminating agents, such as 1,2 dichloroethane ($ClCH_2CH_2Cl$), are added.

## 2.2.2 Living radical technique

It was not until the 1980s that Otsu[114, 115] developed a free radical polymerisation technique with a number of similar features to living ionic polymerisation based on "reversible termination". This method is governed by two components namely the initiator and the chain transfer agent (see Scheme 2.2). A conventional initiator starts a polymer chain, inducing the irreversible addition of monomers to form stable C-C bonds. The second component produces very stable radicals (R-S•) that "terminate" chains, with a C-S bond that breaks easily (reversible termination).

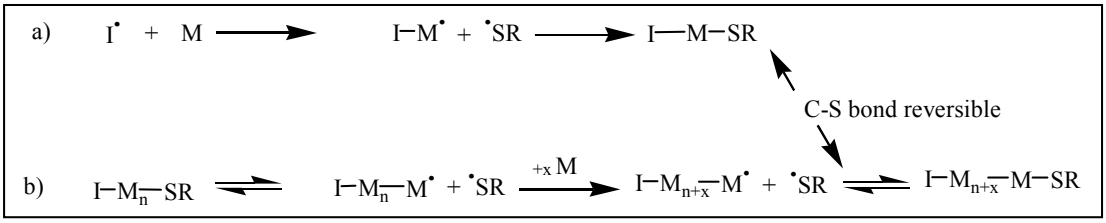


**Scheme 2.2 Reversible termination.**

In this technique, monomer is inserted gradually between chain and iniferter group as the chains are terminated reversibly, and this maintains their ability to grow further. From the mid 1980s until today, other approaches have been investigated in order to develop the concept of controlled free radical polymerisation involving the use of various mediating agents such as

nitroxide radicals, iodine or thiocompounds. The use of nitroxide radicals, for example, has led to the method called stable free radical polymerisation (SFRP)

# 2.3 Stable free radical polymerisation

## 2.3.1 Introduction

Stable free radical polymerisation (SFRP) belongs to the class of reversible free radical termination. A radical polymerisation is conducted in the presence of a nitroxide radical, which reversibly caps the propagating radical chain. This results in a controlled living system and gives polymers with low polydispersity.

The achievement of SFRP as a living mediating technique depends on the nature of stabilized radicals, which range from (arylazo)oxy,[116] substituted triphenyls[117] and triazolinyl,[118] to nitroxide radicals. The latter is the most studied and certainly most successful class of stable radical compounds. These compounds have been successfully developed and used for different applications in the field of living free radical polymerisations. Typical examples are: 2,2,6,6-tetramethyl-1-piperidinyloxy free radical (TEMPO),[119-125] di-tert-butylnitroxide (DBN),[126-128] N-tert-butyl-N-(1-diethylphosphono-2,2-dimethylpropyl) nitroxide (DEPN),[120, 129-131] see Schemes 2.3. The use of such mediators allows the polymerisation of a wide variety of monomers such as styrene derivatives, acrylates, acrylamides, and acrylonitrile etc. Thus, complex copolymers[130, 132, 133] and homopolymers, including polystyrene, with accurate control of molecular weights and polymers with polydispersities as low as 1.05 can be now prepared.[134] The versatile nature of these mediators can be used to control the preparation of random and block copolymers from a wide selection of monomer units.

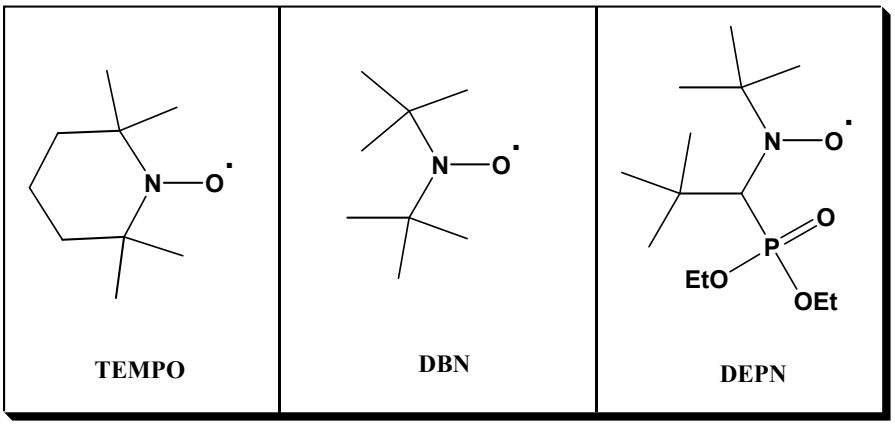


**Scheme 2.3 Examples of nitroxide mediators.**

SFRP is a process which does not only tolerate a number of functional groups[135] but also does not require extremely stringent purification of the starting material as the ionic techniques do.

## 2.3.2 General mechanism of SFRP

In the SFRP process, a capped dormant species (alkoxyamine initiators) (**$P_n$-Y**) is thermally labile and, on heating, decomposes to form a stable nitroxide radical (**Y•**) and a reactive carbon-centered radical (**$P_n$•**). The latter species (**$P_n$•**) can add monomer (**M**) before combining with a nitroxide (**Y•**) to give a new alkoxyamine. The mechanism is illustrated in Scheme 2.4 and by the polymerisation of styrene initiated by TEMPO species in Scheme 2.5.

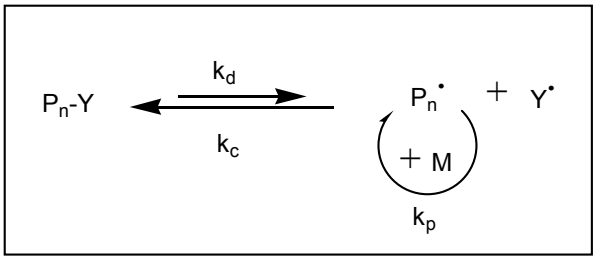


**Scheme 2.4 General mechanism of SFRP.**

Hawker et al.[136] discussed the most important steps in nitroxide mediated radical polymerisations. They noted that the important structural feature in this technique is the ***carbon oxygen (–C-ON) bond*** of the alkoxyamine. In fact, the capping agent, the nitroxide radical (**3**), is generated by the thermolysis process, which causes the homolytic bond cleavage of (–C-ON) of the dormant species (**1**), and produces the active species responsible for the polymerisation, namely the polymeric radical (**2)** (Scheme 2.5). Consequently, while the polymerisation is taking place, the polymeric radical (**2**) can undergo chain extension with monomer (styrene) to yield a new, chain extended polymeric radical (**4**). Chain extension is controlled by the equilibrium between the dormant species and the active (freely propagating) radical. Recombination of (**4**) with the otherwise inert nitroxide (**3)** gives the dormant species (**6)**.

By adding more monomer, the process laid out above can be reactivated. The activation/deactivation, which occurs during the polymerisation cycle, together with the reversible termination of the growing polymeric chain, keeps the level of radicals low, and this leads to a well-controlled polymerisation (Scheme 2.5).[136]

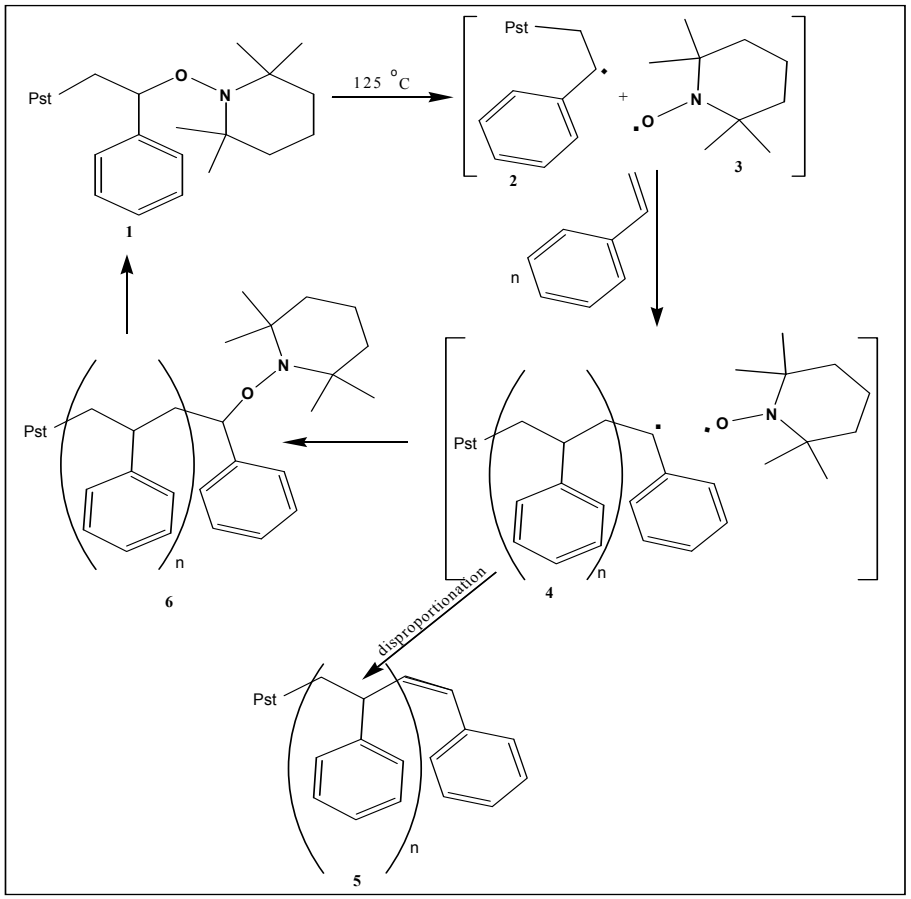


**Scheme 2.5 Polymerisation of styrene mediated by TEMPO.**

It should be noted that instead of adding to a monomer, species (**4**) can terminate via combination or disproportionation to give species (**5**).[136]

Although SFRP has been known since the early 1980s[137, 138] some disadvantages associated with the use of nitroxides as capping agents remain to be overcome (see Table 2.1). These include sensitivity to oxygen and the limited availability of the nitroxides (expensive or difficulty of synthesis), even if TEMPO and some derivatives are currently readily available. Moreover, these mediating agents present a preference to undergo side reactions (disproportionation between propagating species and nitroxide), see Scheme 2.5.

# 2.4 Atom transfer radical polymerisation

## 2.4.1 Introduction

Atom transfer radical polymerisation (ATRP)[139] is a simple, inexpensive polymerisation system, that has found much use in research laboratories because of the commercial

availability of initiators and catalysts.[140, 141] ATRP is mediated by a variety of metal complexes. This living technique was discovered independently by Sawamoto[142] and Matyjaszewski[139] in the 1990s. ATRP combines certain advantages of radical polymerisation, including the ability to polymerise a variety of monomers,[139, 143] with the efficient preparation of block copolymers and the synthesis of polymers with low polydispersities. In addition, like SFRP, ATRP does not require extremely stringent reaction conditions[144] and is applicable over a wide temperature range (Table 2.1). Moreover, the preparation of polymeric materials through ATRP is possible in different media, including emulsion[145] systems.

## 2.4.2 Mechanism of ATRP

Being a member of the reversible termination systems, ATRP polymerisation is based on a capping agent, where halides (R-X) are considered as initiators and X is usually bromide or chloride. As in SFRP, the amount of initiator used in ATRP is very important because the molecular weight of the polymer being formed after consumption of the monomers is a function of the number of radicals produced throughout the polymerisation process.[140]

The mechanism of ATRP[140] is well established (Scheme 2.7); it originates from atom transfer radical addition (ATRA) commonly used in organic synthesis[146-150] (Scheme 2.6).[151]

In ATRA, the mechanism starts by the oxidative addition of a halogen atom X to a transition metal complex $M^n$, due to the abstraction of X from an alkyl halide (R-X), which generates an alkyl radical $R^{\bullet}$ and the oxidized mediator $M^{n+1}$. This radical propagates by adding monomer such as $CH_2$=CHY continuously. The growing chain ($RCH_2CHY\bullet$) will close the catalytic cycle by the abstraction of a halogen from the metal complex $M^{n+1}X$, to form a stable compound ($RCH_2CHXY$).

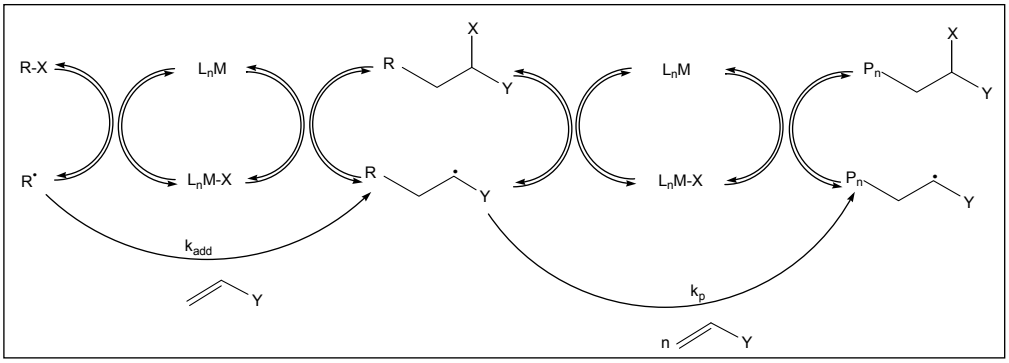


**Scheme 2.6 Catalytic cycles involved in ATRA and ATRP.**

ATRP is a polymerisation technique that was developed on the basis of ATRA and it has the ability of allowing the preparation of growing chains with "active" free radical end-chains according to the ATRA mechanism. One of the advantages of this derivative technique (ATRP) is to allow the reactivation of the polymerisation process in the presence of the additional monomers. Finally, we end up having polymers with high molar masses.[152]

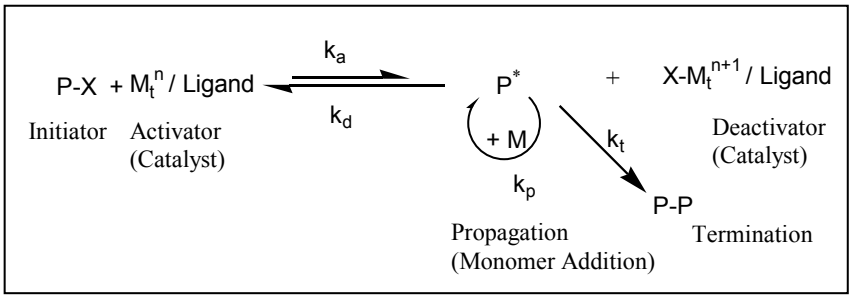


**Scheme 2.7 ATRP and reverse ATRP mechanisms.**

### *2.4.2.1 The ATRP process*

The success of the ATRP technique relies on both the choice of initiator and catalyst complex. In order to minimize the risk of contamination in the final product, the active catalyst selected should provide low levels of transition metal. Due to the fact that oxygen is a contaminant that leads to side reactions (oxidation of the transition metal or reaction with a carbon centered radical), care has to be taken to reduce the amount of dissolved oxygen in the system.

## 2.5 Reversible addition-fragmentation chain transfer polymerisation

### 2.5.1 Introduction

It is increasingly recognized that obtaining polymers with controlled MMD, architecture, etc. through the use of ATRP or SFRP is possible. However, the appropriate choice of monomer is crucial when those aforementioned methods are used in the synthesis of block copolymers and other polymeric materials. For instance, methacrylate and vinyl acetate monomers cannot be polymerised by the use of NMP and ATRP techniques respectively.[153] More recently, a specific technology that has the distinction of being applicable to a wide range of monomers has been developed. This new process is called reversible addition fragmentation chain transfer (RAFT) polymerisation and is mediated by the use of thiocarbonyl thio compounds.

The RAFT process offers several advantages:

- The RAFT process does not need additional experimental precautions compared to conventional radical polymerisation.
- For a given monomer, the chain transfer activity of a RAFT agent can be fine tuned by both substituents *Z* and *R* (see Sections 1.4 and 2.7-2.8).
- The RAFT technique can be applied in both *homogeneous and heterogeneous* polymerisations, such as emulsion[154-156] and miniemulsion[157-160] polymerisations.
- The RAFT technique can be combined with other living techniques, such as ATRP, to produce polymers.

Although RAFT has many advantages, however, they are some disadvantages:

- The synthesis and the purification of thiocarbonyl thio compounds are not too easy and time-consuming.
- Thiocarbonyl thio compounds may have a strong smell and the final products tend to be coloured.
- Inhibition and retardation are often observed in RAFT polymerisations.

Table 2.1 summarizes the characteristics of the three types of living radical polymerisation techniques.

From Table 2.1 and observations discussed in Sections 2.3-2.5.1, the RAFT process appears to be one of the most promising techniques in the field of living free radical polymerisation. The RAFT technique is a sub-class of transfer-based techniques, which depend on the rapid transfer of radical activity among growing chains, where most growing chains are not in their radical form, but in a dormant state. As in all controlled techniques, the termination reactions are not entirely suppressed in a RAFT system. However, the concentration of terminated products can be minimised by using low initiator concentrations.

**Table 2.1 Comparison of SFRP, ATRP, and RAFT processes.[111]**

| Features | SFRP | ATRP | RAFT |
|---|---|---|---|
| Monomers | Styrene, acrylate and acrylamides. No methacrylate. | All monomers except those poisoning the catalytic system (acrylic acid). | Nearly all monomers. |
| Conditions | Generally elevated temperatures are used (>120°C). Sensitive to $O_2$. | From high to low temperatures (-30°C to 150°C). Some tolerance to $O_2$. | All temperatures possible, moderate are preferred. Some tolerance to $O_2$. |
| End-groups | Alkoxyamines. | Alkyl halides. | Thiocarbonylthio compounds. |
| Other features | Conventional radical is used for polymerisations. | Transition metal catalyst /ligand used should be removed and recycled. Conventional radical can be used, too. | Conventional radicals are used for polymerisations. |

The RAFT technique is mainly driven by the presence of a reactive double bound species S=C(Z)SR. This dormant species allows the formation of growing chains when active species are added. Even if the RAFT mechanism is not entirely understood yet,[161] Rizzardo et al.[162] have proposed a general mechanism (Scheme 2.8) that is generally accepted.

It was found that RAFT agents having high reactivity provide polymers with well-controlled molecular weight and narrow molecular weight distribution[162, 163] and these polymers with low polydispersities can be influenced not only by the appropriate choice of the RAFT agent but also by the reaction conditions. The most effective RAFT agents are dithioesters, trithiocarbonates, xanthates, and certain aromatic dithiocarbamates[164] (Section 2.5.2).

## 2.5.2 Mechanism of RAFT

a. Initiation + Propagation:

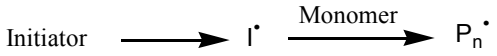


b. Chain transfer:

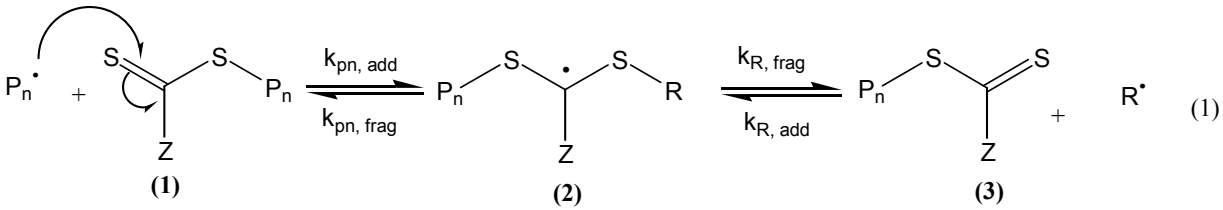


c. Reinitiation:


d. Chain equilibration:

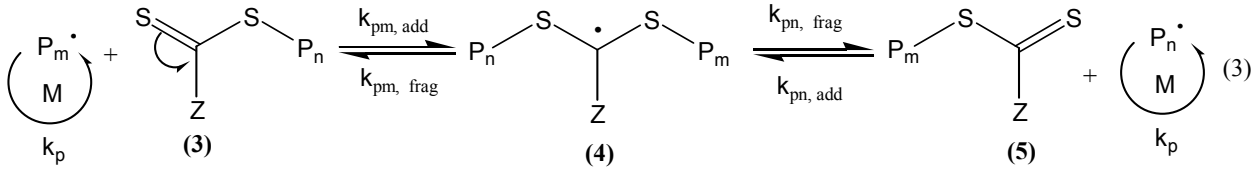


**Scheme 2.8 The RAFT process, as proposed by Rizzardo.**

### *2.5.2.1 The RAFT process*

The RAFT process involves the chain transfer of an active species that reacts with a propagating radical $P_n$•, which is generated by initiator decomposition.

The mechanism proposed by Rizzardo et al.[162] (Scheme 2.8) involves a series of reversible addition fragmentation steps, which begin with the addition of the propagating radical $P_n$• to the dormant chain **(1)**. The resulting intermediate radical **(2)** fragments to a new polymeric thiocarbonylthio compound **(3)** and a new radical R• (equilibrium (1)). It is also possible that the adduct radical **(2)** fragments back to the original polymeric species ((**1)** and $P_n$•. In the former case, the new radical R• formed is added to a monomer M, in order to form a new propagating radical $P_m$•. This propagating radical $P_m$• carries on the polymerisation when it adds to the polymeric RAFT agent **(3)** to form a so-called intermediate radical (species **(4)),**

which can either undergo fragmentation to give a new dormant species **(5),** or fragments back to species **(3)** and $P_m$•. Once the dormant species **(1)** is consumed, an equilibrium is set up between propagating radicals and dormant species (equilibrium (3)).

The following criteria need to be met for an effective RAFT process:

1) A rapid conversion of the RAFT agent into a dormant chain, in order to minimize unwanted termination processes at the earlier stage of the RAFT process. This is called initialization.
2) A dynamic exchange of radicals among all chains.

Both the rates of addition of free polymeric radicals to the RAFT agent and fragmentation of the intermediate radicals must be fast relative to the rate of propagation, in order to give all chains an equal chance to add monomer and to grow at the same rate.

3) Minimal side reactions.

## 2.5.3 The rate of consumption of the transfer agent

Recent studies by Chiefari et al.[165] showed that the consumption of the transfer agent is a function of the propagating radicals [P•] and the ejected radical [R•]. Thus, the consumption of initial RAFT agent (step (1)), can be expressed by the following two transfer coefficients:

$$C_{tr} = k_{tr} / k_p \qquad \text{Eq.2.1.}$$

$$C_{-tr} = k_{-tr} / k_j \qquad \text{Eq.2.2.}$$

- $C_{tr}$ stands for transfer coefficient or transfer constant, which is the ratio of the rate constant for chain transfer to the rate constant for propagation at zero conversion of a given monomer and chain transfer agent (CTA)[166]
- $k_{tr}$ stands for the rate constant for chain transfer
- $k_p$ is the rate constant for propagation
- $C_{-tr}$, $k_{-tr}$ and $k_j$ describe the reverse constants.

For a given RAFT agent, a linear increase in the number-average molecular weight $M_n$ with conversion and a low polydispersity will be obtained, if the chain transfer constant ($C_{tr} = k_{tr} / k_p$) is high (above 100). Moreover, it was observed that $C_{tr}$ varies significantly for different RAFT agents that have the same leaving group (R•) but different activating Z groups. Therefore, $k_{tr}$ values seem to be related to the nature of the activating Z groups contrary to the

leaving moiety R•, which does not play a significant role on the final $k_{tr}$ values as long as it has the ability to reinitiate the polymerisation very quickly.

## 2.5.4 Determination of the transfer rate in the RAFT process

The transfer constant is defined as the ratio of the rate constant for chain transfer to the rate constant for propagation at zero conversion of monomer and RAFT agent.[166] The rate constant for chain transfer agents that occur by addition fragmentation is defined by the following equations:[167]

$$k_{tr} = k_{add} \times k_{\beta} / (k_{-add} + k_{\beta}) \qquad \text{Eq.2.3.}$$

$$k_{-tr} = k_{-add} \times k_{-\beta} / (k_{-add} + k_{\beta}) \qquad \text{Eq.2.4.}$$

where $k_{add}$ is the rate constant for addition to the chain transfer agents, and $k_{-add}$ and $k_{\beta}$ are the rate constants for fragmentation in the reverse and the forward directions respectively.

Studies have shown that the effectiveness of RAFT agent in the RAFT process depends on:

- The rate of reaction of the RAFT agent,[166] with the propagating radicals ($k_{add}$) which is under the influence of (**1**) and (**3**) in Scheme 2.8
- The rate of fragmentation of the intermediate radicals between products and starting materials, determined by the magnitude of $k_{-add}$ and $k_{\beta}$.[166]
- The ability of the expelled radicals, R•, to re-initiate polymerisation.

In the RAFT process, the transfer constant and the polydispersity are strictly related. The preparation of new materials with low polydispersities is achieved by the use of chain transfer agents with higher transfer constants. Aryl (as Z group) dithiobenzoate derivatives, for example, are recommended in the polymerisation of monomers such as styrene and acrylate esters because their transfer constant values with such monomers are estimated to be larger than 20.[166]

## 2.5.5 Determination of molar masses

As will all controlled polymerisation techniques, the RAFT process is characterised by an increase of the molar mass in a linear manner with monomer conversion.[166] With knowledge of the monomer and RAFT agent concentrations, the evolution of $M_n$ can be predicted as follows (Eq. 2.6):[166]

$$M_{n,\,theory} = t\,[M]_0/[RAFT]_0 \times FW_M + FW_{RAFT} \qquad \text{Eq.2.6.}$$

where $[M]_0$ and $[RAFT]_0$ are the initial concentrations of the monomer and the RAFT agent, $FW_M$ and $FW_{RAFT}$ are the molar masses of a monomer and of the RAFT agent, respectively, t is the fractional conversion, $M_{n,\,theory}$ is the theoretical number average molar mass of the formed polymer.

## 2.5.6 The most common Z group of RAFT agents

The chain transfer activity of RAFT agents has been studied extensively and it was found that their activity is a function of the Z and R groups. Among the common Z groups of RAFT agents used, five classes have been identified according to the atom or group atom used to form the C-Z bond (S=C-Z). See Table 2.2 below:

**Table 2.2 Classes of RAFT agents with different Z groups.**

| RAFT agents | Z group |
|---|---|
| Dithioesters | Alkyl-, aryl- |
| Trithiocarbonates | Alkyl-S- |
| Dithiocarbamates | $R_1R_2$-N- |
| Xanthates | Alkyl-O- |
| Phosphoryl-esters | Phosphonate |

Among the five classes, the dithioesters are the most effective and have higher transfer coefficients[166] than the others in the RAFT-mediated polymerisation of styrene for example, where the R group is common.

Trithiocarbonates are relatively simple to synthesise and easier to purify than other RAFT agents, such as dithioesters for example. The role of the activating group is governed by the alkyl-S- moiety, and affords effective RAFT agents,[166] which are often characterised by high transfer coefficients.[168]

Dithiocarbamates (DTCs) are used in agriculture as fungicides, as well as in the rubber industry as vulcanization accelerators and antioxidants.[169] It is noteworthy that the efficiency of the dithiocarbamate groups depends most sensitively on the substituents on the nitrogen (Table 2.2).[166]

Xanthates are easier to synthesise than dithioesters. They are commonly used to manufacture cellulose film. Xanthates are efficient RAFT agents for vinyl esters and amides, but have low transfer constants in polymerisations of certain monomers such as styrene and methyl methacrylate.[166]

The search for new and efficient trapping agents resulted in the use of phosphoryl moieties.[170, 171] Here the phosphoryl group can bear different substituents. Typical examples are methyl diethoxyphosphoryl- or diethoxythiophosphoryl-dithioformiates (Scheme 2.9).[172]

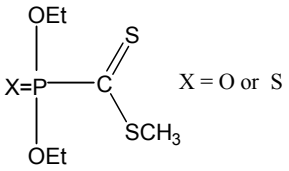


**Scheme 2.9 Example of phosphoryl dithioformates.**

## 2.6 Influence of the Z group on the double bond (S=C)

Among the five classes described above, it has been suggested that within each class of RAFT agents, the differences in transfer coefficient should mainly reflect the influence of the Z group on the rate of free radical addition to the (S=C) double bond. For example, some authors[165] attributed the relative low activity of *O*-alkyl dithiocarbamate and *N,N*-dialkyl xanthates derivatives observed in certain cases to the formation of resonance structures, which arise through interaction between the O or N lone pairs and the double bond (S=C) (Scheme 2.10).[165] In other words, a lowering of the double bond character of the (S=C) bond by conjugation with the lone pair of electrons on the heteroatom substituent explains the low activity of these reagents (Scheme 2.10).

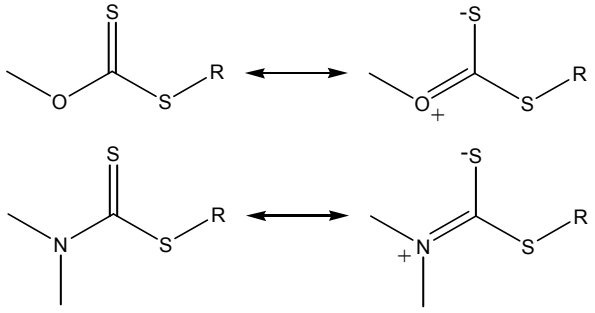


**Scheme 2.10 Resonance structures of xanthates and dithiocarbamates.**

Thus, compounds which present stabilizing effects on the intermediate radical will speed up the rate of addition of the propagating radical to the RAFT agent, and simultaneously lower the fragmentation rate of the leaving groups.

These same considerations should be taken into account with the substituents that are electron withdrawing or which are able to delocalize the lone pair as this should enhance the activity of these compounds. Thus, the efficiency of a RAFT agent should be potentially increased in the case where a Z substituent does not present a stabilizing effect on the intermediate radicals (see Schemes 2.11 and 2.12).

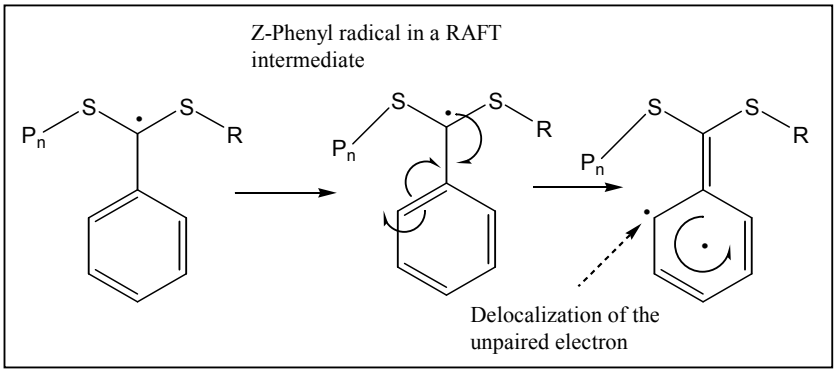


**Scheme 2.11 Proposed stabilization of the intermediate radical by the phenyl Z group during the RAFT process through electron delocalization.**

In addition, Chiefari et al.[165] demonstrated that the transfer coefficient is higher for aromatic compounds if the Z group is taken from the following series: Ph; $SCH_2Ph$; SMe; Me.

By changing the Z group from a phenyl to a benzyl group, (Coote et al.[173]) the radical in the RAFT intermediate is changed from being in a disulfur benzylic position to a less stable disulfur alkyl position (see Schemes 2.11 and 2.12).

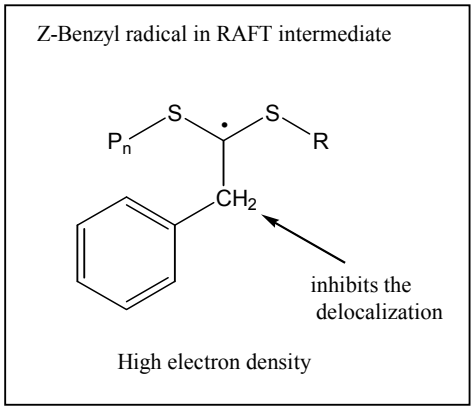


**Scheme 2.12 Intermediate radical in the benzyl group.**

The conjugation along the phenyl group allows the delocalization of the unpaired electron into the aromatic ring, whereas the benzyl substituent inhibits this effect via the insulating $CH_2$ group. These electronic effects provide a better rate of fragmentation. It is for these reasons why in this work the Z groups for styrene and acrylates polymerisation were chosen mostly from S–$(CH_2)_2CH_3$ and S–$(CH_2)_3CH_3$.

## 2.7 Effect of the radical leaving group (R•)

The effect of R as leaving group on the fragmentation step in the RAFT process is as important as the Z group effect.[174] A high rate constant for fragmentation of the intermediate radical **(2)** and **(4)** to polymeric thiocarbonyl thio species **(3)** and **(5)** (Scheme 2.8) is achieved by a R group, which behaves as a good homolytic leaving group with respect to the propagating radical, and which has the ability to reinitiate the polymerisation.

The homolytic leaving ability of a group R appears to increase with electronic factors, the stability of the expelled radicals R• and increasing bulkiness of the R group.[174] Thus, it was found that tertiary radicals R•[174] result in a larger transfer coefficient than primary or secondary radicals R•. Typical examples are shown in Scheme 2.13.

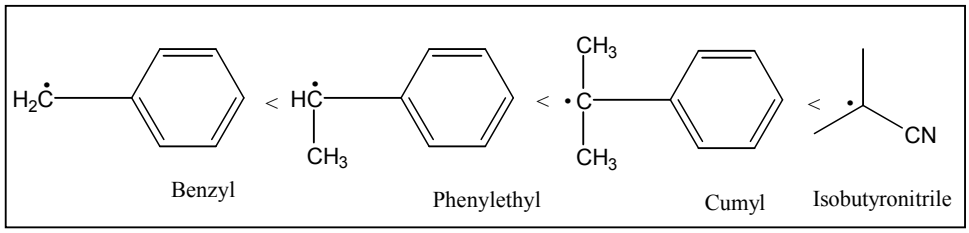


**Scheme 2.13 Examples of different alkyl radicals suited as leaving groups R• in the RAFT process**

The carbon that bears the unpaired electron is electron deficient, and thus electron-releasing alkyl groups attached to this carbon provide a stabilizing effect. Alkyl groups or conjugated groups, such as phenyl, that are attached to this carbon increase the stability of the radical formed.

Beside of both the Z and R groups as important factors in the determination of the value of the transfer coefficient for a given alkyl dithioester, the choice of the monomers also play an essential role. For example, it was shown by Rizzardo et al.[166] that styrene polymerisation is efficient with dithiobenzoate CTAs, in which the Z group is Ph-, and the R group is one of the following: -$C(Me)_2Ph$, -$C(Me)_2CN$, -$C(Me)_2CO_2Alkyl$, -$C(Me)_2CH_2C(Me)_3$, -$C(Me)_3$, -

C(Me)HPh, -$CH_2$Ph, -$CH_2CO_2$H. These CTAs are effective and give polymers with low polydispersities and good control of molecular weight. Contrary, in MMA polymerisation, effectiveness decreases in the order where R is $C(Me)_2$Ph -$C(Me)_2$CN > -$C(Me)_2CO_2$Alkyl > -$C(Me)_2CH_2$C(Me), -$C(Me)_3$ > -C(Me)HPh > -$CH_2$Ph. In fact, in this series only the CTAs where R = -$C(Me)_2$Ph or -$C(Me)_2$CN give polymers with low polydispersities and good control of molecular weight. Therefore, the transfer coefficient is higher when styrene is used with alkyl dithioesters as RAFT agents and the transfer coefficient is lower for the same transfer agents in the case of methyl methacrylate. Accordingly in this work, the R groups for styrene polymerisation were chosen as -$CH_2$Ph.

# 2.8 Choice of monomers

The RAFT process, as mentioned in Section 2.5.1 and Table 2.1, is capable to polymerise most monomers susceptible to free-radical polymerisation. Such monomers can be presented by the following structure (Scheme 2.14).[166]

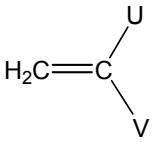


**Scheme 2.14 Example of a monomer unit, where, for example U = H, alkyl, alkoxy groups and halogen; V = phenyl, COOR, OCOR, CN, $CONH_2$ and halogen (there are other possibilities).**

## 2.8.1 Styrene as model monomer in this work

Styrene monomer is a colourless liquid that reacts in the propagation reaction to form polystyrene. Moreover, styrene is the most common monomer used in different polymerisation systems,[136, 140, 165] such as: bulk,[175] solution, emulsion[176, 177] and miniemulsion[178] because it has proved to be successful in the preparation of homopolymers and copolymers. Styrene used alone as monomer in a bulk polymerisation in the presence of a RAFT agent plays two important roles: the first is to initiate the polymerisation via the production of radicals at high temperature generated through the Mayo mechanism[179] and the second is to react with a radical to produce a propagating radical which is responsible for reinitiating the polymerisation (step (2) in the RAFT mechanism, see Section 2.5.2).

Therefore, styrene that is the most commonly studied monomer and appears to be the ideal model to test various RAFT agents.

### 2.8.2 Acrylamide monomers

While a wide range of monomers can be polymerised by traditional living techniques as well as by controlled polymerisation techniques, polymerisation of acrylamido monomers has proven to be difficult. So far, the RAFT process is the only method which can be reliably used for the synthesis of well-defined polyacrylamides and their copolymers. For example, the successful RAFT synthesis of water-soluble block copolymers prepared even from functional acrylamides, such as the nonionic monomer *N*-isopropylacrylamide (**NIPAM**) and the zwitterionic monomer 3-[*N*-(3-methacrylamidopropyl)-*N*,*N*-dimethyl]ammoniopropane sulfonate (**SPP**), have been described.[73] Because of the reasons described above, the RAFT process was selected in this work to prepare **PNIPAM** homo- and block copolymers (Chapter VII).

## 2.9 Choice of initiators

Free radical initiators are molecules which easily decompose into free radicals and serve as reactive intermediates in organic and polymer synthesis. There are several ways of generating radicals, such as by thermal, photochemical or high-energy radiation (electron beam or gamma-radiation).[166] Precautions should be taken that there is no adverse interaction of the initiator or the initiating radicals with the transfer agent under the conditions of the experiment.[166] If radicals are thermally produced, the temperature required should not be unfavourable to the chain transfer agent used. Moreover, the initiator chosen should be soluble in the reaction medium or monomer mixture. Finally, the suitable choice of the initiator is dependent on its half-life at the desired reaction temperature and its initiation ability relative to the monomer employed.

## 2.10 Inhibition periods in the RAFT process

An inhibition period can be defined as a period where there is no polymerisation activity. This is observed at the early stages of polymerisation. Long inhibition periods are frequently observed during RAFT mediated polymerisation. Several attempts have been made to explain these inhibition phenomena. Perrier et al.[180, 181] studied the origin of inhibition effects in the polymerisation of methyl acrylate at 60 °C by varying the initial RAFT agent concentration

(1-phenylethyl dithiobenzoate and 2-(2-cyanopropyl) dithiobenzoate). They found that a cyanoisopropyl leaving group induces a shorter inhibition period than a phenylethyl leaving group. Thus, they suggested that the slow fragmentation of the intermediate RAFT radical **(2)**, (Scheme 2.8) in the preequilibrium could explain the inhibition rather than the weak reinitiation ability of the leaving group.

However, Moad et al.[182] observed an inhibition period lasting up to 1 h for the styrene polymerisation mediated by cumyl dithiobenzoate. This long period has been attributed to the slow initiation of styrene by the cumyl radical.

McLeary et al.[183] investigated the concentration of several characteristic species involved in the first steps of the RAFT polymerisation of styrene in the presence RAFT agent 1-phenylethyl dithiobenzoate and 2-(2-cyanopropyl) dithiobenzoate at 70°C and 80°C. They demonstrated that the RAFT process starts with an initialization period, in which the starting RAFT agent is consumed. The critical process in the initialization of the RAFT controlled polymerisation was found to be the addition of a single monomer unit to the growing chains before the addition of another monomer unit.

## 2.11 Rate retardation in the RAFT process

The phenomenon of retardation in the RAFT process has given rise to numerous discussions. Some research groups claim that the retardation observed is due to the slow fragmentation of intermediate radicals. Thus, Davis et al.[184] assumed that the intermediate radical is stable enough to cause no termination with **P•** (no cross-termination), whereas on the other hand, Monteiro et al.[185] assumed that the intermediate radical undergoes cross-termination between propagating and intermediate radicals, see Scheme 2.15.[174]

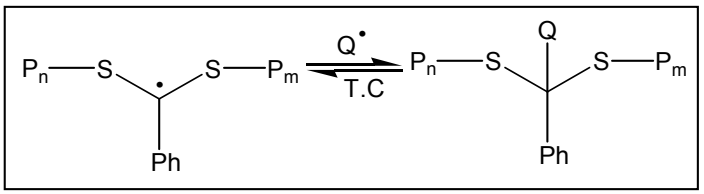


**Scheme 2.15 Possible termination reactions involving the intermediate radical (T.C is termination by combination and Q• is a radical).**

In both cases, a computer simulation was made and the difference between both the fragmentation rate constant in the RAFT process ($k_{fr}$) values used by the two groups was 6-7

orders of magnitude, apart, either $k_{fr}$: $10^{-2}$ $s^{-1}$ from the first group and $k_{fr}$ :$10^{5}$ $s^{-1}$ for the second.[120] The computer simulations brought no solution to this controversy because the rate data for the ratio styrene/dithiobenzoate system used by the two respective groups were more or less similar. However, recently Calitz et al.[186] presented ESR and NMR data about the aforementioned phenomenon; they obtained similar results to those given by Monteiro et al.[185] Despite numerous other studies done by other researchers to clarify this phenomenon of retardation, no satisfying answer has been given up to now. Taking into account studies that have lead to the process of retardation in the RAFT technique (Sections 2.7 and 2.8), several possible origins have been identified as major sources of this retardation, such as:[166]

- The Z group as radical agent stabilizer for the intermediate (**2**) (see Figure 2.10)
- Slow fragmentation of the intermediate radical (**2**) during the polymerisation
- Inability of the R group to re-initiate the polymerisation
- Slow fragmentation of the intermediate radical obtained from the polymeric RAFT agent (**4**)
- The ejected radical (R•) might prefer to add to the RAFT agent rather than to the monomer.

## 2.12 Synthesis of amphiphilic block copolymers

Amphiphilic block copolymers are characterised by the combination of a water soluble part (hydrophilic group) and an insoluble part (hydrophobic group) (see Chapter 1), mostly in form of diblock and symmetrical triblock copolymers. The triblock copolymers can be synthesised through the successive use of monofunctional RAFT agents (CTAs). As seen in section 2.5.6, trithiocarbonates represent the simplest CTAs. Using a monofunctional trithiocarbonate, symmetrical triblock copolymers can be prepared step by step via three subsequent polymerisation steps (see scheme 2.16).

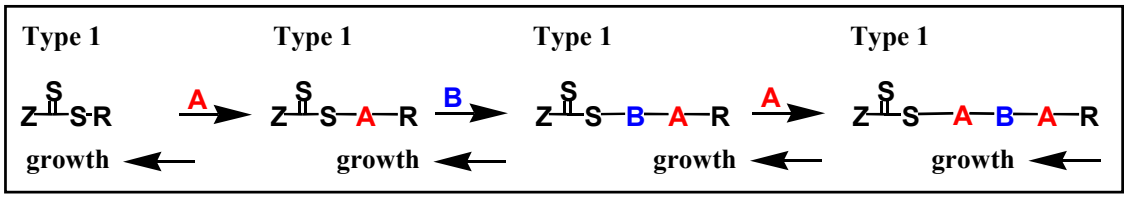


**Scheme 2.16 Synthesis of ABA triblock copolymer using monofunctional CTA in three polymerisation steps.**

Although this procedure allows the synthesis of symmetrical triblock copolymers, some problems inherent to the polymerisation cannot be avoided, including a partial loss of end-group functionality. Thus, the final product can be e.g. contaminated by linear diblock copolymer, which is often hard to remove from the triblock copolymer. In this line, it is more convenient to use bifunctional RAFT agents, so that only two polymerisation steps are needed (see scheme 2.17-2.18).

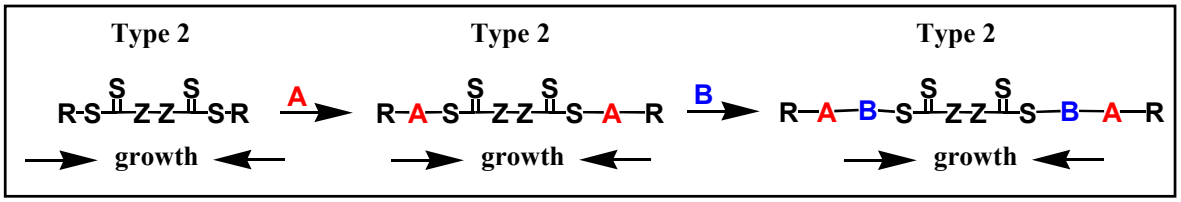


**Scheme 2.17 Synthesis of ABA triblock copolymer using bifunctional CTA in two polymerisation steps.**

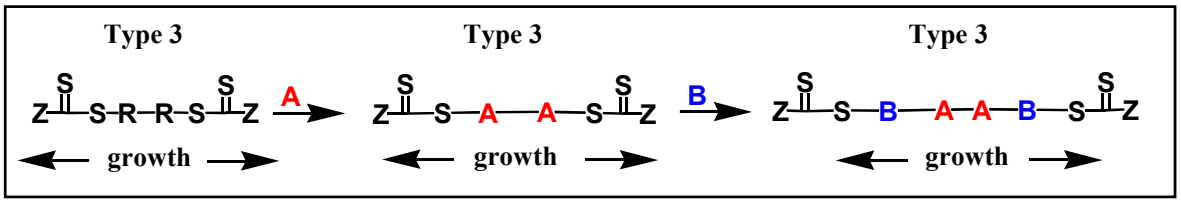


**Scheme 2.18 Synthesis of BAB triblock copolymer using bifunctional CTA in two polymerisation steps.**

The use of bifunctional trithiocarbonates (CTAs) assures both symmetrical segments are of the same lengths and chemical composition (for instance in **ABA** or **BAB**). It should be noted that depending on the growing step with respect to the Z-group, the bifunctional CTAs can differ from one to another by the sequence of insertion of each monomer into the CTA used (Scheme 2.17-2.18). Both strategies have their advantages and inconveniences. For instance, amphiphilic **ABA** and **BAB** copolymers made with type 3 RAFT agents face the risk to degrade into diblock copolymers by hydrolysis of the thiocarbonyl moiety, whereas hydrolysis followed by oxidative thiol coupling may lead to pentablock contaminants, when RAFT agents of type 2 are employed. Several groups have exploited this facile method for preparing sequential blocks **ABA** and **BAB**.[8, 18, 187, 188] Because of the reasons described above, the present work focuses on the use of bifunctional trithiocarbonates with two leaving R-groups.

*"You must judge a man by the work of his hands." African Proverbs*

# *CHAPTER 3: Synthesis of Symmetrical ABA and BAB Triblock Copolymers made of hydrophobic end-groups and poly(N-isopropylacrylamide) as A-block Using Bifunctional Bis(trithiocarbonate)s as RAFT Agents*

Six new bifunctional bistrithiocarbonates were explored as RAFT agents for the polymerisation of styrene and N-isopropylacrylamide, while dibenzyltrithiocarbonate was used as reference. The bifunctional RAFT agents belonged to two types. One type leads to polymers with the active trithiocarbonate groups at the outer ends of the growing polymer chain, while the other type leads to polymers with the trithiocarbonate groups in the middle of the growing polymer. Amphiphilic symmetrical triblock copolymers **ABA** and **BAB** were synthesised in two steps, with hydrophilic **A** blocks made from N-isopropylacrylamide and hydrophobic **B** blocks. Homopolymers were prepared from both monomers, which subsequently were engaged as bifunctional macro-RAFT agents to build the block copolymers. Whereas the extension of poly(N-isopropylacrylamide) macro-RAFT agents by styrene was not effective, polystyrene macro-RAFT agents provided efficiently the desired block copolymers. End-group analysis via $^{1}$H-NMR spectroscopy proved to be a valuable tool to complement molar mass analysis by size exclusion chromatography (SEC). Moreover, end-group analysis by $^{1}$H-NMR revealed an unexpected fragmentation pathway for certain bis(trithiocarbonate)s, converting them to simple trithiocarbonates while extruding ethylenetrithiocarbonate.

# 3.1 Choice of polymerisation methods, monomers and RAFT agents to be used

A number of techniques have been developed to prepare **AB**, **ABA** and **BAB** triblock block copolymers with predetermined molar masses ($M_n$) and low molar mass distributions ($M_w/M_n$). In particular, Reversible Addition Fragmentation chain Transfer (RAFT) technique has shown to be robust, versatile and applicable to classical monomers subject to radical polymerisation. As described in Chapter 2, the RAFT method employs generally thiocarbonyl compounds such as dithioesters, xanthates, and trithiocarbonates, as degenerative chain transfer agents. They may be represented by the general formula Z-C(=S)-S-R, where R is the leaving group that must be capable of reinitiating a new polymer chain, while the Z group modulates the reactivity toward radical addition and the stability of the intermediate radicals formed. Accordingly, a judicious choice of the R and Z groups is necessary to achieve a well controlled polymerisation of a given monomer.[189-191] This implies for the synthesis of block copolymers from monomers of differing reactivity, that the sequence of monomer addition may be not arbitrary, but that a particular order should be respected. For instance, it is advised to polymerise methacrylate monomers before polymerising acrylate or styrenic ones to obtain high blocking efficiencies.[192, 193] The work of the thesis is focused on the use of trithiocarbonates as RAFT agents, as monofunctional and bifunctional trithiocarbonates have been reported to be efficient in the preparation of homo- di- and triblock copolymers. Symmetrical triblock copolymers can be prepared step by step via three subsequent polymerisation steps when monofunctional trithiocarbonates are used as RAFT agents. However, it is more convenient to use bifunctional trithiocarbonate RAFT agents, so that only two polymerisation steps are needed. In this case, two types of RAFT agents can be envisaged, those which place the active group of the growing polymer chain at the outer ends of the polymer (Z-C(=S)-S-R-S-C(=S)-Z, type I, see Figure 3.1), and those which position the active groups in the middle of the growing polymer chain (R-S-C(=S)-Z-C(=S)-S-R, type II, see Figure 3.1). Both strategies have their advantages and inconveniences.[194, 195] For instance, amphiphilic **ABA** and **BAB** copolymers made with type II RAFT agents face the risk to degrade into diblock copolymers by hydrolysis of the thiocarbonyl moiety, whereas hydrolysis followed by oxidative thiol coupling may lead to pentablock contaminants, when RAFT agents of type I are employed.

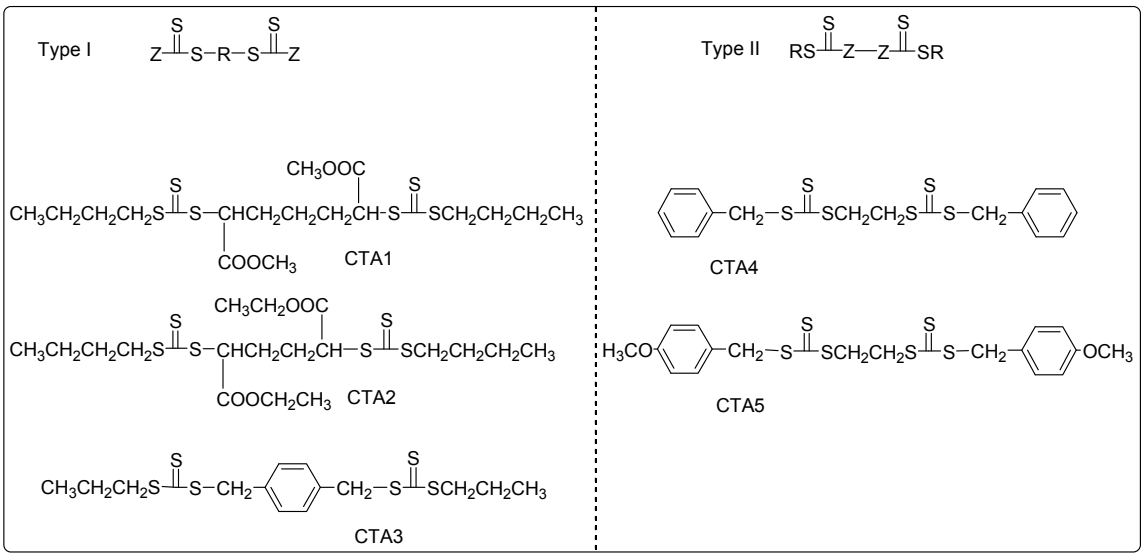


**Figure 3.1 Bifunctional RAFT agents synthesised of Type I and Type II newly used in the thesis (CTA1-CTA5).**

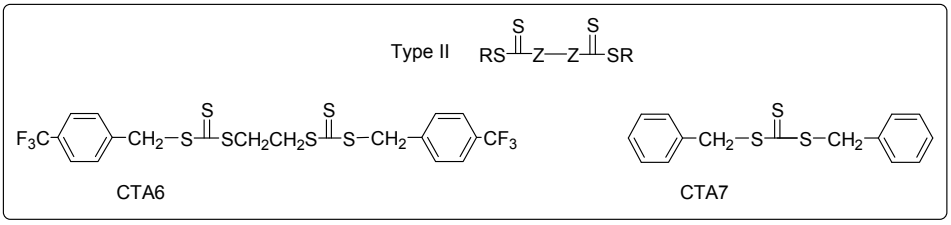


**Figure 3.2 Bifunctional RAFT agents (CTA6-CTA7) included as reference compounds.[8, 196]**

In addition to their inherent importance for efficient chain transfer, the R and Z groups of RAFT agents may be tailored to incorporate functional end-groups in the polymers. If the polymerisation process is well controlled, the degree of end-group functionalisation is close to complete. This is not only useful if a particular functionalisation is aspired, e.g. labelling the polymer with a fluorophore,[197-200] but also for molecular characterisation. Many homopolymers, such as polyacrylamides like **PNIPAM**, pose problems in molar mass analysis by whatsoever method. Moreover, except for a few polymers such as polystyrene or poly(methylmethacrylate), the currently preferred method of size exclusion chromatography (SEC) suffers from the lack of appropriate calibration standards. The problems in molar mass analysis become particularly severe for statistical and block copolymers. In all theses cases, molar mass determination by end-group analysis is an attractive option. Whereas the thiocarbonyl group may serve as inherent UV-label for end-group analysis,[198, 201-204] the use of $^{1}$H-NMR spectroscopy requires the incorporation of moieties, which are easy to identify and well resolved in the spectrum, into the Z or (up to now rarely) the R group of the RAFT

agent.[205-210] Even more, if both R and Z groups are appropriately labeled so that they can be independently quantified,[211, 212] the extent of end-group functionalisation may be estimated by the Z/R ratio in the polymers.[212] This is a precious information e. g. for the synthesis of high quality macroRAFT agents, which can be hardly obtained by other methods.[198, 204, 212]

In this Chapter, six different bifunctional trithiocarbonates as RAFT agents were synthesised and used for the preparation of a series of analogous **ABA** and **BAB** triblock copolymers with a thermo-sensitive hydrophilic block **A**, mostly poly(N-isopropylacrylamide) (**NIPAM**), while the nature of the hydrophobic **B** blocks was varied, using poly(4-*tert*-butyl styrene) (**pM1**), polystyrene (**pM2**), poly(3,5-dibromo benzyl acrylate) (**pM3**), poly(2-ethylhexyl acrylate) (**pM4**), and poly(octadecyl acrylate) (**pM5**) (see Figure 3.3). The R and Z groups in the RAFT agents as well as their positioning in the molecules (type I or type II, see Scheme 1) were varied in order to learn about their usefulness for the particular block copolymer system. Moreover, their potential for end-group analysis by $^{1}$H-NMR spectroscopy should be explored.

The following study starts by exploring the RAFT polymerisation of styrene and **NIPAM** using six different bifunctional trithiocarbonates, five of which were used for the first time in the RAFT process. These two monomers were chosen because they are among the most studied monomers. **PNIPAM** is well known for its lower critical solution temperature (LCST) in aqueous solution. It exhibits not only a convenient switching temperature around 30-35 °C but also, different from many other thermoresponsive polymers (such as polyethylene oxide), **PNIPAM** is also advantageously characterised by a weak dependence only of the transition temperature ("cloud point") on concentration and molar mass. Polystyrene is used in block copolymers to form micelles with ‘‘glassy’’ cores. Such aggregates are of potential interest for solubilizing hydrophobic molecules in aqueous solutions where stable and mechanically robust aggregates are desirable. Furthermore, styrene used in a bulk polymerisation in the presence of a RAFT agent can assume two roles: the first is to initiate the polymerisation via the production of radical generated through the Mayo mechanism[179] and the second is to react with a radical to produce a propagating radical which is responsible for reinitiating the polymerisation (step (2) in the RAFT mechanism, see Section 2.6.2). Thus, styrene appeared to be ideal as a model system to test the various RAFT agents.

The polymerisation of other hydrophobic monomers was also studied (see Figure 3.3).

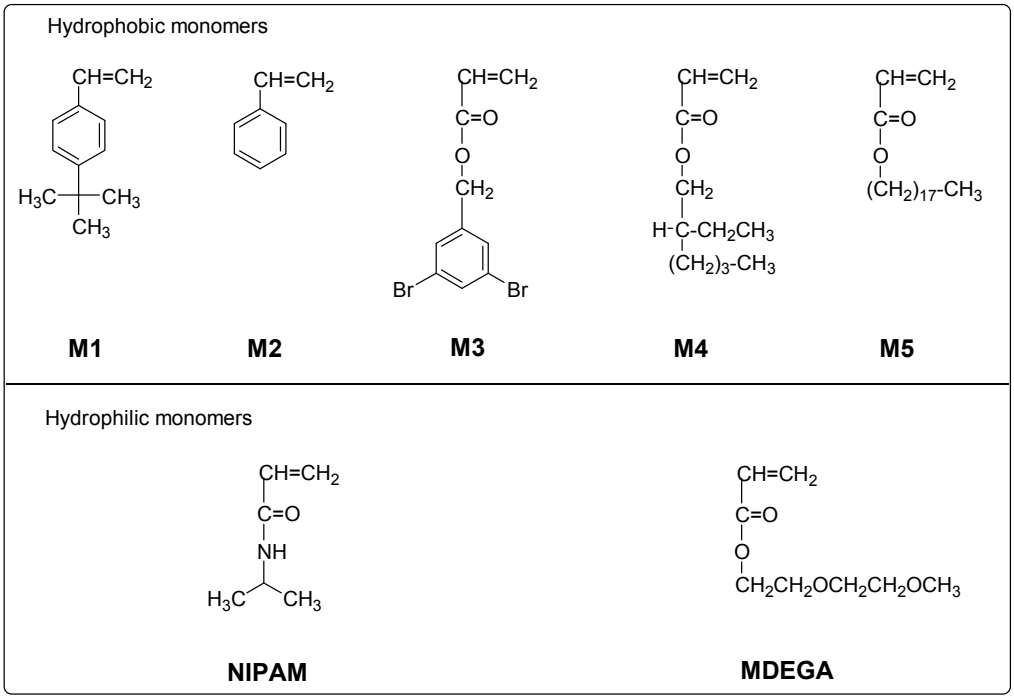


**Figure 3.3 Monomers used in the thesis. M1: 4-tert-butyl styrene, M2: Styrene, M3: 3,5-dibromobenzyl acrylate, M4: 2-ethyl hexyl acrylate, M5: octadecyl acrylate, N-isopropyl acrylamide (NIPAM), Methoxy diethylene glycol acrylate (MDEGA).**

## 3.2 Features of the bistrithiocarbonate RAFT agents

Because of its versatility and usefulness for both classical monomers, several examples of block copolymers from styrenes and **NIPAM**,[7, 213-217] have been reported to be prepared successfully by the RAFT method, mostly employing dithioesters as RAFT agents. Still, molar mass characterisation of **PNIPAM** and even more of such amphiphilic block copolymers is difficult by standard methods for multiple reasons, such as their strong tendency to aggregate or to adsorb on surfaces. Therefore, analysis by end-group determination seems highly attractive. Still, it is difficult to functionalize both R and Z groups in dithioesters with good marker groups, as desirable for efficient end-group analysis. Because this is much easier to implement via trithiocarbonates, the use of unsymmetrical trithiocarbonates was explored, bearing one RAFT active and one RAFT inactive thiol residue. Accordingly, five bistrithiocarbonates as bifunctional chain transfer agents were prepared, and obtained in good yields (see Chapter 8, section 8.3.1). All contain benzyl or secondary α-alkanoyl groups as established R-groups for styrenic and acrylic monomers, [189-191, 193] and are new compounds except for **CTA3** and **CTA4**, which were mentioned briefly in

the past.[7, 187, 218] Both **CTA6** and the well established dibenzyltrithiocarbonate RAFT agent **CTA7** serve as reference, as it is an efficient bifunctional RAFT agent in the polymerisation of styrene and acrylic monomers.[219-222]

The bistrithiocarbonates **CTA1-CTA3** can be classified as type I bifunctional RAFT agents Z-C(=S)-S-R-S-C(=S)-Z, which lead to growing polymer chains that bear the active RAFT group at the outer ends of the polymer. In contrast, **CTA4-CTA7** represent type II bifunctional RAFT agents R-S-C(=S)-Z-C(=S)-S-R, which provide polymers with the active RAFT groups in the center of the growing polymer chains (see Figure 3.1). The trithiocarbonate moiety may be used as inherent end-group label for UV/vis spectroscopy due to its weak absorbance band of the n-π transition at about 440 nm, and generally more practical, the strong absorbance band of the π-π* transition at about 310 nm. Furthermore, the $^1$H-NMR spectra of **CTA1-CTA5** exhibit a number of characteristic groups in both the Z and R fragments which should be resolvable in many polymer spectra (the details of $^1$H-NMR spectrum is reported in the Appendix, Figures A1-A5). For **CTA1**, the methylester signal at 3.8 ppm (-COO-$CH_3$) may serve to identify and quantify the R group in the polymers to be made, while the signals at 3.4 ppm (-S-$CH_2$-) and 0.85 ppm (terminal -$CH_3$) may be used to identify the Z group. The signal at about 4.9 ppm of the functional methine proton (-S-CH-COO-) of the R group will disappear in polymers, while the signal of resulting -C-CH(COO-)-C fragment around 2 ppm will be covered by signals of the polymer backbone. Nevertheless in dependence on the monomers used, the resulting new signal of the methine proton -S-CH-X of the growing end-group in vinyl polymers made from $CH_2$=CHX should appear in the 5 ppm range of the chemical shift for X = carboxyl or aryl, thus offering another potentially useful signal to quantify the number of active, Z-capped polymer chain ends. Analogous considerations apply to the $^1$H-NMR signals of **CTA2** (signal at 4.2 ppm (-COO-$CH_2$-)) to identify R, signals at 3.4 ppm (-S-$CH_2$-) and 0.85 ppm (terminal -$CH_3$) for Z), of **CTA3** (singlet at 7.3 ppm (=CH- aryl) to identify R, signals at 3.4 ppm (-S-$CH_2$-) and 0.9 ppm (terminal -$CH_3$) for Z), of **CTA4** (signal at 7.25 ppm (=CH- aryl) to identify R, singlet at 3.9 ppm (-S-$CH_2$-) for Z), and of **CTA5** (signals at 6.9 and 7.3 ppm (=CH- aryl) and at 3.86 ppm (-O-$CH_3$) to identify R, singlet at 4.01 ppm (-S-$CH_2$-) for Z). Of course, the usefulness of the discussed signals for end-group analysis will depend sensitively on the substituents of the monomers engaged. Still, the multiple options offer a good chance for the feasibility of this approach.

## 3.3 Attempted synthesis of triblock copolymers beginning with the inner hydrophilic PNIPAM block

First, the use of the bifunctional RAFT agents of type I, i.e. of **CTA1-CTA3**, was explored, starting with the polymerisation of **NIPAM**. This constellation should result in macroRAFT agents of **PNIPAM**, which can be extended by styrene to give the desired **BAB** amphiphilic triblock copolymers in only two polymerisation steps. The **PNIPAM** homopolymers were characterised with SEC, $^1$H-NMR and UV spectroscopy (**macroRAFTa-macroRAFTc**, Table 3.1).

**Table 3.1 Synthesis of macroRAFT agents from N-isopropylacrylamide in solution using RAFT agents CTA1 - CTA3.**

| Polymer | RAFT agent used | yield (%) | $M_n^{theo}$ a) | $M_n$ (NMR) b) | $M_n$ (NMR) c) | $M_n$ (UV) d) | $M_n^{app}$ (SEC) e) | PDI e) | Z/R f) |
|---|---|---|---|---|---|---|---|---|---|
| **macroRAFTa** | **CTA1** | 47 | 18200 | 26000 g) | 25000 | 26000 | 21000 | 1.30 | 1.05 |
| **macroRAFTb** | **CTA2** | 48 | 38000 | 36000 h) | 44000 | 48000 | 47000 | 1.30 | 0.82 |
| **macroRAFTc** | **CTA3** | 51 | 50700 | 49000 j) | 46000 | 50000 | 46000 | 1.25 | 1.06 |

a) calculated according to equation 1. b) by end-group determination, calculated from the $^1$H integral of a characteristic signal of the R-group and of the signal at 3.7–4.0 ppm of **PNIPAM**. c) by end-group determination, calculated from the $^1$H integral ratio of the signal at 3.3-3.5 ppm (-$CH_2$-S-) of the Z-group, and of the signal at 3.7–4.0 ppm of **PNIPAM**. d) by end-group determination in $CH_2Cl_2$ assuming full end-group conservation; calculated with the extinction coefficient of the RAFT agents engaged. e) in dimethylacetamide based on polystyrene standards. f) from $^1$H-NMR integration. g) signal at 3.6 ppm used (-$COOCH_3$). h) signal at 4.1 ppm used (-$COOCH_2$-). j) signal at 7.1 ppm used (=CH- aryl).

Figure 3.4 illustrates the $^{1}$H-NMR spectrum, which confirms the incorporation as well the retention of RAFT end-groups (more Figures A9-A10 are shown in the Appendix).

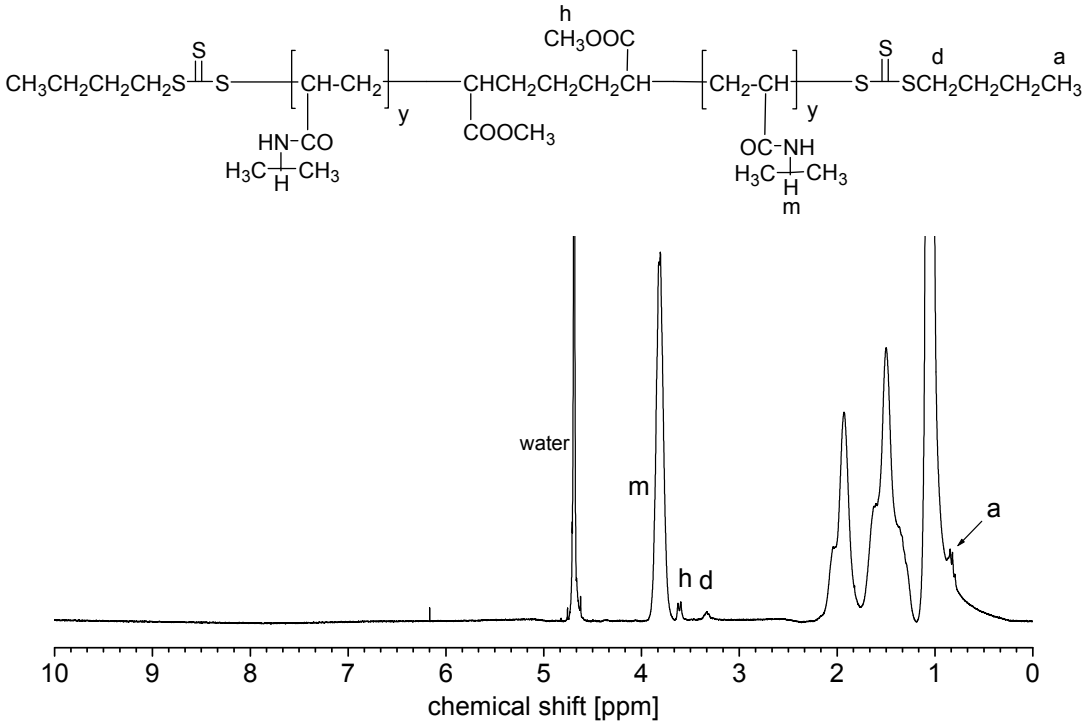


**Figure 3.4 $^{1}$H-NMR spectrum of PNIPAM-macroRAFTa in $D_2O$**

The solvent and polymer signals superpose the signals of the methine proton at the active chain ends at about 4.9 ppm (-SC(=S)S-CH-CON-) and the signal of the terminal -$CH_3$ moiety of the Z-group at 0.9 ppm (the signal is still recognizable in the spectra but cannot be resolved to enable quantification). Still, other functional protons of CTA derived fragments allow to identify and quantify both R and Z residues in all cases, and to calculate accordingly number average molar masses.

The comparison of the molar mass data from the various methods is instructive. First of all, the numbers obtained by the different methods agree well. Noteworthy, even the apparent molar masses derived from SEC analysis in dimethylacetamide seem to deviate not too strongly from the true molar masses (Figure 3.5). The polydispersity indices (PDI) were relatively low, being in the range of about 1.3. It is noted that the theoretically calculated molar mass values are lower than the experimentally determined ones. This discrepancy is attributed to the material losses during the purification of the polymers by dialysis. As the calculations are based on the assumption that the isolated yields reflect the true monomer conversions, the theoretically calculated values must be taken as lower estimates.

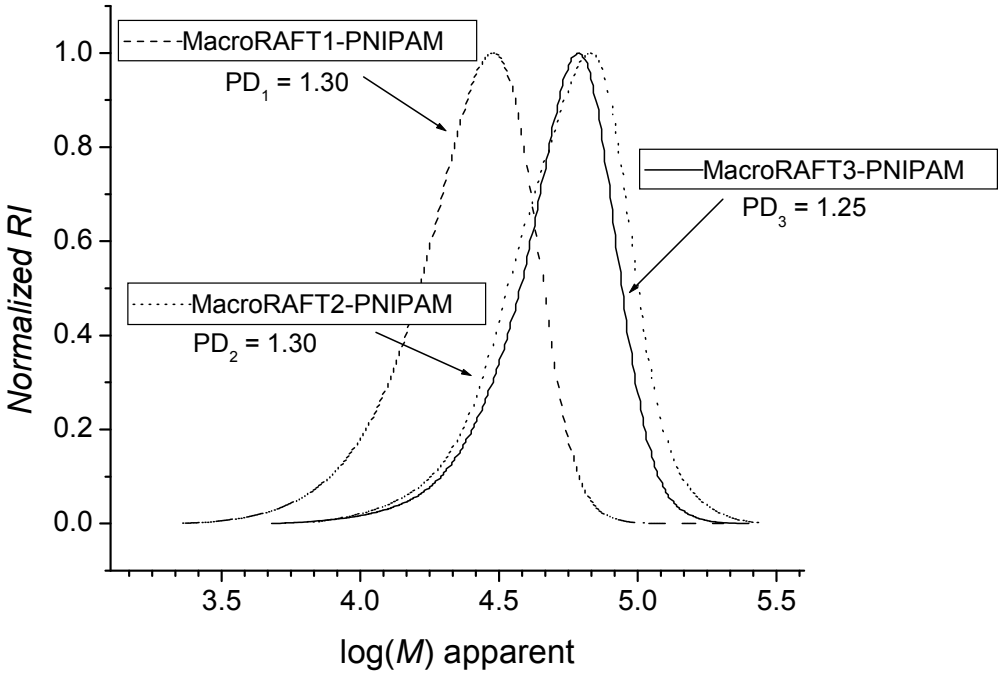


**Figure 3.5 Characterisation of PNIPAM bifunctional macroRAFT agents 1-3 by SEC.**

Considering the weakness of the end-group signals compared to the signals of the constitutional repeat unit, one may not overestimate the precision of the data derived from the NMR spectra. Nevertheless, the molar masses calculated from end-group analysis via signals of the R and of the Z groups agree closely, and thus the extent of end-group functionality must be high (see Z/R ratios in Table 3.1). All these findings demonstrate not only, that the new RAFT agents **CTA1-CTA3** are well suited for the controlled polymerisation of **NIPAM**. Moreover, they provide high quality macroRAFT agents for block copolymer synthesis.

Subsequently, all three **PNIPAM** samples (**macroRAFTa - macroRAFTc)** were employed as macroRAFT agents for chain-extension with styrene, in order to prepare amphiphilic triblock copolymers of the **BAB** type. AIBN was used as initiator and the ratio between [Monomer]/[RAFT]/[initiator] was kept for all **PNIPAM** macroRAFTs at 115 / 1 / 0.1 and at 115 / 0.8 / 0.1. Polymerisation trials were conducted at 65 °C, 70 °C and 90 °C. Although these are classical conditions for the RAFT polymerisation of styrene, virtually no monomer consumption was observed within 60 h of reaction. Obviously, the macroRAFT agents retard the polymerisation of styrene strongly. This was surprising, as successful block copolymerisation via RAFT of styrene and **NIPAM** has been reported for both monomer addition sequences.[223-227] Still, the reported examples of blocking styrene on **PNIPAM** macroRAFT agents used dithioesters. These are known to fragment more easily than

analogous trithiocarbonates.[191, 192] Therefore, the change from a growing acrylic polymer chain to a styrenic one may be difficult, as suggested by recent studies with styrene and dimethylacrylamide,[228] or butyl acrylate, respectively.[183, 229] As discussed in Chapter 2, this very sluggish blocking polymerisation could be due to a very slow initiation period,[183] due to the slow fragmentation of the intermediate radicals,[230] or could be explained by termination reactions of the intermediate radicals, e. g. by cross-termination between propagating and intermediate radicals.[231, 232] In any case, the findings showed that this route to block copolymers of **NIPAM** and styrene using the trithiocarbonate RAFT agents was not practical. Therefore, the opposite blocking sequence of **NIPAM** on polystyrene was investigated.

## 3.4 Synthesis of triblock copolymers beginning with the hydrophobic polystyrene (PS) block

In order to obtain **BAB** amphiphilic triblock copolymers with the hydrophobic **B** blocks at the macromolecules' ends, the bistrithiocarbonate RAFT agents of type I must be replaced by such of type II. Accordingly, RAFT agents **CTA4-5** and **CTA7** (Figure 3.1-3.2) were used to prepare polystyrene macroRAFT agents (Table 3.2).

**Table 3.2 Synthesis of macroRAFT agents from styrene in bulk using RAFT agents CTA1 - CTA7.**

| Polymer | RAFT agent used | yield (%) | $M_n^{theo}$ a) | $M_n$ (NMR) b) | $M_n$ (NMR) c) | $M_n$ (NMR) d) | $M_n^{app}$ (SEC) e) | PDI e) | Z/R f) |
|---|---|---|---|---|---|---|---|---|---|
| **macroRAFT1** | **CTA1** | 52 | 3110 | 3200 g) | 3300 | 3400 m) | 3280 | 1.13 | 0.94 |
| **macroRAFT2** | **CTA2** | 44 | 2500 | 3100 h) | 3200 | 3300 m) | 3180 | 1.17 | 0.94 |
| **macroRAFT3** | **CTA3** | 50 | 2900 | -j) | 3250 | 3200 m) | 2620 | 1.35 | |
| **macroRAFT4** | **CTA4** | 53 | 3070 | -j) | 3100 | | 3080 | 1.23 | |
| **macroRAFT5** | **CTA5** | 56 | 3280 | 3450 k) | 3300 | | 3360 | 1.21 | |
| **macroRAFT6** | **CTA6** | 54 | 2700 | 3400 l) | 3100 | 3400 m) | 3070 | 1.10 | 1.06 |
| **macroRAFT7** | **CTA7** | 40 n) | 2300 | -j) | 2100 | n.a. | 2300 | 1.21 | |

a) calculated according to equation 1. b) by end-group determination via $^1$H-NMR, calculated from the integral of characteristic signals of the initiating end-group (R-group). c) by end-group determination via $^1$H-NMR, calculated from the integral of the active end-group signal of -CH(aryl)-S-C(=S)-S-)-at 4.7-5.1 ppm. d) by end-group determination via $^1$H-NMR, calculated from the integral of characteristic signals the active end-group (Z-group). e) in dimethylacetamide based on polystyrene standards. f) ratio of active end-groups to initiating R groups from $^1$H-NMR integration g) superposed signals of R and Z groups at 3.2-3.6 ppm (-$COOCH_3$ and -S-C(=S)-S-$CH_2$-). h) signal at 4.1 ppm used (-$COOCH_2$-). j) overlapping signals, signals of R groups cannot be resolved. k) signal at 3.8 ppm ($CH_3O$-). l) signal at 7.6 ppm ($CF_3$-C=CHaryl). m) signal at 3.4-3.6 ppm of Z-group (-S-C(=S)-S-$CH_2$-). n) reaction time 18 h only

The polystyrene macroRAFT agents **macroRAFT4** and **macroRAFT7** were chain-extended with **NIPAM** to afford the desired **BAB** triblock copolymers. Typical examples of synthesis are shown in scheme 3.1. The trithiocarbonate functions are located in the middle of the block

copolymer chains following this strategy. For comparison, the analogous **ABA** amphiphilic triblock copolymers were prepared, too, using bistrithiocarbonates **CTA1-CTA3**, and the derived polystyrene macroRAFT agents **macroRAFT1-macroRAFT3**. The trithiocarbonate moieties are positioned for this geometry at the ends of the polymers (see Figures A11-A12 in the Appendix). The polymerisation of styrene was carried out in bulk thermally at 110 °C in the presence of RAFT agent without adding initiator. The ratio of monomer to RAFT agent was the same in all experiments with $[M]_0/[RAFT]_0$ = 48. After about 19 h of polymerisation, very similar yields were obtained for **CTA1-5** and **CTA7**. This implies that the reactivities of the different benzyl and secondary α-alkanoyl R-groups toward styrene are comparable. As for the **PNIPAM** macroRAFT agents, the polystyrene homopolymers were analyzed by with SEC and $^1$H-NMR spectroscopy (**macroRAFT1-5** and **macroRAFT7** (see Table 3.2).

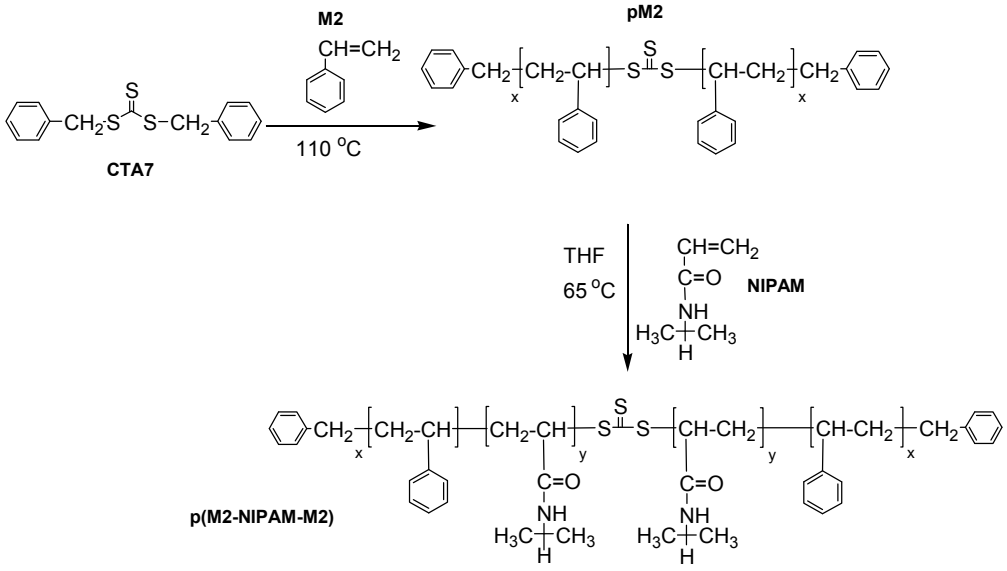


**Scheme 3.1 Synthetic pathway used to BAB block copolymers, exemplified by the series p(M2-NIPAM-M2).**

Again, several characteristic fragments of the respective Z and R groups of **CTA1-CTA5** may be identified and used for end-group analysis by $^1$H-NMR. Typical $^1$H-NMR spectrum of polystyrene macroRAFTs are exemplified in Figures 3.6-3.7 and Figures A11-A12 in the Appendix. Due to the low molar masses, characteristic signals of the R and/or Z groups may be seen in most cases. For instance, in addition to the characteristic polystyrene units at 7.6 ppm, the characteristic signal assigned to protons originating from the propyl of the R-groups of **CTA1** are also observed in Figure 3.5, as well as the signals at 0.89 and 3.6 ppm assigned to butyl protons originating from the Z-group of **CTA1**. It should also be noted that a new broad signal at about 5 ppm assigned to the -S-CH(aryl)-C methine proton of the

terminal styrene unit in the polymer is present. The signals of all these groups are sufficiently resolved to quantify them by integration.

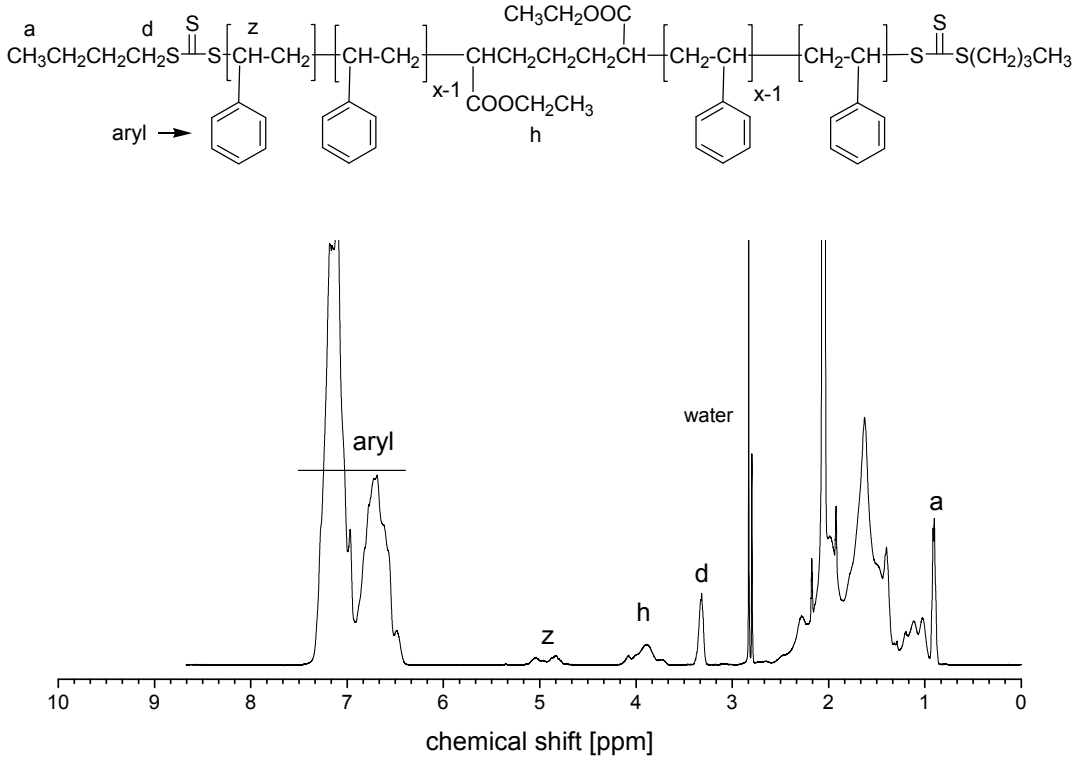


**Figure 3.6 $^{1}$H-NMR spectrum of polystyrene-macroRAFT 1 in acetone-$d_6$.**

Moreover, the experimentally determined molar masses by SEC match well the theoretically calculated ones. The molar mass distributions are relatively narrow, with PDI values between 1.15 and 1.25. All these findings indicate a well controlled polymerisation of styrene using all trithiocarbonate RAFT agents tested, which obviously have high transfer coefficients. The end-group determination by $^{1}$H-NMR spectroscopy gives also molar mass values which match very well with the SEC data (Table 3.2). In particular, characteristic proton signals for the Z or the R groups indicate molar ratios of Z/R which are close to 1. This demonstrates a high degree of end-group functionalisation.

Still, it was most puzzling that in the case of RAFT agents **CTA4** and **CTA5**, end-group analysis using the benzylic methine proton at the active chain ends at about 5 ppm (-SC(=S)S-CH<) for both CTAs and the signal of the terminal -$OCH_3$ moiety of the R-group at 3.8 ppm for **CTA5** (Figure 3.7) provided molar mass data matching with SEC analysis, whereas the expected signal at ca. 4 ppm of the methylene protons (-SC(=S)S-$CH_2$-$CH_2$-SC(=S)S-) of the Z-group gave only a very small integral (thus suggesting very high molar

masses) in the case of **CTA4**, or was even virtually absent in the case of **CTA5** (Figure 3.7 and Figure A12 in the Appendix).

This finding is surprising, as accordingly, the active chain ends of the type -$CH_2$-CHAryl-SC(=S)S-Z are fully preserved within experimental precision, while the Z-groups have apparently mostly disappeared (Figure 3.7).

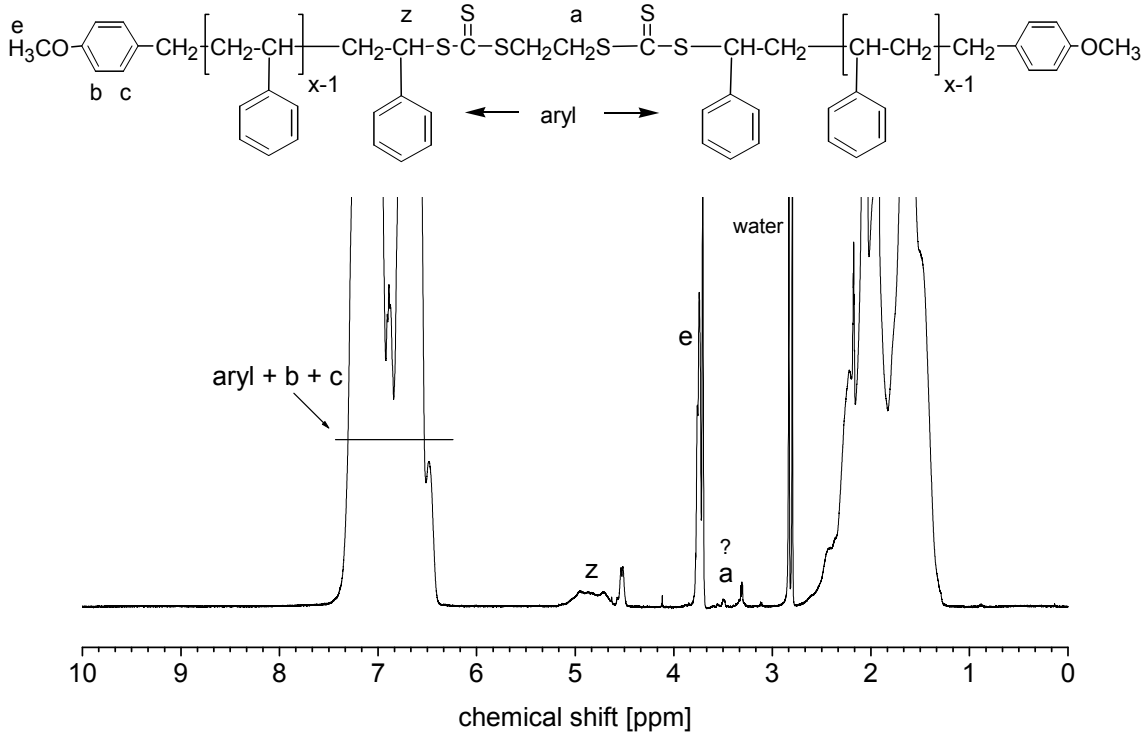


**Figure 3.7 $^1$H-NMR spectrum of polystyrene-macroRAFT 5 in acetone-$d_6$.**

This apparent contradiction is also reflected in the elemental analysis of the macroRAFT agents (Table 3.3). Whereas the sulfur content used for end-group analysis shows an excellent agreement with the molar mass data from SEC for **CTA1-CTA3**, and **CTA7**, the sulfur content is only about ⅔ of the value expected from SEC data in the case of **CTA4**, and only about the half in the case of **CTA5**. Combining the various analytical data, it must be concluded that the number of active RAFT end-groups is preserved, whereas the number of trithiocarbonate groups is reduced by up to 50%.

These apparent contradictory findings indicate an unexpected side reaction during polymerisation. In fact, the solutions obtained after precipitations are yellow coloured during the work up of the polymerisation mixtures containing **CTA4** and **CTA5**, pointing to soluble trithiocarbonates not attached to polymer. This was not observed for the work up of the

polymerisation mixtures when the other CTAs were used. Analysis of the contents of the yellow solutions by chromatography and $^1$H-NMR showed the formation of ethylenetrithiocarbonate in the course of the polymerisation. The combined analytical results indicate, that the bistrithiocarbonate group R-S-C(=S)-$CH_2$-$CH_2$-C(=S)-S-R active chain ends of the growing polymer blocks are converted to monotrithiocarbonate R-S-C(=S)-R chain ends by extrusion of cyclic ethylenetrithiocarbonate. The formed R-S-C(=S)-R chain ends are still bifunctional in the RAFT process, while the liberated ethylenetrithiocarbonate seems to be inert under the reaction conditions. Accordingly, the observed side reaction interferes with end-group functionalisation via the Z group, but not with the RAFT polymerisation process as such.

**Table 3.3 End-group analysis by elemental analysis.**

| Polymer | RAFT agent used | Elemental analysis (in %) | | | $M_n^{app}$ (EA) [a)] | $M_n^{app}$ (SEC) [c)] |
|---|---|---|---|---|---|---|
| **Type ABA** | | C | H | S | | |
| | | | | | | |
| **macroRAFT1** | **CTA1** | 84.17 | 7.56 | 6.33 | 3040 | 3180 |
| **macroRAFT2** | **CTA2** | 84.00 | 7.59 | 6.35 | 3030 | 3170 |
| **macroRAFT3** | **CTA3** | 86.20 | 7.53 | 6.78 | 2840 | 2860 |
| | | | | | | |
| **Type BAB** | | | | | | |
| **macroRAFT4** | **CTA4** | 89.03 | 7.51 | 3.94 | 4850 (2440)c) | 3080 |
| **macroRAFT5** | **CTA5** | 88.87 | 3.16 | 3.16 | 6170 (3050)c) | 3360 |
| **macroRAFT6** | **CTA6** | 83.27 | 6.08 | 6.08 | 2880 | 3070 |
| **macroRAFT7** | **CTA7** | 89.49 | 3.30 | 3.30 | 2570 | 2300 |

[a)] calculated from the sulfur content, assuming full end-group functionality. [b)] in 0.1 M LiBr/dimethylacetamide based on polystyrene standards. [c)] calculated assuming complete extrusion of ethylentrithiocarbonate

In fact, the thermal elimination of ethylenetrithiocarbonate was described for similar xanthogenates, though at much higher temperatures than 110°C,[233] while analogous dithiurams undergo a Čugaev-type elimination.[234] However, no thermal decomposition was found for **CTA4** and **CTA5** after 18 h annealing even at 130°C, so that this pathway can be ruled out in our case. Therefore, a hypothetical radical mechanism is proposed for the elimination of ethylenetrithiocarbonate as outlined in scheme 3.2.

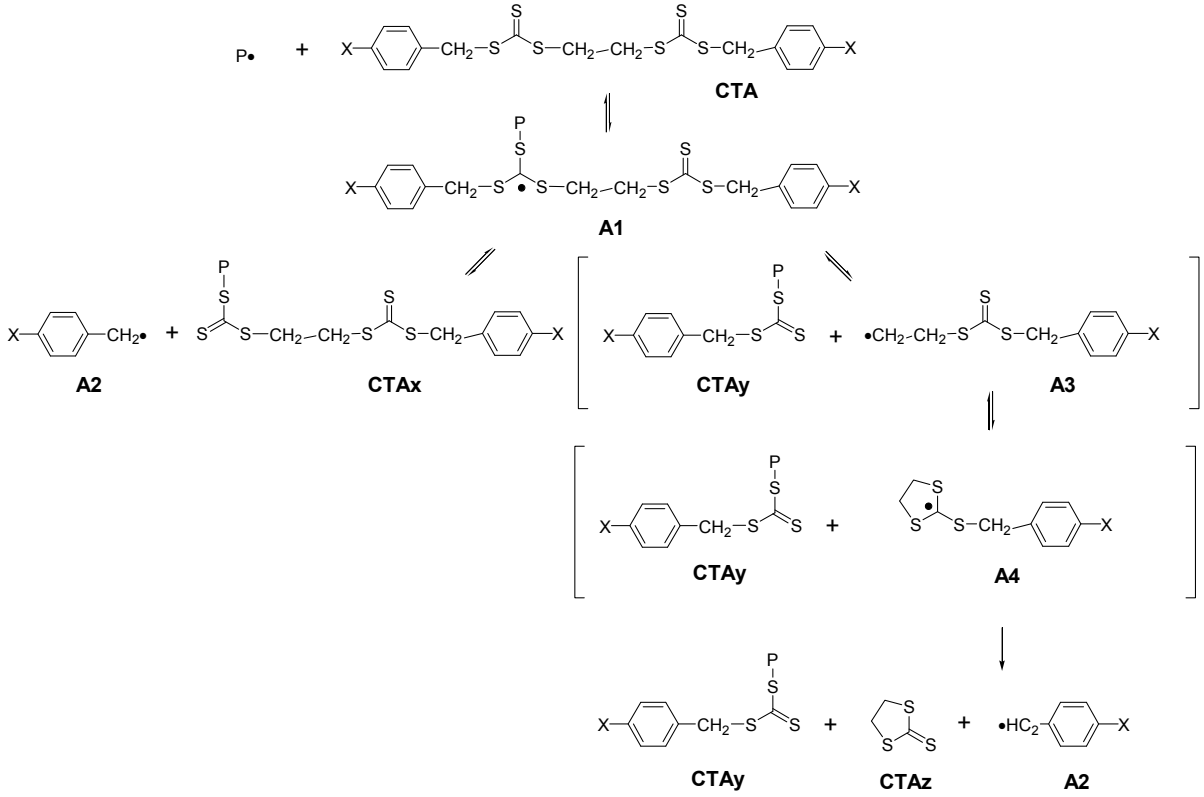


**Scheme 3.2 Possible fragmentation pathways for radical adducts of RAFT agents CTA4 and CTA5.**

Normally, the efficiency and rate of the fragmentation of the radical adduct on a trithiocarbonate increases in the order primary carbon substituent << secondary carbon substituent << tertiary carbon substituent, as well as *n*-alkyl substituent << benzyl substituent,[193] so that in non-symmetrical trithiocarbonates the roles of the reinitiating group R and of the Z group, that modulates the reactivity of the thiocarbonyl moiety, are unambiguously defined. This is the base of using appropriately substituted non-symmetrical trithiocarbonates as monofunctional RAFT agents.[189] However, for **CTA4** and **CTA5** this order seems not to apply. Though the first radical adduct **A1** in Scheme 1 would be a priori expected to follow fragmentation pathway to **CTAx** and the primary benzyl radical **A2**, the hypothesis is that for certain benzyl fragments, the alternative fragmentation to **CTAy** and the

primary alkyl radical **A3** can prevail, in dependence on the nature of the phenyl substituent X. While the non-symmetrical benzyl trithiocarbonate **CTAy** will act as bifunctional RAFT agent in a subsequent addition fragmentation cycle, the primary radical **A3** rearranges to radical **A4**, which in its turn eliminates the cyclic ethylenetrithiocarbonate **CTAz** to produce the benzyl radical **A2**. As the ring tension of the five-membered heterocycle **CTAz** is low, the hypothetical alternative pathway is enthalpically equivalent to the classical addition-fragmentation one, but is entropically favoured. It may be also possible that radical **A1** undergoes fragmentation via a concerted mechanism directly into **CTAy**, **CTAz** and **A2**, without forming the hypothetical intermediate radicals **A3** and **A4**. In any case, the bifunctionality of the RAFT system is maintained overall, though only one trithiocarbonate group is preserved in the growing polymer chains. Consequently, RAFT agent **CTA4** gives the same growing polymer chains as does the classical benzyltrithiocarbonate **CTA7**, whereas **CTA5** produces the same growing polymer chains as would do bis(4-methoxybenzyl)-trithiocarbonate.

In order to understand the elimination pathways, the RAFT agent **CTA6**, which was provided by J. Kristen[196] was used for comparison (Figure 3.2). The **CTA6** differs from **CTA4** and **CTA5** by the electron-withdrawing $-CF_3$ substituent of the benzyl moiety. For **CTA6**, the signals at 7.4 ppm and 7.6 ppm (=CH-aryl) may serve to identify and quantify the R group in the polymers to be made, while the signals at singlet at 3.6 ppm ($-S-CH_2-$) may be used to identify the Z group. As for the **CTA6**, the **polystyrene-macroRAFT6** was also provided by J. Kristen[196] for valuable comparative studies. A typical $^1$H-NMR spectrum of **polystyrene-macroRAFT6** is shown in Figure 3.8.

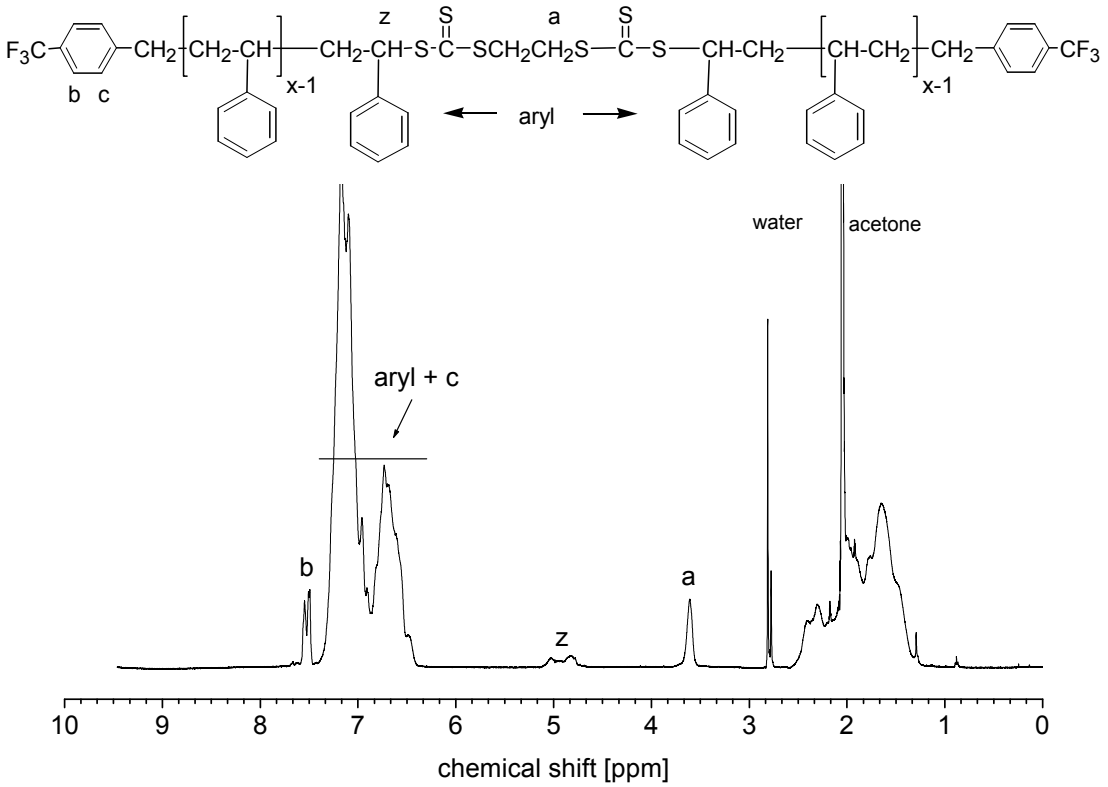


**Figure 3.8 $^{1}$H-NMR spectrum of polystyrene-macroRAFT 6 in acetone-$d_6$.**

Again, as a consequence of the low molar masses, characteristic signals of the R and/or Z groups could be seen. Besides the characteristic chemical shifts of the polystyrene repeating units, the characteristic signal at 7.6 ppm assigned to aromatic protons originating from the R-group of **CTA6** is also observed in Figure 3.8, as well as the signal at 3.6 ppm assigned to aliphatic protons originating from the Z-group of **CTA6**. While the singlet at 4.65 ppm ascribed to the -S-$CH_2$-aryl protons in **CTA6** disappeared in the polymers, a new broad signal at about 5 ppm assigned to the -S-CH(aryl)-C methine proton of the terminal styrene unit in the polymer is present.

Moreover, the molar masses determined by SEC match well the theoretically calculated ones. The molar mass distributions are relatively narrow, with PDI values of 1.1. All these findings indicate a well controlled polymerisation of styrene using **CTA6** as RAFT agent, which obviously has a high transfer coefficient. The molar mass determination by $^{1}$H-NMR spectroscopy matches very well with the SEC data (Table 3.2).

It is most instructive to compare the behaviour of series **CTA4-CTA6**. These RAFT agents all share the (-SC(=S)S-$CH_2$-$CH_2$-SC(=S)S-) fragment as common Z group, and all contain benzylic R groups. Still, they behave differently. When **CTA5** is used, the elimination of

ethylenetrithiocarbonate is complete after the polymerisation reaction, whereas it is only partial, when **CTA4** is engaged. In the case of **CTA6** however, no elimination was observed under identical reaction conditions. As once the polystyrene chain is initiated, all polymers have chemically identical trithiocarbonate end-groups, the differing reactivities must be related to the R groups. This implies that the chemical differentiation must take place when a radical attacks the original RAFT agent, but not later during degenerative chain transfer in the course of polymer growth. Hence, the reactivity for fragmentation after radical attack increases in the order: $CH_3O$-$C_6H_4$-$CH_2$-S-C(=S)S-alkyl < $C_6H_5$-$CH_2$-SC(=S)S-alkyl < $CF_3$-$C_6H_4$-$CH_2$-SC(=S)S-alkyl, $C_6H_5$-CH(alkyl)-S-C(=S)S-alkyl. Only in the first two cases, the fragmentation into a benzyl radical is slow enough to render the alternative fragmentation pathway competitive. The observed reactivities in the series **CTA4-CTA6** may be related to theoretical predictions that electron donating substituents destabilize radical adducts of thiocarbonyl compounds, whereas electron withdrawing substituents stabilize radical adducts.[190, 191] Accordingly, **CTA6** seems particularly suited as benzylic RAFT agent, as it combines enhanced reactivity in the RAFT process with easy-to-identify R and Z fragments for end-group analysis (cf. Table 3.3).

Knowing the high extent of bifunctionality of the macroRAFT agents obtained, **macroRAFT1-5** and **macroRAFT7** were engaged in chain extension reactions with **NIPAM** in THF solution at 70 °C up to high conversions (Table 3.4).

Using this monomer addition sequence, all polystyrenes were successfully chain-extended to give the corresponding **ABA** and **BAB** triblockcopolymers, as already shown qualitatively by the SEC traces (Figure 3.9). The eluograms are monomodal, with no evidence of any residual polystyrene homopolymer. The SEC traces are shifted to shorter elution times, as should be expected for increased molar masses, and indicate relatively low polydispersities between 1.4 and 1.5. Still, the tailing of the signals of the block copolymers to longer elution times points to interactions with the column material superposing the separation by size exclusion. This renders the formally obtained numbers for the molar masses questionable. Unfortunately, end-group analysis by $^1$H-NMR, as done for the macroRAFT agents, could neither be used to determine the absolute molar masses of the triblock copolymers obtained, as the end group signals were much too weak and/or not sufficiently resolved in the spectra to allow quantitative end group analysis. Therefore, other methods were looked for to determine the molar mass of the block copolymers (Table 3.4).

**Table 3.4 Synthesis of symmetrical ABA and BAB triblock copolymers from polystyrene macroRAFT agents and PNIPAM.**

| Block Copolymer | RAFT agent used | yield (%) | $M_n$ (UV) [a] | $M_n$ (NMR) [b] | $M_n^{app}$ (SEC) [c] | PDI [c] |
|---|---|---|---|---|---|---|
| **Type ABA** | | | | | | |
| **p(NIPAM-M2-NIPAM)-1** | **macroRAFT1** | 90.0 | 26000 | 27000 | 23000 | 1.38 |
| **p(NIPAM-M2-NIPAM)-2** | **macroRAFT2** | 87.0 | 25000 | 26000 | 23000 | 1.40 |
| **p(NIPAM-M2-NIPAM)-3** | **macroRAFT3** | 74.0 | 24000 | 21000 | 15000 | 1.33 |
| **Type BAB** | | | | | | |
| **p(M2-NIPAM-M2)-4** | **macroRAFT4** | 83 | 24000 | 22000 | 23000 | 1.36 |
| **p(M2-NIPAM-M2)-5** | **macroRAFT5** | 70 | 29000 | 30000 | 16000 | 1.32 |
| **p(M2-NIPAM-M2)-6** | **macroRAFT6** | 95 [d] | 42000 | 43000 | 14000 | 1.80 |
| **p(M2-NIPAM-M2)-7** | **macroRAFT7** | 73 | 23000 | 27000 | 16000 | 1.34 |

[a] calculated from the absorbance at 260 nm in $CH_2Cl_2$, using the extinction coefficient of 2.14 L·g-1·cm-1 reported for pure PS.[235] [b] from integral ratio of signal at 4 ppm (-CH- of **PNIPAM**), and signal group at 6-8 ppm (superposed aromatic protons of **PS** and -NH- of **PNIPAM**), assuming that the molar mass of the **PS** block corresponds to the one of the macroRAFT agent used. [c] in 0.1 M LiBr/dimethylacetamide, based on polystyrene standards.

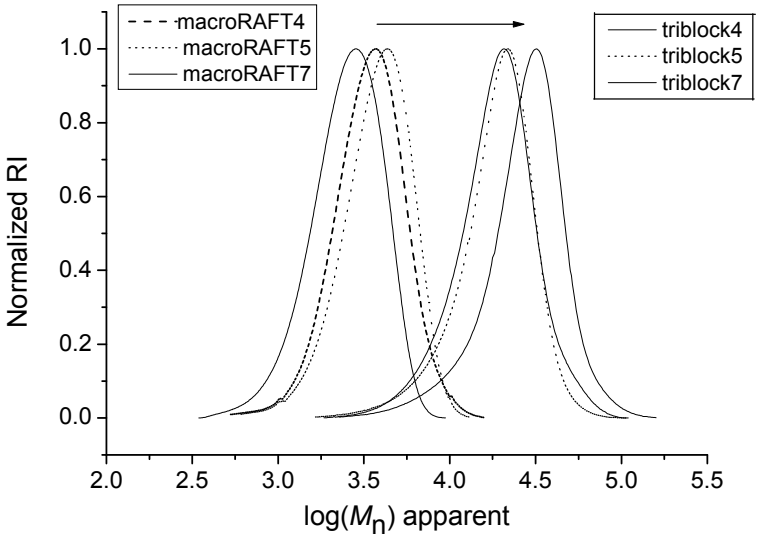


**Figure 3.9 Characterisation of polystyrene bifunctional macroRAFT agents and the derived triblock copolymers with NIPAM.**

Conveniently, absolute molar masses of binary block copolymers can be derived from the elemental analysis of the copolymer composition, if the size of the first block can be accurately determined, and under the - generally granted - premise that the size of the first block is preserved in the block copolymer. However, the hydrophobic polystyrene blocks were designed to be much smaller than the hydrophilic **PNIPAM** blocks in order to provide direct solubility in water.

Therefore, elemental analysis data cannot provide good accuracy, in particular when considering the hygroscopic character of the copolymers. FT-IR spectroscopy proved unsatisfactory, too. The presence of polystyrene in the copolymers is qualitatively demonstrated by the characteristic band at 710 $cm^{-1}$, but the **PNIPAM** bands are so overwhelming in the spectra that quantitative analysis was not possible.

Though often used to analyze copolymer composition, $^1$H-NMR spectroscopy was struck by complications, too. Quantitative analysis by $^1$H-NMR asks for a common good NMR solvent for both blocks, which does not cover the characteristic polymer signals, in order to enable meaningful integration of the signals. Acetone-$d_6$ and DMSO-$d_6$ were well suited for this purpose. The $^1$H-NMR spectra of the **ABA** and **BAB** triblock copolymers confirm qualitatively the presence of both polystyrene and **PNIPAM** blocks, as exemplified in Figure 3.10.

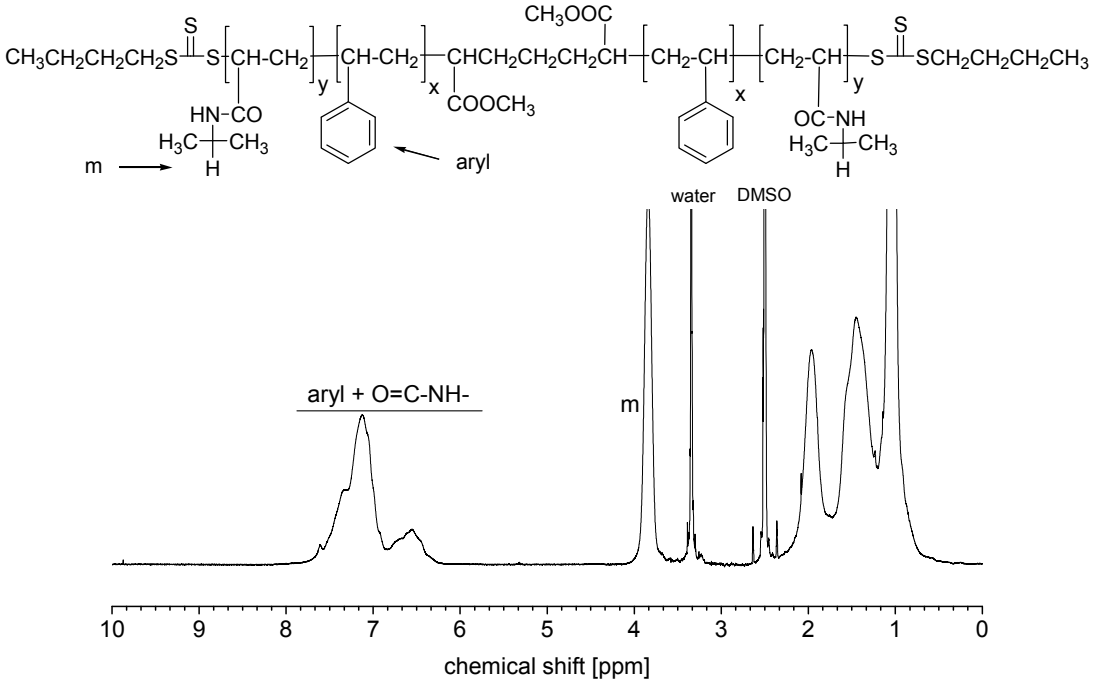


**Figure 3.10 $^1$H-NMR spectrum of poly(NIPAM-M2-NIPAM)-1 in DMSO-$d_6$.**

Characteristic resolved signals are found at 4 ppm for the methine proton of **PNIPAM**, and a complex signal group between 6 and 8 ppm due to the amide proton of **PNIPAM** and the aromatic protons of polystyrene. However in this case, the superposition of the intense signal of the amide proton of **PNIPAM** and of the relative weak signal of the aromatic protons of polystyrene renders the quantitative analysis imprecise: small errors in the integral lead to large deviations in the calculated copolymer composition. Moreover, the integral of the amide proton may be not reliable due to a possible partial H/D exchange, as some water is always present because of the hygroscopy of the long **PNIPAM** block. Indeed, storage of samples resulted in a continuous decrease of the intensity of the signal group at 6-8 ppm. Therefore, molar masses were best calculated from the UV-absorbance data, exploiting the characteristic UV-band of polystyrene at 260 nm.[235] Nevertheless, the compositional data derived from the NMR spectra, do agree reasonably well in most cases (Table 3.4). The data complied in Table 3.4 demonstrate, that all macroRAFT agents prepared enable the successful preparation of the block copolymers, also in the case of **macroRAFT4** and **macroRAFT5** despite of the elimination of ethylenetrithiocarbonate in the early stage of the copolymer synthesis.

## 3.5 Synthesis of triblock copolymers BAB using RAFT agent CTA7

To avoid the inhibition effects observed during the polymerisation of styrene when using **macroRAFT agents CTAa-CTAc** (section 3.3), and any problem connected with the extrusion of ethylenetrithiocarbonate during the bulk polymerisation of styrene with RAFT agents **CTA4-5** (section 3.3), the RAFT agent **CTA7** was employed to extend the studies, toward **BAB** systems, in particular toward block copolymers with a long thermo-sensitive hydrophilic middle block and two strongly hydrophobic outer blocks. While keeping the chemical nature of the hydrophilic block **A** constant by using always **PNIPAM**, the nature and the lengths of the hydrophobic **B** blocks were varied, using poly(4-*tert*-butyl styrene) **pM1**, polystyrene **pM2**, poly(3,5-dibromo benzyl acrylate) **pM3**, poly(2-ethylhexyl acrylate) **pM4**, and poly(octadecyl acrylate) **pM5**. This variation was aimed at exploring the influence of the hydrophobic block on the phase transition as well as on the gel behaviour of the amphiphilic **BAB** copolymers (See Chapters 4-5).

As described in section 3.3, the synthesis of the amphiphilic **BAB** triblock copolymers via the RAFT process starts best by preparing the respective **B** homopolymers, which in a second step are chain extended to **BAB** triblock copolymers. The bifunctional RAFT agent dibenzyltrithiocarbonate (**CTA7**) was used to prepare short hydrophobic polymers from 4-*tert*-butyl styrene (**M1**), styrene (**M2**), 3,5-dibromo benzyl acrylate (**M3**), 2-ethyl hexyl acrylate (**M4**) and octadecyl acrylate (**M5**), which all bear a bifunctional trithiocarbonate moiety in their center. These polymers were employed subsequently as macroRAFT agents for chain extension with **NIPAM**, to produce **BAB** triblock copolymers in overall two polymerisation steps (Scheme 3.5). The chain extension was conducted such that the triblock copolymers dispose of hydrophilic middle block **A** that is much longer than the hydrophobic end blocks **B**. The content of the hydrophobic blocks, with molar masses ranging from 2800 to 22000, was thus between 8 and 13 wt%. The resulting homo- and copolymers were characterised by SEC, $^1$H-NMR and UV spectroscopy (Table 3.5).

SEC demonstrates the synthesis of homo- and block copolymers with a monomodal and narrow molar mass distribution, but due to the calibration with polystyrene standards, the absolute molar mass values are only apparent except for macroRAFT agents **pM2**. Due to characteristic signals of the end-groups derived from the R- and Z-fragments of **CTA7**, both $^1$H-NMR and UV spectroscopy allow to calculate the molar masses of the hydrophobic blocks used as macroRAFT agents. The analysis by UV-spectroscopy is based on the intense $\pi$-$\pi$ band of the C=S trithiocarbonate group. Though less sensitive, end group analysis of the molar mass is alternatively possible in these samples of relatively low molar mass via determination of the sulfur content (Table 3.5).

**Table 3.5 Synthesis of symmetrical BAB triblock copolymers with PNIPAM as hydrophilic middle block.**

| Polymer | RAFT agent used | yield (%) | $M_n^{theo}$ [a] | $M_n$ (NMR) | $M_n$ (UV) | $M_n$ (EA) | $M_n$ (SEC) [b] | PDI [b] |
|---|---|---|---|---|---|---|---|---|
| **PNIPAM-1** | CTA3 | 56 | 56400 | | 66000 | | 35000 | 1.5 |
| **$p(M1)_{17}$** | CTA1 | 48 | 2700 | 3200 [c] | 2800 [d] | 2900 [e] | 2440 | 1.3 |
| **$p(M1)_{34}$** | CTA1 | 46 | 4900 | 5900 [c] | 5400 [d] | 6500 [e] | 5500 | 1.2 |
| **p(M1-NIPA-M1#17)** | $p(M1)_{17}$ | 80 | 50800 | 34000 [f] | | 56000 [i] | 20000 | 1.6 |
| **p(M1-NIPA-M1#34)** | $p(M1)_{34}$ | 82 | 54600 | 60000 [f] | | 54500 [i] | 23600 | 1.7 |
| **$p(M2)_{48}$** | CTA1 | 50 | 5000 | 5600 [c] | 5400 [d] | | 5000 | 1.2 |
| **$p(M2)_{61}$** | CTA1 | 55 | 7800 | 7000 [c] | 6600 [d] | | 6400 | 1.2 |
| **$p(M2)_{81}$** | CTA1 | 48 | 9900 | 8200 [c] | 8400 [d] | | 8400 | 1.2 |
| **$p(M2)_{89}$** | CTA1 | 43 | 11000 | 9600 [c] | 9500 [d] | | 9300 | 1.2 |
| **$p(M2)_{119}$** | CTA1 | 49 | 15000 | 11500 [c] | 12600 [d] | | 12400 | 1.2 |
| **p(M2-NIPA-M2#48)** | $p(M2)_{48}$ | 90 | 59000 | 69000 [f] | 67400 [g] | 51000 [i] | 19600 | 1.4 |
| **p(M2-NIPA-M2#61)** | $p(M2)_{61}$ | 86 | 58000 | 77000 [f] | 66500 [g] | 51100 [i] | 16000 | 1.4 |
| **p(M2-NIPA-M2#81)** | $p(M2)_{81}$ | 100 | 60000 | 106000 [f] | 98000 [g] | 75800 [i] | 21200 | 1.3 |
| **p(M2-NIPA-M2#89)** | $p(M2)_{89}$ | 88 | 62100 | 84000 [f] | 82400 [g] | 64000 [i] | 18100 | 1.4 |
| **p(M2-NIPA-M2#119)** | $p(M2)_{119}$ | 72 | 55600 | 98000 [f] | 91900 [g] | 84000 [i] | 21000 | 1.4 |
| **$p(M3)_{16}$** | CTA1 | 60 | 3300 | | 5000 [d] | 6000 [e] | 2200 | 1.3 |
| **p(M3-NIPA-M3#16)** | $p(M3)_{16}$ | 87.5 | 38000 | 40000 [f] | | 48000 [i] | 19800 | |
| **$p(M4)_{21}$** | CTA1 | 65 | 3500 | 4200 [c] | 3900 [d] | 3900 [e] | 3700 | 1.2 |
| **$p(M4)_{35}$** | CTA1 | 62 | 6500 | 7000 [c] | 6400 [d] | 6700 [e] | 5500 | 1.2 |
| **$p(M4)_{50}$** | CTA1 | 67 | 11000 | 10600 [c] | 9300 [d] | 12000 [i] | 6100 | 1.2 |
| **$p(M4)_{60}$** | CTA1 | 68 | 14000 | 19400 [c] | 11000 [d] | 15700 [i] | 6000 | 1.2 |
| **p(M4-NIPA-M4#21)** | $p(M4)_{21}$ | 92 | 59100 | 47000 [h] | | | 22000 | 1.7 |
| **p(M4-NIPA-M4#35)** | $p(M4)_{35}$ | 92 | 61600 | 77000 [h] | | | 23000 | 1.6 |
| **p(M4-NIPA-M4-50)** | $p(M4)_{50}$ | 96 | 66700 | 88000 [h] | | | 21000 | 1.9 |
| **p(M4-NIPA-M4-60)** | $p(M4)_{60}$ | 94 | 67400 | 87000 [h] | | | 23000 | 1.8 |
| **$p(M5)_{11}$** | CTA1 | 70 | 3800 | 3500 [j] | 3600 [d] | | 4600 | 1.2 |
| **$p(M5)_{36}$** | CTA1 | 59 | 11000 | 12100 [j] | 11700 [d] | | 9100 | 1.3 |
| **$p(M5)_{54}$** | CTA1 | 78 | 16000 | 17800 [j] | 22300 [d] | | 10000 | 1.3 |
| **p(M5-NIPA-M5#11)** | $p(M5)_{11}$ | 74 | 48000 | 35000 [h] | | 53000 [i] | 20000 | 1.5 |
| **p(M5-NIPA-M5#36)** | $p(M5)_{36}$ | 84 | 62000 | 100000 [h] | | 150000 [i] | 20000 | 1.9 |
| **p(M5-NIPA-M5#54)** | $p(M5)_{54}$ | 84 | 73000 | 140000 [h] | | 290000 [i] | 18000 | 2.3 |

calculated according to equation 1. [b] in dimethylacetamide based on polystyrene standards. [c] by end-group determination via $^1$H-NMR, using the integral of the signal of the terminal (-CH-SC(=S)S-) methine group. [d] by end-group determination in $CH_2Cl_2$ assuming full end-group conservation; calculated with the extinction coefficient of the RAFT agent engaged ($\lambda$=309 nm, $\varepsilon$=17000 L mol$^{-1}$ cm$^{-1}$ in $CH_2Cl_2$). [e] by end-group determination using the S content. [f] from integral ratio of signal at 4 ppm (-CH- of **PNIPAM**), and signal group

at 6-8 ppm (superposed aromatic protons of **pM2** and -NH- of **PNIPAM**), assuming that the molar mass of the **pM2** block corresponds to the one of the macroRAFT agent used. [g] calculated from the absorbance at 260 nm in $CH_2Cl_2$, using the extinction coefficient of $\varepsilon$ =2.14 $L \cdot g^{-1} \cdot cm^{-1}$ reported for pure **pM2** [235 h] from integral ratio of signal at 4 ppm (-CH- of **PNIPAM**), and signal group at 0.9 ppm (terminal $-CH_3$ groups of the acrylate monomers), assuming that the molar mass of the hydrophobic blocks corresponds to the one of the macroRAFT agent used. [i] from C/N ratio. [j] by end-group determination via $^1$H NMR, using the integral of the signal of the R group.

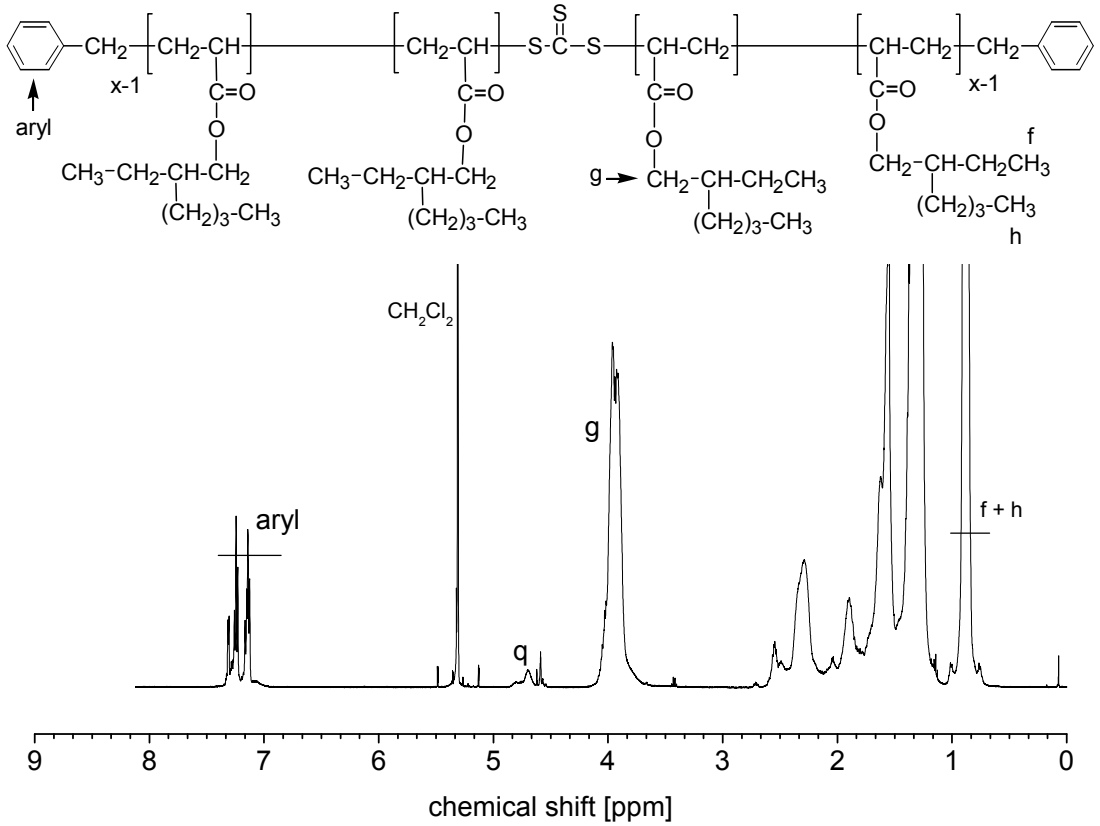


**Figure 3.11 $^1$H-NMR spectrum of p(M4)$_{21}$ macroRAFT CTA in $CD_2Cl_2$.**

Figure 3.11 (above) illustrates exemplarily the $^1$H-NMR spectrum of the macroRAFT agent **p(M4)$_{21}$** which confirms the incorporation and conservation of the RAFT end-groups, as needed for the chain extension reaction. The signals at about 4.7-4.8 ppm (indicated as "q") are assigned to the methine protons of the active chain ends, namely of the protons -CH(COOR)-S-C(=S)-S- in **pM4**. The complex form of the signals is attributed to the atactic nature of the polymers. The comparison with the characteristic signals of the benzylic R-group of **CTA1**, which constitutes the other regular end-group, assuming ideal RAFT

behaviour, is possible in the polyacrylates **pM4** and for **pM5** (see Figure A11 in the Appendix). The close contents of both end-groups, deriving from the R- and Z-groups, and thus of the similar molar masses calculated by end group determination indicate the high functionality of the macroRAFT agents used in the preparation of the block copolymers (Table 3.5). This comparison is not possible for polymers **pM1**, **pM2** and **pM3**, because the signals of the aromatic groups in the repeat units superpose the weak R-group signal. However, the good agreement of the molar mass values calculated by end-group analysis via UV-spectroscopy and the ones determined by SEC in the case of **pM2**, or the values theoretically calculated from the ratio monomer/**CTA1** and the polymer yield in the case of **pM1** and **pM3**, indicate a high functionality of these macroRAFT agents, too.

The SEC traces of the polymers after the chain extension reaction with **NIPAM** are all shifted to shorter elution times, as to be expected for increased molar masses. The elugrams are monomodal with no evidence of residual macroRAFT agent. Accordingly, the hydrophobic macroRAFT agents were successfully chain-extended to give the corresponding block copolymers, see for instance Figure 3.12.

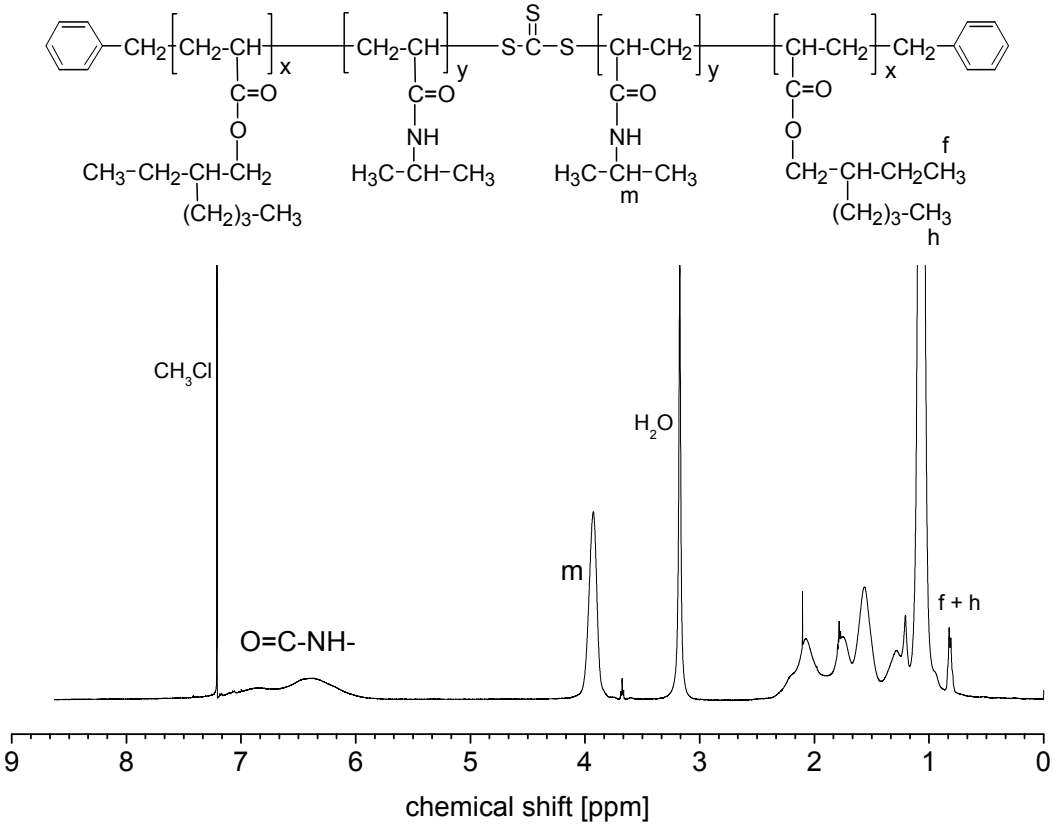


**Figure 3.12 $^{1}$H-NMR spectrum of p(M4-M6-M4) macroRAFT CTA in $CD_2Cl_2$.**

Still, the tailing of the signals of the block copolymers to longer elution times points to interactions with the column material superposing the separation by size exclusion. Therefore, the formally obtained numbers for the molar masses and polydispersities are highly questionable. As end-group signals were much too weak and/or not sufficiently resolved to allow a reliable quantitative analysis, absolute molar masses of the block copolymers were derived from the analysis of the copolymer composition from the $^1$H-NMR spectra (Table 3.5), under the premise that the size of the macroRAFT agent is preserved in the block copolymer. Additionally, copolymer composition and molar masses were calculated from the UV-absorbance data in the series **p(M2-NIPAM-M2)**, exploiting the characteristic UV-band of polystyrene at 260 nm.

The calculated compositions agree reasonably well with the values derived from the NMR spectra (Table 3.5). It should be pointed out that the determination of the molar mass of the block copolymers carrying the hydrophobic **pM4 and pM5** blocks is not straightforward by $^1$H-NMR (See Figure 3.12 and Figures A14-A15 in the Appendix). This is due to the camouflage of the ester protons signal (-COOCH$_2$-) of **pM4** or **pM5** of by the signal of **PNIPAM** originating from the methine proton (–CH). However, from the integrals of the signal groups at 0.89 ppm characteristic for the methyl proton (CH$_3$-) of the **pM4** and **pM5** repeat units and for the **PNIPAM** protons at 6.4 to 7.6 ppm (characteristic for the CONH< proton), one could estimate the molar mass of the block copolymers obtained.

## 3.6 Synthesis of polystyrene-d$_8$ and BAB block copolymers using RAFT agent CTA7

As described in section 3.5, the well established bifunctional RAFT agent **CTA7** was used to prepare the triblock copolymer. The initial thermal polymerisation of styrene-d$_8$ in the presence of the **CTA7** (the ratio of monomer to RAFT agent was set $\mathbf{[M]_0/[RAFT]_0}$ = 45) was conducted to moderate conversions only, in order to guarantee a high degree of end-group functionality of the polymer formed,[236, 237] and thus to produce a highly efficient macroRAFT agent. The $^1$H-NMR spectrum of **P(S-d$_8$) macroRAFT7** exhibits mainly the signals of the initiating benzyl groups at both chain ends, but due to the high degree of deuteration of the styrene-d$_8$ (99%), no other information can be deduced by $^1$H-NMR (Figure 3.13)

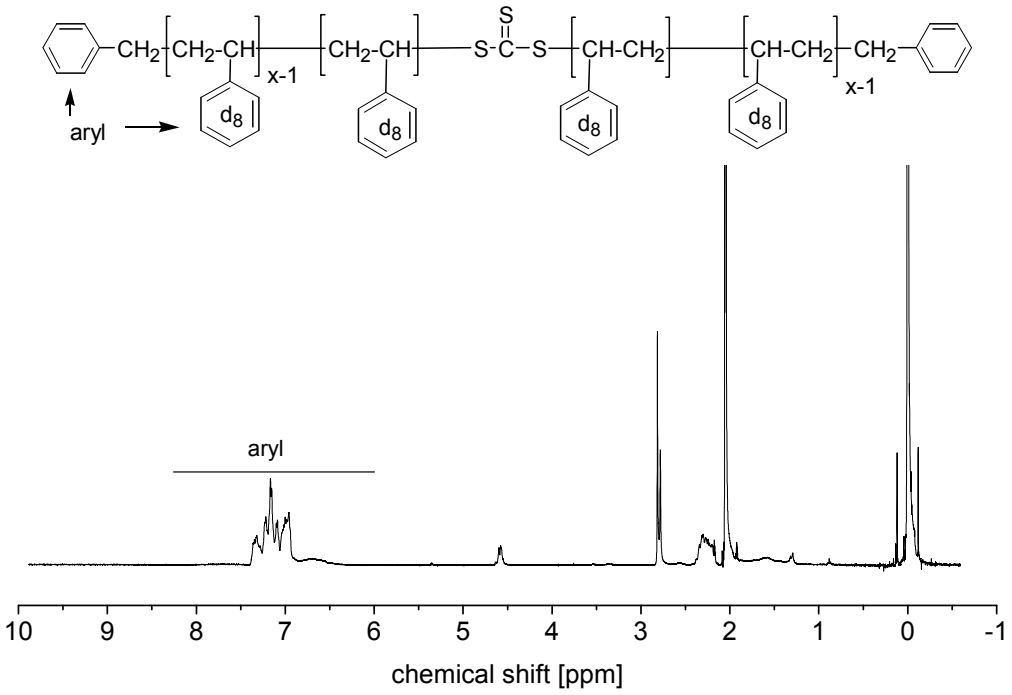


**Figure 3.13 $^{1}$H-NMR spectrum of P(S-d$_8$)$_{20}$-macroRAFT CTA in acetone-d$_6$.**

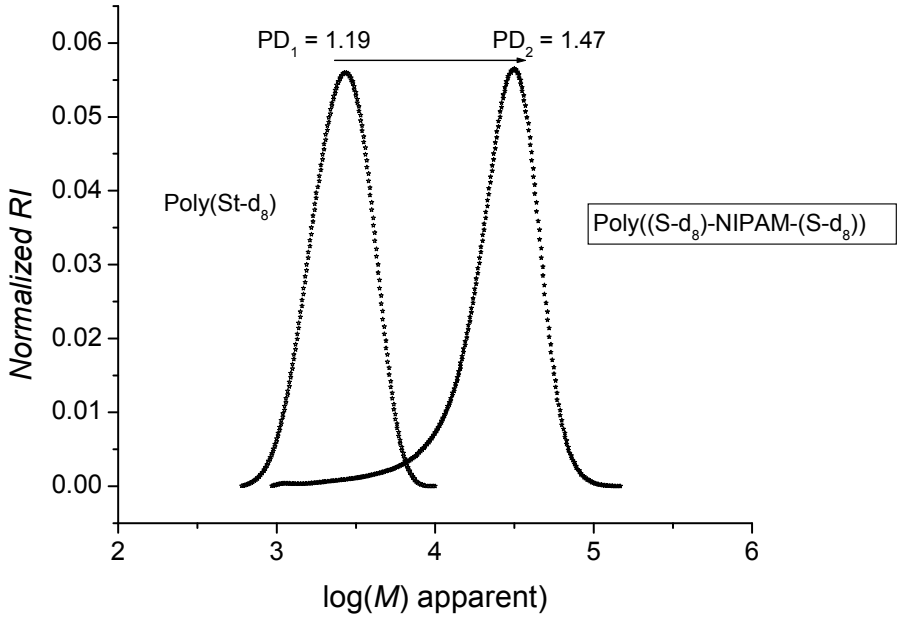


**Figure 3.14 SEC elugrams of P((S-d$_8$)-NIPAM-(S-d$_8$)) and its precursor P(S-d$_8$) macroRAFT.**

The analysis of **P(S-d$_8$) macroRAFT7** by SEC shows a monomodal, relatively narrow molar mass distribution, with a number average molar mass $M_n$ of 2300, and a polydispersity index PDI of 1.19 (Figure 3.14 above). Assuming an ideal RAFT mechanism, the theoretically expected number average molar mass $M_n^{theo}$ is calculated as 2300 using the equation (1). The

good agreement between these values demonstrates the good control over the molar mass of **P(S-$d_8$) macroCTA**, as needed for the synthesis of the triblock copolymers (Table 3.6).

**Table 3.6 Synthesis of polystyrene-$d_8$ using RAFT agent CTA7 and BAB containing PNIPAM as hydrophilic middle block.**

| Polymer | RAFT agent used | yield (%) | $M_n^{theo}$ [a] | $M_n$ (UV) [b] | $M_n$ (EA) [c] | $M_n$ (SEC) [d] | PDI [d] |
|---|---|---|---|---|---|---|---|
| **P(S-$d_8$#20) macroRAFT** | **CTA7** | 40 | 2300 | | | 2300 | 1.19 |
| **p(S-$d_8$-NIPAM#387-S-$d_8$)** | **PS-$d_8$#20** | 80 | 35000 | 46300 | 55700 [1] | 19700 | 1.47 |
| **p(S-$d_8$-NIPAM#387-S-$d_8$)** | **PS-$d_8$#20** | 89 | 30000 | 36000 | 46300 [1] | 16000 | 1.44 |
| **p(S-$d_8$-NIPAM#254-S-$d_8$)** | **PS-$d_8$#20** | 99 | 22000 | 27000 | 29000 [1] | 12000 | 1.45 |

[a] calculated according to equation 1, assuming100% blocking efficiency and that the molar mass of the **P(S-$d_8$)** block corresponds to the one of the macroRAFT agent **P(S-$d_8$)** used. [b] from the absorbance at 262 nm, assuming that the molar mass of the **P(S-$d_8$)** block corresponds to the one of the macroRAFT agent used and using the extinction coefficient of 2.14 $L \cdot g^{-1} \cdot cm^{-1}$ reported for pure polystyrene.[235] [c] Polymerisation calculated from C/N ratio conditions. [d] in dimethylacetamide based on polystyrene standards

Subsequently, the polystyrene-$d_8$ was employed as bifunctional macroRAFT agent for chain-extension with **NIPAM**, in order to prepare amphiphilic triblock copolymers of the **BAB** type. The successful chain extension of the **P(S-$d_8$) macroRAFT7** agent by **NIPAM** is qualitatively shown by $^1$H-NMR. The spectrum shown in Figure 3.15 confirms the incorporation of **NIPAM** into the polymer. Both the signals at 4 ppm characteristic for the CON-CH< methine proton and at 6.4 to 7.6 ppm characteristic for the CONH< amide proton evidence the incorporation of **NIPAM** in large quantities. The benzyl end-groups which were visible in the spectrum of **P(S-$d_8$) macroRAFT7** are camouflaged by the much larger signal of the amide protons.

In agreement, the FT-IR-spectrum corresponds very closely to the spectrum of pure **PNIPAM**, as the polystyrene block is much smaller than the **PNIPAM** block, and its characteristic IR bands are a priori much weaker than e. g. the dominating carbonyl bands of **PNIPAM**. The successful chain extension is further corroborated by SEC. The polymer obtained shows a monomodal molar mass distribution with a PDI value of 1.47, and an apparent number average molar mass of $M_n$(SEC) = 19700 based on calibration with polystyrene (Figure 3.14 and Table 3.6).

The determination of the absolute mass of the triblock copolymer is inherently difficult and inaccurate, as several problems are superposed. This comprises the amphiphilic character of the block copolymer with a strong tendency to aggregate in solution, the unfavourable combination of a very large block, namely of **PNIPAM**, with a very short one, namely of polystyrene-$d_8$, as well as its hygroscopy. Circumventing the problems due to humidity uptake, the C/N ratio from elemental analysis enables in principle to calculate the absolute molar mass, when assuming that the molar mass of the polystyrene-$d_8$ block of 2300 is preserved in the block copolymer. However due to the small size of the polystyrene block, the approach can give only an approximate value. The thus - formally - calculated value of 55700 g/mol for the block copolymer implies a number average degree of polymerisation of 500 of the of **PNIPAM** block.

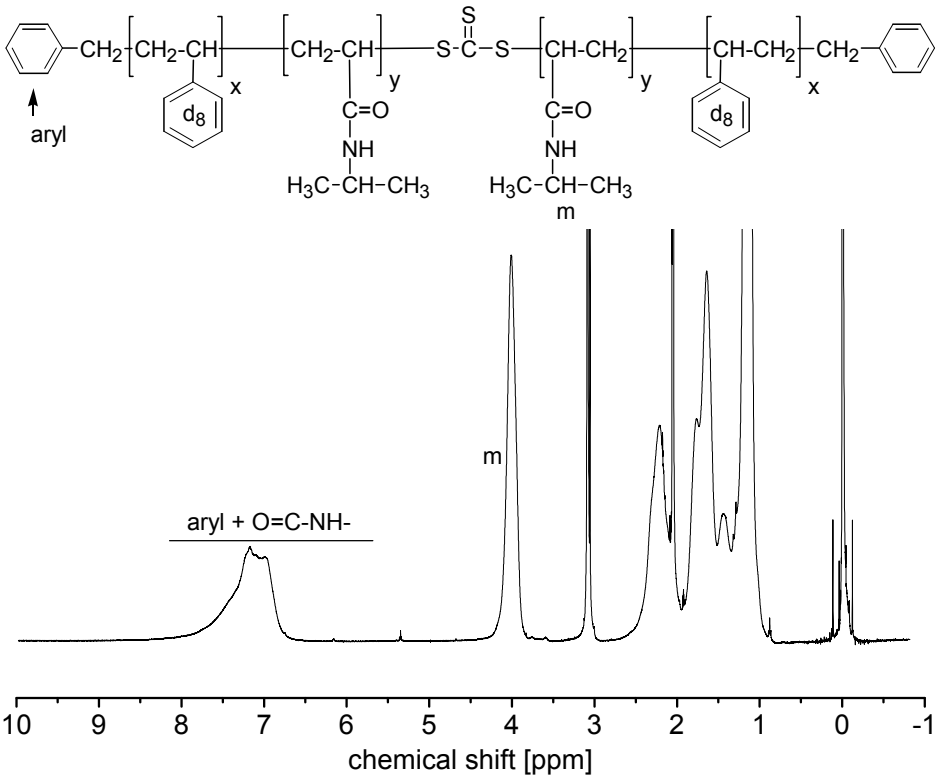


**Figure 3.15 $^1$H-NMR spectrum of P((S-$d_8$)-NIPAM-(S-$d_8$)) in acetone-$d_6$.**

A better estimation can be derived from the absorbance of the styrene moieties in the UV spectrum. On the basis of the extinction coefficient of polystyrene at 262 nm in $CH_2Cl_2$ of 222.5 $L \cdot mol^{-1} \cdot cm^{-1}$,[235] a molar mass of 46300 g/mol for the triblock copolymer was calculated, assuming again that the molar mass of the polystyrene-$d_8$ block of 2300 g/mol is preserved in the block copolymer. This means a number average degree of polymerisation of

389 of the of **PNIPAM** block. The data of the synthesised deuterated polymers are shown in Table 3.6.

As for the **poly((3,5-dibromo benzyl acrylate)-NIPAM-(3,5-dibromo benzyl acrylate)) (p(M3-NIPAM-M3))** hydrogel with a high amount of heavy elements, the **poly((styrene-$d_8$)-NIPAM-(styrene-$d_8$)) [P((S-$d_8$)-NIPAM-(S-$d_8$))]** are interesting compounds, which facilitate the study of the hydrogels by SAXS and SANS techniques (X-ray and neutron scattering are key techniques for structural characterisation of amphiphilic macromolecules and hydrogel systems). These studies on hydrogel networks in water are being investigated at Technische Universität München in collaboration with specialists Peter Müller-Buschbaum and Christine M. Papadakis, the results are still pending.

## 3.7 Conclusions

Bistrithiocarbonates of both Z-C(=S)-S-R-S-C(=S)-Z and R-S-C(=S)-Z-C(=S)-S-R structures are useful and versatile RAFT agents for the synthesis of well-defined amphiphilic triblock copolymers **ABA** and **BAB** consisting of short hydrophobic **B** end blocks and of thermoresponsive **A**-block made of **PNIPAM**. Block copolymer build up is best started with the polystyrene block. Appropriate modifications of the reinitiating R and the active Z end-groups enable a convenient molar mass characterisation of the homopolymers formed by end-group analysis. Combined analysis of the R and Z end-groups helps to evaluate the share of active polymer chains, which can be engaged successfully as macroRAFT agents. Surprisingly, RAFT agents having the R-S-C(=S)-$CH_2$-$CH_2$-C(=S)-S-R group as active part, may extrude ethylene trithiocarbonate during polymerisation, when R is an electron rich benzyl residues. Still, the resulting polymers maintain their bifunctional character, thus enabling the synthesis of symmetrical triblock copolymers.

All these block copolymers are directly soluble in water. The self-organisation into micellar aggregates at low, and into hydrogels at high concentrations as well as their thermoresponsive behaviours are reported in Chapters 4-5.

*"Learning is a treasure that will follow its owner everywhere." Chinese proverb*

# *CHAPTER 4: Self-organization of Thermoresponsive Amphiphilic Symmetrical Triblock Copolymers Containing Poly(N-isopropylacrylamide) as Middle Block in Dilute Aqueous Solution*

In Chapter 3, trithiocarbonates RAFT agents and triblock copolymers **ABA** and **BAB** were synthesised. In this chapter the self-organisation of these thermoresponsive amphiphilic triblock copolymers containing poly(N-isopropylacrylamide) as hydrophilic middle block and small hydrophobic end blocks in dilute aqueous solution is described. The association of these amphiphilic polymers was studied using turbidity and dynamic light scattering. The cloud points of these solutions were nearly the same as compared to the samples of **PNIPAM** homopolymer. Dynamic light scattering measurements showed the presence of aggregates with sizes depending on temperature. The hydrodynamic diameters increase with increasing length of the hydrophobic block within a given copolymer series, whereas the effect of different sizes of the **PNIPAM** middle block seems to be only of minor importance in the molar mass range studied.

## 4.1 Self-assembly of homopolymers and block copolymers in dilute aqueous solution

In comparison to classical low molar mass amphiphiles, amphiphilic block copolymers dispose of a much larger degree of compositional and architectural variability. In addition to the selection of the monomers, parameters such as molar mass, block lengths and architecture can be varied broadly. They all exert a pronounced effect on the block copolymer properties. In the simplest case, a hydrophilic block "**A**" and a hydrophobic block "**B**" form **AB** diblock copolymers, as mostly studied up to now.[238-240] Still, more complex architectures can be realized such as symmetrical triblock copolymers of the **ABA** and **BAB** type, for which the self-assembly depends sensitively on the block sequence.[241-245] Whereas **ABA** block copolymers tend to aggregate into core-shell micelles in aqueous solution, copolymers of the **BAB** type tend to form structures such as flower-like or interconnected micelles and networks. In fact, efficient network formation is an important feature distinguishing **BAB** block copolymers from self-associated **AB** diblock chains.[244] The bridging of micelles in addition to entanglement at high concentrations favours the gelation in **BAB** triblock systems, resulting in physically cross-linked hydrogels. While hydrogels have been studied - and used - in various contexts, a recent focus is on "smart" systems, i.e. hydrogels whose swelling behaviour is controlled by an external stimulus.[246, 247] A particularly interesting stimulus is temperature, as this can be applied in a materially closed system.[239, 248]

A highly efficient "switching" behaviour is achieved when phase transitions of the hydrophilic block **A** are exploited, namely when the block exhibits an upper critical solution temperature (UCST),[73, 249, 250] or a lower critical solution temperature (LCST).[61, 251-254] As the latter is frequently found for non-ionic water-soluble polymers, such hydrophilic blocks have attracted most interest so far in the context of smart hydrogels.[246, 247] Out of the many polymers bearing ether or amide moieties that show LCST behaviour, the most popular example is poly(N-isopropylacrylamide) (**PNIPAM**), by virtue of the weak dependence of the transition temperature ("cloud point") on concentration and molar mass, as well as of the convenient switching temperature around 30-35 °C.[26] The choice of an appropriate hydrophobic **B** block seems a priori nearly unlimited from the pool of water-insoluble polymers. Still, whereas for micellar systems, hydrophobic blocks with low glass transition temperatures are favoured in order to avoid "frozen" hydrophobic domains.[255-259] Such "frozen" systems [260] seem attractive for hydrogel applications, as a high glass transition

temperature of the physical cross-links should enhance the mechanical stability of the gels formed.

After the successful synthesis of **ABA** and **BAB** block polymers using the RAFT technique (Chapter 3), the behaviour of these block copolymers in aqueous solution was investigated. By keeping the chemical nature of the hydrophilic block **A** constant by using always **PNIPAM**, the nature and the lengths of the hydrophobic **B** blocks were varied, using poly(4-*tert*-butyl styrene) **pM1**, polystyrene **pM2**, poly(3,5-dibromo benzyl acrylate) **pM3**, poly(2-ethylhexyl acrylate) **pM4**, and poly(octadecyl acrylate) **pM5** (see Figure 1). The strong hydrophobic **pM1** shows a high glass transition temperature $T_g$ of about 139 °C, **pM2** shows a high glass transition temperature $T_g$, too, of about 100 °C. In contrast, the strongly hydrophobic polyacrylate **pM4** is known for its very low $T_g$ of about -70 °C. The glass transition temperature of the new brominated hydrophobic polyacrylate **pM3** was expected to be in the intermediate range, exceeding somewhat $T_g$ of its parent structure poly(benzylacrylate), which is reported as 6 °C. In fact, $T_g$ of **pM3** was found to be 38 °C (see below). The glass transition temperature of **pM5** is reported to occur in the intermediate temperature range, too, with a $T_g$ of about 57 °C. However, due to the long alkyl side chains that confer extreme hydrophobicity to the polymer, **pM5** is semi-crystalline with a melting point of the side chains of ca. 48 °C. The effect of the different $T_g$ hydrophobic blocks on the thermo-sensitive self-organization of these block copolymers into micelles was studied in dilute aqueous solution, respectively, by $^1$H-NMR, turbidimetry and dynamic light scattering.

## 4.2 $^1$H-NMR of ABA and BAB block copolymers in $D_2O$

Due to the combination of relatively small hydrophobic blocks and much longer hydrophilic **PNIPAM** block, all copolymers made could be dispersed directly in water to give clear mixtures, without the need of an indirect process, such as dissolving the polymers first in an organic, water-miscible solvent followed by the addition of water and the removal of the organic solvent. Different from aqueous solutions of low molar mass amphiphiles, the solutions do not foam notably. $^1$H-NMR spectra of solutions in deuterated water show only the characteristic signals of the hydrophilic **PNIPAM** block,[261] while the characteristic signals of the **B** blocks are suppressed, indicating qualitatively the formation of hydrophobic aggregates (Figure 4.1). The signal at 4 ppm (m in Figure 4.1) evidences the methyl proton of the isopropyl group (-CON-C<u>H</u>$(CH_3)_2$) of **PNIPAM** block.[261, 262]

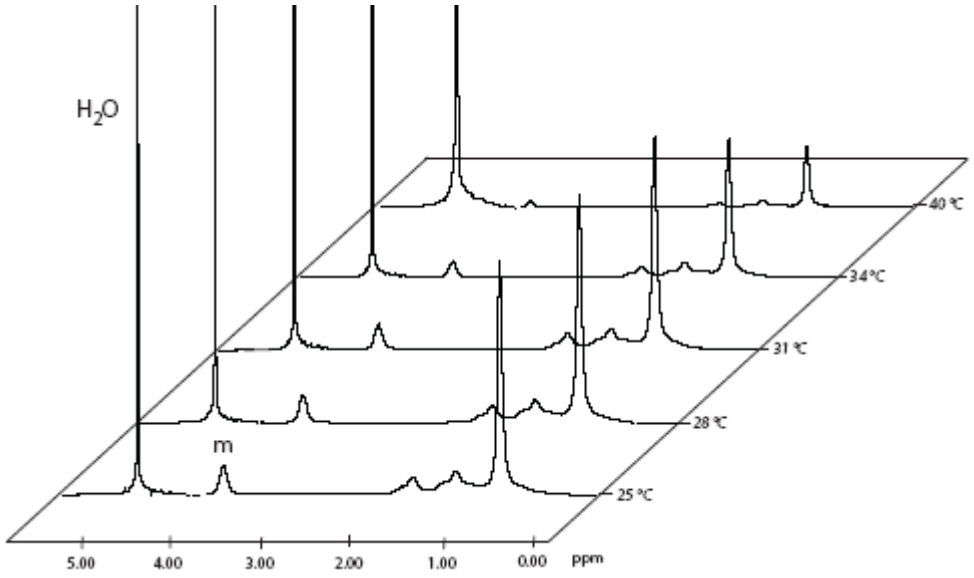


**Figure 4.1 Example of temperature dependent $^1$H-NMR spectrum of p(M1-NIPAM-M1) in $D_20$.**

## 4.3 Turbidimetry: LCST of PNIPAM and its derivatives

As discussed in Chapter1, the cloud point of **PNIPAM** system is caused by a balance between hydrophobic and hydrophilic forces. Below the cloud point of **PNIPAM**, hydrogen bonding interactions between water molecules and amide groups (-NH and –C=O) dominate, so that the polymer is miscible with water. Above the cloud point of **PNIPAM**, hydrophobic interactions between the isopropyl groups dominate, and water is expelled from the polymer. This results in the precipitation of the polymer. Consequently, the addition of hydrophobic segments to a **PNIPAM** block when generating amphiphilic block copolymers is expected to deteriorate the interactions between water molecules with **PNIPAM**. This type of chain extension of **PNIPAM** might lower the value of the cloud point of the block copolymer. To evaluate the behaviour of the block copolymers described in Chapter 3 in dilute aqueous solution, turbidimetric measurements were carried out. The following part focuses on the examination of the effect of the $T_g$ hydrophobic blocks of the symmetrical triblock copolymers **BAB** on the cloud point of **PNIPAM**. The analogous **ABA** architecture and pure **PNIPAM** were studied as comparison, too. All samples were investigated at a concentration of 1 g/L.

## 4.3.1 Series (a): PNIPAM

All samples dissolve directly in water. The aqueous solutions were optically clear below the cloud point, but became turbid in response to increasing temperature. In a first study, the cloud point of homopolymers **PNIPAM-1** and **PNIPAM-3** (Figure 4.2 and Table 4.1) was investigated by turbidimetry at a fixed heating/cooling rate of 1 °C/min in the temperature range from 20 to 60 °C.

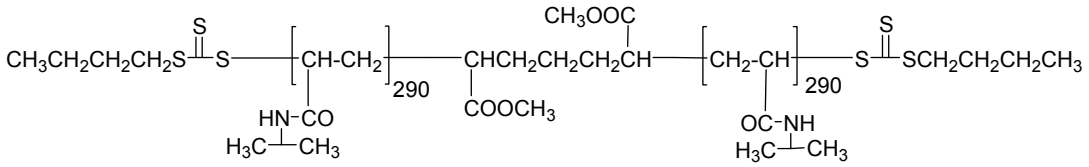


**Figure 4.2 PNIPAM-1 as an example of PNIPAM homopolymer with RAFT agent 1.**

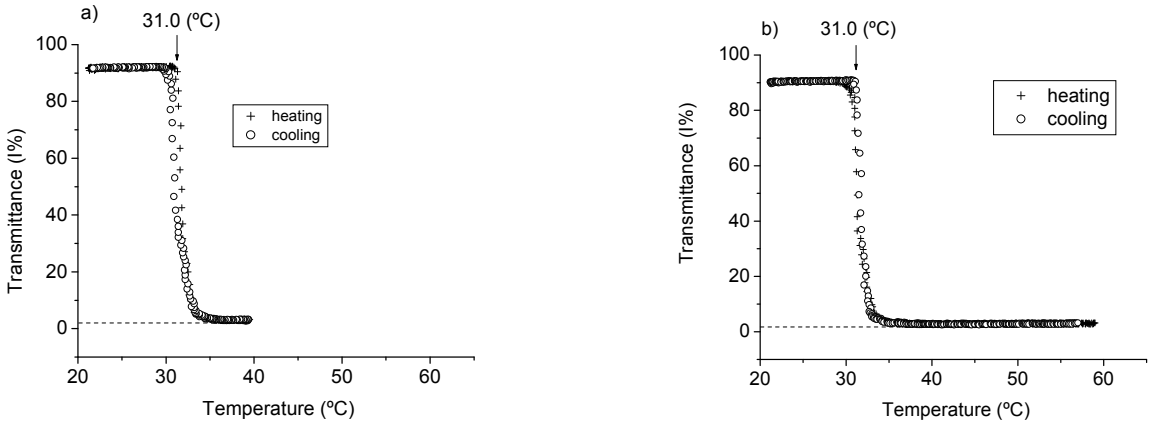


**Figure 4.3a-b Transmittance (I/Io) of aqueous solution of (a) PNIPAM-1 and (b) PNIPAM-3 as a function of the temperature at a fixed heating/cooling rate.**

Figure 4.3a-b shows the results for the homopolymers. These are characterised by a sigmoidal curve that covers two distinctive temperature ranges: the first one corresponds to the transparent **PNIPAM** solution (temperature below the cloud point), the second one to the phase separated system upon heating beyond the cloud point. When the solutions were heated, the transmission decreases steeply above a temperature of 31 °C and reaches quickly a plateau at 36 °C with no remaining transmission. The cloudiness of the solution can be explained by the increase strength of hydrophobic interactions of the **PNIPAM** chains when the temperature is raised, resulting in larger aggregates that causes an augmentation in the turbidity values (see Chapter 1, sections 1.4-1.6).

Upon cooling, very small hystereses of less than 1 °C are observed and the full transmission is recovered (Figure 4.3a-b). The process is fully reversible.

Noteworthy, the cloud points found are very similar to the ones reported in the literature.[28, 43, 263] This implies that the RAFT end-groups used for the synthesis of the **PNIPAM** homopolymers do have a negligible effect on the cloud point of these homopolymers. The small hystereses seen in the cooling process were also reported by Fujishige et al.[43] They postulated that these effects could be attributed to a restricted free rotation on the total conformation of this polymer due to the presence of the methylene group in the main chain unit structure. Additionally, taking into account that the phase transition temperature of **PNIPAM** is related to a conformational change from well-solvated random coils at lower temperature to tightly packed globular particles at higher temperature and vice versa,[25, 264-267] it is plausible that these conformations delay hydration of the **PNIPAM** chains upon cooling as shown in Figure 4.3 a-b.

## 4.3.2 Series (b): p(NIPAM-M2-NIPAM) ABA triblock block copolymers

In order to learn on possible hydrophobic effects on the thermally-induced phase transition of **PMIPAM**, **ABA triblock copolymers** made of **PNIPAM** as end blocks and polystyrene as hydrophobic **B**-middle block were employed for comparison, too. These block copolymers have degrees of polymerisation (*D*P) of 27 and 30 for the polystyrene block and 160 and 210 for the **PNIPAM** blocks, respectively. Typical models are: **p(NIPAM-M2#27-NIPAM)** and **p(NIPAM-M2#30-NIPAM)**, see Figure 4.4 and Table 4.1. Figure 4.4 shows a typical example for the **ABA** structure.

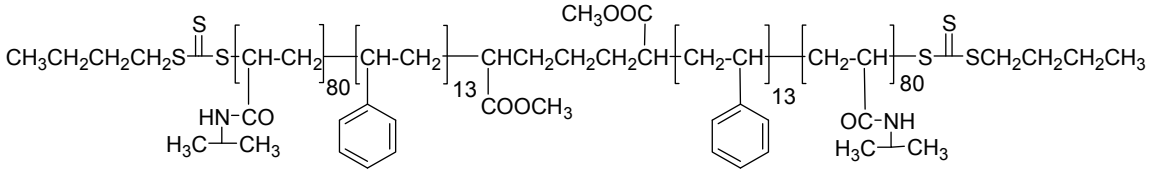


**Figure 4.4 p(NIPAM#80-M2#26-NIPAM#80) as an example of an amphiphilic block copolymer with ABA structure.**

The results of turbidimetric studies of these block copolymers are displayed in Figure 4.5a-b. The experimental results show that for the solutions of the **ABA** triblock copolymers, the transmission decreases above a temperature of 30 °C, too, but the transmission decreases

more gradually than for the homopolymers and reaches a plateau only at 40-45 °C with some transmission remaining. Upon cooling, a notable hysteresis is observed between 45 and 25 °C before the full transmission is recovered (Figure 4.5a-b).

The fact that the cloud point of the **p(NIPAM-M2-NIPAM)** samples is virtually the same as for **PNIPAM** homopolymers (30.0 °C to 31.0 °C) was surprising. As discussed before, the addition of hydrophobic blocks to **PNIPAM** was expected to decrease the cloud point. This suggests that the hydrophobic polystyrene blocks cannot influence directly the **PNIPAM** blocks in aqueous media. That is achieved when **p(NIPAM-M2-NIPAM)** polymers form a core-shell structure, with **PNIPAM** blocks forming the shell and **PNIPAM** the core of the micelles. A similar behaviour was reported for **PNIPAM** block copolymers with polystyrene[57] as well as amphiphilic **PNIPAM** bearing two n-octadecyl end-groups.[268]

The addition of polystyrene end blocks to **PNIPAM** chains induces the formation of reversible phase transitions with notable hystereses (Figure 4.5a-b). The hysteresis can be explained by interchain association in the collapsed state of **PNIPAM** due to the hydrophobic end blocks. Consequently, longer equilibration times are required for remixing to be complete at low temperature.

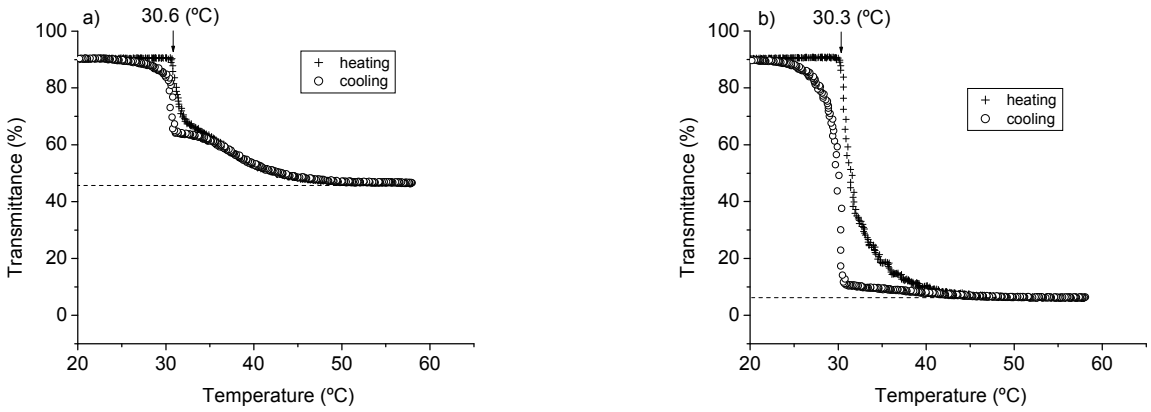


**Figure 4.5a-b Transmittance (I/Io) of aqueous solution of p(NIPAM-M2-NIPAM#27) (a) and p(NIPAM-M2-NIPAM#30) (b) as a function of the temperature at a fixed heating/cooling rate.**

The fact that the transmittance above the cloud point is lower in **p(NIPAM-M2#27-NIPAM)** compared to **p(NIPAM-M2#30-NIPAM)** is unusual. Due to the higher content in polystyrene in **p(NIPAM-M2#30-NIPAM) (pM2#30)**, a lower scattered-light intensity was expected in the latter case. However, this is not the case. The reasons for this behaviour are uncertain. Subsequent measurements on **BAB** solutions (series **(d-g)**) show a similar behaviour.

### 4.3.3 Series (c): p(M1-NIPAM-M1) (BAB) triblock block copolymers

To find out whether the addition of hydrophobic end blocks to **PNIPAM** triggers the phase transition of the pure **PNIPAM** at lower solution temperatures, the phase transition temperatures of block copolymers having **PNIPAM** as **A**-middle block and hydrophobic **B** end blocks of the linear **BAB** block copolymers were addressed. First, **poly(tert-butyl styrene) (pM1**) was investigated. This polymer is characterised with a high glass transition in the range of 139 °C. Figure 4.6 presents the general structure of this series **(c)**. For the solubility reasons, *D*P of **pM1** was limited to 17 and 34, and *D*P of **PNIPAM** was set as 280 and 490, respectively, in **p(M1-NIPAM-M1#17)** and **p(M1-NIPAM-M1#34)** (Table 4.1 and Figure 4.7).

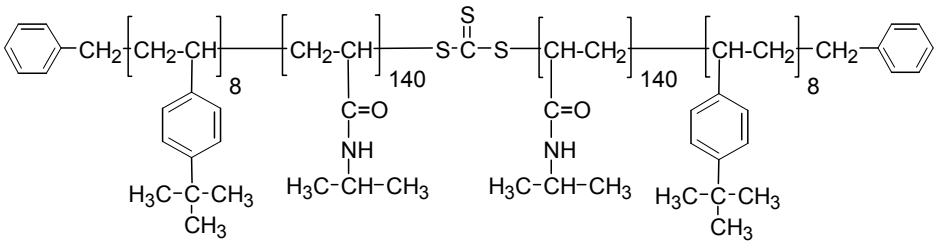


**Figure 4.6 p(M1-NIPAM#280-M1#16) as an example of an amphiphilic block copolymer with BAB structure.**

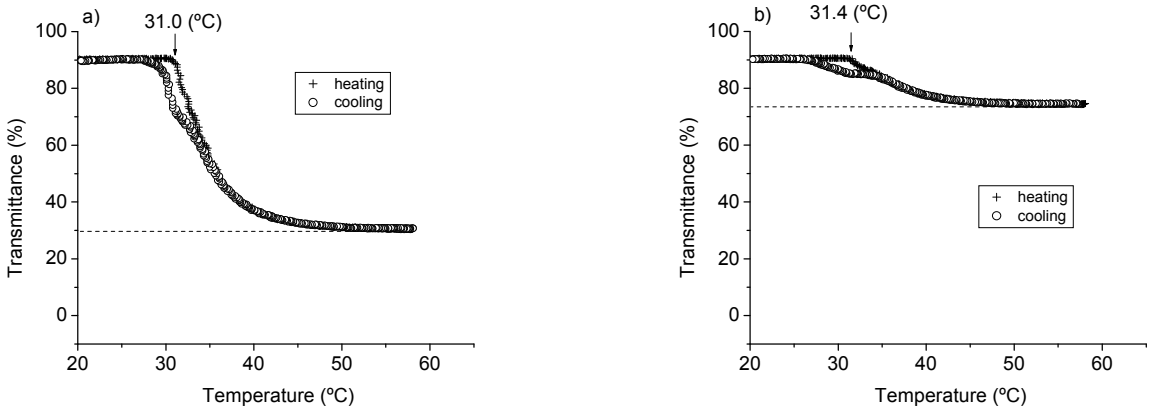


**Figure 4.7 Transmittance (I/Io) of aqueous solution of (a) p(M1-NIPAM-M1#17) and (b) p(M1-NIPAM-M1#34) copolymers as a function of the temperature at a fixed heating/cooling rate.**

Inspection of Figure 4.7 indicates first an evolution of turbidity within two distinctive temperature ranges, as observed for the **PNIPAM** homopolymer. Also, it shows that both copolymer solutions exhibit almost same the cloud point (31.0 °C), with only slight

differences. Note that the transitions are reversible, but show a notable hysteresis in heating and cooling runs. In contrast to **PNIPAM** homopolymers, the transmittances decreased by 74 % for **p(M1-NIPAM-M1#17)** and 30 % for **p(M1-NIPAM-M1#34)**. The hysteresis results probably also from a retarded recovery of the conformational change of polymer due to interchain associations in the collapsed state of **PNIPAM**. The fact that the cloud point of **p(M1-NIPAM-M1)** samples is virtually the same as for **PNIPAM** homopolymers and the **ABA** block copolymer type (31.0 °C to 31.0, 30.0 °C) is remarkable. As discussed before, the addition of hydrophobic end blocks into **PNIPAM** would be expected to lower the cloud point. This unusual trend suggests that in solutions of the **p(M1-NIPAM-M1)** copolymers, the **p(M1)** blocks are not exposed to water but rather form a micellar structure protected from the water, and therefore do not make a hydrophobic contribution to the LCST.[269] Similarly, Troll et al.[7] reported that micellar structures formed from **AB** block copolymers comprising the **PNIPAM** block with polystyrene show a similar LCST to the linear **PNIPAM** chains. Chung et al.[57] observed also comparable values for the phase transition of **PNIPAM** and diblock copolymers made of **PNIPAM** block with polystyrene or poly(butyl methacrylate) hydrophobic segments. They attributed this effect to phase-separated micellar structures due to strong interaction of the hydrophobic blocks formed.[58, 270-272]

## 4.3.4 Series (d): p(M2-NIPAM-M2) (BAB) triblock block copolymers

The hydrophobic group investigated in this series **(d)** concerns **polystyrene** (**pM2**) and its derivatives. The *D*P of the **pM2** blocks varied from 22, 30, 48, 61, 81, 89 to 119, while the *D*P of the **PNIPAM** block varied as 1185, 185, 550, 530, 790, 650 and 700, respectively (Table 4.1). The general structure of the series **(d)** is shown in Figure 4.8.

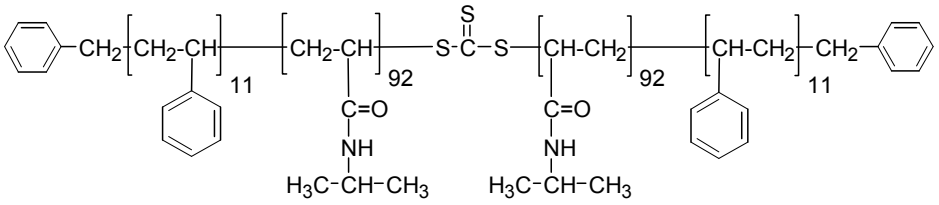


**Figure 4.8 p(M2#11-NIPAM#184-M2#11) as an example of an amphiphilic block copolymer with BAB structure.**

Figure 4.9a-d displays the phase transition of this series. Despite the differences in the polystyrene lengths of the triblock copolymers, these figures indicate that the block copolymers have comparable cloud points in the range of 31.0 °C. Again, notable hystereses

are observed between 35 and 25 °C, before the full transmission is recovered (Figure 4.9a-d). According to the varying length of the hydrophobic end blocks of the six triblock copolymers, one would expect to see a significant difference in their cloud points with the order increasing as **pM2#119 < pM2#89 < pM2#81 < pM2#61 < pM2#48 < pM2#22**. In contrast to the expectation almost the same cloud point was found for the six triblock copolymers in the turbidimetry measurements. This suggests that the attached hydrophobic group does not play a significant role for the cloud point of **PNIPAM** block.

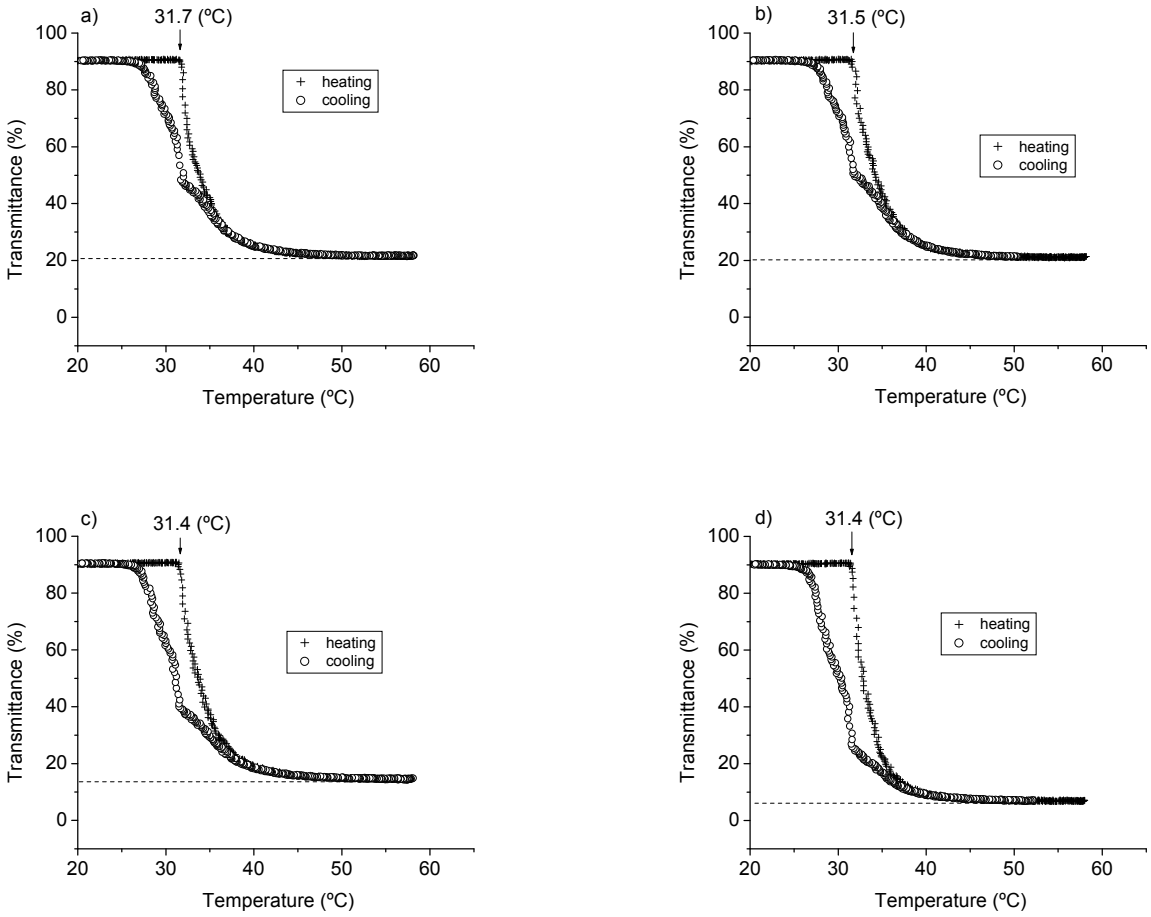


**Figure 4.9 Transmittance (I/Io) of aqueous solution of a) p(M2-NIPAM-M2#48), b) p(M2-NIPAM-M2#81), c) p(M2-NIPAM-M2#89) and d) p(M2-NIPAM-M2#119) copolymers as a function of the temperature at a fixed heating/cooling rate.**

## 4.3.5 PNIPAM mixed with P(M2-NIPAM-M2#48)

As mixtures of thermoresponsive polymers have been reported to show non-additive behaviour, an exemplary test was performed with a mixture of **PNIPAM-1** homopolymer and triblock copolymer **p(M2-NIPAM-M2#48)** in water. Figure 4.10 shows the occurrence of one

transition temperature, corresponding to the cloud point of the both individual polymers. Therefore, no specific effects seem to occur on such mixed systems.

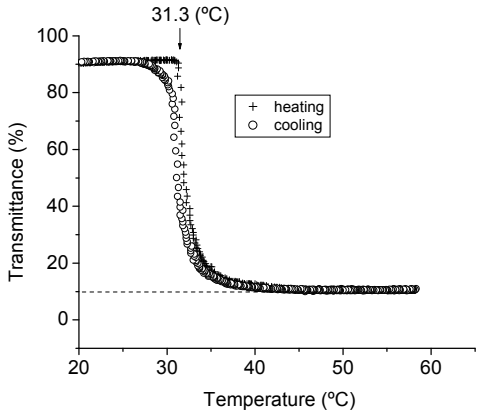


**Figure 4.10 Transmittance (I/Io) of aqueous solution mixed of PNIPAM-1 with p(M2-NIPAM-M2#48) as a function of the temperature at a fixed heating/cooling rate.**

## 4.3.6 Series (e): p(M3-NIPAM-M3) (BAB) triblock block copolymers

In order to gain further insight into the influence of the end block, the new **poly(3,5-dibromobenzyl acrylate) (pM3)** was used for the **BAB** block copolymers, Figure 4.11, which is characterised by a $T_g$ = 37 °C.

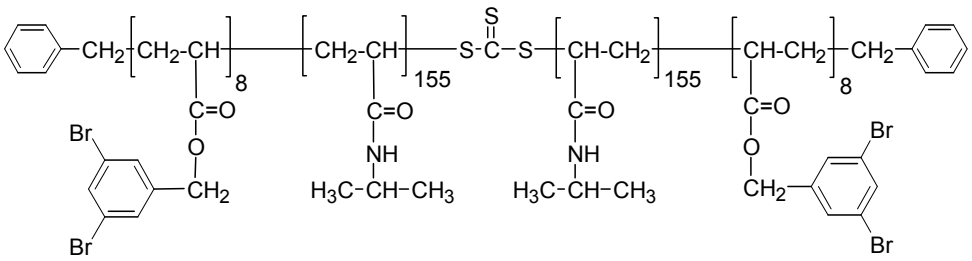


**Figure 4.11 p(M3#8-NIPAM#310-M3#8) as an example of an amphiphilic block copolymer with BAB structure.**

Figure 4.12 presents the turbidimetric studies of this block copolymer. Independent of **pM3** having a low $T_g$, the result of turbidity measurements of the **p(M3-NIPAM-M3#16)** solution is similar to that of the previous systems. As seen above, the transmission decreases progressively above 31.7 °C and does not reach zero, but reaches a plateau at 22% of the initial value at 35 °C. Upon cooling, a hysteresis is observed between 35 and 25 °C, and then the full transmission is recovered. The process is thus fully reversible with a hysteresis loop.

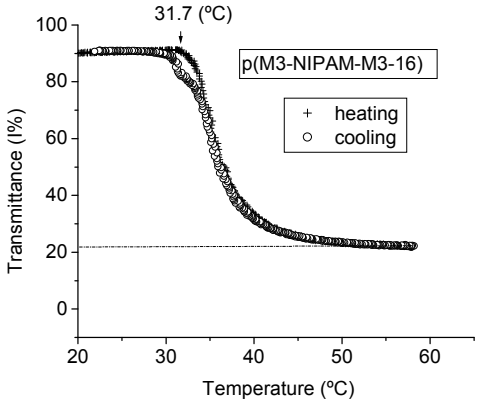


**Figure 4.12 Transmittance (I/Io) of aqueous solution of p(M3-NIPAM-M3#16) copolymers as a function of the temperature at a fixed heating/cooling rate.**

Thus far, it has been demonstrated that the attachment of the various hydrophobic blocks onto the thermoresponsive block copolymers only has a small affect on the cloud point of the **PNIPAM** based block copolymers.

## 4.3.7 Series (f): p(M4-NIPAM-M4) (BAB) triblock block copolymers

The influence of the end block on the cloud point of **PNIPAM** block copolymers was extended using **poly(2-ethyl hexyl acrylate) (pM4)**. **pM4** is characterised by a $T_g$ = -70 °C. The four thermoresponsive triblock copolymers of this series **(f)** studied vary the *D*P of the hydrophobic blocks from 21, 35, 50 to 60, while the *D*P of the **PNIPAM** block varies from 380, 610, 700 to 670, respectively (Table 4.1). Figure 4.13 displays the general structure of this series **(f)**.

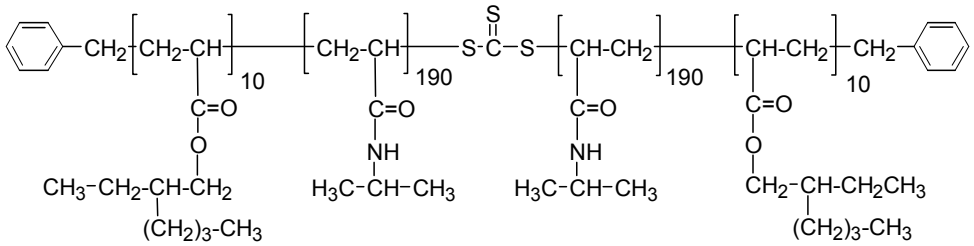


**Figure 4.1.3 p(M4#10-NIPAM#380-M4#10) as an example of an amphiphilic block copolymer with BAB structure.**

Figure 4.14a-d displays their phase transitions in dilute aqueous solution. As seen in the previous series **(b-e)**, in the series **(f)** the four triblock copolymer solutions display phase

transitions at almost the same temperature (31.7 °C), with only slight differences (Figure 4.14a-d).

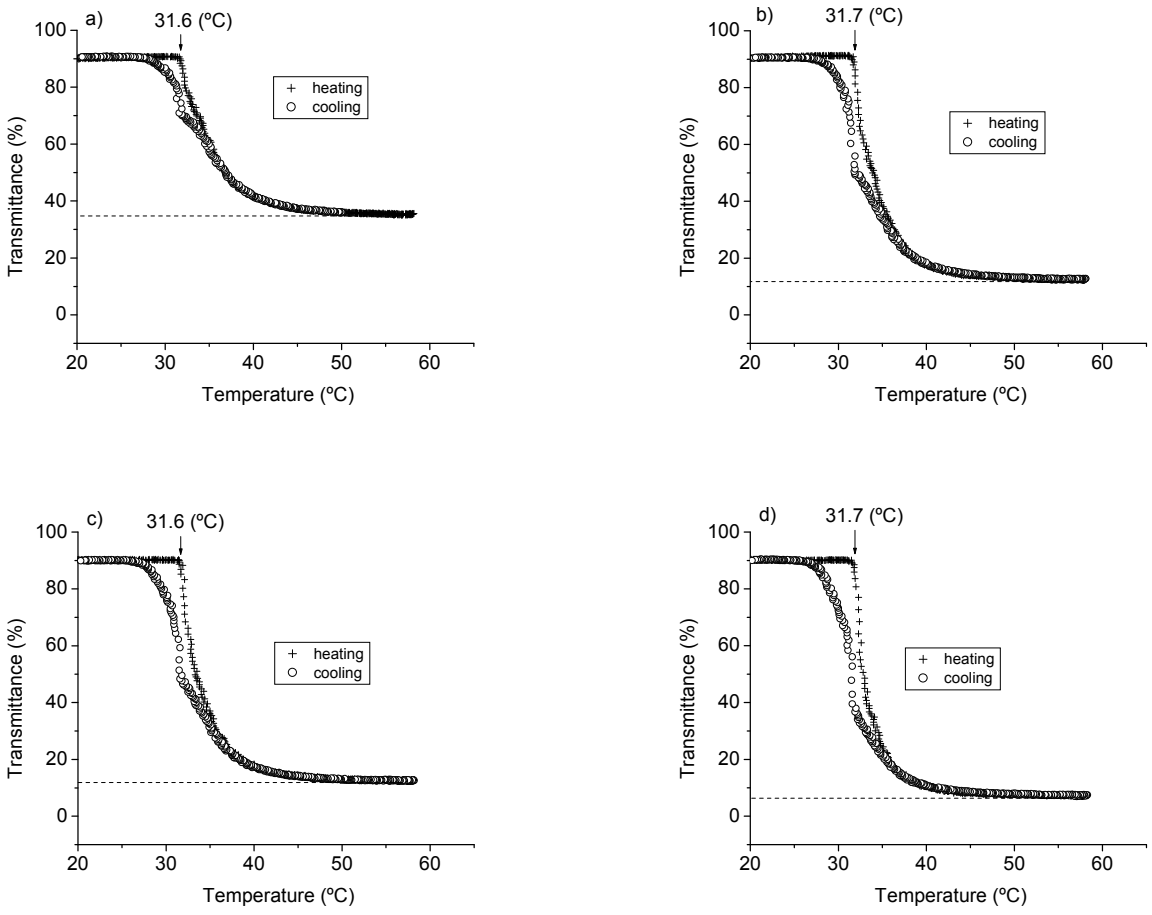


**Figure 4.14 Transmittance (I/Io) of aqueous solution of a) p(M4-NIPAM-M4#21), b) p(M4-NIPAM-M4#35), c) p(M4-NIPAM-M4#50) and d) p(M4-NIPAM-M4#60) copolymers as a function of the temperature at a fixed heating/cooling rate.**

The finding corroborates that the hydrophobic blocks attached to the thermoresponsive centre block of **PNIPAM** do not play a significant role for the cloud point, also for blocks with very low $T_g$.

It should be noted that hysteresis remains present as discussed in the above series.

## 4.3.8 Series (g): p(M5-NIPAM-M5) (BAB) triblock block copolymers

In the final series, the hydrophobic block is made of **poly(octadecyl acrylate)(pM5)**. **pM5** is semi-crystalline with a melting point of the side chains of ca. 48 °C. The triblock copolymers of this series have combined *D*P of the hydrophobic blocks from 11, 36 and 54 while the *D*P

of the **PNIPAM** block varied as 280, 900 and 1250, respectively (Table 4.1). Figure 4.15 demonstrates the general formula of **p(M5-NIPAM-#M5)** block copolymers.

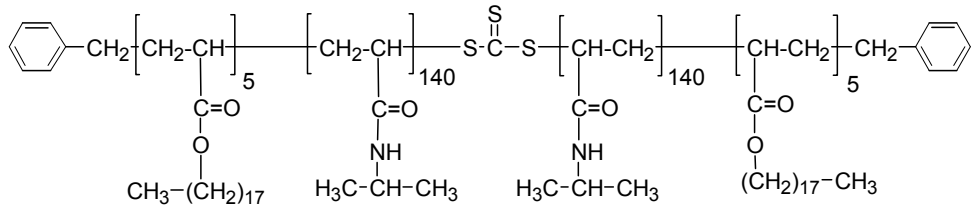


**Figure 4.15 p(M5#5-NIPAM#280-M5#5) as an example of an amphiphilic block copolymer with BAB structure.**

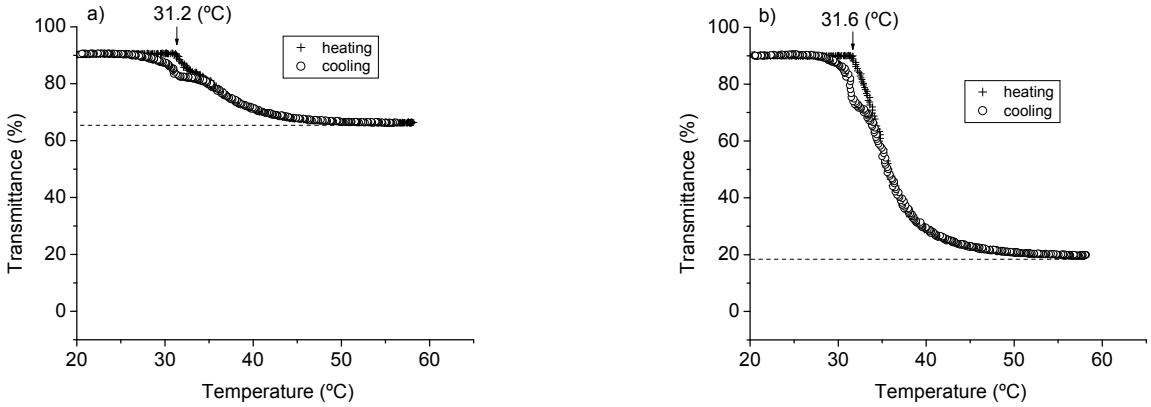


**Figure 4.16a-b Transmittance (I/Io) of aqueous solution of a) p(M5-NIPAM-M5#11) and b) p(M5-NIPAM-M5#54) copolymers as a function of the temperature at a fixed heating/cooling rate.**

Figure 4.16a-b shows that the triblock copolymers of series **(g)**, display reversible phase transitions at almost the same temperature (31.2 °C) with only slight differences in agreement with the previous series **(b-f)**.

In addition, hystereses and transmittance demonstrate the influence of hydrophobic end blocks in the phase transition. Looking at the molar mass composition, one would also expect a decrease of the cloud point with increasing molar mass. This is not, however, what it is observed.

## 4.4 Summary of the turbidimetry measurements

For comparison, Figure 4.17 results from the plot of the cloud points as a function of the molar mass for homopolymers and block copolymers. The cloud points are found in the temperature range of 31-32 °C.

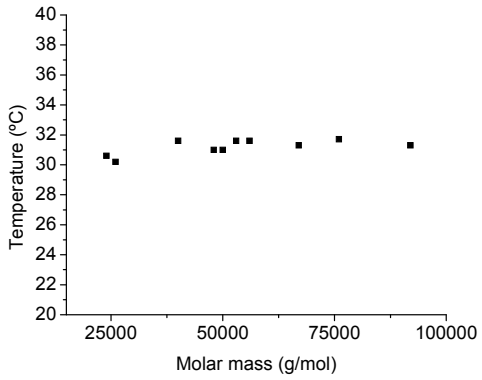


**Figure 4.17 Cloud point temperature of aqueous solution of the PNIPAM homopolymers and ABA and BAB amphiphilic triblock copolymers as a function of the molar mass (of the PNIPAM block).**

Different from these findings, Duan'group[47] reported that the presence of hydrophobic end blocks in the polymer may alter markedly the cloud point of **PNIPAM**. This effect becomes weaker with increasing molar masses, and depends sensitively on chemical nature of the initiator or chain transfer agents used. Recent other reports have also confirmed that for very small molar masses or very low concentrations, the cloud point of **PNIPAM** may vary notably from the 31-32°C range reported usually. However, these reports seem to concern extreme scenarios only (see Chapter 1, section 1.7).

The fact that the cloud points measured in the heating runs are virtually the same within experimental precision for reference samples of **PNIPAM** homopolymer as well as all the block copolymers investigated, independent of the presence, the nature and the length of the hydrophobic blocks can be explained by the formation of micelles. When micelles are formed, the hydrophobic groups are no more exposed to water, but reside in the micellar cores, where they are protected from water by the **PNIPAM** chains. Therefore the hydrophobic blocks are not effective to lower the LCST.[46] This model accounts for the surprising behaviour, that moderately hydrophobic end-groups, which are not strong enough to induce micellization, influence much more strongly the phase behaviour in dilute aqueous solution than strong hydrophobic end blocks, as polymers **p(M1)-p(M5)** do.

The current dilute aqueous solutions of **PNIPAM** homopolymers and nonionic amphiphiles **ABA** and **BAB** copolymers made of **PNIPAM** as **A block** exhibit nearly an identical phase separation temperature around 30-32 °C. Thus, despite differences in the molecular architecture, the results demonstrate that $T_g$ and molar mass have little effect on the LCST of **PNIPAM**. It is possible that the polymer solutions present some similarity in their respective micellar solutions.

## 4.5 DLS of PNIPAM and its derivatives

**Table 4.1 Cloud points (from heating run) and hydrodynamic diameters of dilute micellar solutions (1g/L) of BAB triblock copolymers and some reference polymers.**

| Polymer | $DP_n$ of hydro-phobic blocks | $DP_n$ of **PNIPAM** block | hydro-phobe content [wt%] | Cloud point [ °C ] | $D_h$ [nm] 20 °C | PDI 20 °C | $D_h$ [nm] 60 °C | PDI 60 °C |
|---|---|---|---|---|---|---|---|---|
| **PNIPAM-1** | - | 580 | - | 31.0 | | | | |
| **PNIPAM-2** | - | 430 | - | 31.0 | 12 | 0.76 | 250 | 0.14 |
| **PNIPAM-3** | - | 320 | - | 31.0 | 11 | 0.60 | 280 | 0.12 |
| | | | | | | | | |
| **p(NIPAM-M2-NIPAM)-1** | 27 | 160 | 13.6 | 30.5 | 33 | 0.21 | 120 | 0.03 |
| **p(NIPAM-M2-NIPAM)-2** | 30 | 210 | 11.8 | 30.0 | 36 [a)] | 0.27 [a)] | 190 [a)] | 0.04 [a)] |
| | | | | | | | | |
| **p(M1-NIPAM-M1#17)** | 17 | 280 | 8.0 | 31.6 | 40 | 0.17 | 130 | 0.04 |
| **p(M1-NIPAM-M1#34)** | 34 | 490 | 9.0 | 31.4 | 50 | 0.18 | 100 | 0.04 |
| | | | | | | | | |
| **p(M2-NIPAM-M2#22)** | 22 | 185 | 10.0 | 30.9 | 32 [a)] | 0.28 [a)] | 120 [a)] | 0.03 [a)] |
| **p(M2-NIPAM-M2#30)** | 30 | 185 | 12.8 | 30.9 | 30 [a)] | 0.26 [a)] | 150 [a)] | 0.03 [a)] |
| **p(M2-NIPAM-M2#48)** | 48 | 550 | 7.4 | 31.3 | 51 | 0.18 | 200 | 0.03 |
| **p(M2-NIPAM-M2#61)** | 61 | 530 | 10.5 | 31.3 | 44 | 0.18 | 170 | 0.02 |
| **p(M2-NIPAM-M2#81)** | 81 | 790 | 8.6 | 31.4 | 47 | 0.14 | 180 | 0.03 |
| **p(M2-NIPAM-M2#89)** | 89 | 650 | 11.3 | 31.4 | 48 | 0.12 | 150 | 0.03 |
| **p(M2-NIPAM-M2#119)** | 119 | 700 | 13.4 | 31.3 | 58 | 0.15 | 190 | 0.05 |
| | | | | | | | | |
| **p(M3-NIPAM-M3#16)** | 16 | 310 | 12.5 | 31.6 | 37 | 0.30 | 155 | 0.03 |
| | | | | | | | | |
| **p(M4-NIPAM-M4#21)** | 21 | 380 | 8.4 | 31.4 | 36 | 0.15 | 165 | 0.01 |
| **p(M4-NIPAM-M4#35)** | 35 | 610 | 9.2 | 31.7 | 49 | 0.16 | 180 | 0.06 |
| **p(M4-NIPAM-M4#50)** | 50 | 700 | 10.6 | 31.5 | 52 | 0.19 | 185 | 0.03 |
| **p(M4-NIPAM-M4#60)** | 60 | 670 | 12.6 | 31.5 | 55 | 0.12 | 185 | 0.03 |
| | | | | | | | | |
| **p(M5-NIPAM-M5#11)** | 11 | 280 | 10.0 | 31.4 | 50 | 0.18 | 111 | 0.03 |
| **p(M5-NIPAM-M5#36)** | 36 | 900 | 10.7 | 31.5 | 62 | 0.11 | 142 | 0.04 |
| **p(M5-NIPAM-M5#54)** | 54 | 1250 | 11.3 | 31.6 | 65 | 0.12 | 165 | 0.03 |

[a)] measured at 25 °C.

The second part of this Chapter focuses on the investigation of block copolymers solutions by dynamic light scattering (DLS). The samples were prepared at concentrations covering 1 g/L as mentioned above. The DLS measurements were carried out at the temperatures of 20, 40, 50, and 60 °C. The results are presented in Figures 4.18-4.23 and Table 4.1.

## 4.5.1 DLS of PNIPAM homopolymer solutions

Looking at the hydrodynamic diameters ($D_h$) of **PNIPAM** solutions, below the cloud point at 20 °C, small particles sizes with about 11 nm and PDI = 0.6 are observed (see Table 4.1). This result reflects the size of single molecule coils (unimers). With increasing temperature from 20 °C to 50 °C, the solutions become turbid and DLS indicates a sudden increase in their hydrodynamic diameter with a PDI ($D_h$ of about 300 and PDI = 0.12). It should be noted that with further increase of the temperature (50 °C to 60 °C) the particle size stagnates and, no precipitation was observed for the sample. Additionally, when more concentrated solutions up to 20 wt% of the polymers were studied, only monomodal distributions of small aggregates were observed. These behaviours were seen for all **PNIPAM** homopolymers.

The differences in the $D_h$ of the **PNIPAM** homopolymers (11-300 nm) below and above the cloud point are obvious. As below the cloud point, water is a good solvent for **PNIPAM**, the polymer adopts a random coil conformation. Above the cloud point, water becomes a poor solvent for **PNIPAM** chains so that the intra- and intermolecular (polymer-polymer intermolecular) hydrophobic interactions prevail. Thus, the polymer chains collapse and aggregate to colloidal particles with increased diversity and hydrodynamic diameters. This phenomenon has been reported in the case poly(N-isopropylmethacrylamide), poly(N-propylmethacrylamide), poly(N-vinylcaprolactam), and poly(vinyl methyl ether).[273, 274]

## 4.5.2 DLS of p(NIPAM-M2-NIPAM) (ABA) triblock block copolymers

The following section addresses the role of hydrophobic blocks on the particle size of the block copolymers studied in the earlier section. First, the results for **p(NIPAM-M2-NIPAM)** block copolymers are illustrated in Figure 4.18 taking **p(NIPAM-M2#27-NIPAM)** as an example.

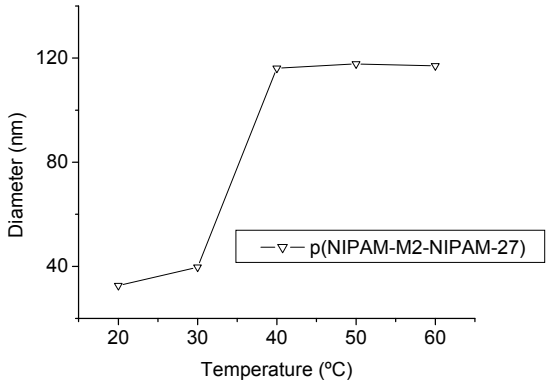


**Figure 4.18 Evolution of the hydrodynamic diameter ($D_h$) as a function of temperature for 1g/L of aqueous solutions of p(NIPAM-M2#27-NIPAM).**

The investigation of the $D_h$ of **p(NIPAM-M2-NIPAM)** samples showed similar trends as in the case of **PNIPAM** homopolymers. Taking **p(NIPAM-M2#27-NIPAM-1)** as an example (see Table 4.1), when the temperature was below 30 °C, the apparent hydrodynamic size was 33 nm and PDI = 0.21. The size of the colloids is characteristic for the formation of micelles with a core made of polystyrene and the corona of **PNIPAM** chains. With the increase of the temperature above 50 °C, the micelles augment in size 120 nm, while the size distribution becomes narrower (PDI = 0.03), indicating the formation of compact and dense aggregates with uniform size. The large aggregates formed do not reflect the collapse of the **PNIPAM** corona with increasing temperature, but is attributed to a secondary association of the primary micelles into larger clusters. Further heating up to 60 °C induces no significant changes and, no precipitation was observed for the sample; this indicates the formation of stable aggregates. Again, when concentrated solutions up to 20 wt% of the block polymers were employed, only monomodal distributions of small aggregates were observed at room temperature. These tendencies were seen also for all block copolymers solutions studied. The current experiments show that the short hydrophobic end blocks of the triblock copolymers are sufficient to induce micelle formation. This observation is in good accordance with the findings of Eisenberg et al.[275] who demonstrated that micelle formation of **PS-b-poly(sodium acrylates)** block copolymers was possible with 2-3 styrene units only.[275]

A closer inspection of the data in Figure 4.18 (and Table 4.1) above the cloud point, reveal that **p(NIPAM-M2-NIPAM)** block copolymers form aggregates with smaller size compared to those of pure **PNIPAM**. The difference can be explained by the formation of micellar clusters. Despite of the collapsed corona, micellar clusters with reduced sizes are formed, as

the immobilization of the hydrophobic blocks on the cases of the micelles seems to hinder large scale aggregation.[276, 277]

## 4.5.3 DLS of p(M1-NIPAM-M1) (BAB) triblock block copolymers

In order to get information concerning the effect of hydrophobic blocks on the micellization of **BAB** architecture, studies were carried out with **pM1**, **pM2**, **pM3**, **pM4**, and **pM5** (see section above).

Figures 4.19-4.23 illustrate typical DLS results obtained for the five different series of **BAB** triblock copolymer solutions including **p(M1-NIPAM-M1)**, **p(M2-NIPAM-M2)**, **p(M3-NIPAM-M3)**, **p(M4-NIPAM-M4)** and **p(M5-NIPAM-M5)**. The values of $D_h$ can be found in Table 4.1. Comparing copolymers of a given series, **p(M1-NIPAM-M1)**, **p(M2-NIPAM-M2)**, **p(M3-NIPAM-M3)**, **p(M4-NIPAM-M4)** and **p(M5-NIPAM-M5)**, the general pattern of the evolution of the hydrodynamic diameter as a function of temperature is the same within a series. The hydrodynamic diameter changes with temperature and with length of the hydrophobic blocks.

Concerning the **p(M1-NIPAM-M1)** block copolymers, Figure 4.19 reveals at 20 °C, the formation micelles with small particle size and a low size distribution as well (40 and 50 nm and PDI = 0.17 and 0.18 for **p(M1-NIPAM-M1#17)** and **p(M1-NIPAM-M1#34)**, Table 4.1).

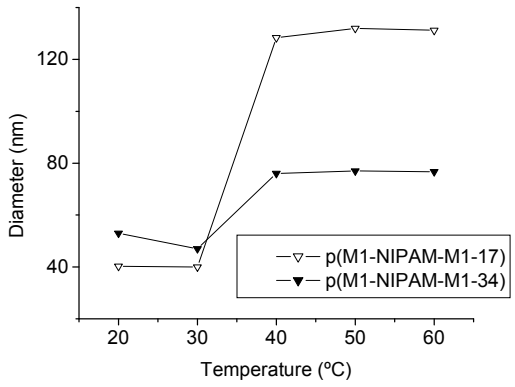


**Figure 4.19 Evolution of the hydrodynamic diameter ($D_h$) as a function of temperature for 1g/L of aqueous solutions of p(M1-NIPAM-M1).**

This clearly reinforces the idea that the incorporation of hydrophobic end blocks in the **PNIPAM** chains is crucial for micelle formation. When the temperature rises above the cloud point, the particle size shifted toward high values while the size distribution turned narrower

(130 and 100 nm and PDI = 0.04) for **p(M1-NIPAM-M1#17)** and **p(M1-NIPAM-M1#34)**. These observations indicate that the thermoresponsive blocks **p(M1-NIPAM-M1)** form micellar aggregates with the temperature. In fact, at low temperatures strong hydrogen-bonding between the hydrophilic groups and surrounding water ensure good solubility of PNIPAM units. When the temperature rises, these hydrogen-bridges are broken, **PNIPAM** shell become more hydrophobic and intermolecular interactions occur, resulting in the formation of aggregates with large size.[278, 279]

A moderate decrease of the hydrodynamic diameter with increasing temperature below the cloud point has been previously observed with di- and triblock copolymers from polystyrene and **PNIPAM**.[214, 280] This may be due to the gradual collapse of the hydrophilic corona of the micelles.[7]

It is worth noting that the value of $D_h$ of the micelles increases with increasing hydrophobic end block lengths. Typically at 20 °C, the sizes of micelles of **p(M1-NIPAM-M1#34)** are slightly larger than those of **p(M1-NIPAM-pM1#17)**, likely because of the high content of hydrophobic end block in **pM1#34 > pM1#17**. Consequently, the micelles formed from **p(M1-NIPAM-M1#34)** should have larger cores compared to those resulting from **p(M1-NIPAM-M1#17)**.

## 4.5.4 DLS of p(M2-NIPAM-M2) (BAB) triblock block copolymers

Similar to **p(M1-NIPAM-M1)**, **p(M2-NIPAM-M2)** exhibits the same trend of the hydrodynamic diameter as a function of temperature, Figure 4.20.

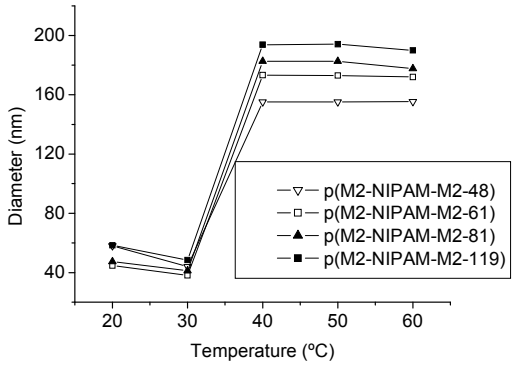


**Figure 4.20 Evolution of the hydrodynamic diameter ($D_h$) as a function of temperature for 1g/L of aqueous solutions of p(M2-NIPAM-M2).**

In all cases the diameters of the particles formed by the polymers **p(M2-NIPAM-M2)** vary between 30 and 60 nm with polydispersity indexes between 0.10 and 0.60 at 20 °C (Figure 4.20 and Table 4.1). These data indicate the formation of micelles with a small polystyrene core and an extended **PNIPAM** shell. The increase of temperature up to 60 °C leads to a substantial increase in the particle size of the polymeric micelles with narrow polydispersity indexes (120 and 200 nm and PDI between 0.02 and 0.05, Table 4.1). This behaviour reveals intermicellar interactions leading to cluster structures with high hydrodynamic diameter.

Whereas a direct comparison of all samples of the series is difficult due to their different molar masses, a comparison between **p(M2-NIPAM-M2#22)** and **p(M2-NIPAM-M2#30)**, which have **PNIPAM** block with similar molar masses is instructive. The particle sizes increased with the hydrophobic end blocks length. **p(M2-NIPAM-M2#22)** makes aggregates with a hydrodynamic diameter of 32 nm at 20 °C and 120 nm at 60 °C, while aggregates of **p(M2-NIPAM-M2#30)** show hydrodynamic diameter of 30 nm at 20 °C and 150 nm at 60 °C. Accordingly, the micelles increase in size with increasing **pM2** content. This is in good accordance with the work of Liu et al.[281] They studied the effects of block lengths on the association of triblock copolymers of poly(ethylene oxide) (**PEO**) and poly(butylene oxide) (**PBO**) in aqueous solution including: **$PBO_5$-$PEO_{91}$-$B_5$**, **$PBO_6$-$PEO_{46}$-$PBO_6$**, **$PBO_7$-$PEO_{22}$-$PBO_7$**, **$PBO_{10}$-$PEO_{27}$-$PBO_{10}$**, and **$PBO_{12}$-$PEO_{260}$-$PBO_{12}$**. They reported that the hydrodynamic radius of the micelles increases with the length of the hydrophobic **PBO** block.

To gain insight into the effect of the triblock architectures **ABA** and **BAB**, it is interesting to compare the behaviour of **p(M2-NIPAM-M2#30)** and **p(M6-NIPAM-M6#30)**, since both block copolymers have the same hydrophobe content (Table 4.1). Looking at the hydrodynamic diameters below and beyond the cloud point, the size of the particles is similar (30 and 31 nm). This suggests that the overall size of the hydrophobic blocks rather than the triblock architecture determines the micelles formed.

## 4.5.5 DLS of p(M3-NIPAM-M3#16) (BAB) triblock block copolymers

The micellization behaviour of the **p(M3-NIPAM-M3#16**) block copolymer as function of temperature is depicted in Figure 4.21 (Table 4.1). The general picture that emerges is the same as described for the above series. Typically, the hydrophobic diameter of the aggregates

is smaller at 20 °C and increases up to 60 °C. The former is attributed to disperse micelles formed with cores made of poly(3,5-dibromobenzyl acrylate ) **(pM3)** and a shell of **PNIPAM**, whereas the latter corresponds to the association of many micelles. Although the **pM3** block is less hydrophobic than **pM1** or **pM2**, its hydrophobicity is enough to induce formation of microdomains at low and high temperatures.

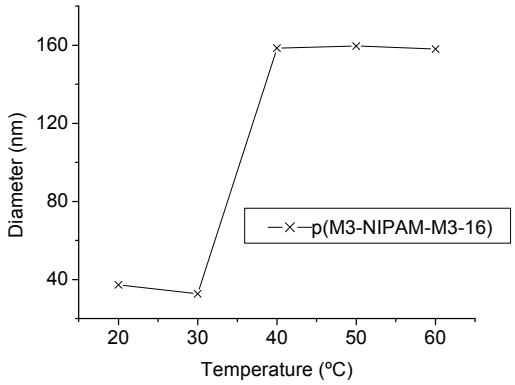


**Figure 4.21 Evolution of the hydrodynamic diameter ($D_h$) as a function of temperature for 1g/L of aqueous solutions of p(M3-NIPAM-M3#16).**

## 4.5.6 DLS of p(M4-NIPAM-M4) (BAB) triblock block copolymers

The data of micellization of the **p(M4-NIPAM-M4)** block copolymers show the same general behaviour over the temperature range investigated. The variation of the hydrodynamic diameters of the **p(M4-NIPAM-M4)** block copolymers is presented as a function of temperature in Figure 4.22.

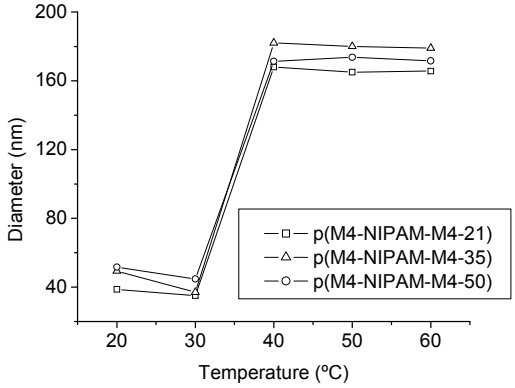


**Figure 4.22 Evolution of the hydrodynamic diameter ($D_h$) as a function of temperature for 1g/L of aqueous solutions of p(M4-NIPAM-M4).**

At low temperature, the **p(M4-NIPAM-M4)** block copolymers form also micelles with size in the range of 36-55 nm for hydrodynamic diameter (Table 4.1). Upon increasing the temperature, the block copolymer micelles show aggregate formation. As for series **p(M2-NIPAM-M2)**, the hydrodynamic diameters of the block copolymer micelles increases with increasing the molar mass in the series **p(M4-NIPAM-M4)**. The size of the micellar clusters formed above the cloud point is about the same, however.

Concerning the influence of the hydrophobic monomers used, a comparison of **p(M3-NIPAM-M3#16)** and **p(M4-NIPAM-M4#21)** seems instructive, since both block copolymers have almost the same degree of polymerisation. Both polymers form micelles with comparable hydrodynamic diameters of 36-37 nm at 20 °C, and of 155-165 nm at 60 °C, respectively. As both blocks differ from each other by the level of hydrophobicity, the size of the micelles seems to be mostly influenced by the length rather than by the hydrophobicity of the **B** blocks.

## 4.5.7 DLS of p(M5-NIPAM-M5) (BAB) triblock block copolymers

The final variation of the hydrophobic blocks concerns the polymeric solutions of **p(M5-NIPAM-M5)**. The results of the DLS studies are included in Figure 4.23 (and Table 4.1). There was no difference in the general appearance of the hydrodynamic diameter as a function of temperature compared to the other series. Again, the micelles tend to become larger with the higher hydrophobic content. The results of this series support once again the conjecture that the size of micelles is determined by the hydrophobic end blocks.

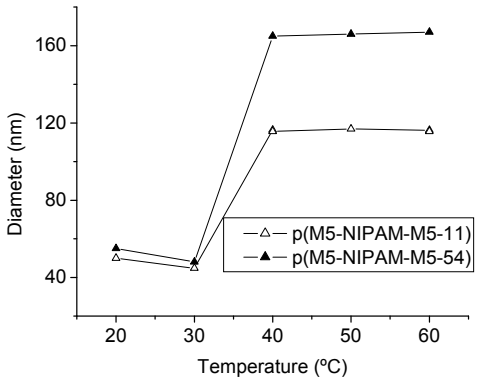


**Figure 4.23 Evolution of the hydrodynamic diameter ($D_h$) as a function of temperature for 1g/L of aqueous solutions of p(M5-NIPAM-M5).**

The main results concerning the aggregation of block copolymers in dilute aqueous solutions are summarized in the following: all samples show different aggregate sizes at the temperatures (20 to 60 °C) studied. The colloids are small below the cloud point and large above it. This is observed for all block copolymers studied, independently of how big the particles are. In contrast, below the cloud point, pure **PNIPAM** exists as unimers, while the **ABA** and **BAB** block copolymers form micelles with a hydrophobic core and a **PNIPAM** corona. Above the cloud point, **PNIPAM** unimers associate to form larger aggregates compared to those obtained from the associating micelles of the block copolymers. Apparently, when aqueous solutions of pure **PNIPAM** are heated to high temperatures, the polymer collapses to generate mesoglobular aggregates, due to attractive polymer-polymer interactions. The situation is different when the block copolymer micelles are heated above the cloud point, as they aggregate into dense micellar clusters.

Within a series of block copolymers, the hydrodynamic diameters of the aggregates generally increase with increasing length of the hydrophobic block for a given copolymer series. Also, it seems that for a given length of the hydrophobic blocks, the size of the aggregates increases with **pM2** < **pM3** < **pM1** < **pM5**, i.e. with the size of the repeat unit. Comparing **p(NIPAM-M2-NIPAM-1)** and **p(NIPAM-M2-NIPAM-2)** of Table 4.1 with **p(M2-NIPAM-M2#22)** and **p(M2-NIPAM-M2#30)**, i.e. comparing triblock copolymers **ABA** with **BAB** of analogous composition, the aggregate sizes are the same within the accuracy of the data.

Even when more concentrated solutions up to 20 wt% of the copolymers were studied, only monomodal distributions of small aggregates were observed. Different from reports on other **BAB** triblock copolymers, such as poly(butylene oxide)-poly(ethylene oxide)-poly(butylene oxide), or poly(styrene oxide)-poly(ethylene oxide)-poly(styrene oxide), no indication for the formation of micellar clusters was found. The apparent hydrodynamic diameters of the aggregates decrease with increasing concentration, as is typical for repulsive hard spheres.

## 4.6 Conclusions

The self-assembly of amphiphilic triblock copolymers **ABA** and **BAB** synthesised in Chapter 3, bearing **PNIPAM** as thermoresponsive moiety, was studied by turbidity and DLS. Due to the combination of relatively small hydrophobic blocks and much longer hydrophilic **PNIPAM** block, all copolymers made could be dispersed directly in water to give clear mixtures.

The turbidity measurements showed that for the pure **PNIPAM** samples, only a small hysteresis is observed in the thermally induced aggregation and disaggregation when passing the cloud point, while a marked hysteresis is found for the block copolymers. The hysteresis is explained by the hindrance of reswelling of the collapsed **PNIPAM** shells once the polymer micelles have formed clusters at temperatures high enough above the cloud point, which need some time to disentangle and thus to allow the hydrophilic shell of the micelles to recover their fully swollen state.

It is worth noticing that the cloud points measured in the heating runs are virtually the same within experimental precision for reference samples of **PNIPAM** homopolymer as well as the entire block copolymers investigated, independent of the presence, the nature and the length of the hydrophobic blocks. This finding corroborates the particular usefulness of **PNIPAM** as thermo-sensitive block for potential applications, as the cloud point varies hardly with concentration and molar mass, or end-groups, if concentration and molar mass exceed a minimum value.

Dynamic light scattering measurements showed the presence of small aggregates, with hydrodynamic diameters in the range of about 40 to 70 nm at ambient temperature, with a certain polydispersity. The hydrodynamic diameters seemingly increase with increasing length of the hydrophobic block within a given copolymer series, whereas the effect of different sizes of the **PNIPAM** middle block seems to be only of minor importance in the molar mass range studied. The small hydrodynamic diameters suggest that aggregates formed are micelles, rather than vesicles or micellar clusters.

Although being insoluble above the cloud point, the polymers did not precipitate from the solutions, but formed stable larger aggregates of well-defined size. The reasons for this behaviour are not fully clear yet. One may speculate that kinetic effects play a role, and that the tethering of both ends of the thermo-sensitive block on the micellar surface hinders the growth of larger clusters made of collapsed micelles. The contribution of kinetic effects induced by the presence of the hydrophobic blocks to the self-organization is evident from the cooling runs of the turbidimetric studies.

*"If we knew what it was we were doing, it would not be called research would it?" Albert Einstein*

# *CHAPTER 5: Hydrogel Formation of Thermoresponsive BAB Copolymers Containing Poly(N-isopropylacrylamide) as Hydrophilic Middle Block*

In Chapter 4, the reversible thermoresponsive behaviour of the **BAB** containing poly(N-isopropylacrylamide) as hydrophilic **A** middle block aggregate was studied in dilute and semi-concentrated aqueous solutions. It was found that the cloud point for the copolymers was nearly identical to the cloud point of the homopolymer (30-32 °C) and that small micelles are formed below the cloud point temperatures, while large aggregates are obtained above the cloud points.

Here, the influence of the hydrophobic end blocks on the hydrogel formation and the thermo-sensitive rheological behaviour was investigated, by varying the length and the nature of the hydrophobic **B** end blocks, namely polystyrene, poly(2-ethylhexyl acrylate) and poly(*n*-octadecyl acrylate). The mechanical strength was found to increase with the hydrophobicity of the end blocks, either by increasing their length, or by using a more hydrophobic monomer. Because of the thermo-sensitivity of the poly(N-isopropylacrylamide) as hydrophilic middle block, all systems exhibit a cloud point at 30-32 °C, which stays nearly constant in the concentration range of 0.01 - 50 wt% block copolymer. Heating beyond the cloud point initially favours hydrogel formation, but continued heating results in macroscopic phase separation.

# 5.1 Introduction

In Chapter 4, it was shown that aqueous solutions of **PNIPAM** and its corresponding symmetrical triblock copolymers exhibit a lower critical solution temperature (LCST) around 30-35 °C. Different from many other non-ionic polymers (such as polyethylene oxide), **PNIPAM** is also characterised advantageously by a weak dependence only of the transition temperature ("cloud point") on concentration and molar mass.[26, 282] Here, the preliminary studies focussing on thermal behaviour of **BAB** copolymers in dilute and semi-concentrated aqueous solutions (Chapter 4) are extended to highly concentrated solutions. These copolymers have **PNIPAM** as a long thermo-sensitive hydrophilic **A** middle block and two strongly hydrophobic **B** outer blocks. While keeping the chemical nature of the hydrophilic block **A** constant by using always **PNIPAM**, the nature and the lengths of the hydrophobic **B** blocks were varied broadly. The variation was aimed at exploring the influence of the hydrophobic block on the micellization and the gel behaviour as well as on the phase transition of the amphiphilic **BAB** copolymers. As hydrophobic **B** blocks, polystyrene **pM2**, poly(2-ethylhexyl acrylate) **pM4**, and poly(octadecyl acrylate) **pM5** were studied (see Chapter 4). The strongly hydrophobic **pM2** shows a high glass transition temperature $T_g$ of about 105 °C[283] and the strongly hydrophobic polyacrylate **pM4** is known for its very low $T_g$ of about -50 °C.[284] The glass transition of **pM5** was reported to occur in the intermediate temperature range, too, with a $T_g$ of about 57 °C.[285] However, due to the long alkyl side chains that confer extreme hydrophobicity to the polymer, **pM5** is semi-crystalline with a melting point of the side chains of ca. 48 °C.[285] This variation was aimed at exploring the influence of the hydrophobic block on the phase transition as well as on the gel behaviour of the amphiphilic **BAB** copolymers. Gel formation was studied by the tube inversion method and by rheological measurements, revealing sol to gel transitions, as well as gel to macrophase separation transitions with increasing temperature of the formed micellar hydrogels.

# 5.2 Partial Phase Diagram by Tube Inversion Method (TIM)

In a first, qualitative survey, the sol-gel and gel-macrophase separation transitions of the amphiphilic triblock copolymers in water were investigated by the tube inversion method (TIM) in the temperature range of 5- 45 °C. Figure 5.1 exemplifies the resulting partial phase

diagrams for the three copolymer classes studied **p(M2-NIPAM-M2)**, **p(M4-NIPAM-M4)**, and **p(M5-NIPAM-M5)**, together with the reference **PNIPAM-1**.

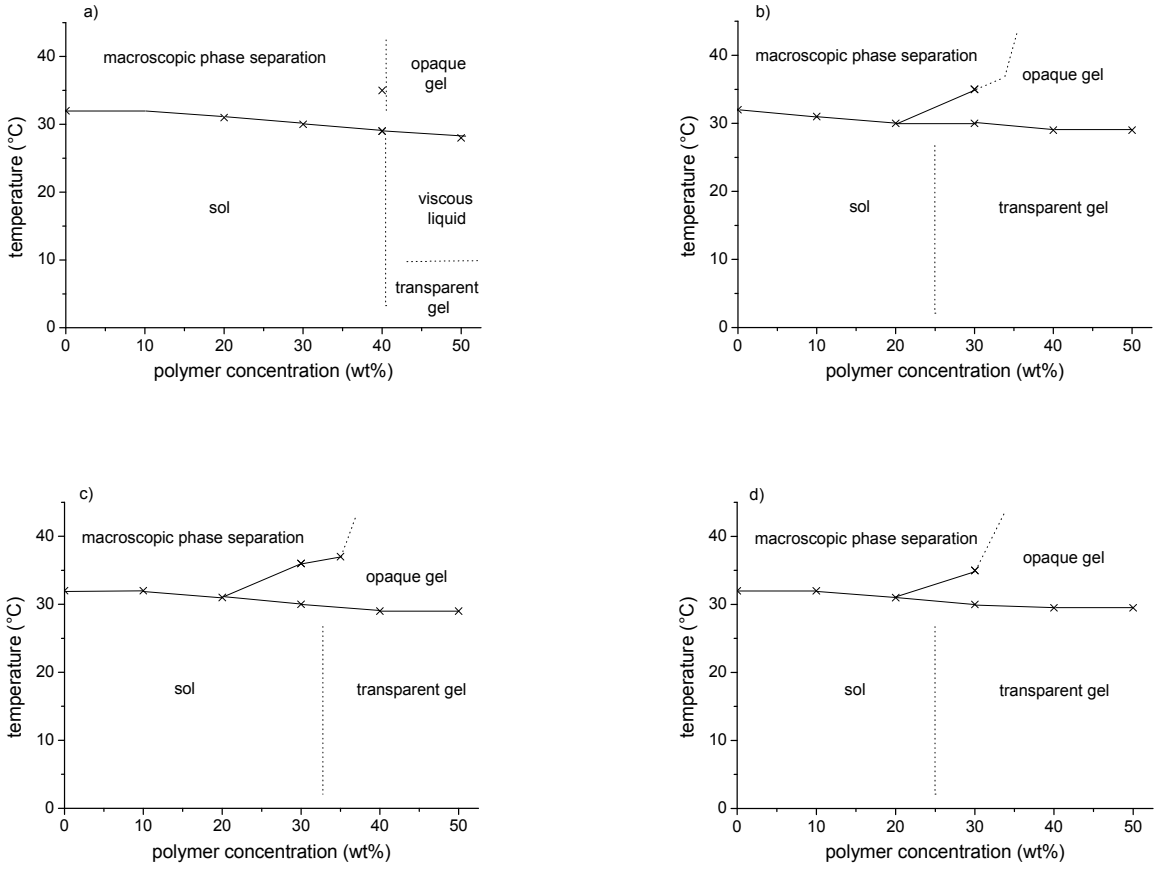


**Figure 5.1 Partial phase diagrams of amphiphilic BAB triblock copolymers in water. (a) PNIPAM-1, (b) p(M2-NIPAM-M2#48), (c) p(M4-NIPAM-M4#50), (d) p(M5-NIPAM-M5#11).**

Figure 5.1 illustrates that the homopolymer requires the highest concentrations to form visually a gel. In the molar mass range given, aqueous solutions of **PNIPAM-1** visually do not even gelify at ambient temperature at concentrations of 50 wt%, but form only highly viscous liquids (Figure 5.1a). Gel formation is only seen below 10 °C. Inevitably, the systems are thermo-sensitive, becoming cloudy above 28-32 °C. The cloud point changes only weakly in the concentration range of 1 - 50 wt% studied, in agreement with the literature.[26, 282] For concentrations below 40 wt%, macroscopic phase separation is observed above the cloud point. Interestingly, the viscosity of the sols increases notably when reaching the cloud point. For the highest concentrations studied, an opaque gel is formed above the cloud point.

Looking at the behaviour of the micellar solutions of the various **BAB** block copolymer by TIM, the differences to the behaviour of the homopolymer are obvious. Though high

concentrations are required, typically of 30-40 wt%, the copolymer solutions gelify beyond a certain concentration at ambient temperature, as exemplified in Figure 5.1b-d. All copolymer systems are thermo-sensitive in the temperature range studied. At concentrations below 30 wt%, i. e. when the copolymer micellar solutions form a sol, the polymers precipitate above a cloud point of about 32 °C and undergo macroscopic phase separation. Again, the transition temperature of the copolymers is remarkably close to the cloud point of **PNIPAM** homopolymer even at these high concentrations, independent of the nature of the hydrophobic end blocks. At concentrations above 35-40 wt%, opaque gels are formed above the cloud point, which is now slightly lowered to about 28 °C. At these high concentrations, the opaque gels do not phase separate visually even on annealing in the studied temperature range, i.e. temperatures below 45 °C. In contrast, phase separation of the opaque gels upon further heating beyond 35-37 °C is observed when the copolymer concentration is reduced to about 30-35 wt%, i.e. when the concentration is only slightly higher than the minimum value needed to give a gel. Particular to samples **p(M4-NIPAM-M4)**, the intermediate formation of opaque hydrogels was observed within a narrow temperature window between 30 and 35 °C, though no clear gel was formed, in a transition regime with concentrations of about 30 wt%. This opaque hydrogel phase separates the sol state from the phase separated regime (Figure 5.1c).

Comparing copolymers of a given series, **p(M2-NIPAM-M2)** or **p(M4-NIPAM-M4)**, the general appearance of the phase diagrams is the same within a series, but the minimum concentration for gel formation decreases somewhat with increasing length of the hydrophobic blocks. In the series **p(M2-NIPAM-M2)**, gels are formed at 30 wt%, but not yet at 20 wt% concentration. In the series **p(M4-NIPAM-M4)**, samples **p(M4-NIPAM-M4#21)** and **p(M4-NIPAM-M4#35)** need concentrations as high as 40 wt% to form a gel, and only copolymer **p(M4-NIPAM-M4#50)** with the longest hydrophobic **B** blocks gels already at 35 wt%.

Comparing the three copolymer series for a given length of the hydrophobic block, the results demonstrate that the series **p(M2-NIPAM-M2)** and **p(M5-NIPAM-M5)** form gels typically between 20 and 30 wt% polymer, while the concentration needed in the case of series **p(M4-NIPAM-M4)** is somewhat higher, between 30 and 40 wt%.

Clearly, the gelling behaviour of block copolymers differs from the behaviour of the **PNIPAM** homopolymer. This and the observed differences within, as well as between, the analogous series indicate that the cores of the micelles contribute to the gel formation,

presumably acting as weak crosslinking sites. Increasing the length of the hydrophobic micelle forming blocks favours gelation. Still, an increased hydrophobicity of the end blocks seems not to be the determining factor. This is demonstrated by comparing copolymers with similar length of the end blocks, such as **p(M2-NIPAM-M2#48)** and **p(M4-NIPAM-M4#50)**. As the latter copolymer is less efficient in forming hydrogels, although **M4** is more hydrophobic than **M2**, the lower efficiency of the **pM4** block may be rather ascribed to its lower glass transition temperature. The influence of both nature and length of the hydrophobic blocks for a given length of the hydrophilic block implies, that at least some bridging of micelles by amphiphilic **BAB** triblock copolymers[286-288] should occur in these systems, and contributes to their behaviour. Nonetheless, the high concentrations needed to achieve gelation for all the block copolymers investigated suggest that only a small percentage of them are involved in micelle bridging, so that the effect plays only a minor role for gelation.

These findings that high concentration of **BAB** block copolymer are needed for forming hydrogels, is contrast with the recent report of Nykänen et al.[213] on aqueous mixtures of analogous copolymers **p(M2-NIPAM-M2)** with similar compositions to samples **p(M2-NIPAM-M2#48)** to **p(M2-NIPAM-M2#119)**, for which highly swelling hydrogels were inferred. However, a closer inspection shows that the reported systems were studied far from hydration equilibrium (1h immersion in excess water), and it is not clear whether the amount of bound water is due to true swelling or at least in parts due to physical trapping in/on the samples. Alternatively it is possible, that the samples became chemically cross-linked during the annealing procedure (3-4 days at 180 °C) applied prior to swelling experiments, thus changing the mechanism of hydrogel formation completely. Chemical crosslinking is possible e.g. via the -COOH end-groups present in these samples, or as a follow-up of thermal elimination of the thiocarbonyl groups under these harsh conditions.[289-292]

The comparison with the few other studied **BAB** triblock copolymers studied with respect to their gelling in water, in particular of **PPO-PEO-PPO**,[286-288] **PBO-PEO-PBO**,[287, 293, 294] or poly(lactide)-poly(ethylene oxide)-poly(lactide) gels,[295] but also to poly(isotactic **NIPAM**)-poly(atactic **NIPAM**)-poly(isotactic **NIPAM**) gels,[296] is instructive. These polymers with relatively weak hydrophobic blocks compared to the polymers studied here, gel already at concentrations of 5-10 wt% for lengths of the hydrophilic middle block, which are similar to the ones of the **BAB** block copolymers studied. Similarly, **PNIPAM** α,ω-end-capped simply with two octadecyl chains forms hydrogels at concentrations of 5-10 wt%, too.[297] These

different performances might seem surprising at first sight, but go well along with theoretical and modelling studies on micelle forming **BAB** block copolymers,[16] when assuming a weak segregation regime for **PBO** and poly(lactide) as hydrophobic blocks,[287] and a strong segregation regime in the case of **pM2**, **pM4** and **pM5**.[16] Accordingly, the strongly hydrophobic character of these blocks interferes with the formation of temporary networks of the hydrophobic chains. The probability of the strongly hydrophobic chains to leave the micellar core and to associate with other "dangling" hydrophobic chains in the solution, or to insert in a neighbouring micellar core, becomes so low, that the total number of cross-links in form of bridged micelles stays small.

In Figure 5.1, it is interesting to note, that the tendency to form gels seems to be enhanced at the onset of phase separation of the **PNIPAM** block, when the systems become opaque. Only at markedly higher temperatures, macroscopic phase separation with a break down of the macroscopically coherent gel is observed. This finding may be explained by two counteracting effects. On the one hand, the strongly decreasing solvent quality of water for the **PNIPAM** blocks above the cloud point results in an increasing number of intra- and interpolymeric hydrophobic contacts. The latter ones act as cross-linking points that strengthen the gels. On the other hand, increasing dehydration makes the swollen **PNIPAM** coils contract until a space-filling network of micelles cannot be maintained anymore. With increasing difference to the phase transition temperature, the second effect becomes more important and results in the observed temperature profile. Alternatively, these observations may be attributed to an increased share of micelle bridging copolymers, as discussed for analogous **BAB** amphiphilic copolymers poly(lactide-block-ethylene oxide-block lactide).[295] However, the latter explanation seems unlikely considering that the general thermal effects are the same for the copolymer series **p(M2-NIPAM-M2)** and **p(M4-NIPAM-M4)**, albeit their hydrophobic blocks have strongly differing glass transition temperatures $T_g$, namely much above and much below the cloud point. A much more marked increase of micelle bridging copolymers would be expected for the series **p(M4-NIPAM-M4)** with the low $T_g$, which is not the case.

## 5.3 Rheological properties of concentrated solutions of BAB block copolymers

Following the qualitative tests by TIM, the rheological behaviour of the concentrated polymer solutions was studied in more detail. First, they were subjected to flow shear tests at 25 °C.

Typical flow curves with the apparent viscosity (stress divided by shear rate) as a function of the shear rate are shown for 30 wt% solutions in Figure 5.2.

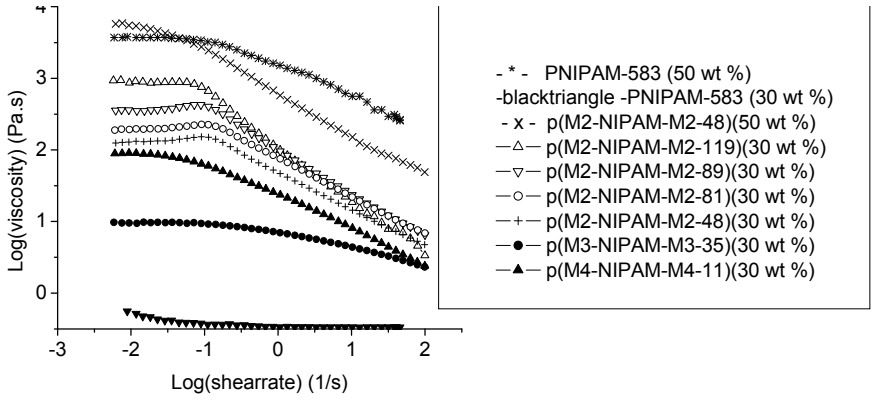


**Figure 5.2 Shear rate dependency of the apparent viscosities of hydrogels formed at 25 °C by aqueous solutions of: (+) = 30 wt% of p(M2-NIPAM-M2#48), (x ) = 50 wt% of p(M2-NIPAM-M2#48), (o) = 30 wt% of p(M2-NIPAM-M2#81), (▽) = 30 wt% of p(M2-NIPAM-M2#89), (Δ) = 30 wt% of p(M2-NIPAM-M2#119), (●) = 30 wt% of p(M4-NIPAM-M4#35), (▲) = 30 wt% of p(M5-NIPAM-M5#11), (▼) = 30 wt% of PNIPAM, (✳) = 50 wt% of PNIPAM-1**

All copolymer samples showed Newtonian behaviour, i.e. nearly constant viscosity, at shear rates below about 0.1 $s^{-1}$, while shear thinning is observed for higher shear rates. In the series **p(M2-NIPAM-M2)**, the onset of the shear thinning regime is anticipated by a small dilatant maximum. The viscosity depends on the length and the chemical nature of the hydrophobic blocks. The series **p(M2-NIPAM-M2)** illustrates that for a given concentration, viscosity increases with the length of the hydrophobic blocks. The comparison of copolymer samples, which all contain about 10 wt% of hydrophobic outer blocks, demonstrates the influence of the chemical nature of the latter. The viscosities increase with **p(M4-NIPAM-M4#35)** < **p(M5-NIPAM-M5#11**) < **p(M2-NIPAM-M2#48)**. This sequence does neither correlate with the hydrophobicities of the blocks, which is **pM2** < **pM4** < **pM5**, nor with the lengths of the blocks, but may be related to their increasing glass transition temperatures (-50 °C < 57 °C < 105 °C).

As also exemplified in Figure 5.2, the viscosity increases markedly with the concentration rising from 30 to 50 wt%, as is expected. This effect is much more pronounced for the homopolymer **PNIPAM** than for the amphiphilic copolymers, in agreement with the results of the TIM studies (see Figure 5.1). While for 30 wt% solutions, the viscosity of the homopolymer is much lower than of the block copolymer, viscosities at 50 wt% solutions of **PNIPAM-1** and **p(M2-NIPAM-M2#48)** are comparable for low shear rates. Shear thinning

of **PNIPAM** solutions is much less pronounced than of block copolymer solutions, for which the effect increases with increasing length of the hydrophobic block (Figure 5.2). Accordingly, the shear thinning effect may be mainly attributed to a local restructuring and disruption of micelles with increasing shear.[99] It may be speculated that the disruption of flower-like micelles initially induces a slight increase in the share of bridged micelles, thus accounting for the small dilatant maximum, before a gradual breakdown of the associative network structure occurs at even higher shear deformation.

Next, the concentrated polymer solutions were subjected to dynamic oscillation stress ramping. Figure 5.3 exemplifies the linear viscoelastic regime found for a stress smaller than 10 Pa, over which the storage modulus G' is independent of the applied stress.

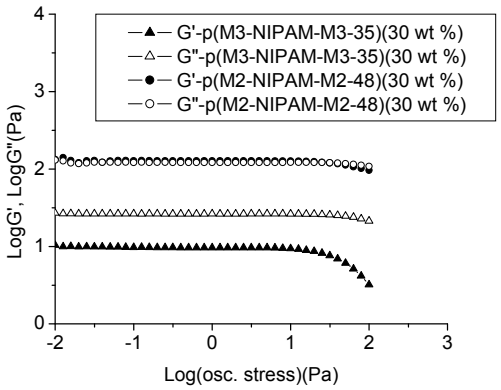


**Figure 5.3 Oscillation shear stress (at 1 Hz) of the storage modulus G' (solid symbols) and loss modulus G" (open symbols) of 30 wt% hydrogels at 25 °C. (o, ●) = p(M2-NIPAM-M2#48), (Δ, ▲) = p(M4-NIPAM-M4#35)**

In order to stay in the viscoelastic regime, all following experiments, which explored the dynamic viscoelastic properties, were conducted with an oscillating shear stress of 5 Pa.

Figure 5.4 shows the storage modulus G' and loss modulus G" plotted against angular frequency ω for the 50 wt% aqueous solution of **PNIPAM-1** at 25 °C.

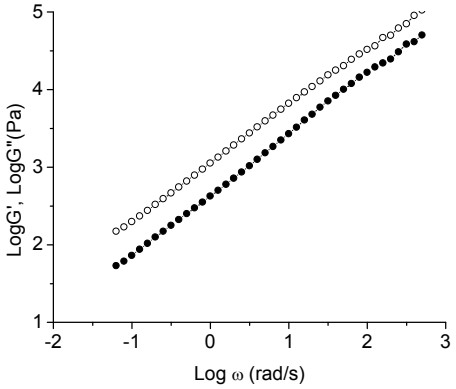


**Figure 5.4 Frequency dependence of the dynamic moduli of 50 wt% aqueous solutions of PNIPAM-1 at 25 °C at 5 Pa oscillatory stress: solid symbol = storage modulus G', open symbol = loss modulus G").**

Even at this high concentration, the frequency dependencies of G' and G" are almost parallel over the full frequency window studied, with G" larger than G', and tan $\delta \geq 1$. This behaviour is considered characteristic for a viscous liquid.[298] These findings agree with the visual inspection by TIM experiments, which reveal the formation of a highly viscous solution even at this high concentration (see Figure 5.1a).

The situation is quite different for the block copolymer solutions, as illustrated by copolymer series **p(M2-NIPAM-M2)** (Figure 5.5). As shown for sample **p(M2-NIPAM-M2#48)**, the general increase of both G' and G" with the concentration is more pronounced for the storage modulus G' (Figure 5.5a). Consequently, at 20 wt%, the frequency dependencies of G' and G" are parallel, with G" larger than G', indicating viscous liquid-like behaviour. Increasing the concentration to 30 wt%, G' and G" become of similar size, but G' is less frequency dependent than G". Therefore, G' is slightly smaller than G" at low frequencies, but slightly larger than G' at high frequencies, indicating soft gel behaviour. Increasing the concentration further to 50 wt%, the frequency dependence of G' is even more reduced, and G' is generally larger than G', indicating hard gel behaviour. This behaviour agrees very well with the visual inspection by TIM experiments (see Figure 5.1b). A similar effect to increasing the concentration is obtained, when increasing the length of the hydrophobic blocks for a given block copolymer concentration (Figure 5.5b).

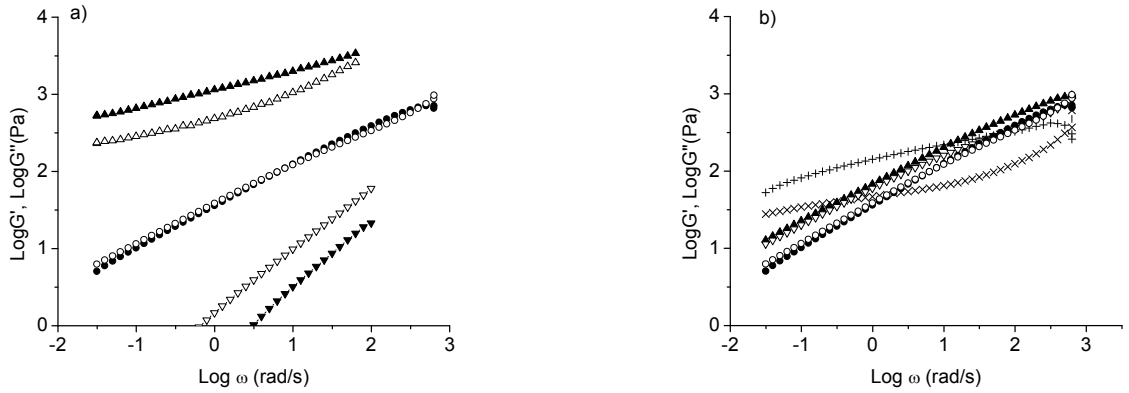


**Figure 5.5 Frequency dependence of the dynamic moduli of aqueous micellar solutions made from BAB triblock copolymers p(M2-NIPAM-M2) at 5 Pa oscillatory stress at 25 °C. a) Influence of the copolymer concentration on hydrogel formation of p(M2-NIPAM-M2#48): (▼, ▽) = 20 wt%, (●, o) = 30 wt%, (▲, Δ) = 50 wt%. Solid symbols = storage modulus G', open symbols = loss modulus G". b) Influence of the length of the hydrophobic blocks of 30 wt% hydrogels of p(M2-NIPAM-M2#48) (●, o), p(M2-NIPAM-M2#89) (▲,▽), and p(M2-NIPAM-M2#119) (+, x) at 5 Pa oscillatory stress at 25 °C: Solid symbols and "+" = storage modulus G', open symbols and "x" = loss modulus G".**

While at 30 wt%, **p(M2-NIPAM-M2#48)** behaves as a soft gel, in the case of **p(M2-NIPAM-M2#89)** G' is slightly higher than G" in the full frequency range studied and is notably higher in the case of **p(M2-NIPAM-M2#119)**, thus demonstrating the continuous shift from a soft gel to a hard gel behaviour.

The evolution of the **BAB** block copolymer solutions from viscous liquid via soft gel to hard gel behaviour with increasing concentration is also reflected in the temperature dependence of the dynamic moduli (Figure 5.6). Below the cloud point, both storage modulus G' and loss modulus G" decrease continuously with the temperature. At all concentrations, the passing over the cloud point at 30-32°C is accompanied by a marked initial increase of both moduli, which levels off with further heating up to 45 °C. However, the relative increase of the moduli is much higher for lower concentrations. Importantly, the values of G'and G" become close above the cloud point (and also during almost the whole cooling cycles even if both moduli differ notably at the beginning of the experiment (Figure 5.6a) ). This induces the transition from a viscous liquid-like to a soft gel behaviour at intermediate block copolymer concentrations. The hysteresis of the heating and cooling cycles increases with decreasing concentration, which is not surprising considering the increasing tendency for macroscopic phase separation (cf. Figure 5.1b). Again, the behaviour studied by rheology agrees well with the visual inspection by TIM experiments (see Figure 5.1b). Note that at the highest concentrations of 50 wt%, the general appearance of the temperature dependence of the

moduli is very similar for the amphiphilic triblock copolymer and the pure **PNIPAM** (Figure 5.6d), though the absolute values differ and G" is higher than G'.

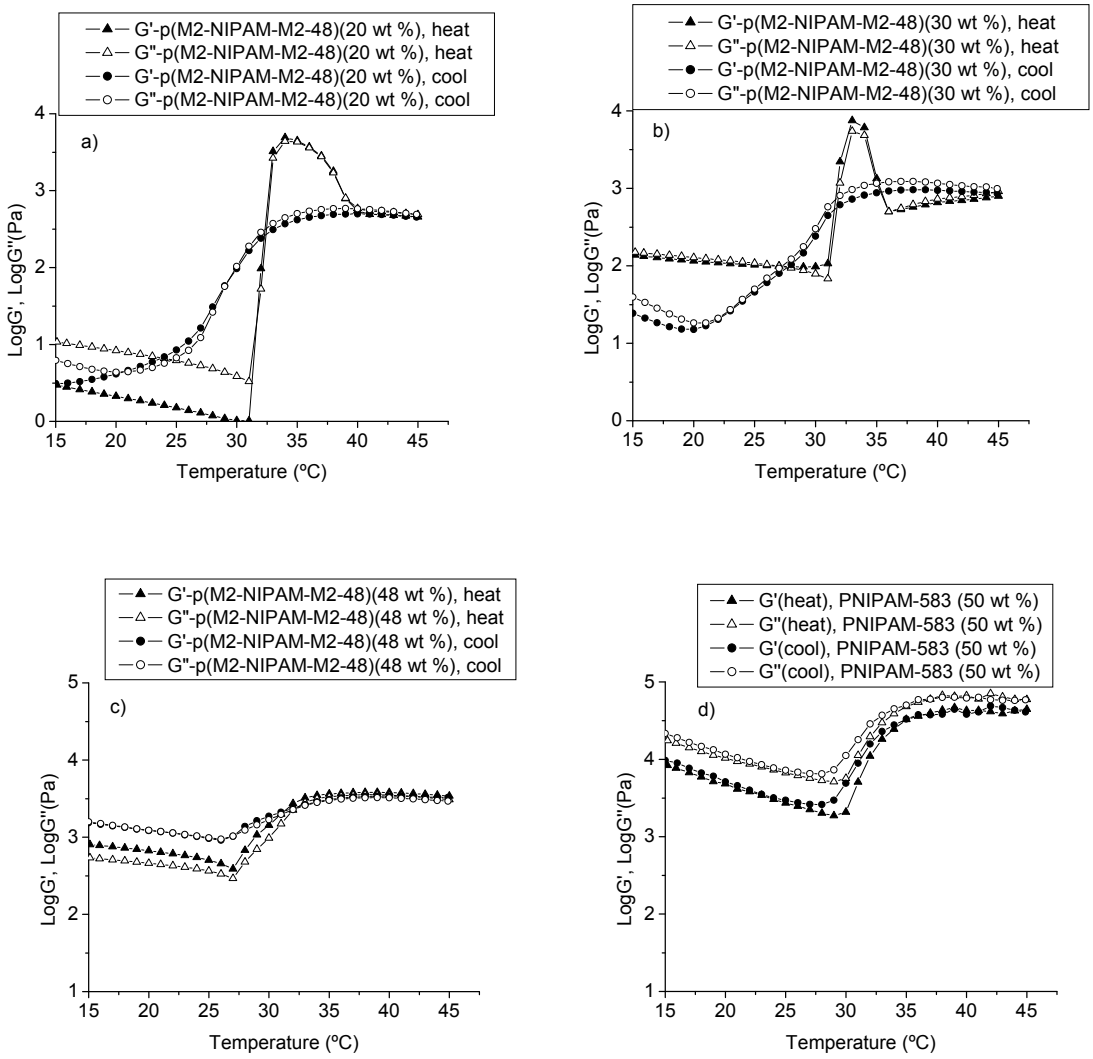


**Figure 5.6 Temperature dependence of the dynamic moduli of aqueous solutions at 5 Pa oscillatory stress and the frequency of 1 Hz: (a) of p(M2-NIPAM-M2#48) at 20 wt%, (b) of p(M2-NIPAM-M2#48) at 30wt% (c) p(M2-NIPAM-M2#48) at 50 wt%, and (d) PNIPAM at 50 wt%. Solid symbols = storage modulus G', open symbols = loss modulus G". (▲, Δ) = heating curves, (●, o) = cooling curves (heating and cooling rates 2 °C·min-1).**

Still, a closer inspection reveals that below the cloud point, the decrease of the moduli with increasing temperature is stronger for the homopolymer. This difference suggests that the observed decrease of G' and G" is not only related to the standard reduction of viscosity with warming, but may be also attributed to the increasingly reduced solvent quality of water for **PNIPAM** with rising temperatures, already well below the phase transition temperature.

The general features of the rheological behaviour discussed for the series **p(M2-NIPAM-M2)** are also found for the series **p(M4-NIPAM-M4)** (Figures 5.3 and 5.4) and for sample **p(M5-NIPAM-M5#11)** (Figure 5.9). The general increase of both G' and G" with the concentration is more pronounced for the storage modulus G' (Figure 5.7a).

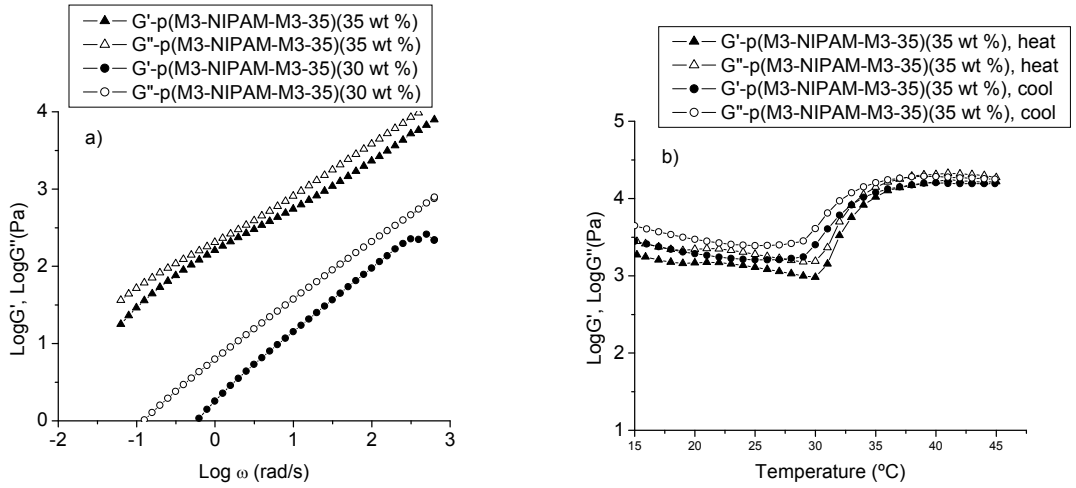


**Figure 5.7 Dynamic moduli of aqueous solutions of p(M3-NIPAM-M3#35) at 5 Pa oscillatory stress. Solid symbols = storage modulus G', open symbols = loss modulus G". (a) Frequency dependence at 25 °C for 30wt% (●, o) and 40 wt% (▲, Δ). (b) Temperature dependence at the oscillatory frequency of 1 Hz for 40 wt% concentration: (▲, Δ) = heating curves, (●, o) = cooling curves ( heating and cooling rates 2 °C·min-1).**

Hence at 30 wt%, the frequency dependencies of G' and G" are parallel for **p(M4-NIPAM-M4#35)**, with G" larger than G', indicating viscous liquid-like behaviour. Increasing the concentration to 40 wt%, G' and G" become of similar size, so that the system is approaching a soft gel behaviour. Alternatively, the behaviour shifts from viscous liquid-like toward gel-like when increasing the length of the hydrophobic blocks (Figure 5.8a). For **p(M4-NIPAM-M4#50)** at 35 wt%, G' is slightly smaller than G" at low frequencies, but becomes slightly larger than G' at high frequencies, indicating the formation of a soft gel. The thermal dependences of the moduli of these samples (Figures 5.7b and 5.8b), i.e. the slow decrease up to the cloud point and the marked increase when passing the cloud point, correspond very well to the behaviour of the soft gel obtained for a 30 wt% solution of **p(M2-NIPAM-M2#48)** as described above. The behaviour of **p(M5-NIPAM-M5#11)** fits well into this general pattern.

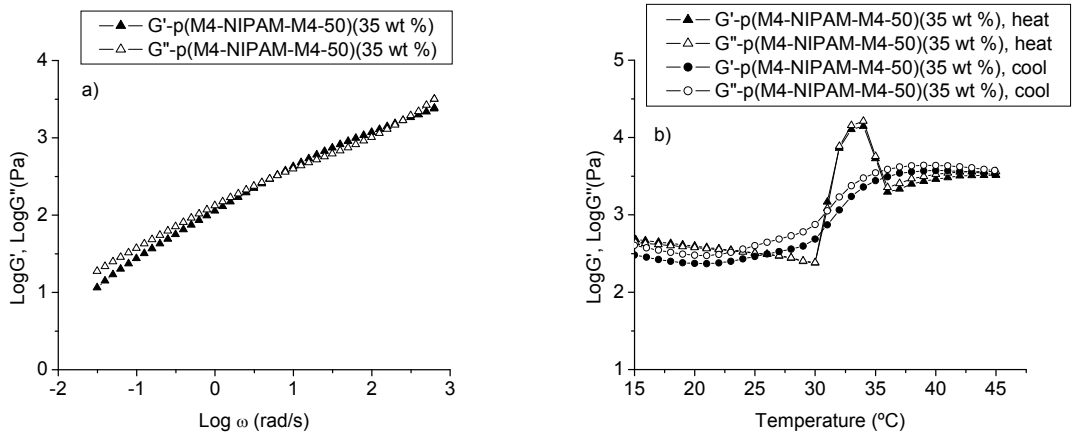


**Figure 5.8 Dynamic moduli of 35 wt% hydrogels of p(M4-NIPAM-M4#50) at 5 Pa oscillatory stress. Solid symbols = storage modulus G', open symbols = loss modulus G". (a) Frequency dependence at 25 °C, and (b) temperature dependence at the oscillatory frequency of 1 Hz: (▲, Δ) = heating curves, (●, o) = cooling curves ( heating and cooling rates 2 °C·min-1).**

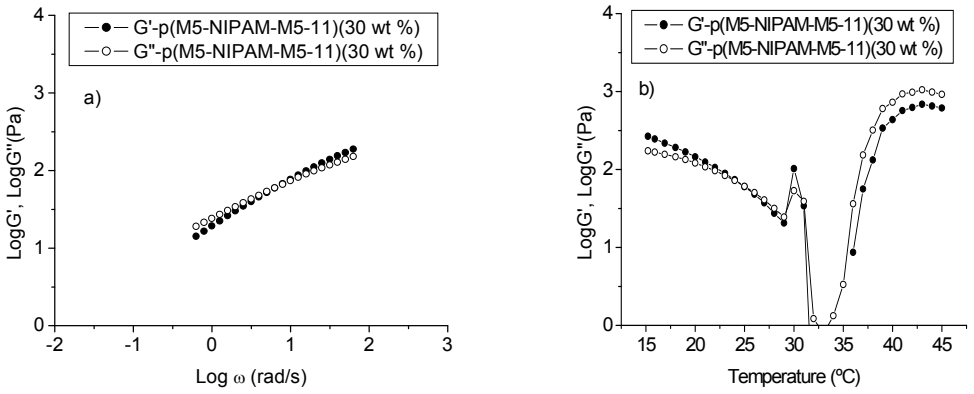


**Figure 5.9 Dynamic moduli of 30 wt% hydrogels of p(M5-NIPAM-M5#11) at 5 Pa oscillatory stress. Solid symbols = storage modulus G', open symbols = loss modulus G". (a) Frequency dependence at 25 °C, and (b) temperature dependence at the oscillatory frequency of 1 Hz: (▲, Δ) = heating curves, (heating rate 2 °C·min-1).**

The 30 wt% solution shows G' to be slightly smaller than G" at low frequencies, but to become slightly larger than G" at high frequencies, indicative of a soft gel (Figure 5.9). The thermal dependences of the moduli exhibits a small decrease until reaching the cloud point, at which both moduli make a jump upwards and then level off.

As for the series **p(M2-NIPAM-M2)**, the rheological behaviour of the block copolymer samples **p(M4-NIPAM-M4)** and **p(M5-NIPAM-M5)** matches well the findings of the TIM experiments (cf. Figures 2c and 2d). The rheological studies confirm that the tendency to form

gels depends not only on the length of a hydrophobic block, but also on its chemical nature, and that it increases with **p(M4-NIPAM-M4)** < **p(M5-NIPAM-M5)** < **p(M2-NIPAM-M2)**. Also, they confirm that the tendency to form hydrogels is enhanced when passing above the cloud point. Note that an analogous pronounced maximum of the shear viscosity was reported for dilute (1g/L) solutions of homopolymer **PNIPAM** at the cloud point, too, albeit an increased viscosity was only found in a very narrow temperature interval of ca 2-3 °C, beyond which the viscosity decreased rapidly to very low values.[299] Possible reasons for the enhanced viscosity shortly above the cloud point, which might seem counter-intuitive at first sight, are discussed above when analyzing the results of the TIM experiments with respect to enhanced gelling in the vicinity of the cloud point. The observation may be understood by the interplay of hydrophobic "sticky" contacts between **PNIPAM** coronas above the cloud point and their decreasing hydration until the space-filling network of micelles breaks apart.

## 5.4 Conclusions

The RAFT method enables the straightforward synthesis of amphiphilic triblock copolymers in only two steps, allowing to vary the nature of the hydrophobic blocks as well as the length of the hydrophobic and hydrophilic blocks broadly. The amphiphilic polymers here are characterised by a long hydrophilic middle block and relatively small, but strongly hydrophobic end blocks. These triblock copolymers associate in dilute and semi-concentrated aqueous solution into small flower-like micelles, while only at high concentrations, hydrogels are formed. This is attributed to the low tendency to form interconnected, bridged micelles despite of the **BAB** architecture, as the strong segregation regime applies for these copolymers due to the strongly hydrophobic end blocks. Accordingly, such triblock copolymers are not particularly efficient as viscosifier or gelling agents. However in turn, they allow to prepare freely flowing polymeric, micellar solutions at concentrations as high as 30 wt%, or even beyond, which is interesting for the effective solubilization of hydrophobic active agents, the more as these solutions are low foaming. The minimum concentration to form hydrogels decreases while their mechanical strength increases with the length of the end blocks. Nevertheless, the glass transition temperature of the hydrophobic blocks seems to be more important than the detailed hydrophobicity of the polymer blocks used, with high glass transitions favouring hydrogel formation and mechanical strength of the gels formed.

The hydrophilic poly(N-isopropylacrylamide) block used renders all systems studied thermo-sensitive. The cloud point for the copolymers was between 28-32 °C and thus varied little in the full concentration range of 0.01-50 wt%, being very close to the cloud point of the homopolymer. The absent effect of the hydrophobic blocks onto the cloud point is attributed to the minimization of hydrophobic contacts by micelle formation. Heating beyond the cloud point initially favours hydrogel formation due to additional interpolymeric hydrophobic contacts of the corona forming middle blocks, but continued heating results in macroscopic phase separation when the space filling network of polymeric micelles collapses due to increasing dehydration of the coronas.

*"Imagination is more important than knowledge. Knowledge is limited. Imagination encircles the world."*

*Albert Einstein.*

# *CHAPTER 6: Micellization of Thermoresponsive BAB Triblock Copolymers Containing Poly(methoxy diethylene glycol acrylate) as Middle Block*

This chapter describes the synthesis of homopolymers and block copolymers **BAB** with the thermoresponsive poly(methoxy diethylene glycol acrylate) **A** block and small hydrophobic **B** end blocks using the RAFT process. The self-organization of these polymers was studied using turbidity and dynamic light scattering. Different cloud points were found. Dynamic light scattering measurements showed the presence of aggregates with sizes depending on temperature. The hydrodynamic diameters increase with increasing length of the hydrophilic and hydrophobic blocks. The rheological behaviour of the block copolymer suggests that the block copolymer associates basically into flower-like micelles, with only a small share of polymers which bridge micelles and thus can act as efficient physical cross-linkers.

# 6.1 Introduction

Polyethylene oxide (**PEO**) or poly(ethylene glycol) (**PEG**) for low molar masses is a polyether that has attracted much attention in the field of biomedical applications mostly because of its biocompatibility and good water solubility. As **PNIPAM**, **PEO** is thermoresponsive in aqueous solution, with a lower critical solution temperature.[300, 301] Up to now, a number of water-soluble triblock copolymers **BAB** made of hydrophobic **B** end blocks and **A** as **PEO** or modified **PEO** block have been developed. Aqueous solutions of several block copolymers show thermoresponsive behaviours which depend sensitively on the balance between the hydrophobic and the hydrophilic blocks. At low temperature and concentration, the block copolymers form flower-like micelles. If the middle block is large, bridge conformations can form. When the temperature is raised, these conformations result from the attachment of the end blocks of linear block cores to different micelles. Such processes are believed to be responsible for the viscoelastic behaviour of the block copolymers.[302] Typical examples include poly(caprolactone-ethylene glycol-caprolactone)(**PCL-PEO-PCL**) triblock copolymers[100] etc. These form transient physical networks at certain temperatures, resulting in hydrogels. For instance, **PCL-PEO-PCL** aqueous solutions show a sol-gel transition sequence with the increase of temperature. Such systems have been exploited in drug delivery systems. Still, the phase transition of triblock copolymers **BAB** is only partially understood and there are little reports on their rheological properties so far.

Although block copolymers containing linear **PEO** chains have been the most described so far in the context of biomedicine, interesting alternatives are based on **PEO** brushes with oligoethylene oxide units, which are increasingly being studied.[303-306] Such **PEO** brushes have attracted much interest for potential applications including biomedical materials,[307] surfactants[308, 309] and flocculants. Recently, the addition of short oligo(ethylene glycol) side chains to the polymer backbone has been exploited to prepare new water-soluble polymers with thermoresponsive properties. The polymerisation of vinyl, acrylate and methacrylate monomers with such side chains by controlled polymerisation techniques has been demonstrated. Typical examples include oligo(ethylene glycol) vinyl ethers by living cationic polymerisation,[310, 311] methoxyoligo(ethylene glycol) methacrylates by living anionic polymerisation[312] and atom transfer radical polymerisation (ATRP),[313-316] styrenics and acrylates with short oligo(ethylene glycol) pendants by nitroxide-mediated radical

polymerisation (NMRP).[79, 317, 318] Possible molecular structures containing ethylene oxide units are shown in Figure 6.1.

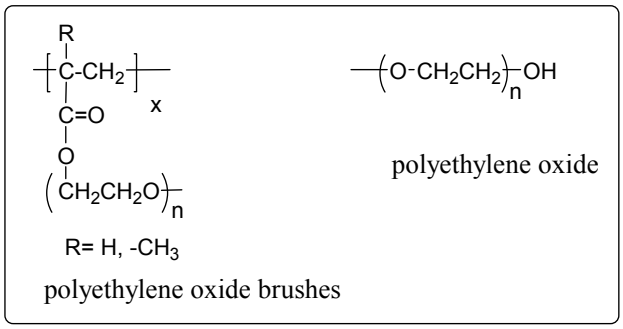


**Figure 6.1 Examples of thermoresponsive polymers containing polyethylene oxide units.**

Poly(methoxy diethylene glycol acrylate)(**PMDEGA**) homopolymer prepared by NMRP exhibits a cloud point in a temperature range of 35-38 °C,[36] which is close to the **PNIPAM** cloud point. It is therefore instructive to compare its aqueous behaviours to those of **PNIPAM**.

The current chapter describes the thermal property relationship of poly(methoxy diethylene glycol acrylate)(**PMDEGA**) homopolymers and the triblock block copolymers poly(styrene-methoxy diethylene glycol acrylate-styrene). Initial efforts were first the synthesis of the polymers using the RAFT method. Then, the association behaviours of the synthesised polymers in dilute and concentrated aqueous solutions were studied using turbidity and dynamic light scattering. The dynamic rheological properties of the triblock copolymer solutions were also part of this study. To date, there is no literature reporting the synthesis and micellization of the copolymer poly(styrene-methoxy diethylene glycol acrylate-styrene). This novel system should give more insight in the relationship between micellization and gelation processes.

## 6.2 Synthesis of homopolymer (A) and block copolymers BAB

The synthetic strategy to **BAB** amphiphilic triblock copolymers of polystyrene **(pM2)** and poly(methoxy diethylene glycol acrylate) (**PMDEGA**) via the RAFT process is similar to the one to the analogous triblock copolymers **BAB** described in Chapter 3 (scheme 3.1) which are made from **PNIPAM** as **A**-block and polystyrene as **B**-block.[8] The polymerisation conditions are listed in Table 6.1 and Chapter 8, section 8.5.

**Table 6.1 Synthesis of amphiphilic block copolymers from polystyrene macroRAFT agents and MDEGA.**

| Polymer | RAFT agent used | Yield (in %) | $M_n$theor a) | $M_n$ b) | $M_n$ (UV) c) | $M_n$ (SEC) d) | PDI d) |
|---|---|---|---|---|---|---|---|
| **PMDEGA#69** | **CTA3** | 70 | 7400 | 7600 | 12000 | 8000 | 1.3 |
| **PMDEGA#138** | **CTA2** | 72 | 29000 | 17000 b- | 24000 | 9700 | 1.7 |
| **pM2#22** | **CTA7** | 40 | 2300 | 2100 e) | | 2300 | 1.2 |
| **pM2#81** | **CTA7** | 48 | 9900 | 8200 e) | 8400 | 8400 | 1.2 |
| **p(M2-MDEGA-M2#22)** | **pM2-22** | 94 | 21000 | 24000 b- | 19000* | 9700 | 1.5 |
| **p(M2-MDEGA-M2#81)** | **pM2-81** | 65 | 65400 | 68000 b- | 71000* | 15000 | 1.4 |

[a)] calculated according to equation 1. [b)] from integral ratio of signal at 4 ppm (-$CH_2$- of **PMDEGA**), and signal group at 7-8 ppm (aromatic protons of **PS**), assuming that the molar mass of the **PS** block corresponds to the one of the macroRAFT agent used. [c)] by end-group determination in $CH_2Cl_2$ assuming full end-group conservation; calculated with the extinction coefficient of the RAFT agents engaged at 310 nm with the extinction coefficient of 16100 L $mol^{-1}$ $cm^{-1}$. [d)] in dimethylacetamide based on polystyrene standards. [e)] by end-group determination via $^1$H-NMR (via active methine group), calculated from the integral of the active end-group signal of -CH(aryl)-S-C(=S)-S-)-at 4.7-5.1 ppm. [b-)] $^1$H-NMR calculated from integral ratio of signal at 4 ppm (-$CH_2$- of **PMDEGA**), and signal group at 7-8 ppm (aromatic protons of **PS**) in the **P(S-MDEGA-S)**. [*)] calculated from the absorbance at 260 nm in $CH_2Cl_2$, using the extinction coefficient of 2.14 $L \cdot g^{-1} \cdot cm^{-1}$ reported for pure polystyrene.[235]

The copolymer **p(M2-MDEGA#96-M2#22)** was obtained by chain extension of the macroRAFT **CTA7** (see Chapter 3, section 3.5) with **PMDEGA** in THF at 70 °C up to high conversions (Table 6.1). The $^1$H-NMR spectrum of **p(M2-MDEGA#96-M2#22)** triblock copolymer confirms qualitatively the presence of both **pM2#22** and **PMDEGA** blocks, as illustrated in Figure 6.2. The signals at 6.4 to 7.6 ppm are assigned to the aromatic protons of the **pM2** block whereas the peak at about 4.1 ppm is assigned to the ester protons **-$COOCH_2$-** of **PMDEGA**. These peaks confirm that macroRAFT agent **pM2#22** enables the preparation of **p(M2-MDEGA-M2)** block copolymers. The chemical structure of **p(M2-MDEGA-M2)** was further characterised by SEC and UV. The elugram is monomodal, with no evidence of any residual polystyrene homopolymer **pM2#22**. The SEC traces are shifted to shorter elution times, as should be expected for increased molar masses, and indicate relatively low polydispersities between 1.4 and 1.5. Nevertheless, the tailing of the signals of the block copolymers to longer elution times indicates interactions with the column material

superposing the separation by size exclusion, thus rendering the formally obtained numbers for the molar masses questionable.

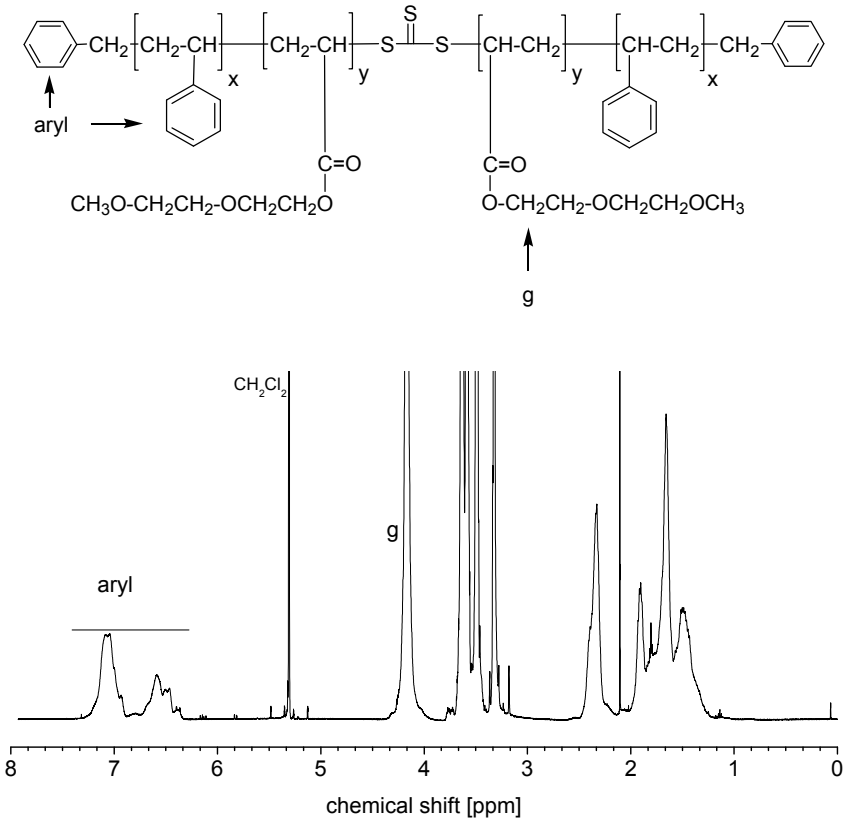


**Figure 6.2 $^{1}$H-NMR spectrum of p(M2-MDEGA#96-M2#22) in $CD_2Cl_2$.**

UV analysis reveals the retention of the trithiocarbonate as well as the presence of **pM2**. The estimation of the molar masses of the resulting triblock copolymers was possible from the absorbance of the styrene moieties in the UV spectrum. The extinction coefficient of polystyrene at 262 nm in $CH_2Cl_2$ of 222.5 $L \cdot mol^{-1} \cdot cm^{-1}$.[235] Two homopolymers **PMDEGA** (**PMDEGA#138** and **PMDEGA#69**) were prepared with **RAFT agents 3** and **8** as references (Table 6.1 and Figures A3 and A8 in the Appendix). The homopolymers are shown in Figure 6.3a-b.

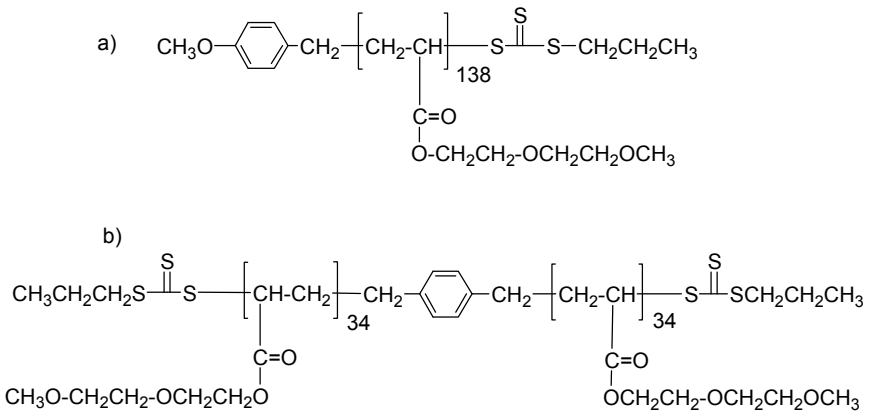


**Figure 6.3 Homopolymers PMDEGA#138 (a) and (b) PMDEGA#69.**

An example of the $^{1}$H-NMR spectrum of the homopolymer **PMDEGA#138** via RAFT agent **CTA8** is displayed in Figure 6.4. The signal at 4.1 ppm (g in Figure 6.4) evidences the ester protons **-COOCH$_2$-** of **PMDEGA** and the signals at 6.7 to 7.1 ppm are assigned to the aryl protons of the R-group of the RAFT agent 8 (Figure A8 in the Appendix).

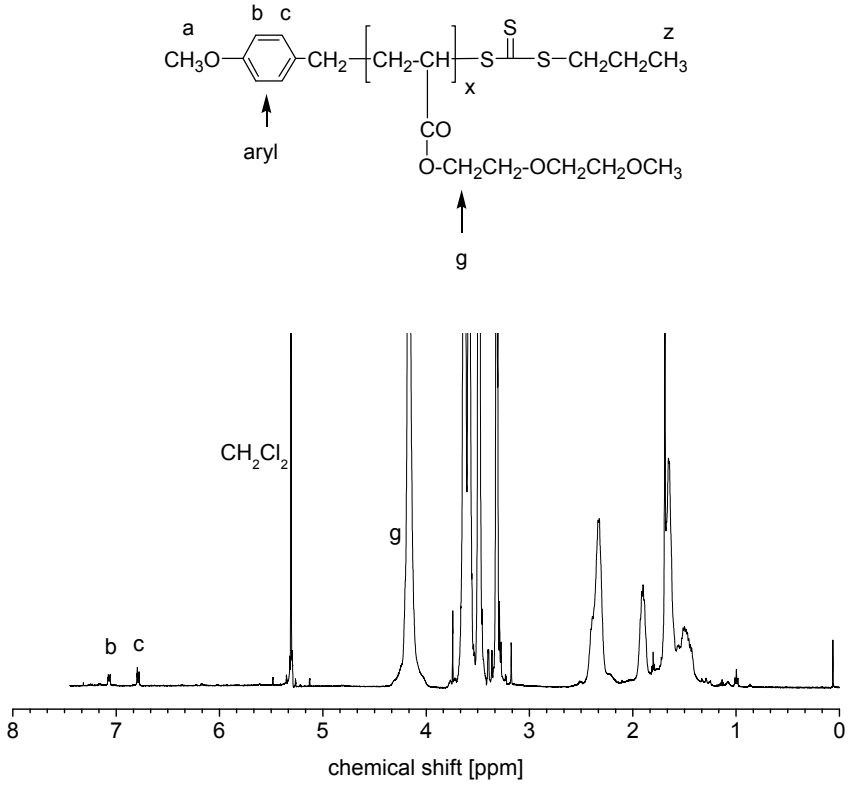


**Figure 6.4 $^{1}$H-NMR spectrum of PMDEGA#138 in $CD_2Cl_2$.**

To confirm the incorporation of the RAFT end-groups, UV spectroscopy was applied (Table 6.1).

# 6.3 Behaviour in dilute aqueous solutions

All the samples used in the following discussion were prepared by direct dissolution of the polymers in water. The thermoresponsive behaviour of the polymers was examined by turbidimetry, dynamic light scattering, and rheology. The cloud points of the aqueous solutions (at c = 1 g/l) were measured by turbidimetry at a fixed heating/cooling rate of 1 °C/min. The temperature at which the first deviation of the scattered light intensity from the baseline of the turbidity curve occurred, was taken as the cloud point. At this temperature the solutions start to become opaque.

## 6.3.1 Cloud points of PMDEGA (A) and block copolymers (BAB)

In Chapter 4, it was found for the triblock copolymers **BAB** with **PNIPAM** as thermoresponsive **A** segment and short hydrophobic **B** blocks, that the **B** end blocks hardly affect the cloud point, even if they induce the formation of micelles. Two triblock copolymers were selected with different polystyrene **p(M2)** and **PMDEGA** blocks, namely **p(M2-MDEGA#96-M2#22)** and **p(M2-MDEGA#359-M2#81)**. They were studied with the aim of assessing the hydrophobic effects on the cloud point of **PMDEGA**, while homopolymers **PMDEGA#69** and **PMDEGA#138** were used as references (Figure 6.3a-b and Table 6.1). **PMDEGA** shows a glass transition at about -50 °C.[319]

The cloud points of both homopolymers **PMDEGA#69** and **PMDEGA#138** in water were investigated in the temperature range from 20 to 80 °C (Figure 6.5).

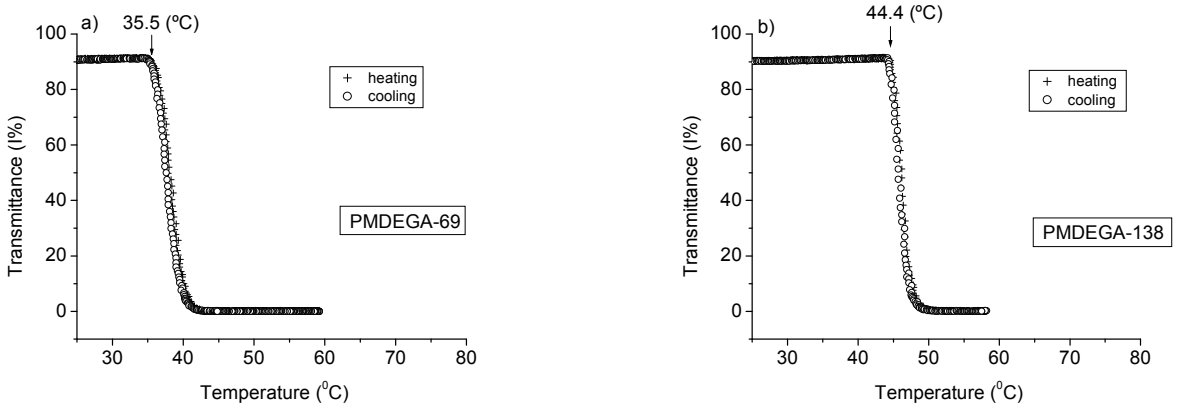


**Figure 6.5 Transmittance (I/Io) of aqueous solution of a) PMDEGA#69 and b) PMDEGA#138.**

The cloud point curves of both polymers comprised two reversible states as in the case of the **PNIPAM** (series a-g in Chapter 4, section 4.3). The homogenous transparent phase (temperature below the cloud point) and the separated turbid phase beyond the cloud point. Noteworthy, **PMDEGA#69** and **PMDEGA#138** exhibit two distinct cloud points at 35.5 and 44.4 °C with small hystereses between heating and cooling cycles. The cloud point of **PMDEGA#69** was similar to the value reported in the literature for the homopolymer of 38-39 °C by Fengjunhua et al.[36] Fengjunhua et al. prepared **PMDEGA** of 9000 g/mol via nitroxide mediated radical polymerisation with 1,1,2,2-tetraphenyl-1,2-diphenoxyethane (TPPA) as initiator. This polymer has a similar molar mass to **PMDEGA#69** synthesised by RAFT agent 3 (Figure 6.3b) (12000 g/mol). The cloud points determined for **PMDEGA#138** is higher than the one of **PMDEGA#69**. This discrepancy is attributed to the difference of the RAFT agent end-group used for their synthesis.[317] It is known that the cloud point of stimuli responsive polymers can vary because of parameters such as the polymerisation method, molar mass and end-group effects.[313, 320-322] It is difficult to assign this difference to the different molar masses. If this would be the reason, then **PMDEGA#138** should have the lower cloud point due to its higher molar mass.

As in the case of the homopolymers, the aqueous solution of triblock copolymers **p(M2-MDEGA#96-M2#22)** and **p(M2-MDEGA#359-M2#81)** exhibit reversible thermal phase transitions in the temperature range from 20 to 80 °C. Figure 6.6 shows the dependence of the solution turbidity of **p(M2-MDEGA#96-M2#22)** and **p(M2-MDEGA#359-M2#81)** on the temperature. The transmittance decreases at 36.6 and 56.0 °C, respectively.

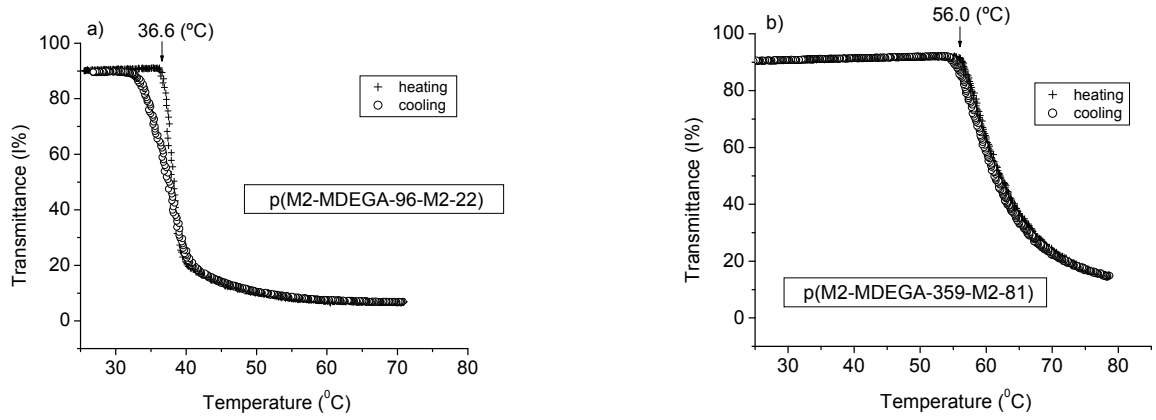


**Figure 6.6. Transmittance (I/Io) of aqueous solution of a) p(M2-MDEGA#96-M2#22) and b) p(M2-MDEGA#359-M2#81) as a function of the temperature at a fixed heating/cooling rate of 1 °C/min.**

The curve of **p(M2-MDEGA#96-M2#22)** has a pronounced hysteresis compared to the one of **p(M2-MDEGA#359-M2#81)**. In general, the chain extension of a thermoresponsive polymer with hydrophobic units should increase the hydrophobic interactions and reduce the solubility of formed block copolymer. Such a situation should result in a lower value of the cloud point of the thermoresponsive polymer, and thus cannot explain the high value of 56.0 °C for the **p(M2-MDEGA#359-M2#81)** block copolymer. The reasons for this high value are unknown.

The hysteresis observed for **p(M2-MDEGA#96-M2#22)** and **p(M2-MDEGA#359-M2#81)** suggests that the inherent change in the conformation of these polymers in water occurs with some differences. At low temperatures, these polymers form flower-like micelles with polystyrene core and **PMDEGA** as coronas. When temperature increases, the coronas of the flower-like micelles collapse and simultaneously interchain association leads to "stable mesoglobules". Because of the presence of the high $T_g$ core (polystyrene), the mesoglobules might be partially "frozen" and consequently, longer times will be required for rehydration to be complete upon cooling below the cloud point. The difference hysteresis observed in **p(M2-MDEGA#96-M2#22)** compared to **p(M2-MDEGA#359-M2#81)** could also be explained by the different annealing times after reaching the individual cloud points, when cycling both solutions between 20 and 80 °C.

## 6.3.2 DLS of PMDEGA (A) and block copolymers (BAB)

In addition to the cloud point measurements, studies were performed by DLS to determine the evolution of the hydrodynamic radii upon heating from 20 to 60 °C. The data of Table 6.2 demonstrate that the homopolymer form single molecular chains (unimers) while the block copolymers form micelles, and that the aggregate size dramatically increases above the cloud points (60 °C).

**Table 6.2 Evolution of hydrodynamic diameter of thermoresponsive polymers made of MDEGA in water, as a function of the temperature at a concentration of 1g/L.**

| **Polymer** | Cloud point [ °C ] | Dh [nm] 20 °C | PDI 20 °C | Dh [nm] 60 °C | PDI 60 °C |
|---|---|---|---|---|---|
| **PMDEGA#138** | 44.4 | 5 | 0.83 | 712 | 0.06 |
| **p(M2-MDEGA-96-M2#22)** | 36.6 | 20 | 0.13 | 91 | 0.06 |
| **p(M2-MDEGA-359-M2#81)** | 56.0 | 75 | 0.23 | 357 | 0.54 |

At 20 °C, DLS of **PMDEGA#138** solution revealed the formation of small particles with a monomodal size distribution. The peak $D_h$ was about 5 nm with a polydispersity (PDI) of 0.83 below the cloud point. With increasing temperature from 20 °C to 60 °C, the solution becomes turbid and DLS indicates a sudden increase in the average hydrodynamic diameter with a decrease of PDI (Table 6.2). It should be noted that with further increase of the temperature, the colloidal size stagnates and no precipitation was observed for the sample. The difference in the apparent hydrodynamic diameter ($D_h$) observed below and above the cloud point suggests changes of conformation of **PMDEGA**. Below the cloud point, the polymer adopts a random coil conformation. At high temperature, water becomes a poor solvent for the polymer and the polymer shrinks. This gives rise to the development of intermolecular hydrophobic interactions, which lead to compact colloidal particles (mesoglobules) with large hydrodynamic diameters.

Examination by DLS of the hydrodynamic diameters $D_h$ of triblock copolymer **p(M2-MDEGA#96-M2#22)** solution below and above the cloud points shows some similarities with the homopolymer (see Table 6.2). In fact at 20 °C, the copolymer forms small colloid particles with $D_h$ of 20 nm and PDI = 0.18. The size of the colloids is characteristic for the formation of micelles with a core made of the hydrophobic **B** blocks and a corona of **PMDEGA**. As the temperature increases up to 60 °C, the colloids increases in size to 91 nm with a narrow size distribution PDI = 0.06. Because above the cloud point, the size of the individual polymeric micelles must shrink due to the collapse of the corona, the large aggregates formed may be attributed to the reassociation of the primary micelles to multichain aggregates with high hydrodynamic diameters.[279, 323, 324] Analogous observations were made for the copolymer **p(M2-MDEGA#359-M2#81)**, Table 6.2.

The difference in the $D_h$ values between both triblock copolymers below and above the cloud points demonstrates that the size of micelles increases with the size of the hydrophilic and hydrophobic blocks. This finding was seen for the triblock copolymers **BAB** with **PNIPAM** as thermoresponsive **A** block and short hydrophobic **B** blocks (Chapter 4, section 4.6).

Note also that at 60 °C, both copolymers form multichain aggregates with smaller size compared to those formed by the homopolymer **PMDEGA#138**. This behaviour is comparable to the finding for **PNIPAM** series (Chapter 4, section 4.6). The reasons for this behaviour are uncertain (see also Chapter 4, section 4.6).

# 6.4 Behaviour in concentrated aqueous solutions

## 6.4.1 Tube Inversion Method (TIM) for block copolymer solutions

In order to learn about the behaviour of amphiphilic **BAB** block copolymer with **PMDEGA** as hydrophiphilic block, **p(M2-MDEGA#96-M2#22)** was used as model. Six concentrations were prepared: 0.1 wt%, 10 wt%, 20 wt%, 30 wt%, 40 wt% and 50 wt%, and characterised by means of TIM. The derived partial phase diagram of **p(M2-MDEGA#96-M2#22)** in aqueous solution is shown in Figure 6.7.

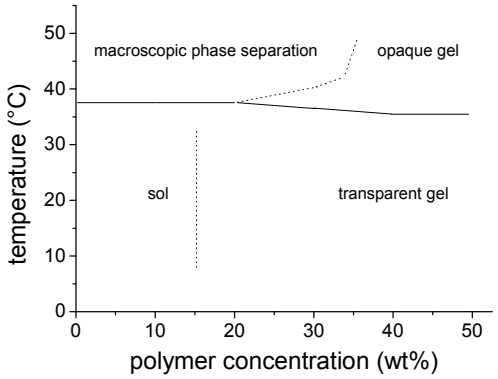


**Figure 6.7 Schematic phase diagram of triblock copolymer p(M2-MDEGA#96-M2#22) in aqueous solutions at concentrations from 0.10-50 wt%.**

Typical for **p(M2-MDEGA#96-M2#22)**, viscosity increases only at higher concentrations. Below 20 wt%, low viscous solutions are obtained, though a gradual increase in viscosity is observed at temperatures near the cloud point. At concentrations of 20 wt% and above, the mobile fluid changes to an immobile gel at 20 °C. Above 37 °C, the **p(M2-MDEGA#96-M2#22)** systems become cloudy and undergo macroscopic phase separation, if the concentration is below 40 wt%. At higher concentrations an opaque gel is formed. The sol-gel transition is attributed to intermicellar association and dense packing of micelles at high polymer concentrations. More details are given later.

It is seen that when comparing the results of the Chapter 5 on **p(M2-NIPAM-M2)** block copolymers with the results for **p(M2-MDEGA#96-M2#22)** polymer, the increase in viscosity and gelation depend on the chemical nature of the thermoresponsive middle block. When for instance, **BAB** block copolymers with identical hydrophobic end blocks are compared no gel formation occurred with copolymer **p(M2-NIPAM-M2#22)** at 20 wt%

concentration. This is interesting because both **p(M2-NIPAM#183-M2#22)** and **p(M2-MDEGA#96-M2#22)** have same hydrophobic block length and almost similar hydrophilic block sizes: **PNIPAM#183 = 20700** and **PMDEGA#96 = 19000**. Still, the minimum concentration for gel formation is about at 40 wt% for **p(M2-NIPAM#183-M2#22)**, but only about at 20 wt% for **p(M2-MDEGA#96-M2#22)**. Hence, the use of **PMDEGA** in with styrene end blocks, means that equivalent effects can be obtained with much shorter **PMDEGA** block lengths than is possible using **PNIPAM**. An explanation of the observed difference might be related to the swelling ratio of the coronae of the micelles leading to gel formation. The gelation of **p(M2-MDEGA#96-M2#22)** at concentration 20 wt% suggests that the middle block **PMDEGA#96** is able to bind more water molecules. Thus, the middle block of **p(M2-MDEGA#96-M2#22)** is in a more extended conformation leading to a more voluminous corona, so that the gel is formed already at 20 wt%.

## 6.4.2 Rheological properties of concentrated solutions of block copolymers

Rheological properties were exemplarily studied for solutions of 20, 30, 40 and 50 wt% of **p(M2-MDEGA#96-M2#22)**

- **Shear rate sweep tests**

First, the block copolymer solutions were subjected to flow shear tests at 25 °C. Figure 6.8 displays the apparent viscosity as a function of the shear rate.

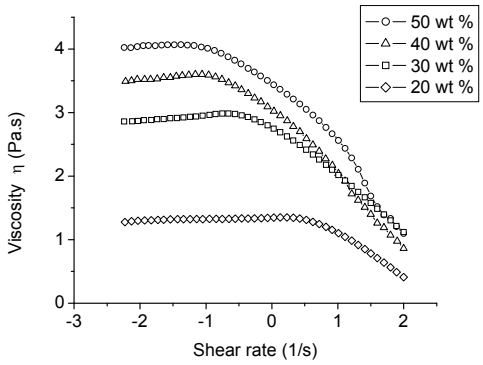


**Figure 6.8 Shear rate dependence of the apparent viscosity of p(M2-M7#96-M2#22) samples at concentrations 50 wt% (O), 40 wt% (Δ), 30 wt% (□), 20 wt% (◊) at 25 °C.**

All measurements were reproducible with only slight differences between individual runs. As seen in the case of **p(M2-NIPAM-M2)**, all samples showed similar behaviour. As expected,

the viscosity decreases markedly with the concentration. It decreases in the order from 50 wt% (10000 Pa·s) > 40 wt% (3500 Pa·s) > 30 wt% (960 Pa·s) > 20 wt% (22 Pa·s). At low shear rates, they showed Newtonian behaviour until a critical shear rate at which shear thinning started. The transition to the shear-thinning regime shifts to lower critical rates with increasing concentration. A plausible interpretation of the Newton regime observed in all the cases is ascribed to transient network via intermicellar hydrophobic interactions arising from the polystyrene end blocks. With increasing shear, this network breaks down, resulting in a gradual drop of the viscosity. Such a behaviour has also been reported before e.g. by Dimitris et al.,[325] Annable et al.,[326] and Jenkins et al.[327]

- **Frequency Sweep for Sol-Gel and Gel-Sol transitions**

After studying the flow properties, the concentrated polymer solutions were subjected to dynamic oscillation stress ramping. All experiments were conducted in the viscoelastic regime, namely with an oscillating shear stress of 5 Pa and frequency sweep of 0.03-628 rads$^{-1}$. Figure 6.9 illustrates the viscoelastic properties of **p(M2-MDEGA#96-M2#22)** solution of 40 wt%, at 15, 20, 25 and 30 °C.

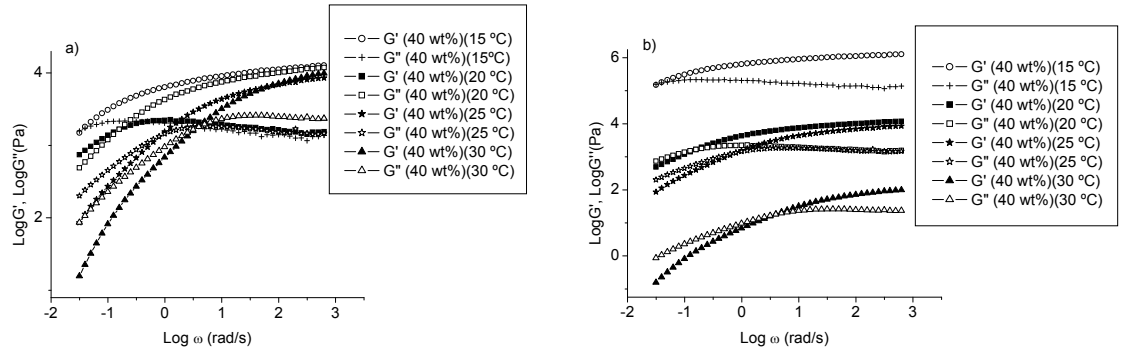


**Figure 6.9. a) Frequency dependence of the dynamic moduli of the p(M2-MDEGA#96-M2#22) hydrogel at concentration of 40 wt%, showing the crossing of the two moduli. Storage modulus (G', solid symbol) and loss modulus (G", open symbol) were measured at 15, 20, 25 and 30 °C, at 5 Pa.**

**b). For better viewing the data shown on the right side are vertically shifted by log100 for 15 °C, and by -log100 for 30 °C to avoid overlapping.**

At 15 °C, the aqueous solution behaves nearly as a "hard gel";[328] the system exhibits nearly frequency independent viscoelastic moduli, G' > G" at the entire frequencies investigated with tan $\delta$ < 1. Only for the lowest value of ω (logω = 0.60 rad/s), G" is found to be slightly higher than G'. This behaviour suggests that a network structure of **p(M2-MDEGA#96-M2#22)** molecules is formed. At 25-30 °C, the copolymer solution behaves as a soft-gel.

There are three distinct regimes to note. The first regime is marked by a viscous character in the low angular frequency range; G" > G' with tan $\delta$ > 1 (logω < -1 rad/s). With the increase of frequency, both moduli increase and reach a crossing point (G' = G"; and tan $\delta$ = 1). This second regime corresponds to the gel point. The cross point implies the transition of a sol to a gel marked by the formation a transient physical network. Above this cross point (logω > 1 rad/s), the third regime, G' becomes larger than G", indicating the formation of a viscoelastic solid at high angular frequency.

With the increase of temperature, the gel point shifts toward lower frequency values. Clearly, the change from an elastic to a viscoelastic state is a function of temperature. This implies that the junctions or crosslinks are constantly formed and deformed under the applied frequency. These findings contrast with the visual inspection by TIM experiments, which shows the gel behaviour up to 35 °C at this concentration (Figure 6.7).

- **Effect of polymer concentration on physical network formation at 25 °C**

To compare the effect of polymer concentration, the frequency dependence of the moduli G' and G'' for **p(M2-MDEGA#96-M2#22)** was determined at a given temperature (25 °C) for solutions of concentrations 20, 30, 40 and 50 wt% (Figure 6.10).

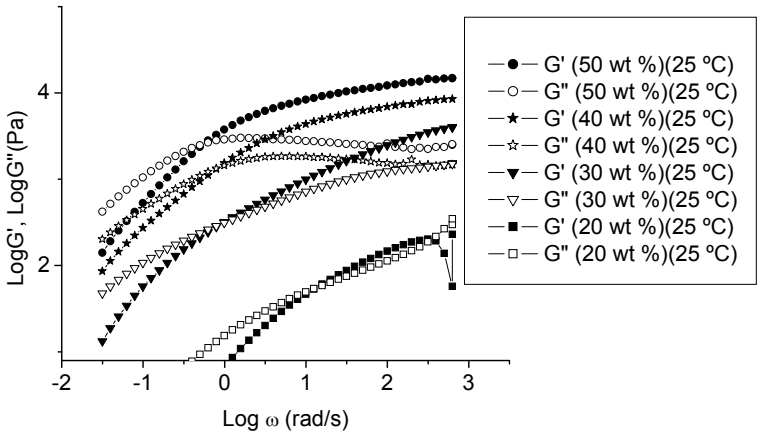


**Figure 6.10 Frequency dependence of the dynamic moduli of the p(M2-MDEGA#96-M2#22) hydrogel at concentrations of 20, 30, 40 and 50 wt%, showing the crossing of the two moduli. Storage modulus (G', solid symbol) and loss modulus (G", open symbol) were measured at 25 ºC and at 5 Pa.**

All four solutions were immobile fluids in the tube inversion test (Figure 6.7). The logarithmic plots of the moduli G' and G" showed the same trend as discussed previously at (25 °C). All the samples behaved as soft-gel at the entire frequencies investigated. They have dominantly viscous character at the low frequency range (G" > G'). Viscosity decreases with

concentration as 50 wt% (G”: 1644 Pa) > 40 wt% (G”: 680 Pa) > 30 wt% (G”: 157 Pa) >20 wt% (G”: 5.00 Pa) at 0.20 rad/s. With the increase of frequency, the storage modulus increases faster than the loss modulus and reaches a crossing point where G’ = G’’. Beyond the crossing point, G’ exceeds G” over the rest of the frequency range investigated. The curves of G’ and G’’ for 40 and 50 wt% attained nearly plateaus at high frequency with a weak dependence on the frequency. This indicates that a “hard” gel state had formed.[328] In contrast, the sample with 20 wt% showed a strong dependence of its G’ and G’’ on the frequency while no plateau was observed in the whole frequency range investigated, so that this sample behaves as weak soft gel. Thus, the order of gelation decreases with concentration as 50 wt% (G’: 13500 Pa) > 40 wt% (G’: 7800 Pa) > 30 wt% (G’: 3300 Pa) >20 wt% (G’: 195 Pa) at 249 rad/s.

- **Temperature Sweep for Gel-Sol and Sol-Gel transitions**

Temperature ramp experiments illustrate the profound change in rheology that occurs upon heating and cooling over a moderate temperature range from 20 to 50 °C and vice-versa in the block copolymer solutions. The measurements were performed at 6.268 rad/s and 5 Pa. Figure 6.11a-d illustrates the temperature dependent properties of **p(M2-MDEGA#96-M2#22)** as 20, 30, 40 and 50 wt% solutions.

The 30-50 wt% samples show below 30 °C (Figure 6.11b-d) viscoelastic solid-like behaviour, with G’ > G’’. As the temperatures increases to 35 °C, both moduli decrease progressively so that a crossing point is reached where G’ = G”, indicating the change from an elastic gel-like to a viscous liquid-like response. Both G’ and G” reach their minimum values around 37 °C (except for 50 wt%), which coincides with the cloud point of **p(M2-MDEGA#96-M2#22)** (Figure 6.11b-d). Above this temperature up to 43 °C, the values of G’ and G” increase to a maximum, before falling back again, with G’’ always larger than G’. When the sample is cooled from 50 to 20 °C, a reverse transition from sol to gel without hysteresis is observed, indicating the reversibility of the gelation process in **p(M2-MDEGA#96-M2#22)**. The gelation processes in the current case are therefore thermodynamically controlled.

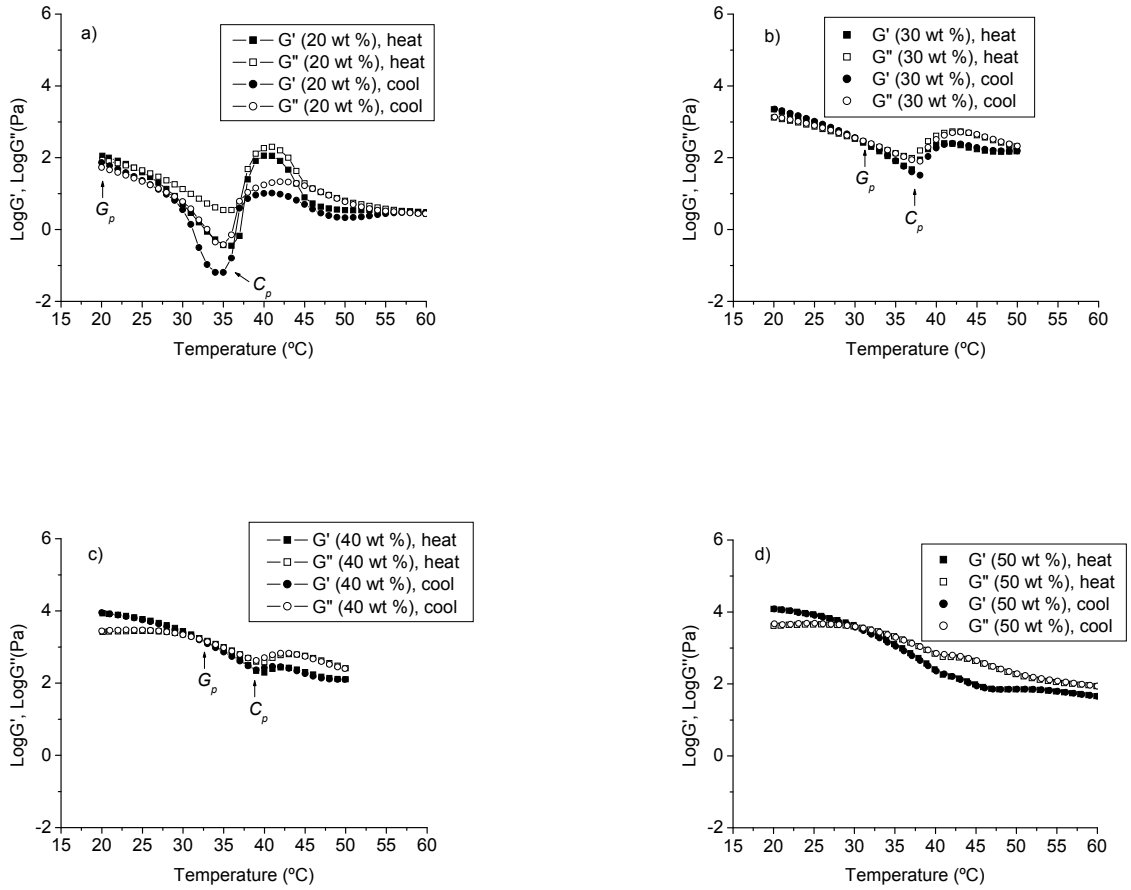


**Figure 6.11a-d Temperature dependence of the dynamic moduli of the p(M2-MDEGA#96-M2#22) hydrogels at concentrations of 20 (a), 30 (b), 40 (c) and 50 wt% (d), showing the crossing of the two moduli. Storage modulus (G', solid symbol) and loss modulus (G", open symbol) were measured on heating and cooling at a heating rate of 2 °C/min and at 6.268 rad/s, 5 Pa.**

The investigation of the dynamic viscoelastic properties of the 20 wt% sample showed similar trends, except that a pronounced hysteresis is observed. The degelation process starts at 24 °C (G' = G") and the cloud point is observed at 37 °C, where G'' is larger than G' (Figure 6.11a). Above 37 °C up to 41 °C, the values of G' and G" increase rapidly before falling back, with G'' still larger than G'. The solution at 20 wt% thus remained in a viscoelastic liquid state. The heating and cooling curves were all reproducible and fully reversible with slight differences (Figure 6.11a).

## 6.4.3 Discussion for BAB in concentrated aqueous solutions

The rheological results indicate significant differences in the behaviour of the thermo-reversible **p(M2-MDEGA#96-M2#22) (BAB)** hydrogels from the one made of the polystyrene end blocks and the middle block of **PMDEGA**. In order to better understand

these results, it worth reminding the possible associations that can occur when a **BAB** copolymer is dissolved in dilute and concentrate solutions. In dilute solution, the triblock copolymer can adopt several conformations including ring, dumbbell shapes and flower micelles, stripped flower (dangling chain) and loose branched structures.[329] These associations are governed by the competition between the attractive hydrophobic interactions of the sticky outer blocks **B** and the repulsive interactions along the hydrophilic middle block **A**. Above a certain concentration, transient binding between micelles can take place. Different scenarios are possible. Bridge conformations result either, when the polymer places its **B** ends into the cores of two different micelles, or when dangling chain attaches its free **B** end to the core of a second micelle.[330] Additionally, it is also possible to have interlocked micelles. These situations occur when the distance between two micelles is short enough that micellar loops with the "sticky" blocks at the opposite ends entangle heavily with each other. Additionally, the transient network can also occur by the packing of micelles, when the total volume fraction of micelles is larger than the maximum packing fraction (see Chapter 1, section 1.8.2).

Because of the thermoresponsive character the triblock copolymer **BAB**, the temporal junctions described above will split when the temperature is raised above the cloud point. As the collapsed **A** block cannot bridge the distance between two micelles anymore, this leads to a sol state. The temporary junctions are eventually reformed at low temperature.[331]

Following the aforementioned explanation, it is plausible that the solutions with concentrations below 20 wt% (Figure 6.7) do not gelify either due to the insufficient number of cross-links or to the low total volume filling of micelles. In contrast, polymer solutions with concentrations above 20 wt%, form transient networks due to sufficient bridging of micelles. Therefore these systems behave as solid-like (Figure 6.7). The viscosity of solutions of the block copolymers increases with increasing concentration possibly because the effective volume fraction of the micelles approaches that of close packing (Figure 6.8).

For all the four given block copolymer samples (20, 30, 40 and 50 wt%) at 25 °C, the viscoelastic response strongly depends on the applied frequency. They show a liquid-like behaviour at lower frequencies, but a solid-like behaviour at high frequencies (Figures 6.9-6.10). Similar behaviour has been previously observed with triblock copolymers from

ethylene oxide and styrene.[96] The explanation of this process is not straightforward. The most likely explanation to the observed increase of viscosity (gel formation), as the frequency is increased, lies in physical changes of the macromolecules with time.[332] Contrary to the case of chemical crosslinked polymer gels where the branch points have fixed positions along the chemical block, here the connections result either by the mechanism of bridged micelles or due to sliding of micelles. Because of these temporary junctions, transient networks are characterised by reversible breakdown processes.[83] Possibly, at low frequency, the transient network formed by **p(M2-MDEGA#96-M2#22)** has a very short life-time in which case the entangled micelles could break from each other almost freely conferring to these systems a high fluidity behaviour. Thus, no effective bridges between micelles are established. Over a long period of time (high frequency), the relaxation time of molecules is reduced so that the bridge phenomena dominate over the breaking processes, leading thus to transient network (solid-like behaviour).

Following the dynamic oscillation tests, the concentrated polymer solutions were subjected to temperature ramp tests (Figure 6.11). The results indicate that both moduli G' and G'' decreased gradually with temperature before reaching the cloud point. This behaviour could be ascribed to the gradual shrinking of **PMDEGA** chains. In particular, an increase in temperature favours the contraction of the **PMDEGA** chains and thus, induces disentanglement of the micelles thus destroying the network connectivity. This is the beginning of the degelation process. Near the cloud point, a thermothickening (or an increase of viscosity with temperature) of the polymer solutions is observed (Figure 6.11). In addition to the change in the volume packing micelles, the jump in moduli or viscosity might also be ascribed to the collapse of macromolecules that were still surrounded by water molecules, which could only be removed upon further heating. These macromolecules first form small networks with each other, which induce the increase of viscosity with temperature. At higher temperature, the **PMDEGA** block collapses and the networks lately formed split. Beside, the formation of few new networks, the jump in viscosity observed at the cloud point might indicate also the formation of independent globules by the collapse of free **PMDEGA** chains, which were still in the swollen state.[333]

When the temperature is decreased, the solvent quality for **PMDEGA** block improves and the block polymer chains are more swollen. This process increases the mobility of the block copolymers. Further decrease in temperature allows a full change in conformation and therefore a change in volume phase transition going from sol to gel is observed (Figure 6.11). It should be pointed out that a pronounced hysteresis is observed during the gelation and degelation processes of the block copolymer solution of 20 w% (Figure 6.11a). The hysteresis of the heating and cooling cycles increases with decreasing concentration, which is not surprising considering the increasing tendency for macroscopic phase separation (Figure 6.11a-b, this is discussed in Chapter 5, section 5.3).

In Chapter 5 the features of **PNIPAM** and its corresponding block copolymers are discussed. Although it is difficult to make specific conclusions between **PNIPAM** systems with those of **PMDEGA**, however, the self-organization of these two systems reveals some similarities and some differences. The investigation of dilute aqueous solutions of **PMDEGA** homopolymers and block copolymers suggests that their cloud points appear to be markedly end-groups dependent, while the dilute aqueous solutions of **PNIPAM** and its corresponding block copolymers showed only a weak variation of the transition temperature ("cloud point") around 32 °C. Both systems have their advantages and inconveniences. For instance, for any instantaneous application which solicits the adjustment of the cloud point, it seems more effortless to use **PMDEGA** instead of **PNIPAM**.

The studies of dilute aqueous solutions of homopolymers **PMDEGA** or **PNIPAM** and their corresponding block copolymers show at ambient temperature the formation of unimers and micelles, respectively. Above the cloud points (60 °C), the size of these colloidal particles is considerably increased. This is due to the formation of multichain associations.

Interestingly, concentrated aqueous solutions of **PMDEGA** and **PNIPAM** polymer systems exhibit transient network formation. However, the self-organization of block copolymers into micellar hydrogels seems to be more efficient when **PMDEGA** is used as a middle block than with **PNIPAM**. This difference can be assigned not only to their difference in solubility in water but also to their interaction with the hydrophobic end blocks. It should also be mentioned that the heating/cooling cycles of the **PMDEGA** block copolymer hydrogels are characterised by the reversible gel-sol-gel transitions without any hysteresis except for the sample made of 20 w% **PMDEGA** block copolymer, whereas **PNIPAM** triblock copolymers

solutions were marked with poorly reversible gel-sol transitions accompanied with pronounced hystereses. These differences suggest that the formation of **PMDEGA** block copolymer hydrogels are closer to thermodynamic control while those formed by **PNIPAM** triblock copolymers are under kinetic control.

Finally, contrary to the thermal experiments of the triblock copolymer made of **PNIPAM** as middle block (Chapter 5, section 5.3), the temperature ramp of the triblock copolymer **p(M2-MDEGA#96-M2#22)** shows that degelation or gel point $G_p$ and cloud point ($C_p$) are processes that might occur at different stages. This observation might imply that the both triblock copolymer systems follow different physical processes (Figure 6.11).

## 6.5 Conclusions

Thermoresponsive homopolymers **PMDEGA#69** and **PMDEGA#138**, and amphiphilic triblock copolymers **p(M2-MDEGA#96-M2#22)** and **p(M2-MDEGA#359-M2#81)** consisting of short hydrophobic polystyrene end blocks and of poly(methoxy diethylene glycol acrylate) as thermoresponsive block were successful prepared by the RAFT process using trithiocarbonates as the chain transfer agents.

All these polymers dissolve directly in water without using any co-solvent. Thermoresponsiveness has been observed for these polymers. When these solutions were heated, different phase transition temperatures were observed. Some differences were attributed to specific end-group effects of the RAFT agents used for the synthesis of polymers (**PMDEGA#69** and **PMDEGA#138**).

Dynamic light scattering of the homopolymers and triblock copolymers solutions revealed that the size of colloid particles formed depends on temperature. Small colloid particles were formed at low temperature, while much larger ones were observed at high temperature.

From the rheology experiments, it was found that **p(M2-MDEGA#96-M2#22)** triblock copolymer solutions exhibit a reversible gel-sol transition in the concentration range from 20-50 wt% below the cloud point of the **PMDEGA** block. The reversible break down of

physically crosslinked micelles has an important influence on the viscoelastic properties of **p(M2-MDEGA#96-M2#22)** triblock copolymer.

*"The limits of the possible can only be defined by going beyond them into the impossible." Arthur C. Clarke*

# CHAPTER 7: Conclusions and perspectives

# 7.1 Conclusions

The use of bifunctional bistrithiocarbonate compounds of the general structure Z-C(=S)-S-R-S-C(=S)-Z (type I), as well as R-S-C(=S)-Z-C(=S)-S-R (type II) enables the convenient synthesis of **ABA** and **BAB** triblock copolymers by reversible addition-fragmentation chain transfer (RAFT) polymerisation. The bistrithiocarbonates are effective chain transfer agents, characterised by high transfer coefficients and may be tailored to incorporate functional end-groups in the polymer, which can support the molar mass determination. Additionally, the new bistrithiocarbonates are relatively simple to prepare and to purify, and they permit to synthesise symmetrical block copolymers in only two polymerisation steps.

RAFT polymerisations gave access to copolymers of various chemical nature with hydrophilic monomers such as N-isopropylacrylamide (**PNIPAM**), and methoxy diethylene glycol acrylate (**PMDEGA**) for the **A** blocks, and hydrophobic monomers including 4-*tert*-butyl styrene (**M1**), styrene (**M2**), 3,5-dibromo benzyl acrylate (**M3**), 2-ethylhexyl acrylate (**M4**), and octadecyl acrylate (**M5**) for the **B** blocks. The synthesis of homopolymers **A** and **B** as well as of triblock copolymers **ABA** and **BAB** via the RAFT process produces polymers with good control of the molar mass and with narrow molar mass distributions.

The self-assembly of **ABA** and **BAB** triblock copolymers containing **PNIPAM** as long hydrophilic middle block in dilute, semi-concentrated, and high concentrated aqueous solution leads to a rich aggregation behaviour. These triblock copolymers associate in dilute and semi-concentrated aqueous solution into small micelles, while at high concentrations, hydrogels are formed. Comparing triblock copolymers **ABA** with **BAB** of analogous composition, the aggregate sizes were the same within the accuracy of the data. For **BAB** architectures, the size of the cores of the polymer micelles increases with the size of the hydrophobic end blocks. Also, it seems that for a given length of the hydrophobic blocks, the size of the micelles increases with **pM2** < **pM3** < **pM1** < **pM5**, i.e. in the order of their steric demands.

Noteworthy in the full concentration range of 0.01 - 50 wt%, the addition of hydrophobic end blocks onto the **PNIPAM** chains does not shift the LCST to lower values. This is attributed to the high tendency of hydrophobic associations reducing their contact with water by micelles formation. Due to the stable transition temperature, amphiphilic block copolymers based on **PNIPAM**, are good candidates for practical uses as thermo-sensitive amphiphiles.

Different from expectations, rheological studies indicate that physical networks (hydrogels) are only formed at high concentrations, typically above 30-35 wt%. The minimum concentration to form hydrogels decreases slightly with the length of the hydrophobic end blocks. The tendency to form gels depends not only on the length of a hydrophobic block, but also on its chemical nature, and increases with **p(M3-NIPAM-M3)** < **p(M5-PNIPAM-M5)** < **p(M2-NIPAM-M2)**. It appears that the glass transition temperature of the hydrophobic end blocks affects gel formation. High glass transitions favour hydrogel formation with high mechanical strength.

For comparison with the extensive systematic study on the micellization of triblock copolymers bearing **PNIPAM** as thermoresponsive polymer, **PMDEGA** and its copolymers were studied. These polymers show a more complex thermoresponsive behaviour. The **PMDEGA** homopolymers exhibit a marked dependence of the cloud points on the polymer end-groups, and the **BAB** triblock copolymers showed an increase of the cloud-point temperatures with increasing the length of the middle hydrophilic block **A** (**PMDEGA**). The understanding of these phenomena awaits further investigations.

The block copolymer aggregates into micelles in aqueous solution, as for the **PNIPAM** based analogs, but forms already hydrogels when the concentration exceeds 18 wt%. The increased ability to form gels in comparison to the block copolymers based on **PNIPAM**, suggests a better swelling capacity of **PMDEGA**. This might be attributed the presence of a high density of strongly interacting methoxy diethyleneglycol side chains on the polymer backbone. This new copolymer system is therefore considered to be of special interest for future uses.

## 7.2 Perspectives for future research

Amphiphilic block copolymers have been extensively used to solubilize hydrophobic molecules, in particular Pluronic ® block copolymers have been employed to solubilize organics compounds which are immiscible in water. It should be therefore instructive to compare the solubilization of the amphiphilic block copolymers described in this work with those of pluronic block copolymers.

Supplementary studies on the phase transition temperatures of **PMDEGA** and its copolymers are needed for understanding the mechanical behaviour that reflects the various physical processes in the micellization of these systems

As the attempted chain extension of **PNIPAM** homopolymers of the general structure Z-C(=S)-S-R-S-C(=S)-Z (type I) with styrene gave results that differ most from results expected (long inhibition period) for the common understanding of the RAFT process, future research should include a detailed kinetic study of the polymerisation reaction.

**p(M2-MDEGA#96-M2#22)** triblock copolymer.

*"One never notices what has been done; one can only see what remains to be done." Marie Currie*

# *CHAPTER 8: Synthesis and characterisation of RAFT agents and polymers*

This chapter describes the analytical methods, the synthesis of RAFT agents, homopolymers, monomers and block copolymers.

# 8.1 Experimental PART

# 8.2 Analytical Methods

**$^{1}$H-**, **$^{13}$C-NMR** spectra were taken with an apparatus Bruker Avance 300 (300 MHz).

**Mass spectra** were recorded by a GC/MS-system Trace DSQII (Thermo Scientific).

**Elemental analyses** were carried out using a Vario ELIII microanalyzer (Elementar Analysensysteme, Germany).

**UV-vis spectra** were recorded on a spectrophotometer Cary-1 (Varian) equipped with temperature controller (Julabo F-10). Quartz cuvettes (Suprasil, Hellma, Germany) with an optical path length of 10 mm were used.

**Thermal properties** of the polymers were measured with a TGA/SDTA 851 thermal gravimetric analyzer (TGA) (Mettler Toledo) and a DSC 822 differential scanning calorimeter (DSC) (Mettler Toledo) under nitrogen atmosphere, with a heating and cooling rate of 20 $K \cdot min^{-1}$.

**Size-exclusion chromatography** (SEC) of the polymers was run in N,N-dimethylacetamide containing 0.1 % LiBr as eluent at a column temperature of 45°C, with a set-up consisting of an Agilent 1200 isocratic pump, an Agilent 1200 refractive index detector, and two GRAM columns (10µm, 8x300mm, pore sizes 100 and 1000; PSS GmbH, Mainz, Germany). The SEC set-up was calibrated using low polydispersity polystyrene standards (PSS GmbH, Mainz, Germany).

**Turbiditmetry** was performed on a temperature-controlled turbidimeter (model TP1, E. Tepper, Germany) with heating and cooling rates of 1.0 K/min, respectively. The transmittance of polymer solutions was set automatically to 90% at the beginning of each measurement. Temperatures are precise within 0.5 K.

**Dynamic light scattering** (DLS) for the characterisation of the association of the polymers in aqueous solutions was studied by using a high-performance particle sizer (HPPS-ET, Malvern Instruments, UK) equipped with a He-Ne laser ($\lambda$ = 633 nm) and a thermoelectric Peltier temperature controller. Polymers were directly dissolved at ambient temperature in deionised water with a concentration of 1.0 g/L. The measurements were made at the scattering angle of $\theta$ = 173º ("backscattering detection"), and the autocorrelation functions were analyzed with the CONTIN method.

**Tube inversion method** (**TIM**) was used to study qualitatively the sol-gel and gel-macrophase separation transitions in the temperature range of 5- 45 °C. The samples in 15 ml tightly screw-capped vials were thermostated by a water bath, and sol or gel formation or macrophase separation at the given temperature was judged visually. When the vials were inverted and the mixture flew freely, the system was classified as "sol". When the mixture did not flow freely, but showed slow plastic deformation within a period of 1 h, it was classified as "highly viscous liquid". When the mixture did not flow within a period of 1 h, the system was classified as “gel”. In fact, the mixtures classified as “gel” did not show plastic deformation after 24 h, either.

**Rheological experiments** were performed with an AR-G2 rheometer (TA Instruments) equipped with cone-plate geometry and a Peltier plate for temperature control. The cone diameter was 40 mm, cone angle 1° and the truncation gap 30 μm, thus enabling to measure sample volumes as small as 0.3 mL. A water-filled solvent trap was used to minimize solvent evaporation during the measurements. Steady shear flow experiments were performed under stress control in the shear rate range between 0.01 and 100 $s^{-1}$. Oscillation stress sweep studies in order to specify the linear viscoelastic regime were conducted over the range of 0.01-1000 Pa (log mode) at 25 °C and with a frequency of 1 Hz. For frequency sweeps, the samples were subjected to frequencies ranging from 0.001 to 100 Hz at 25 °C and an oscillatory stress of 5 Pa. Temperature dependent experiments were conducted in a controlled gap compensation mode in the temperature range between 15 °C and 45 °C with a heating/cooling rate of 2 °C·$min^{-1}$, applying an oscillatory stress of 5 Pa at a frequency of 1 Hz. Based on the ratio of the values for the storage modulus G’ and the loss modulus G”, a system was considered as viscous liquid-like for G’’< G’, as soft-gel for G’ equal to G”, and as hard gel for G’ > G”.[298]

## 8.3 Synthesis of chain transfer agents (CTAs)

The chemicals used for the synthesis of the chain transfer agents (CTAs) were used without further purification if not stated otherwise. **CTA6** was synthesised by J. Kristen.[196]

## 8.3.1 Synthesis of CTA1

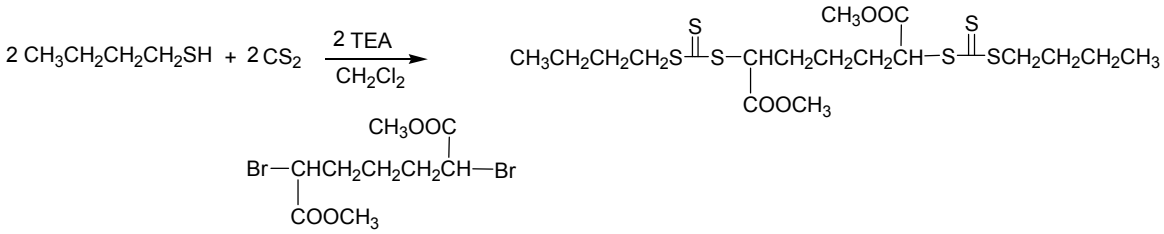


**Scheme 8.1 Structure of CTA1**

### *Materials*

Butanethiol [109-79-5] (99%, Acros Organics), carbon disulfide [75-15-0] (99.9%, Acros Organics), dichloromethane [75-09-2] (Acros Organics), dimethyl-2,6-dibromoheptanedioate [868-73-5] (97%, Sigma-Aldrich), triethylamine [121-44-8] (99%, Acros Organics); magnesium sulfate [7487-88-9] (97%, Acros Organics) were used as received.

### *Procedure*

The compound **CTA1** was synthesised by alkylation of trithiocarbonate salts with alkyl halides following a general procedure.[334] Butanethiol (7.5 mL, 0.066 mol), $CS_2$ (4 mL, 0.066 mol) and dry $CHCl_3$ (20 mL) were placed in a dry three necked round-bottomed flask. Triethylamine (6.4 mL, 0.068 mol) was added dropwise at room temperature with stirring. The solution became yellow/orange as the addition proceeded with formation of the intermediate triethylammonium butyl trithiocarbonate. After 30 min of stirring, dimethyl 2,6-dibromoheptanedioate (5 mL, 0.033 mol) was added slowly, causing the mixture to thicken with formation of the bromide salt. The reaction mixture was stirred for 16 h, then diluted with an additional $CHCl_3$ (20 mL) prior to washing sequentially with three portions of 100 mL of deionised water. The solution was dried over $MgSO_4$, concentrated by evaporation and passed over a short column of basic $Al_2O_3$. The solvent was removed by rotary evaporation to give a orange oil.

Yield: 16.35g (95.90%). MS (EI, negative ions): m/z = 516 (M-1). EA ($C_{19}H_{32}O_4S_6$, Mr=516.85): Calc.: %C = 44.15; %H = 6.24; %S = 37.22. Found: %C = 44.29; %H = 6.28; %S = 36.98. $^1$H-NMR (300 MHz in $CDCl_3$, δ in ppm): δ = 0.93 (t, 6H $CH_3$-), 1.42 (m, 4H, S-C-C-$CH_2$-), 1.50-1.60 (m, 2H, -$CH_2$-C-C(COO)-S-), 1.68 (m, 4H, S-C-$CH_2$-), 2.09-1.84

(m, 4H, -$CH_2$-C(COO)-S-), 3.36 (t, 4H, -S-$CH_2$-), 3.73 (s, 6H, O-$CH_3$), 4.83 (m, 2H, S-CH-COO-). $^{13}$C-NMR (75 MHz in $CDCl_3$, δ in ppm): δ = 13.55 (-$CH_3$), 22.00 (-$\underline{C}H_2$-$CH_3$), 24.44 (-$\underline{C}H_2$-C(COO)-C-S-), 29.85 (-S-C-$\underline{C}H_2$-, 30.87 (-$\underline{C}H_2$-C-C(COO)-C-S-), 37.05 (-S-$CH_2$-), 52.24 ($CH_3$O-), 52.73 (-OOC-$\underline{C}$H-S), 170.86 (-COO), 221.88 (-S-(C=S)-S-).

## 8.3.2 Synthesis of CTA2 - CTA5 and CTA7 - CTA8

RAFT agents **CTA2 - CTA5** and **CTA7 – CTA8** were synthesised by analogous procedures and were also obtained in more than 90% yields. **CTA2** was synthesised using diethyl-meso-2,5-dibromoadipate as alkylating agent. **CTA3** was prepared from 1-propanethiol and 1,4-bis-chloromethyl-benzene. The synthesis of **CTA4** started from 1,2-ethandithiol and benzyl bromide, the synthesis of **CTA5** from 1,2-ethandithiol and p-methoxybenzylbromide. Different from the procedure reported in the literature, **CTA7** was also synthesised in the analogous way from benzylmercaptane and benzyl bromide. **CTA8** was synthesised from 4-methoxy-benzyl mercaptane and bromopropane as alkylating agent.

***Materials***

Carbon disulfide [75-15-0] (99.9%, Acros Organics); propanethiol [2107-03-9] (99%, Sigma-Aldrich), butanethiol [109-79-5] (99%, Acros Organics); benzylmercaptane [100-53-8] (99%, Sigma-Aldrich), 1,2-ethanedithiol [540-63-6] (98%, Fluka), 1-bromopropane [106-94-5] (99%, Sigma-Aldrich), benzyl bromide [100-39-0] (98%, Sigma-Aldrich), 4-methoxy-benzylbromide [2746-25-0] (with 3 w% $K_2CO_3$ , Sigma-Aldrich), 4-methoxy-α-toluenethiol [6258-60-2] (Sigma-Aldrich), α,α'-dichloro-p-xylene [623-25-6] (98%, Sigma-Aldrich), diethyl-meso-2,5-dibromoadipate [869-10-3] (98%, Sigma-Aldrich), dichloromethane [75-09-2] (Acros Organics), CHCl3 [37-297-8] (99%, Sigma-Aldrich), triethylamine [121-44-8] (99%, Acros Organics), Aliquat® 336 (Acros Organics, average molar mass 442 g mol-1) and magnesium sulphate [7487-88-9] (97%, Acros Organics) were used as received. basic $Al_2O_3$ (Acros Organics, activated, 50-200 micron).

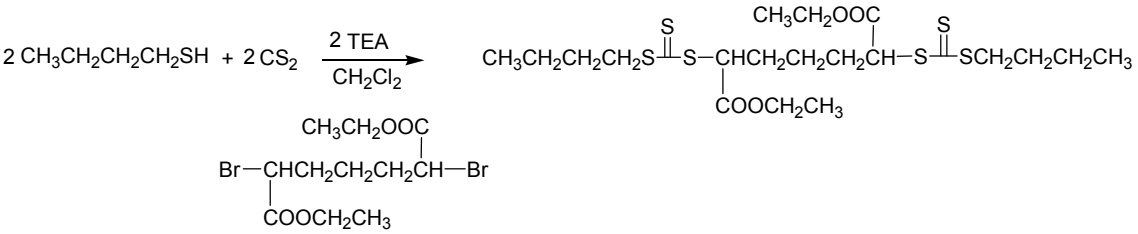

**Scheme 8.2 Structure of CTA2**

**CTA2**. Yield: 15.80g (90.20%). MS (EI, negative ions): m/z = 530. (M-1). EA ($C_{20}H_{34}O_4S_6$, Mr=530.88) : EA: Mr= Calc.: %C: 45.25; %H: 6.46; %S: 36.24. Found: %C = 45.65; %H = 6.53; %S = 35.38. $^1$H-NMR (300 MHz in $CDCl_3$, δ in ppm): δ = 0.93 (t, 6H $CH_3$-), 1.26 (t, 6H $\underline{C}H_3$-C-O), 1.42 (m, 4H -S-C-C-$CH_2$-), 1.66 (m, 4H -S-C-$CH_2$-), 1.95-2.22 (m, 4H, -$CH_2$-C(COOR)-S-), 3.35 (t, 4H, -S-$CH_2$-), 4.22 (q, 4H, -O-$CH_2$-), 4.84 (m, 2H, OOC-CH-S). $^{13}$C-NMR (75 MHz in $CDCl_3$, δ in ppm): δ = 13.54 ($CH_3$-), 14.07 ($\underline{C}H_3$-C-O), 22.01 ($\underline{C}H_2$-$CH_3$), 28.86 (-S-C(COOR)-$\underline{C}H_2$-), 29.87 (S-C-$\underline{C}H_2$-), 36.07 (-S-$\underline{C}H_2$-alkyl), 52.29 (-S-$\underline{C}$H(COOR)-), 61.95 (O-$CH_2$-), 169.92 (-COO-), 221.63 (-S-(C=S)-S-).

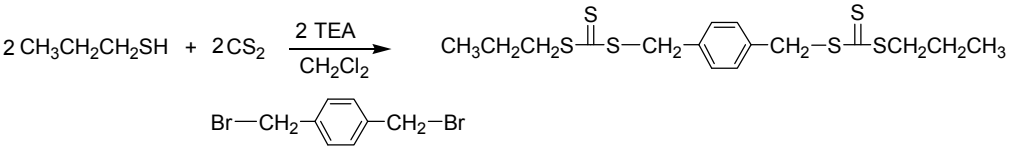

**Scheme 8.3 Structure of CTA3**

**CTA3**. Yield: 13.03g (97.12%). MS (EI, negative ions): m/z = 406 (M-1). EA ($C_{16}H_{22}S_6$, Mr=406.74):. Calc.: %C: 47.25; %H: 5.45; %S: 47.30. Found: %C = 47.58; %H = 5.48; %S = 46.72. $^1$H-NMR (300 MHz in $CDCl_3$, δ in ppm): δ = 1.02 (t, 6H, $CH_3$-), 1.74 (m, 4H, S-C-$CH_2$-), 3.35 (t, 4H, -S-$CH_2$-alkyl), 4.58 (s, 4H, S-$CH_2$-aryl), 7.28 (s, 4H, CHaryl). $^{13}$C-NMR (75 MHz in $CDCl_3$, δ in ppm): δ = 13.44 ($CH_3$-), 21.52 (-$\underline{C}H_2$-$CH_3$), 38.91 (-S-$CH_2$-), 40.84 (-$CH_2$-aryl), 129.52 (CH aryl), 134.78 (C-aryl), 223.58 (-S-(C=S)-S-).

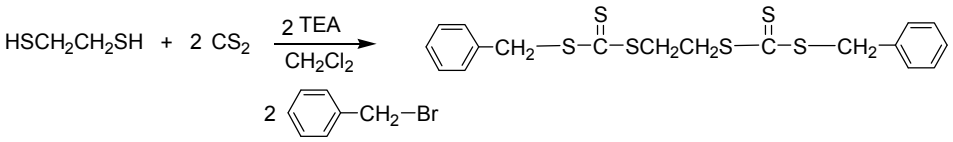


**Scheme 8.4 Structure of CTA4**

**CTA4**. Yield: 12.02g (85.40%). MS (EI, negative ions): m/z = 426. (M-1). EA ($C_{18}H_{18}S_6$, Mr=426.73): Calc.: %C: 50.66; %H: 4.25; %S: 45.09. Found: %C = 49.60; %H = 4.21; %S = 46.02. $^1$H-NMR (300 MHz in $CDCl_3$, δ in ppm): δ = 3.94 (s, 4H, S-$CH_2$-$CH_2$-S), 4.63 (s, 4H, S-$CH_2$-aryl), 7.28-7.36 (m, 10H, CHaryl). $^{13}$C-NMR (75 MHz in $CDCl_3$, δ in ppm): δ = 41.47 (-S-$\underline{C}H_2$-), 41.47 (-S-$\underline{C}H_2$-aryl), 43.67 (-S-$\underline{C}H_2$-$CH_2$-), 127.72 ($\underline{C}$H aryl-para), 128.64 ($\underline{C}$H aryl-ortho), 129.19 ($\underline{C}$H aryl-meta), 134.87 (C-aryl), 222.63 (-S-($\underline{C}$=S)-S-).

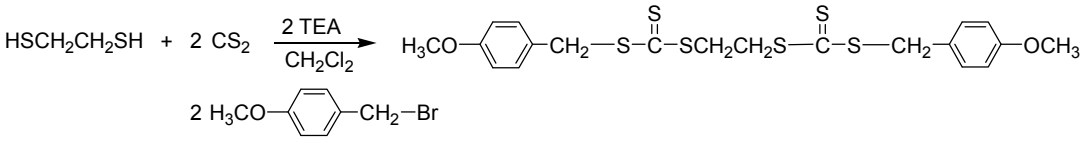


**Scheme 8.5 Structure of CTA5**

**CTA5**. Yield: 14.57g (90.750%). MS (EI, negative ions): m/z = 486 (M-1). EA ($C_{20}H_{22}O_2S_6$, Mr=486.78): Calc.: %C: 49.35; %H: 4.56; %O: 6.57; %S: 39.52. Found: %C = 49.09; %H = 4.63; %S = 40.51. $^1$H-NMR (300 MHz in $CDCl_3$, δ in ppm): δ = 3.86 (s, 4H, S-$CH_2$-$CH_2$-S), 4.01 (s, 6H, $CH_3$-O), 4.64 (s, 4H, S-$CH_2$-aryl), 6.93 (d, 4H, -CH=C-O aryl), 7.34 (d, 4H, =CH-C=C-O aryl). $^{13}$C-NMR (75 MHz in $CDCl_3$, δ in ppm): δ = 41.04 (-S-$\underline{C}H_2$-aryl), 43.67 (-S-$\underline{C}H_2$-$CH_2$), 55.20 ($\underline{C}H_3$-O-) 114.04 ($\underline{C}$H aryl-ortho), 126.61 ($\underline{C}$-$CH_2$ aryl), 130.38 ($\underline{C}$H aryl-meta), 159.13 ($\underline{C}$-O aryl), 223.02 (-S-($\underline{C}$=S)-S-).

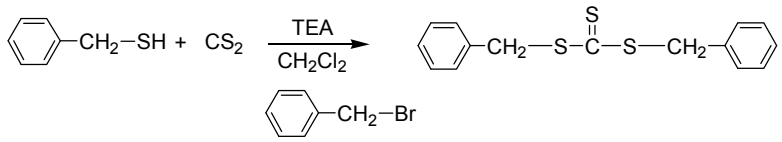

**Scheme 8.6 Structure of CTA7**

**CTA7**. Yield: 8.86.4g (92.50%). EA ($C_{15}H_{14}S_3$, Mr=290.47): Calc.: %C: 62.02; %H: 4.86; %S: 33.12. Found: %C = 62.36; %H = 4.90; %S = 32.91. $^1$H-NMR (300 MHz in $CDCl_3$, δ in ppm): δ = 4.65 (s, 4H, $CH_2$-aryl), 7.38-7.28 (m, 10H, aromatic H). $^{13}$C-NMR (75 MHz in $CDCl_3$, δ in ppm): δ = 41.48 (-S-$\underline{C}H_2$-), 127.72 ($\underline{C}$H aryl-para), 128.64 ($\underline{C}$H aryl-ortho), 129.20 ($\underline{C}$H aryl-meta), 134.84 ($\underline{C}$-aryl), 222.63 (-S-($\underline{C}$=S)-S-).

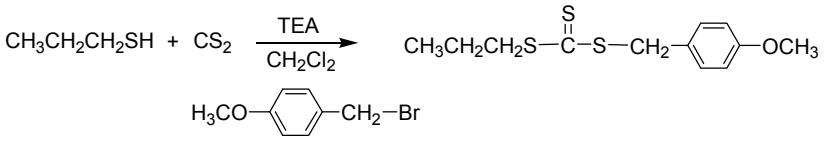

**Scheme 8.7 Structure of CTA8**

**CTA8**. Yield: 15.68 g (90%). MS (EI, negative ions): m/z = 272.45. EA ($C_{12}H_{16}OS_3$, $M_r$ = 272.46): Calc. C 52.90%, H 5.92%, S 35.31%; found: C 53.13%, H 5.90%, S 34.63 %. $^1$H-NMR (300 MHz in $CDCl_3$, δ in ppm): δ = 1.12 (t, 3H, $CH_3$-), 1.83 (m, 2H S-C-$CH_2$-), 3.45 (t, 4H, S-$CH_2$-), 3.88 (s, 3H, $CH_3O$-), 4.66 (s, 2H, $CH_2$-aryl), 6.93 (d, 2H, -CH=C-O-) , 7.34 (d, 2H, =CH-C=C-O-). $^{13}$C-NMR (75 MHz in $CDCl_3$, δ in ppm): δ = 13.41 ($\underline{C}H_3$-), 21.50 ($CH_3$-$\underline{C}H_2$-), 38.72 (-S-$\underline{C}H_2$-alkyl), 40.92 (-S-$\underline{C}H_2$-aryl), 114.05 (-$\underline{C}$H=C-O aryl), 126.60 (=$\underline{C}$< aryl), 130.38 (=$\underline{C}$H-C=C-O aryl), 159.12 (=$\underline{C}$-O aryl), 223.90 (-S-(-($\underline{C}$=S)-S-). UV-vis (in $CH_2Cl_2$): bands at $\lambda_{max1}$ = 310 nm (π-π*, ε = 16100 L mol$^{-1}$ cm$^{-1}$), $\lambda_{max2}$ = 433 nm (n-π*, ε = 62.5 L mol$^{-1}$ cm$^{-1}$).

# 8.4 Synthesis of monomers

## 8.4.1 Synthesis of methoxy diethylene glycol acrylate (MDEGA)

Methoxy diethylene glycol acrylate ***(MDEGA)*** was synthesised following a general procedure described by Fengjunhua et al.[36]

## 8.4.2 Synthesis of 3,5-dibromo benzyl acrylate (M3)

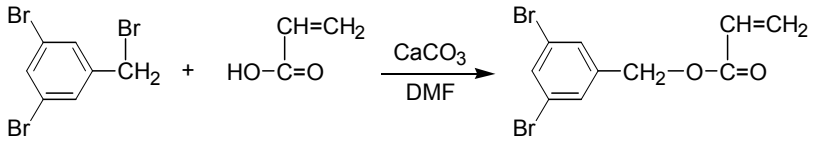


**Scheme 8.8 synthesis of 3,5-dibromo benzyl acrylate (M3)**

### *Materials*

Acrylic acid [79-10-7] (99,5%, Sigma-Aldrich), acryloyl chloride [814-68-6] (99,5%, Sigma-Aldrich), 3,5-dibromobenzyl bromide [56908-88-4] (Acros Organics), caesium carbonate [534-17-8] (99%, Sigma-Aldrich), N,N-dimethylformamide [68-12-2] (99,8%, Fluka) dried over molecular sieve, $CH_2Cl_2$ [75-09-2] (Acros Organics), and magnesium sulphate [7487-88-9] (97%, Acros Organics) were used as received.

### *Procedure*

After activating molecular sieve (3 g) and drying caesium carbonate (10 g; 0.030 mol) at 120°C at 2 x$10^{-4}$ mbar, acrylic acid (3 ml; 0.03 mol) and hydroquinone (0.2 g) in dry DMF (40 ml) were added at 0°C. After 10 min, 3,5-dibromo benzyl bromide (5.0 g; 0.0152 mol) was added dropwise in dry DMF (40 ml) in an nitrogen atmosphere, and the reaction mixture was stirred for 48 h. After dilution with $CH_2Cl_2$ (200 mL), the mixture was washed thrice with portions of 100 mL of deionised water. The solution was dried over $MgSO_4$, passed over a short column of basic $Al_2O_3$, and concentrated by rotary evaporation at ambient temperature. Kugelrohr distillation at 130-160 °C at 2 x$10^{-4}$ mbar gave a white solid.

Yield: 3.70 g (74%).

MS (EI, selected positive ions): m/z = 318, 320, 322 ($M^+$). EA ($C_{10}H_8Br_2O_2$, $M_r$=319.98): Calc.: %C: 37.54; %H: 2.52; %Br: 49.94; %O: 10.00. Found: %C =38.94; %H = 2.51; %Br = 47.99. $^1$H-NMR (300 MHz in DMOS-$d_6$, δ in ppm): δ = 5.16 (s, 2H, -O-$CH_2$-), 5.99 (m, 1H, =CH- E), 6.24 (m, 1H, =CH-COO- ), 6.38 (m, 1H, =CH Z), 7.62 (s, 2H, =CH- aryl, ortho), 7.79 (s, $^1$H, =CH- aryl, para). $^{13}$C-NMR (75 MHz in $CDCl_3$, δ in ppm): δ = 63.66 (-O-$\underline{C}H_2$-l), 122.10, 127.45, 129.44, 132.08, 132.61, 140.34 (-$\underline{C}$= aryl and vinyl), 164.86 (-$\underline{C}$OO-).

# 8.5 Polymerisations

## 8.5.1 Materials

4-*tert*butyl-styrene (**M1**) [1746-23-2] (93%, Sigma-Aldrich), styrene (**M2**) [100-42-5] (99%, Sigma-Aldrich), 2-Ethylhexyl acrylate (**M4**) [103-11-7] (99%, Acros Organics) and octadecyl acrylate (**M5**) [4813-57-4] (99,7%, Sigma-Aldrich) were purified by passing through a column filled with basic $Al_2O_3$ (Acros Organics, activated, 50-200 micron). Styrene-$d_8$ [PS 07150] (99,0%, Chemotrade) was distilled in vacuo in the presence of hydroquinone, N-isopropylacrylamide (**M6**) [2210-25-5] (99%, Acros Organics) was recrystallized from hexane and dried in vacuo. Azoisobutyronitrile AIBN (Wako) was recrystallized from methanol. Tetrahydrofurane (THF) was distilled over K-Na. Regenerated cellulose dialysis tubing was obtained from Roth, Germany (Zellu Trans 3,5, nominal cut-off 4.000-6.000).

## 8.5.2 Synthesis of hydrophilic macroCTAs

***Typical procedure for RAFT polymerisation of NIPAM***

In a typical polymerisation, **NIPAM** (27.65 g; 0.244mol), AIBN (0.00453 g; 2.764 x10-5 mol) previously dissolved in distilled THF (3 mL), **CTA3** (0.1124 g; 2.764 x10-5 mol) and THF (128 mL) were accurately weighed and then transferred to a round-bottom flask (250 mL), equipped with a magnetic stirrer bar. The reaction flask was sealed with a rubber septum, and the contents were degassed with argon for 55 min. The flask was then immersed into an oil bath preheated to 70 °C. After 130 min, the reaction was quenched by placing the flask into liquid nitrogen. The reaction mixture was diluted with acetone and the polymer was precipitated one time in diethyl ether (600 mL), dissolved in acetone and dialysised for 3 d. The polymer was isolated by lyophilization from water to give a white-off powder: Yield: 14.10 g (51.0 %).

***Typical procedure for RAFT polymerisation of MDEGA***

In a typical procedure, **MDEGA** (5 g; 0.0087 mol), **CTA8** (0.0686 g; 2.5 x10-4 mol) were dissolved in toluene (8 mL), AIBN (0.0082 g; 5.0 x10-5 mol) previously dissolved in (2 mL) in THF were added, and the contents were purged with argon for 15 min. The sealed reaction flask was then immersed into an oil bath preheated to 70 °C. After 6 h, the reaction was

quenched by placing the flask in liquid nitrogen. The reaction mixture was diluted with acetone and precipitated three times into hexane (300 mL). The polymer obtained was a viscous yellow oil.

Yield: 3.6 g (72 %).

## 8.5.3 Synthesis of hydrophobic macroCTAs

***Typical procedure for RAFT polymerisation of 4-tert-butyl styrene (M1)***

In a typical procedure, 4-*tert*-butyl styrene (5.0 g; 0.031mol), **CTA1** (0.289 g; 9.95 $x10^{-4}$ mol), and AIBN (0.0163 g; 9.95 $x10^{-5}$ mol) in THF (4 mL) were purged with argon for 15 min, and reacted at 65 °C for 24 h. The reaction was quenched by placing the flask in liquid nitrogen. The mixture was diluted with THF and precipitated into methanol (300 mL). The polymer was purified by a second precipitation from THF into methanol, collected by filtration and dried in vacuo at 50 °C, to give a yellow powder. Yield: 2.3 g (46 %).

***Typical procedure for RAFT polymerisation of styrene (M2)***

Styrene (10.0 g; 0.096 mol) and the selected RAFT agent (0.002 mol), **CTA1**, were placed in a 100 mL flask equipped with a magnetic stirrer. The homogeneous mixture was sealed with a rubber septum, and the contents were purged with argon for 25 min. The flask was then immersed in an oil bath at 110 °C for 18 h. The polymerisation was quenched by placing the flask into liquid nitrogen, the mixture diluted with acetone and precipitated into methanol. The precipitation was repeated twice, and the yellow polymer dried in vacuo at 50 °C for 16 h. Yield 5.20 g (52.0 %).

***Polymerisation of styrene-$d_8$: synthesis of macroRAFT-$d_8$***

Styrene-$d_8$ (10.0 g; 0.089 mol) and the selected RAFT agent (0.002 mol) were placed in a 100 mL flask equipped with a magnetic stirrer. The homogeneous mixture was sealed with a rubber septum, and the contents were degassed with argon for 28 min to eliminate oxygen. The flask was then immersed in an oil bath at 110 °C. After 19 h, the polymerisation was quenched by placing the flask into liquid nitrogen. The reaction mixture was diluted with acetone and precipitated in methanol. The precipitation was repeated twice, and the collected polymer was dried in vacuo at 50 °C for 16 h.

Yield 4.0 g (40.0 %) of a yellow powder.

***Typical procedure for RAFT polymerisation of 3,5-dibromo benzyl acrylate (M3)***

3,5-dibromo benzyl acrylate (2.8 g; 0.0087 mol), **CTA1** (0.1626 g; 5.6 x$10^{-4}$ mol), and AIBN (0.0184 g; 1.12 x$10^{-4}$ mol) in THF (5 mL), and the contents were degassed with argon for 15 min. The sealed reaction flask was then immersed into an oil bath preheated to 70 °C. After 5 h, the reaction was quenched by placing the flask in liquid nitrogen, the reaction mixture diluted with THF, and precipitated into acetone (300 mL). The polymer was collected by filtration, to give a yellow powder. Yield: 1.68 g (60.0 %).

***Typical procedure for RAFT polymerisation of 2-ethyl hexyl acrylate (M4)***

In a typical procedure, 2-ethyl hexyl acrylate (10.07 g; 0.054 mol), **CTA1** (0.58 g; 2.0 x$10^{-3}$ mol), and AIBN (0.065 g; 4.0 x$10^{-4}$ mol) in THF (10 mL) were purged with argon for 30 min, and immersed into an oil bath preheated to 70 °C. After 6 h, the reaction was quenched in liquid nitrogen, the mixture diluted with acetone, and precipitated into cold methanol/water (50:50) (300 mL). The polymer was collected by decantation and dried, to give a viscous yellow oil. Yield: 6.54 g (65 %).

***Typical procedure for RAFT polymerisation of octadecyl acrylate (M5)***

In a typical procedure, octadecyl acrylate (10 g; 0.0308 mol), **CTA1** (0.580 g; 2.0 x$10^{-3}$ mol), and AIBN (0.0656 g; 4.0 x$10^{-4}$ mol) in THF (10 mL) were purged with argon for 20 min, and immersed into an oil bath preheated to 70 °C. After 5 h, the reaction was quenched in liquid nitrogen, the mixture diluted with THF, precipitated into methanol (300 mL). The polymer was filtered off to give a yellow powder.

Yield: 5.9 g (59 %).

## 8.5.4 Synthesis of amphiphilic triblock copolymers

***Polymer chain extension with NIPAM***

In a typical procedure, **NIPAM** (5.10g; 0.044mol), the selected macroRAFT agent, here **pM1#17** (0.79 g; 2.7 x10-4 mol), AIBN (0.0040 g; 2.4 x10-5 mol) in THF (28 mL) were

purged with argon for 30 min. The sealed reaction flask was immersed into an oil bath preheated to 70 °C. After 130 min, the reaction was quenched by placing the flask in liquid nitrogen. The reaction mixture was diluted with acetone, and precipitated into diethyl ether (300 mL). The polymer was collected by filtration, dissolved in acetone and dialyzed against water for 3 d with regenerated cellulose dialysis tubing (Roth, nominal cut-off 4.000-6.000). The polymer was recovered and lyophilized to give a white-off powder. Yield: 4.38 g (86 %).

***Polymer chain extension of macroRAFT-$d_8$ with NIPAM***

In a typical polymerisation, **NIPAM** (5.10 g; 0.045 mol), the selected macroRAFT agent (macroRAFT1 (0.2875 g; Mn=2300 g/mol; 1.25 x10-4 mol), AIBN (0.0025 g; 1.5625 x10-5 mol) dissolved in THF (3 mL) and THF (25 mL) were accurately weighed and then transferred to a round-bottom flask (100 mL), equipped with a magnetic stirrer bar. The reaction flask was sealed with a rubber septum, and the contents were degassed with argon for 15 min. The reaction flask was then immersed into an oil bath preheated to 65 °C. After 62 h, the reaction was quenched by placing the flask in liquid nitrogen. The reaction mixture was diluted with acetone, and precipitated in diethyl ether (300 mL). The polymer was collected by filtration, dissolved in acetone and dialyzed for 3 d against water. The polymer was recovered and freeze-dried.

Yield: 4.08 g (80.0 %) of white-off powder. Elemental analysis: Found %C = 59.68; %N = 11.00.

***Polymer chain extension with MDEGA***

In a typical procedure, **MDEGA** (5.7 g; 0.0327 mol), macroRAFT agent1 (0.0575 g; 1.42 x10-4 mol; 2300 g/mol), AIBN (0.0045 g; 2.85 x10-5 mol) were dissolved in THF (20 mL), and the contents were degassed with argon for 20 min. The sealed reaction flask was then immersed into an oil bath preheated to 65 °C. After 63 h, the reaction was quenched by placing the flask in liquid nitrogen. The reaction mixture was diluted with acetone, and precipitated into cold hexane (300 mL). The polymer was collected by filtration, dried in vacuum oven to give a viscous yellow oil.

Yield: 5.36 g (94 %).

## 8.6 Preparation of micellar aqueous solutions

***Dilute aqueous solutions of thermoresponsive polymers***

Aqueous solutions of polymers at low concentrations (1g/L) are referred as *dilute* solutions. They were prepared by dissolving dried polymer samples directly in water.

***Semi-Concentrated to concentrated aqueous solutions of thermoresponsive polymers***

Aqueous solutions of polymers with concentrations lower than 40 wt% were also prepared by dissolving freeze dried polymer samples directly in water, supporting the mixing and dissolution with a Lab shaker HS 250 at ambient temperature (about 20 °C) for 1 week. These solutions were referred as *semi-concentrat*e. In order to obtain more *concentrated* aqueous solutions, the copolymers were first dissolved in acetone and then allowed to evaporate the solvent on the wall of a vessel in order to form a thin polymer film. Then the desired volume of water was added, and samples were left for 2 weeks at ambient temperature (about 20 °C).

*"Learn from yesterday, live for today, hope for tomorrow. The important thing is not to stop questioning."*
*Albert Einstein*

# *References*

# References


1. Schmolka, I. *J. Am. Oil Chem. Soc* **1977,** 54, 110-116.

2. Alexandridis, P.; Olsson, U.; Lindman, B. *Macromolecules* **1995,** 28, 7700-7710.

3. Hurter, P. N.; Hatton, T. A. *Langmuir* **2002,** 8, 1291-1299.

4. Schmolka, I. R. *Cosmet. Toiletries* **1984,** 69, 99.

5. Moghimi, S. M.; Hunter, A. C. *Trends Biotechnol.* **2000,** 18, 412-420.

6. Firestone, M. A.; Williams, D. E.; Seifert, S.; Csencsits, R. *Nano Lett.* **2001,** 1, 129-135.

7. Troll, K.; Kulkarni, A.; Wang, W.; Darko, C.; Bivigou Koumba, A. M.; Laschewsky, A.; Müller-Buschbaum, P.; Papadakis, C. *Colloid Polym. Sci.* **2008,** 286, 1079-1092.

8. Bivigou Koumba, A. M.; Kristen, J.; Laschewsky, A.; Müller-Buschbaum, P.; Papadakis, C. M. *Macromol. Chem. Phys.* **2009,** 210, 565-578.

9. Li, C.; Buurma, N. J.; Haq, I.; Turner, C.; Armes, S. P.; Castelletto, V.; Hamley, I. W.; Lewis, A. L. *Langmuir* **2005,** 21, 11026-11033.

10. Chu, B. *Langmuir* **1995,** 11, 414-421.

11. Laurer, J. H.; Khan, S. A.; Spontak, R. J.; Satkowski, M. M.; Grothaus, J. T.; Smith, S. D.; Lin, J. S. *Langmuir* **1999**, 7947-7955.

12. Wu, W.; Matyjaszewski, K.; Kowalewski, T. *Langmuir* **2005,** 21, 1143-1148.

13. Matsen, M. W.; Schick, M. *Macromolecules* **1994,** 27, 187-192.

14. Ten Brinke, G.; Hadziioannou, G. *Macromolecules* **1987,** 20, 486-489.

15. Balsara, N. P.; Tirrell, M.; Lodge, T. P. *Macromolecules* **1991,** 24, 1975-1986.

16. Wang, Y.; Mattice, W. L.; Napper, D. H. *Macromolecules* **1992,** 25, 4073-4077.

17. Rodrigues, K.; Mattice, W. L. *Polym. Bull.* **1991,** 25, 239-243.

18. Kirkland, S. E.; Hensarling, R. M.; McConaughy, S. D.; Guo, Y.; Jarrett, W. L.; McCormick, C. L. *Biomacromolecules* **2008,** 9, 481-486.

19. Kim, S. H.; Jo, W. H. *Macromolecules* **2001,** 34, 7210-7218.

20. Jeong, B.; Gutowska, A. *Trends Biotechnol.* **2002,** 20, 305-311.

21. Mamada, A.; Tanaka, T.; Kungwatchakun, D.; Irie, M. *Macromolecules* **1990,** 23, 1517-1519.

22. Qiu, Y.; Park, K. *Adv. Drug Delivery Rev.* **2001,** 53, 321-339.

23. Bromberg, L. E.; Ron, E. S. *Adv. Drug Delivery Rev.* **1998**, 197-221.

24. Taylor, L. D.; Cerankowski, L. D. *J. Polym. Sci.* **1975,** 13, 2551-2570.

25. Tiktopulo, E. I.; Uversky, V. N.; Lushchik, V. B.; Klenin, S. I.; Bychkova, V. E.; Ptitsyn, O. B. *Macromolecules* **1995,** 28, 7519-7524.

26. Schild, H. G. *Progress in Polymer Science* **1992,** 17, 163-249.

27. Wang, X.; Qiu, X.; Wu, C. *Macromolecules* **1998,** 31, 2972-2976.

28. Heskins, M.; Guillet, J. E. *J. Macromol. Sci., Part A: Pure Appl. Chem.* **1968,** 2, 1441 - 1455.

29. Schild, H. G.; Tirrell, D. A. *J. Phys. Chem.* **1990,** 94, 4352-4356.

30. Ingo, B.; Crisan, P.; Franz-Josef, W.; Walter, R. *Angew. Chem., Int. Ed.* **2006,** 118, 1099-1102.

31. Kanazawa, H.; Kashiwase, Y.; Yamamoto, K.; Matsushima, Y.; Kikuchi, A.; Sakurai, Y.; Okano, T. *Anal. Chem.* **1997,** 69, 823-830.

32. Kanazawa, H.; Yamamoto, K.; Matsushima, Y.; Takai, N.; Kikuchi, A.; Sakurai, Y.; Okano, T. *Anal. Chem.* **1996,** 68, 100-105.

33. Markus, G.; Katsunori, N.; Norio, I.; Hiromi, K. *Die Makromolekulare Chemie* **1992,** 193, 249-256.

34. Hosoya, K.; Sawada, E.; Kimata, K.; Araki, T.; Tanaka, N.; Frechet, J. M. J. *Macromolecules* **2002,** 27, 3973-3976.

35. Kanazawa, H.; Yamamoto, K.; Kashiwase, Y.; Matsushima, Y.; Takai, N.; Kikuchi, A.; Sakurai, Y.; Okano, T. *J. Pharm. Biomed. Anal.* **1997,** 15, 1545-1550.

36. Hua., F.; Jiang., X.; Li., D.; Zhao., B. *J. Polym. Sci., Part A: Polym. Chem.* **2006,** 44, 2454-2467.

37. Zalipsky, S. *Adv. Drug Delivery Rev.* **1995,** 16, 157-182.

38. Kainthan, R. K.; Janzen, J.; Levin, E.; Devine, D. V.; Brooks, D. E. *Biomacromolecules* **2006,** 7, 703-709.

39. Roberts, M. J.; Bentley, M. D.; Harris, J. M. *Adv. Drug Delivery Rev.* **2002,** 54, 459-476.

40. Schild, H. G.; Tirrell, D. A. *Langmuir* **1990,** 6, 1676-1679.

41. Furyk, S.; Yanjie, Z.; Ortiz-Acosta, D.; Cremer, P. S.; Bergbreiter, D. *J. Polym. Sci., Part A: Polym. Chem.* **2006,** 44, 1492-1501.

42. Tong, Z.; Zeng, F.; Zheng, X.; Sato, T. *Macromolecules* **1999,** 32, 4488-4490.

43. Fujishige, S.; Kubota, K.; Ando, I. *J. Phys. Chem.* **1989,** 93, 3311-3313.

44. Takei, Y. G.; Aoki, T.; Sanui, K.; Ogata, N.; Okano, T.; Sakurai, Y. *Bioconjugate Chem.* **1993,** 4, 42-46.

45. Ding, Z.; Chen, G.; Hoffman, A. S. *Bioconjugate Chem.* **1996,** 7, 121-125.

46. Winnik, F. M.; Adronov, A.; Kitano, H. *Can. J. Chem.* **1995,** 73, 2030-2040

47. Duan, Q.; Miura, Y.; Narumi, A.; Shen, X.; Sato, S.-I.; Satoh, T.; Kakuchi, T. *J. Polym. Sci., Part A: Polym. Chem.* **2006,** 44, 1117-1124.

48. Baltes, T.; Garret-Flaudy, F.; Freitag, R. *J. Polym. Sci., Part A: Polym. Chem.* **1999,** 37, 2977.

49. Freitag, R.; Baltes, T.; Eggert, M.; Schuegerl, K.; Ute, B. *Bioseparation* **1994,** 4, 353.

50. Mana Ito, T. I. *J. Polym. Sci., Part A: Polym. Chem.* **2006,** 44, 4832-4845.

51. Isobe, Y.; Fujioka, D.; Habaue, S.; Okamoto, Y. *J. Am. Chem. Soc.* **2001,** 123, 7180-7181.

52. Katsumoto, Y.; Kubosaki, N. *Macromolecules* **2008,** 41, 5955-5956.

53. Tomohiro, H.; Yuya, O.; Hiroko, K.; Makiko, S.; Tsuneyuki, S. *J. Polym. Sci., Part A: Polym. Chem.* **2006,** 44, 4450-4460.

54. Feil, H.; Bae, Y. H.; Feijen, J.; Kim, S. W. *Macromolecules* **1993,** 26, 2496-2500.

55. Beltran, S.; Baker, J. P.; Hooper, H. H.; Blanch, H. W.; Prausnitz, J. M. *Macromolecules* **1991,** 24, 549-551.

56. Bokias, G.; Hourdet, D.; Iliopoulos, I. *Macromolecules* **2000,** 33, 2929-2935.

57. Chung, J. E.; Yokoyama, M.; Okano, T. *J. Controlled Release* **2000,** 65, 93-103.

58. Chung, J. E.; Yokoyama, M.; Suzuki, K.; Aoyagi, T.; Sakurai, Y.; Okano, T. *Colloids Surf., B* **1997,** 9, 37-48.

59. Zhang, G.; Wu, C. *J. Am. Chem. Soc.* **2001,** 123, 1376-1380.

60. Winnik, F. M.; Ringsdorf, H.; Venzmer, J. *Macromolecules* **1990,** 23, 2415-2416.

61. Winnik, F. M.; Ottaviani, M. F.; Bossmann, S. H.; Garcia-Garibay, M.; Turro, N. J. *Macromolecules* **1992,** 25, 6007-6017.

62. Asano, M.; Winnik, F. M.; Yamashita, T.; Horie, K. *Macromolecules* **1995,** 28, 5861-5866.

63. Costa Ricardo, O. R.; Freitas Roberto, F. S. *Polymer* **2002,** 43, 5879-5885.

64. Mukae, K.; Sakurai, M.; Sawamura, S.; Makino, K.; Kim, S. W.; Ueda, I.; Shirahama, K. *J. Phys. Chem.* **1993,** 97, 737-741.

65. Freitag, R.; Garret-Flaudy, F. *Langmuir* **2002,** 18, 3434-3440.

66. Zhang, Y.; Furyk, S.; Bergbreiter, D. E.; Cremer, P. S. *J. Am. Chem. Soc.* **2005,** 127, 14505-14510.

67. Freitag, R.; Garret-Flaudy, F. *Langmuir* **2002**, 3434-3440.

68. Schild, H. G.; Tirrell, D. A. *The Journal of Physical Chemistry* **1990,** 94, 4352-4356.

69. Zhang, Y.; Furyk, S.; Sagle, L. B.; Cho, Y.; Bergbreiter, D. E.; Cremer, P. S. *J. Phys. Chem. C* **2007,** 111, 8916-8924.

70. Yuan, G.; Wang, X.; Han, C. C.; Wu, C. *Macromolecules* **2006,** 39, 6207-6209.

71. Elena Krasovitski; Yachin Cohen; Bianco-Peled, H. *J. Polym. Sci., Part B: Polym. Phys.* **2004,** 42, 3713-3720.

72. Currie, E. P. K.; Borisov, O. V. *Macromolecules* **2001,** 34, 1018-1030.

73. Arotcarena, M.; Heise, B.; Ishaya, S.; Laschewsky, A. *J. Am. Chem. Soc.* **2002,** 124, 3787-3793.

74. Qiu, X.; Wu, C. *Macromolecules* **1997,** 30, 7921-7926.

75. Topp, M. D. C.; Dijkstra, P. J.; Talsma, H.; Feijen, J. *Macromolecules* **1997,** 30, 8518-8520.

76. Zhu, P. W.; Napper, D. H. *Macromolecules* **1999,** 32, 2068-2070.

77. Zhu, P. W.; Napper, D. H. *Langmuir* **2000,** 16, 8543-8545.

78. Van Durme, K.; Van Assche, G.; Aseyev, V.; Raula, J.; Tenhu, H.; Van Mele, B. *Macromolecules* **2007,** 40, 3765-3772.

79. Hua, F.; Jiang, X.; Zhao, B. *Macromolecules* **2006,** 39, 3476-3479.

80. Allen, C.; Maysinger, D.; Eisenberg, A. *Colloids Surf., B* **1999,** 16, 3-27.

81. Colin Booth, D. A. *Macromol. Rapid Comm.* **2000,** 21, 501-527.

82. Kelarakis, A.; Havredaki, V.; Booth, C. *Macromol. Chem. Phys.* **2003,** 204, 15-21.

83. Mortensen, K.; Brown, W.; Joergensen, E. *Macromolecules* **1994,** 27, 5654-5666.

84. Luo, Y. Z.; Nicholas, C. V.; Attwood, D.; Collett, J. H.; Price, C.; Booth, C. *Colloid Polym. Sci.* **1992,** 270, 1094-1105.

85. Yang, Z.; Sharma, R. *Langmuir* **2001,** 17, 6254-6261.

86. Mortensen, K.; Pedersen, J. S. *Macromolecules* **1993,** 26, 805-812.

87. Hvidt, S.; Joergensen, E. B.; Brown, W.; Schillen, K. *J. Phys. Chem.* **1994,** 98, 12320-12328.

88. Yang, Y.-W.; Ali-Adib, Z.; McKeown, N. B.; Ryan, A. J.; Attwood, D.; Booth, C. *Langmuir* **1997,** 13, 1860-1861.

89. Mortensen, K.; Brown, W. *Macromolecules* **1993,** 26, 4128-4135.

90. Boon Kiak Lau; Qiqiang Wang; Wei Sun; Li, L. *J. Polym. Sci., Part B: Polym. Phys.* **2004,** 42, 2014-2025.

91. Brown, W.; Schillen, K.; Hvidt, S. *J. Phys. Chem.* **1992,** 96, 6038-6044.

92. Jeong, B.; Bae, Y. H.; Kim, S. W. *J. Controlled Release* **2000,** 63, 155-163.

93. Balsara, N. P.; Tirrell, M.; Lodge, T. P. *Macromolecules* **1991,** 24, 1975-1986.

94. Zhou, Z.; Chu, B.; Peiffer, D. G. *Langmuir* **1995,** 11, 1956-1965.

95. Nguyen-Misra, M.; Mattice, W. L. *Macromolecules* **1995,** 28, 6976-6985.

96. Ricardo, N. M. P. S.; Honorato, S. B.; Yang, Z.; Castelletto, V.; Hamley, I. W.; Yuan, X.-F.; Attwood, D.; Booth, C. *Langmuir* **2004,** 20, 4272-4278.

97. Liu, T.; Zhou, Z.; Wu, C.; Nace, V. M.; Chu, B. *J. Polym. Sci., Part B: Polym. Phys.* **1998,** 102, 2875-2882.

98. Lee, D. S.; Shim, M. S.; Kim, S. W.; Lee, H.; Park, I.; Chang, T. *Macromol. Rapid Comm.* **2001,** 22, 587-592.

99. Annable, T.; Buscall, R.; Ettelaie, R.; Whittlestone, D. *J. Rheol.* **1993,** 37, 695-726.

100. Bae, S. J.; Suh, J. M.; Sohn, Y. S.; Bae, Y. H.; Kim, S. W.; Jeong, B. *Macromolecules* **2005,** 38, 5260-5265.

101. Zhou, Z.; Chu, B.; Nace, V. M.; Yang, Y.-W.; Booth, C. *Macromolecules* **1996,** 29, 3663-3664.

102. Liu, T.; Nace, V. M.; Chu, B. *J. Polym. Sci., Part B: Polym. Phys.* **1997,** 101, 8074-8078.

103. Kabanov, A. V.; Batrakova, E. V.; Melik-Nubarov, N. S.; Fedoseev, N. A.; Dorodnich, T. Y.; Alakhov, V. Y.; Chekhonin, V. P.; Nazarova, I. R.; Kabanov, V. A. *J. Controlled Release* **1992,** 22, 141-157.

104. Yu, G.-E.; Masters, A. J.; Heatley, F.; Booth, C.; Blease, T. G. *Macromol. Chem. Phys* **1994,** 195, 1517.

105. Zhou, Z.; Yang, Y.-W.; Booth, C.; Chu, B. *Macromolecules* **1996,** 29, 8357-8361.

106. Yang, Z.; Yang, Y. W.; Zhou, Z. K.; Attwood, D.; Booth, C. *Journal of the Chemical Society-Faraday Transactions* **1996,** 92, 257-265.

107. Liu, T.; Zhou, Z.; Wu, C.; Chu, B.; Schneider, D. K.; Nace, V. M. *J. Polym. Sci., Part B: Polym. Phys.* **1997,** 101, 8808-8815.

108. Matyjaszewski, K.; Müller, A. H. E. *Polym. Prepr.* **1997,** 1, 6-9.

109. Szwarc, M. *J. Polym. Sci., Polym. Chem. Ed.* **1998,** 36, 9-15.

110. Szwarc, M. *Nature* **1956,** 178, 1168-69.

111. Matyjaszewski, K.; Davis, T. P., John Wiley and Sons, Inc: 2002; Vol. 1Ed, p 398-401.

112. Szwarc, M.; Levy, M.; Milkovich, R. M. *J. Am. Chem. Soc.* **1956,** 78, 2656-2657.

113. Von, B. J. S.; Schulz, G. V. *Die Makromolekulare Chemie* **1969,** 121, 184-204.

114. Otsu, T.; Matsunaga, T.; Doi, T.; Matsumoto, A. *Eur. Polym. J.* **1995,** 31, 67-78.

115. Otsu, T. *J. Polym. Sci., Part A: Polym. Chem.* **2000,** 38, 2121-2136.

116. Druliner, J. D. *Macromolecules* **1991,** 24, 6079-6082.

117. Leon-Saenz, E. D.; Morales, G.; Guerrero-santos, R.; Gnanou, Y. *Macromol. Chem. Phys.* **2000,** 201, 74-83.

118. Steenbock, M.; Klapper, M.; Mullen, K. *Macromol. Chem. Phys.* **1998,** 199, 763-769.

119. Moroni, M.; Hilberer, A.; Hadziioannou, G. *Macromol. Rapid Comm.* **1996,** 17, 693-702.

120. Goto, A.; Fukuda, T. *Prog. Polym. Sci* **2004,** 29, 329-385.

121. Georges, M. K.; Veregin, R. P. N.; Kazmaier, P. M.; Hamer, G. K.; Saban, M. D. *Macromolecules* **1994,** 27, 7228-7229.

122. Baldovi, M. V.; Mohtat, N.; Scaiano, J. C. *Macromolecules* **1996,** 29, 5497-5499.

123. Pradel, J. L.; Boutevin, B.; Ameduri, B. *J. Polym. Sci., Part A: Polym. Chem.* **2000,** 38, 3293-3302.

124. Ciriano, M. V.; Korth, H. G.; Van Scheppingen, W. B.; Milder, P. *J. Am. Chem. Soc* **1999,** 121 (27), 6375-6381.

125. Miura, Y.; Nakamura, N.; Taniguchi, I. *Macromolecules* **2001,** 34, 447-455.

126. Greszta, D.; Matyjaszewski, K. *Macromolecules* **1996,** 29, 7661-7670.

127. Jousset, S.; Hammouch, S. O.; Catala, J. M. *Macromolecules* **1997,** 30 (21), 6685-6687.

128. Hammouch, S. O.; Catala, J. M. *Macromol. Rapid Comm.* **1996,** 17, 683-691.

129. Benoit, D.; Grimaldi, S.; Robin, S.; Finet, J. P.; Tordo, P.; Gnanou, Y. *J. Am. Chem. Soc* **2000,** 122 (25), 5929-5939.

130. Benoit, D.; Chaplinski, V.; Braslau, R.; Hawker, C. J. *J. Am. Chem. Soc* **1999,** 121, 3904-20.

131. Farcet, C.; Lansalot, M.; Charleux, B.; Pirri, R.; Vairon, J. P. *Macromolecules* **2000,** 33, 8559-8570.

132. Benoit, D.; Hawker, C. J.; Huang, E. E.; Lin, Z.; Russell, T. P. *Macromolecules* **2000,** 33, 1505-1507.

133. Robin, S.; Gnanou, Y. *ACS Symp Ser* **2000,** 768, 334-46.

134. Benoit, D.; Harth, E.; Fox, P.; Waymouth, R. M.; Hawker, C. J. *Macromolecules* **2000,** 33(2), 363-370.

135. Dasgupta, A.; Sivaram, S., J. M. S. *Rev. Macromol. Chem. Phys* **1997,** 37, 1-59.

136. Hawker, C. J.; Bosman, A. W.; Harth, E. *Chem. Rev.* **2001,** 101, 3661-3688.

137. Georges, M. K.; Veregin, R. P. N.; Kazmaier, P. M.; Hamer, G. K. *Macromolecules* **1993,** 26, 2987-8.

138. Moad, G.; Rizzardo, E.; Solomon, D. H. *Macromolecules* **1982,** 15, 909-914.

139. Wang, J.-S.; Matyjaszewski, K. *J. Am. Chem. Soc.* **1995,** 117, 5614-5615.

140. Matyjaszewski, K.; Xia, J. *Chem. Rev.* **2001,** 101, 2921-2990.

141. Kamigaito, M.; Ando, T.; Sawamoto, M. *Chem. Rev.* **2001,** 101, 3689-3745.

142. Sawamoto, M.; Kamigaito, M. *Trends Polym Sci* **1996,** 4, 371-377.

143. Wang, J.-S.; Matyjaszewski, K. *Macromolecules* **1995,** 28, 7572-7573.

144. Matyjaszewski, K.; Coca, S.; Gaynor, S. G.; Wei, M.; Woodworth, B. E. *Macromolecules* **1998,** 31, 5967-5969.

145. Matyjaszewski, K.; Qiu, J.; Tsarevsky, N. V.; Charleux, B. *J. Polym. Sci., Part A: Polym. Chem.* **2000,** 38, 4724-4734.

146. Gossage, R. A.; Van de Kuil, L. A.; Van Koten, G. *Acc. Chem. Res* **1998,** 31, 423-431.

147. Curran, D. P. *Synthesis* **1998,** 417-439.

148. Asscher, M.; Vofsi, D. J. *Chem. Soc* **1963,** 1887-1896.

149. Bellus, D. *Pure Appl. Chem* **1985,** 57, 1827-1833.

150. Minisci, F. *Acc. Chem. Res* **1975,** 8, 165-171.

151. Matyjaszewski, K.; Paik, H.-J.; Shipp, D. A.; Isobe, Y.; Okamoto, Y. *Macromolecules* **2001,** 34, 3127-3129.

152. Matyjaszewski, K. *Macromolecules* **1999,** 32, 9051-9053.

153. Shim, S. E.; Jung, H.; Lee, H.; Biswas, J.; Choe, S. *Polymer* **2003,** 44, 5563-5572.

154. Uzulina, I.; Kanagasabapathy, S.; Claverie, J. *Macromol. Symp.* **2000,** 150, 33-38.

155. Monteiro, M. J.; de Barbeyrac, J. *Macromolecules* **2001,** 34, 4416-4423.

156. Monteiro, M. J.; Hodgson, M.; de Brouwer, H. *J. Polym. Sci., Part A: Polym. Chem.* **2000,** 38, 3864-3874.

157. Lansalot, M.; Davis, P. T.; Heuts, J. P. A. *Macromolecules* **2002,** 35, 7582-7591.

158. Butte, A.; Storti, G.; Morbidelli, M. *Macromolecules* **2001,** 34, 5885-5896.

159. Vosloo, J. J.; Wet-Roos, D. D.; Tonge, M. P.; Sanderson, R. D. *Macromolecules* **2002,** 35, 4894-4902.

160. De Brouwer, H.; Tsavalas, J. G.; Schork, F. J.; Monteiro, M. J. *Macromolecules* **2000,** 33, 9239-9246.

161. Calitz, F. M.; Tonge, M. P.; Sanderson, R. D. *Macromol. Symp* **2003,** 193, 277-288.

162. Chiefari, J.; Chong, Y. K. B.; Ercole, F.; Krstina, J.; Jeffery, J.; Le, T. P. T.; Mayadunne, R. T. A.; Meijs, G. F.; Moad, C. L.; Moad, G.; Rizzardo, E.; Thang, S. H. *Macromolecules* **1998,** 31, 5559-5562.

163. Chong, B. Y. K.; Le, T. P. T.; Moad, G.; Rizzardo, E.; Thang, S. H. *Macromolecules* **1999,** 32, 2071-2074.

164. Thang, S. H.; Chong, Y. K. B.; Mayadunne, R. T. A.; Moad, G.; Rizzardo, E. *Tetrahedron Lett.* **1999,** 40, 2435-2438.

165. Chiefari, J.; Mayadunne, R. T. A.; Moad, C. L.; Moad, G.; Rizzardo, E.; Postma, A.; Skidmore, M. A.; Thang, S. H. *Macromolecules* **2003,** 36, 2273-2282.

166. Le, T. P.; Moad, G.; Rizzardo, E.; Thang, S. H. *PCT Int. Appl* **Jan. 25, 1998**, WO 9801478 A1 980115.

167. Moad, C. L.; Moad, G.; Rizzardo, E.; Thang, S. H. *Macromolecules* **1996,** 29, 7717-7726.

168. Lai, J. T.; Filla, D.; Shea, R. *Macromolecules* **2002,** 35, 6754-6756.

169. Ashok, K. M.; Werner, F., In *Methods of analysis of dithiocarbamate pesticides: a review*, 1999; Vol. 55, pp 965-970.

170. Laus, M.; Papa, R.; Sparnacci, K.; Alberti, A.; Benaglia, M.; Macciantelli, D. *Macromolecules* **2001,** 34, 7269-7275.

171. Alberti, A.; Benaglia, M.; Laus, M.; Macciantelli, D.; Sparnacci, K. *Macromolecules* **2003,** 36, 736-740.

172. Levillain, J.; Masson, S.; Hudson, A.; Alberti, A. *J. Am. Chem. Soc* **1993,** 115, 8444-8446.

173. Coote, M. L.; Wood, G. P. F.; Radom, L. *J. Polym. Sci., Part A: Polym. Chem.* **2002,** 106, 12124-12138.

174. Chong, Y. K. B.; Krstina, J.; Le, T. P. T.; Moad, G.; Postma, A.; Rizzardo, E.; Thang, S. H. *Macromolecules* **2003,** 36, 2256-2272.

175. Zhu, J.; Zhu, X.; Zhou, D.; Chen, J. *J. Eur. Polym. J.* **2003**, 1618-7229.

176. Asua, J. M. *J. Polym. Sci., Part A: Polym. Chem.* **2004,** 42, 1025-1041.

177. Zaragoza-Contreras, E. A.; Navarro-Rodriguez, D. *Polymer* **2003,** 44, 5541-5546.

178. Uzulina, I.; Gaillard, N.; Guyot, A.; Claverie, J. *Comptes Rendus Chimie* **2003,** 6, 1375-1384.

179. Mayo, F. R. *J. Am. Chem. Soc.* **1968,** 90, 1289-1295.

180. Perrier, S.; Barner-Kowollik, C.; Quinn, J. F.; Vana, P.; Davis, T. P. *Macromolecules* **2002,** 35, 8300-8306.

181. Kwak, Y.; Goto, A.; Tsujii, Y.; Murata, Y.; Komatsu, K.; Fukuda, T. *Macromolecules* **2002,** 35, 3026-3029.

182. Moad, G.; Chiefari, J.; Chong, B. Y.; Krstina, J.; Mayadunne, R. T.; Postma, A.; Rizzardo, E.; Thang, S. H. *Polym. Int.* **2000,** 49, 993-1001.

183. McLeary, J. B.; Calitz, F. M.; McKenzie, J. M.; Tonge, M. P.; Sanderson, R. D.; Klumperman, B. *Macromolecules* **2004,** 37, 2383-2394.

184. Barner-Kowollik, C.; Quinn, J. F.; Morsley, D. R.; Davis, T. P. *J. Polym. Sci., Part A: Polym. Chem.* **2001,** 39, 1353-1365.

185. Monteiro, M. J.; de Brouwer, H. *Macromolecules* **2000,** 34, 349-352.

186. Calitz, F. M.; Tonge, M. P.; Sanderson, R. D. *Macromolecules* **2003,** 36, 5-8.

187. Skrabania, K.; Li, W.; Laschewsky, A. *Macromol. Chem. Phys.* **2008,** 209, 1389-1403.

188. Strube, O. I.; Schmidt-Naake, G. *Macromol. Symp.* **2009,** 275-276, 13-23.

189. Moad, G.; Rizzardo, E.; Thang, S. H. *Polymer* **2008,** 49, 1079-1131.

190. Coote, M. L.; Henry, D. J. *Macromolecules* **2005,** 38, 1415-1433.

191. Coote, M. L.; Krenske, E. H.; Izgorodina, E. I. *Macromol. Rapid Commun.* **2006,** 27, 473-497.

192. Chong, Y. K.; Le, T. P. T.; Moad, G.; Rizzardo, E.; Thang, S. H. *Macromolecules* **1999,** 32, 2071-2074.

193. Chong, Y. K.; Krstina, J.; Le, T. P. T.; Moad, G.; Postma, A.; Rizzardo, E.; Thang, S. H. *Macromolecules* **2003,** 36, 2256-2272.

194. Mayadunne, R. T. A.; Jeffery, J.; Moad, G.; Rizzardo, E. *Macromolecules* **2003,** 36, 1505-1513.

195. Barner, L.; Davis, T. P.; Stenzel, M. H.; Barner-Kowollik, C. *Macromol. Rapid Commun.* **2007,** 28, 539-559.

196. Kristen, J. Thesis in preparation. University Potsdam, 2009.

197. Chen, M.; Ghiggino, K. P.; Mau, A. W. H.; Rizzardo, E.; Sasse, W. H. F.; Thang, S. H.; Wilson, G. J. *Macromolecules* **2004,** 37, 5479-5481.

198. Mertoglu, M.; Laschewsky, A.; Skrabania, K.; Wieland, C. *Macromolecules* **2005,** 38, 3601-3614.

199. Xiao, X.; Fu, Y.-Q.; Zhou, J. J.; Bo, Z. S.; Li, L.; Chan, C.-M. *Macromol. Rapid Commun.* **2007,** 28, 1003-1009.

200. Bonné, T. B.; Papadakis, C. M.; Lüdtke, K.; Jordan, R. *Colloid Polym. Sci.* **2007,** 285, 491-497.

201. Donovan, M. S.; Lowe, A. B.; Sumerlin, B. S.; McCormick, C. L. *Macromolecules* **2002,** 35, 4123-4132.

202. Baussard, J.-F.; Habib-Jiwan, J.-L.; Laschewsky, A.; Mertoglu, M.; Storsberg, J. *Polymer* **2004,** 45, 3615-3626.

203. Kujawa, P.; Segui, F.; Shaban, S.; Diab, C.; Okada, Y.; Tanaka, F.; Winnik, F. M. *Macromolecules* **2006,** 39, 341-348.

204. Laschewsky, A.; Mertoglu, M.; S. Kubowicz; Thünemann, A. F. *Macromolecules* **2006,** 39, 9337-9345.

205. Lowe, A. B.; Wang, R. *Polymer* **2007,** 48, 2221-2230.

206. Metz, N.; Theato, P. *Eur. Polym. J.* **2007,** 43, 1202-1209.

207. Grignard, B.; Jérôme, C.; Calberg, C.; Detrembleur, C.; Jérôme, R. *J. Polym. Sci., Part A: Polym. Chem.* **2007,** 45, 1499-1506.

208. Fournier, D.; Hoogenboom, R.; Thijs, H. M. L.; Paulus, R. M.; Schubert, U. S. *Macromolecules* **2007,** 40, 915-920.

209. Liu, J.; Barner-Kowollik, C.; Bulmus, V.; Stenzel, M. H.; Davis, T. P. *Macromol. Rapid Commun.* **2007,** 28, 305-314.

210. Li, J.; He, W.-D.; Sun, X.-L. *J. Polym. Sci. Part A: Polym. Chem.* **2007,** 45, 5156-5163.

211. Chong, Y. K.; Moad, G.; Rizzardo, E.; Thang, S. H. *Macromolecules* **2007,** 40, 4446-4455.

212. Skrabania, K.; Li, W.; Laschewsky, A. *Macromol. Chem. Phys.* **2008,** 209, 1389-1403.

213. Nykanen, A.; Nuopponen, M.; Laukkanen, A.; Hirvonen, S.-P.; Rytela, M.; Turunen, O.; Tenhu, H.; Mezzenga, R.; Ikkala, O.; Ruokolainen, J. *Macromolecules* **2007,** 40, 5827-5834.

214. Zhou, X.; Ye, X.; Zhang, G. *J. Phys. Chem. B* **2007,** 111, 5111-5115.

215. Ray, B.; Isobe, Y.; Matsumoto, K.; Habaue, S.; Okamoto, Y.; Kamigaito, M.; Sawamoto, M. *Macromolecules* **2004,** 37, 1702-1710.

216. Zheng, G.; Pan, C. *Polymer* **2005,** 46, 2802-2810.

217. Zhang, W.; Zhang, W.; Zhou, N.; Cheng, Z.; Zhu, J.; Zhu, X. *Polymer* **2008,** 49, 4569-4575.

218. Tanimoto, S.; Oida, T. H., K.; Sugimoto, T. *Tetrahedron Lett.* **1981,** 22, 655-658.

219. Mayadunne, R. T. A.; Rizzardo, E.; Chiefari, J.; Krstina, J.; Moad, G.; Postma, A.; Thang, S. H. *Macromolecules* **2000,** 33, 243-245.

220. Loiseau, J.; Doerr, N.; Suau, J. M.; Egraz, J. B.; Llauro, M. F.; Ladavière, C.; Clavérie, J. *Macromolecules* **2003,** 36, 3066-3077.

221. Freal-Saison, S.; Save, M.; Bui, C.; Charleux, B.; Magnet, S. *Macromolecules* **2006,** 39, 8632-8638.

222. Mayadunne, R. T. A.; Rizzardo, E.; Chiefari, J.; Krstina, J.; Moad, G.; Postma, A.; Thang, S. H. *Macromolecules* **2000,** 33, 243-245.

223. Zhou, X. C.; Ye, X. D.; Zhang, G. Z. *J. Phys. Chem. B* **2007,** 111, 5111-5115.

224. Nykänen, A.; Nuopponen, M.; Laukkanen, A.; Hirvonen, S.-P.; Rytelä, M.; Turanen, O.; Tenhu, H.; Mezzenga, R.; Ikkala, O.; Ruokolainen, J. *Macromolecules* **2007,** 40, 5827-5834.

225. Ray, B.; Isobe, Y.; Matsumoto, K.; Habaue, S.; Okamoto, Y.; Kamigaito, M.; Sawamoto, M. *Macromolecules* **2004,** 37, 1702-1710.

226. Nuopponen, M.; Ojala, J.; Tenhu, H. *Polymer* **2004,** 45, 3643-3650.

227. Zheng, G.; Pan, C. *Polymer* **2005,** 46, 2802-2810.

228. Wong, K. H.; Davis, T. P.; Barner-Kowollik, C.; Stenzel, M. H. *Polymer* **2007,** 48, 4950-4965.

229. Bowes, A.; McLeary, J. B.; Sanderson, R. D. *J. Polym. Sci., Part A: Polym. Chem.* **2007,** 45, 588-604.

230. Barner-Kowollik, C.; Quinn, J. F.; Morsley, D. R.; Davis, T. P. *J. Polym. Sci. Part A: Polym. Chem.* **2001,** 39, 1353-1365.

231. Monteiro, M. J.; de Brouwer, H. *Macromolecules* **2000,** 34, 349-352.

232. Konkolewicz, D.; Hawkett, B. S.; Gray-Weale, A.; Perrier, S. *Macromolecules* **2008,** 41, 6400-6412.

233. Lefort, D.; Hugel, G. *Bull. Soc. Chim. France* **1952**, 172-176.

234. Nakai, T.; Shioya, K.; Okawara, M. *Makromol. Chem.* **1967,** 108, 95-103.

235. Larque, A. M.; Maire, C.; Belissent, H.; Galin, M.; Galin, J. C. *L'Actualité chimique* **1988**, 187-193.

236. Souaille, M.; Fischer, H. *Macromolecules* **2002,** 35, 248-261.

237. Pallares, J.; Jaramillo-Soto, G.; Flores-Catano, C.; Lima, E. V.; Lona, L. M. F.; Penlidis, A. *J. Macromol. Sci., Part A: Pure Appl. Chem.* **2006,** 43, 1293 - 1322.

238. Förster, S.; Plantenberg, T. *Angew. Chem., Int. Ed.* **2002,** 41, 688-714.

239. Rodríguez-Hernández, J.; Chécot, F.; Gnanou, Y.; Lecommandoux, S. *Prog. Polym. Sci.* **2005,** 30, 691-724.

240. Riess, G. *Prog. Polym. Sci.* **2003,** 28, 1107-1170.

241. Booth, C.; Attwood, D. *Macromol. Rapid Commun.* **2000,** 21, 501-527.

242. Mortensen, K. *Coll. Surf. A* **2001,** 183-185, 277.

243. Battaglia, G.; Ryan, A. J. *J. Am. Chem. Soc.* **2005,** 127, 8757-8764.

244. Halperin, A. *J. Macromol. Sci. C: Polym. Rev.* **2006,** 46, 173-214.

245. Bonné, T. B.; Lüdtke, K.; Jordan, R.; Papadakis, C. M. *Macromol. Chem. Phys.* **2007,** 208, 1402-1408.

246. Chaterji, S.; Kwon, I. K.; Park, K. *Prog. Polym. Sci.* 32, 1083-1122.

247. Kumar, A.; Srivastava, A.; Galaev, I. Y.; Mattiasson, B. *Prog. Polym. Sci.* **2007,** 32, 1205-1237.

248. Skrabania, K.; Kristen, J.; Laschewsky, A.; Akdemir, O.; Hoth, A.; Lutz, J.-F. *Langmuir* **2006,** 23, 84-93.

249. Maeda, Y.; Mochiduki, H.; Ikeda, I. *Macromol. Rapid Comm.* **2004,** 25, 1330-1334.

250. Mertoglu, M.; Garnier, S.; Laschewsky, A.; Skrabania, K.; Storsberg, J. *Polymer* **2005,** 46, 7726-7740.

251. Liu, S.; Billingham, N. C.; Armes, P. S. *Angew. Chem., Int. Ed.* **2001,** 40, 2328-2331.

252. Yang, Z.; Pickard, S.; Deng, N.-J.; Barlow, R. J.; Attwood, D.; Booth, C. *Macromolecules* **1994,** 27, 2371-2379.

253. Dimitrov, P.; Utrata-Wesolek, A.; Rangelov, S.; Walach, W.; Trzebicka, B.; Dworak, A. *Polymer* **2006,** 47, 4905-4915.

254. Muñoz-Bonilla, A.; Fernández-García, M.; Haddleton, D. M. *Soft Matter* **2007,** 3, 725 - 731.

255. Garnier, S.; Laschewsky, A. *Colloid Polym. Sci.* **2006,** 284, 1243-1254.

256. Garnier, S.; Laschewsky, A. *Macromolecules* **2005,** 38, 7580-7592.

257. Amado, E.; Augsten, C.; Mader, K.; Blume, A.; Kressler, J. *Macromolecules* **2006,** 39, 9486-9496.

258. Colombani, O.; Ruppel, M.; Schubert, F.; Zettl, H.; Pergushov, D. V.; Muller, A. H. E. *Macromolecules* **2007,** 40, 4338-4350.

259. Booth, C.; Attwood, D.; Price, C. *Phys. Chem. Chem. Phys.* **2006,** 8, 3612 - 3622.

260. Cameron, N. S.; Corbierre, M. K.; Eisenberg, A. *Can. J. Chem.* **1999,** 77, 1311-1326.

261. Burba, C. M.; Carter, S. M.; Meyer, K. J.; Rice, C. V. *J. Phys. Chem. B* **2008,** 112, 10399-10404.

262. Tokuhiro, T.; Amiya, T.; Mamada, A.; Tanaka, T. *Macromolecules* **2002,** 24, 2936-2943.

263. Ringsdorf, H.; Simon, J.; Winnik, F. M. *Macromolecules* **1992,** 25, 7306-7312.

264. Kubota, K.; Fujishige, S.; Ando, I. *J. Phys. Chem.* **1990,** 94, 5154-5158.

265. Wu, C.; Zhou, S. *Macromolecules* **1995,** 28, 5388-5390.

266. Wu, C.; Zhou, S. *Phys. Rev. Lett.* **1996,** 77, 3053.

267. Wu, C.; Wang, X. *Phys. Rev. Lett.* **1998,** 80, 4092.

268. Winnik, F. M.; Davidson, A. R.; Hamer, G. K.; Kitano, H. *Macromolecules* **1992,** 25, 1876-1880.

269. Ringsdorf, H.; Venzmer, J.; Winnik, F. M. *Macromolecules* **1991,** 24, 1678-1686.

270. Cammas, S.; Suzuki, K.; Sone, C.; Sakurai, Y.; Kataoka, K.; Okano, T. *J. Controlled Release* **1997,** 48, 157-164.

271. Kohori, F.; Sakai, K.; Aoyagi, T.; Yokoyama, M.; Sakurai, Y.; Okano, T. *J. Controlled Release* **1998,** 55, 87-98.

272. Takei, Y. G.; Aoki, T.; Sanui, K.; Ogata, N.; Okano, T.; Sakurai, Y. *Bioconjugate Chem.* **1993,** 4, 341-346.

273. Laukkanen, A.; Valtola, L.; Winnik, F. M.; Tenhu, H. *Macromolecules* **2004,** 37, 2268-2274.

274. Chan, K.; Pelton, R.; Zhang, J. *Langmuir* **1999,** 15, 4018-4020.

275. Zhong, X. F.; Varshney, S. K.; Eisenberg, A. *Macromolecules* **2002,** 25, 7160-7167.

276. Vasilevskaya, V. V.; Khalatur, P. G.; Khokhlov, A. R. *Macromolecules* **2003,** 36, 10103-10111.

277. Wu, C.; Li, W.; Zhu, X. X. *Macromolecules* **2004,** 37, 4989-4992.

278. Kelarakis, A.; Tang, T.; Havredaki, V.; Viras, K.; Hamley, I. W. *J. Colloid Interface Sci.* **2008,** 320, 70-73.

279. Tian, T.; Valeria, C.; Petros, P.; Ian, W. H.; Stephen, M. K.; Debashish, R.; Sebastien, P.; Richard, H.; Ulrich, S. S. *Macromol. Chem. Phys.* **2006,** 207, 1718-1726.

280. Zhang, W.; Zhou, X.; Li, H.; Fang, Y.; Zhang, G. *Macromolecules* **2005,** 38, 909-914.

281. Liu, T.; Zhou, Z.; Wu, C.; Nace, V. M.; Chu, B. *Macromolecules* **1997,** 30, 7624-7626.

282. Aseyev, V.; Tenhu, H.; Winnik, F. *Adv. Polym. Sci.* **2006,** 196, 1-85.

283. Blanchard, L.-P.; Hesse, J.; Malhotta, S. L. *Can. J. Chem.* **1974,** 52, 3170-3175.

284. Sonja, K.; James, J. G.; Nicholas, R.; John, A. S.; Warren, H. W. *J. Polym. Sci., Part A: General Papers* **1965**, 3573-3586.

285. Leyrer, R. J.; Mächtle, W. *Macromol. Chem. Phys.* **2000,** 201, 1235-1243.

286. Hamley, I. W. *Block Copolymers in Solution: Fundamentals and Applications; John Wiley & Sons: Chichester* **2005**.

287. Booth, C.; Attwood, D. *Macromol. Rapid Commun.* **2000,** 21, 501-527.

288. Mortensen, K. *Coll. Surf. A* **2001,** 183-185, 277-292.

289. Xu, J.; He, J.; Fan, D.; Tang, W.; Yang, Y. *Macromolecules* **2006,** 39, 3753-3759.

290. Laschewsky, A.; Pound, G.; Skrabania, K.; Holdt, H.-J.; Teller, J. *Colloid Polym. Sci.* **2007,** 285, 947-952.

291. Moad, G.; Chong, Y. K.; Postma, A.; Rizzardo, E.; Thang, S. H. *Polymer* **2005,** 46, 8458-8468.

292. Mayer, R.; Schäfer, K. *J. Prakt. Chemie (4. Reihe)* **1964,** 26, 279-295.

293. Mistry, D.; Annable, T.; Yuan, X.-F.; Booth, C. *Langmuir* **2006,** 22, 2986-2992.

294. Kelarakis, A.; Havredaki, V.; Yuan, X.-F.; Chaibundit, C.; Booth, C. *Macromol. Chem. Phys.* **2006,** 207, 903-909.

295. Lee, D. S.; Shim, M. S.; Kim, S. W.; Lee, H.; Park, I.; Chang, T. Y. *Macromol. Rapid Commun.* **2001,** 22, 587-592.

296. Hietala, S.; Nuopponen, M.; Kalliomäki, K.; Tenhu, H. *Macromolecules* **2008,** 41, 2627-2631.

297. Kujawa, P.; Watanabe, H.; Tanaka, F.; Winnik, F. M. *Eur. Phys. J. E.* **2005,** 17, 129-137.

298. Ferry, J. D., *Viscoelastic Properties of Polymers, 3rd ed.; Wiley: New York*. 1980.

299. Tam, K. C.; Wu, X. Y.; Pelton, R. H. *J. Polym. Sci., Part A: Polym. Chem.* **1993,** 31, 963-969.

300. Dormidontova, E. E. *Macromolecules* **2002,** 35, 987-1001.

301. Willauer, H. D.; Huddleston, J. G.; Rogers, R. D. *Ind. Eng. Chem. Res.* **2002,** 41, 1892-1904.

302. Odenwald, M.; Eicke, H. F.; Meier, W. *Macromolecules* **1995,** 28, 5069-5074.

303. Laschewsky, A.; Mertoglu, M.; Kubowicz, S.; Thunemann, A. F. *Macromolecules* **2006,** 39, 9337-9345.

304. Lutz, J.-F. *J. Polym. Sci., Part A: Polym. Chem.* **2008,** 46, 3459-3470.

305. Lutz, J.-F.; Hoth, A. *Macromolecules* **2006,** 39, 893-896.

306. Du, J.-Z.; Chen, D.-P.; Wang, Y.-C.; Xiao, C.-S.; Lu, Y.-J.; Wang, J.; Zhang, G.-Z. *Biomacromolecules* **2006,** 7, 1898-1903.

307. A. Oyane; T. Ishizone; M. Uchida; K. Furukawa; T. Ushida; Yokoyama, H. *Adv. Mater.* **2005,** 17, 2329-2332.

308. Geetha, B.; Mandal, A. B.; Ramasami, T. *Macromolecules* **1993,** 26, 4083-4088.

309. Olugebefola, S. C.; Park, S. Y.; Banerjee, P.; Mayes, A. M.; Santini, C. M. B.; Iyer, J.; Hammond, P. T. *Langmuir* **2002**, 1098-1103.

310. Sugihara, S.; Kanaoka, S.; Aoshima, S. *Macromolecules* **2005,** 38, 1919-1927.

311. Shibata, T.; Kanaoka, S.; Aoshima, S. *J. Am. Chem. Soc.* **2006,** 128, 7497-7504.

312. Han, S.; Hagiwara, M.; Ishizone, T. *Macromolecules* **2003,** 36, 8312-8319.

313. Simon, J. H.; Geraldine, G. D.; Chert-Tsun, Y.; Elodie, I.; Nicholas, J. H.; Tim, H. R. *J. Polym. Sci., Part A: Polym. Chem.* **2008,** 46, 7739-7756.

314. Fechler, N.; Badi, N.; Schade, K.; Pfeifer, S.; Lutz, J.-F. o. *Macromolecules* **2009,** 42, 33-36.

315. Lutz, J.-F.; Weichenhan, K.; Akdemir, O.; Hoth, A. *Macromolecules* **2007,** 40, 2503-2508.

316. Lutz, J.-F.; Andrieu, J.; Uzgun, S.; Rudolph, C.; Agarwal, S. *Macromolecules* **2007,** 40, 8540-8543.

317. Xueguang Jiang, B. Z. *J. Polym. Sci., Part A: Polym. Chem.* **2007,** 45, 3707-3721.

318. Zhao, B.; Li, D.; Hua, F.; Green, D. R. *Macromolecules* **2005,** 38, 9509-9517.

319. Xu, W.; Siow, K. S.; Gao, Z.; Lee, S. Y. *Chem. Mater.* **1998,** 10, 1951-1957.

320. Idziak, I.; Avoce, D.; Lessard, D.; Gravel, D.; Zhu, X. X. *Macromolecules* **1999,** 32, 1260.

321. Liu, H. Y.; Zhu, X. X. *Polymer* **1999,** 40, 6985.

322. Baltes, T.; Garret-Flaudy, F.; Freitag, R. *J. Polym. Sci., Part A: Polym. Chem.* **1990,** 37, 2977.

323. Wu, C.; Qiu, X. *Phys. Rev. Lett.* **1998,** 80, 620.

324. Chen, H.; Li, J.; Ding, Y.; Zhang, G.; Zhang, Q.; Wu, C. *Macromolecules* **2005,** 38, 4403-4408.

325. Dimitris, V.; Constantinos, T. *Macromol. Chem. Phys.* **2001,** 202, 3284-3292.

326. Annable, T.; Buscall, R.; Ettelate, R.; Whittlestone, D. *J. Rheol.* **1993,** 37, 695-726.

327. Jenkins, R. D.; Silebi, C. A.; El-Aasser, M. S. *Polym. Mater. Sci. Eng* **1989,** 61, 629-633.

328. Desbrieres, J.; Hirrien, M.; Ross-Murphy, S. B. *Polymer* **2000,** 41, 2451.

329. Raspaud, E.; Lairez, D.; Adam, M.; Carton, J. P. *Macromolecules* **1994,** 27, 2956-2964.

330. Mortensen, K. *Macromolecules* **1997,** 30, 503-507.

331. Quintana, J. R.; Díaz, E.; Katime, I. *Macromol. Chem. Phys.* **1996,** 197, 3017-3026.

332. Tanaka, F.; Edwards, S. F. *Macromolecules* **1992,** 25, 1516-1523.

333. Virtanen, J.; Tenhu, H. *Macromolecules* **2000,** 33, 5970-5975.

334. Postma, A.; Davis, T. P.; Evans, R. A.; Li, G.; Moad, G.; O'Shea, M. S. *Macromolecules* **2006,** 39, 5293-5306.

# *Appendix*

# RAFT agent 1 (CTA1)

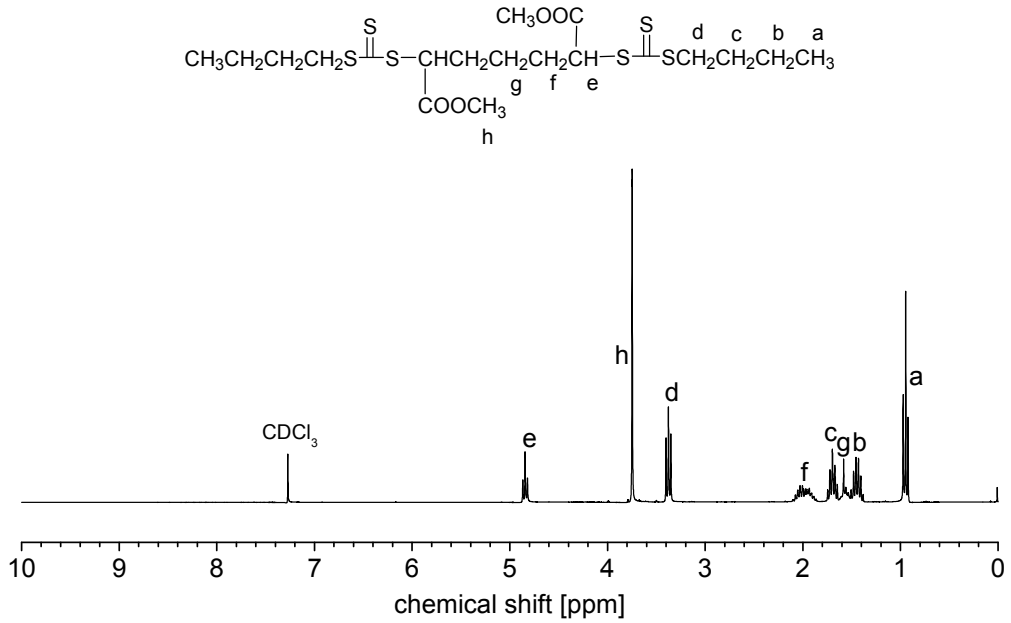


**Figure A1 $^{1}$H-NMR spectrum of RAFT agent 1 in $CDCl_3$**

# RAFT agent 2 (CTA2)

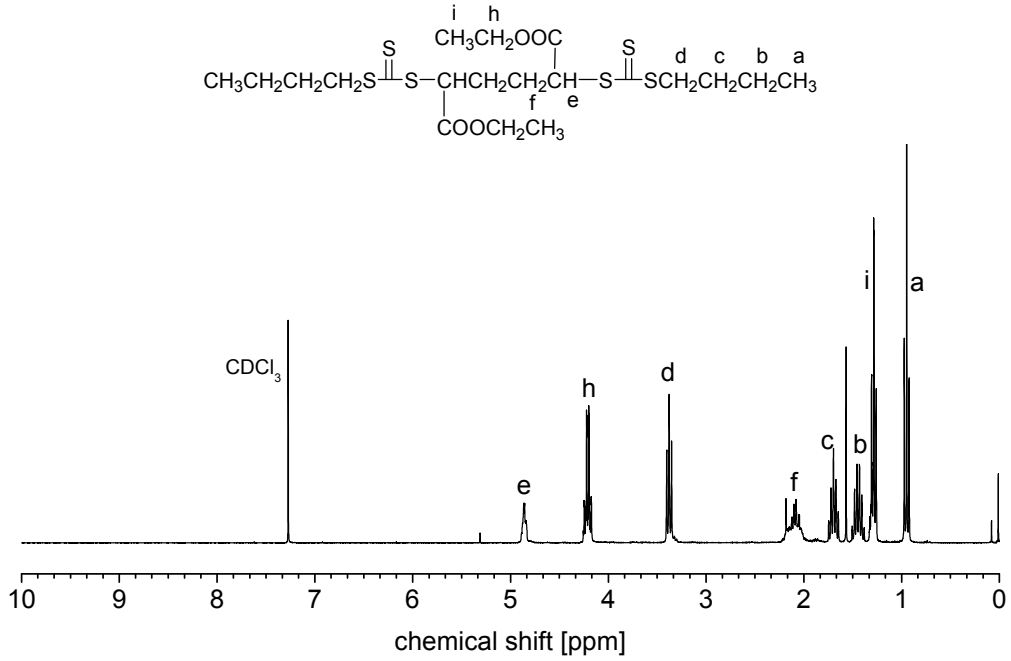


**Figure A2 $^{1}$H-NMR spectrum of RAFT agent 2 in $CDCl_3$**

# RAFT agent 3 (CTA3)

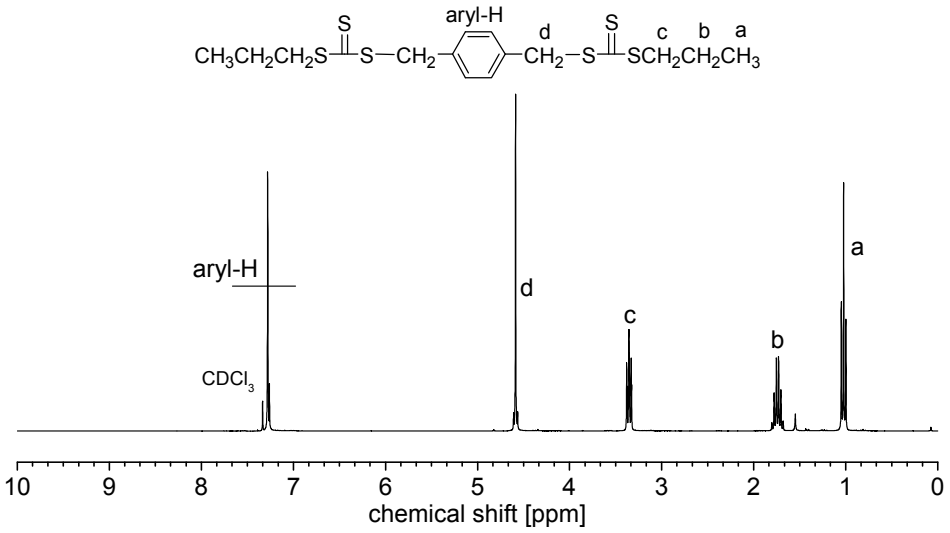


**Figure A3 $^{1}$H-NMR spectrum of RAFT agent 3 in $CDCl_3$**

# RAFT agent 4 (CTA4)

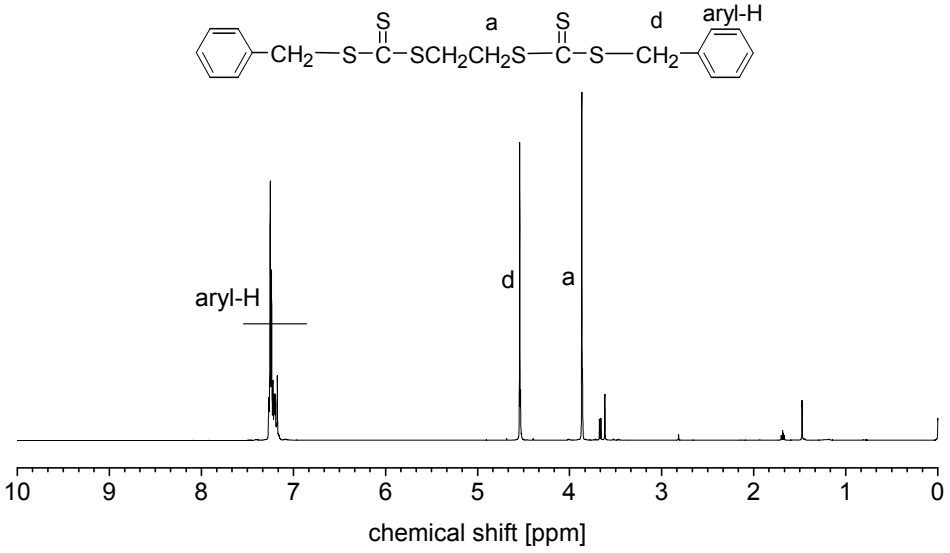


**Figure A4 $^{1}$H-NMR spectrum of RAFT agent 4 in $CDCl_3$**

# RAFT agent 5 (CTA5)

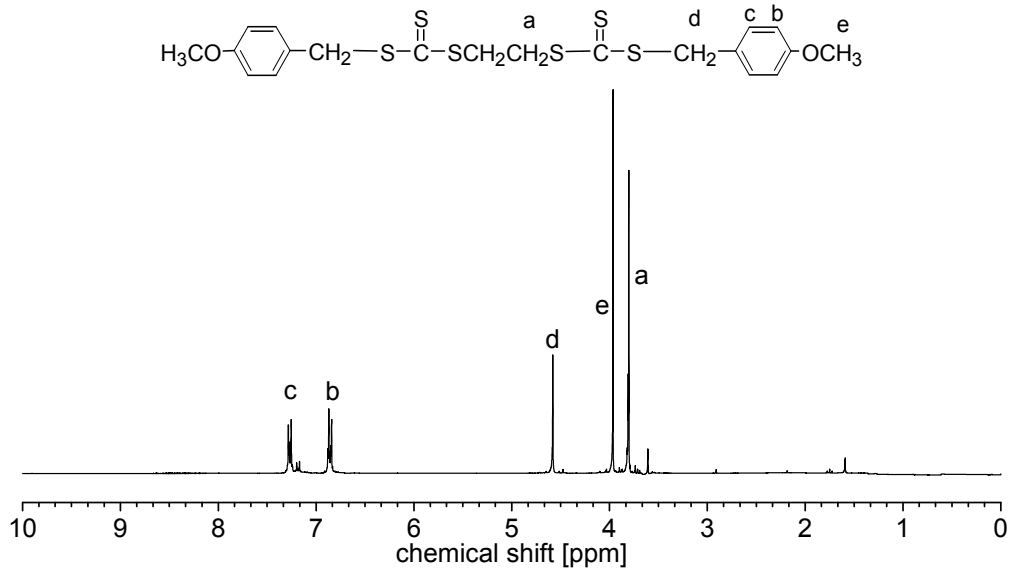


**Figure A5 $^{1}$H-NMR spectrum of RAFT agent 5 in $CDCl_3$**

# RAFT agent 7 (CTA7)

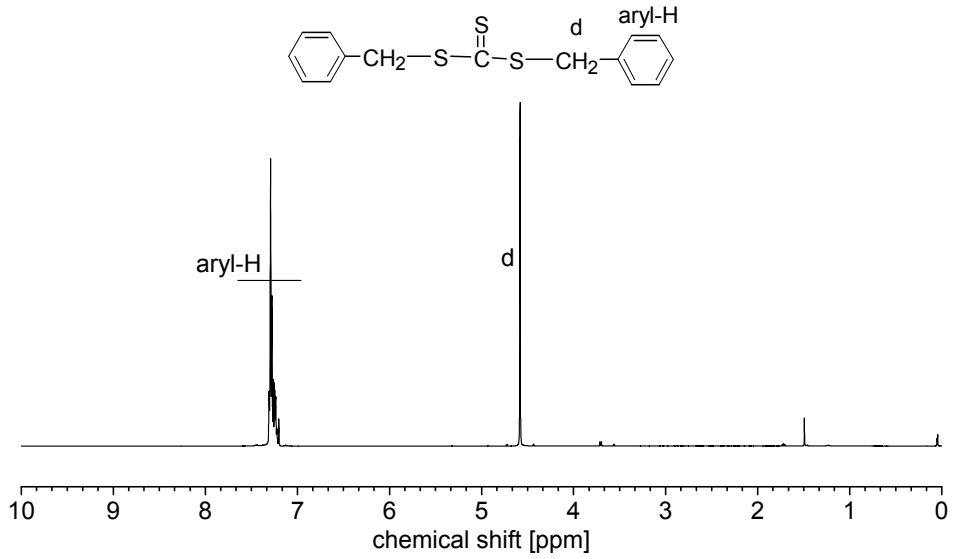


**Figure A6 $^{1}$H-NMR spectrum of RAFT agent 7 in $CDCl_3$**

# RAFT agent 8 (CTA8)

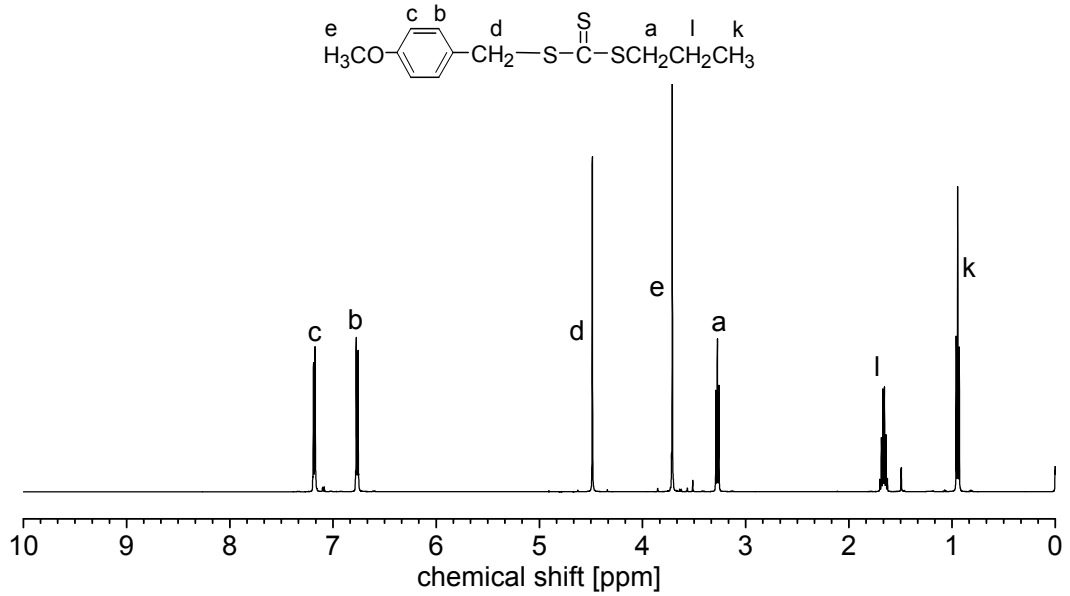


**Figure A7 $^{1}$H-NMR spectrum of RAFT agent 8 in $CDCl_3$**

# 3,5-dibromo benzyl acrylate

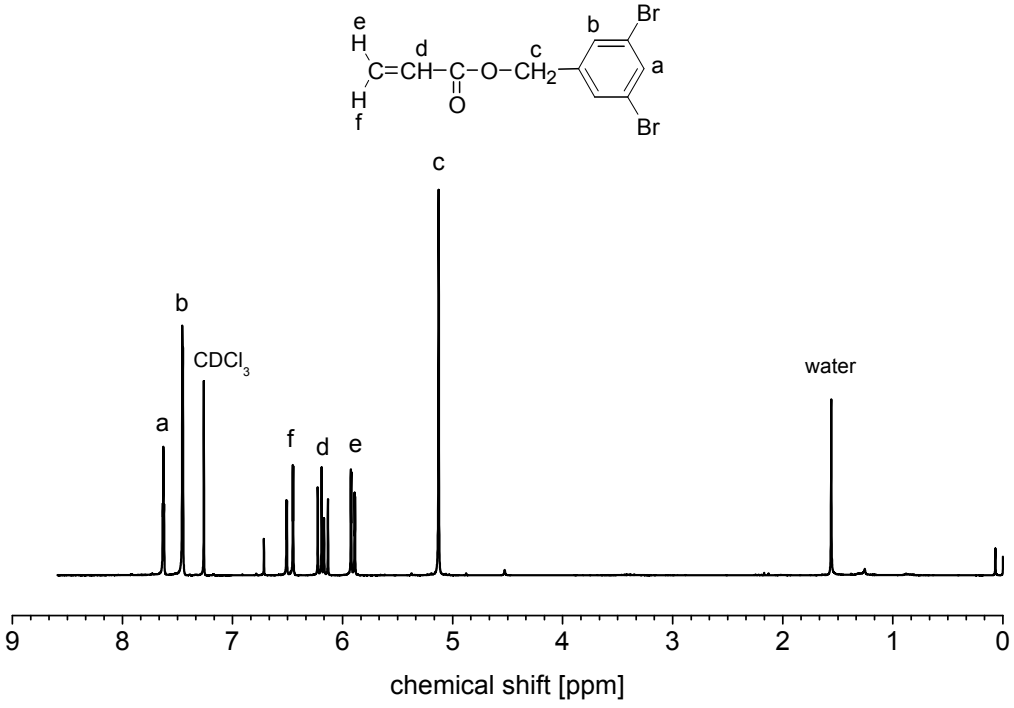


**Figure A8 $^{1}$H-NMR spectrum of 3,5-dibromo benzyl acrylate in $CDCl_3$.**

# PNIPAM-macroRAFT2

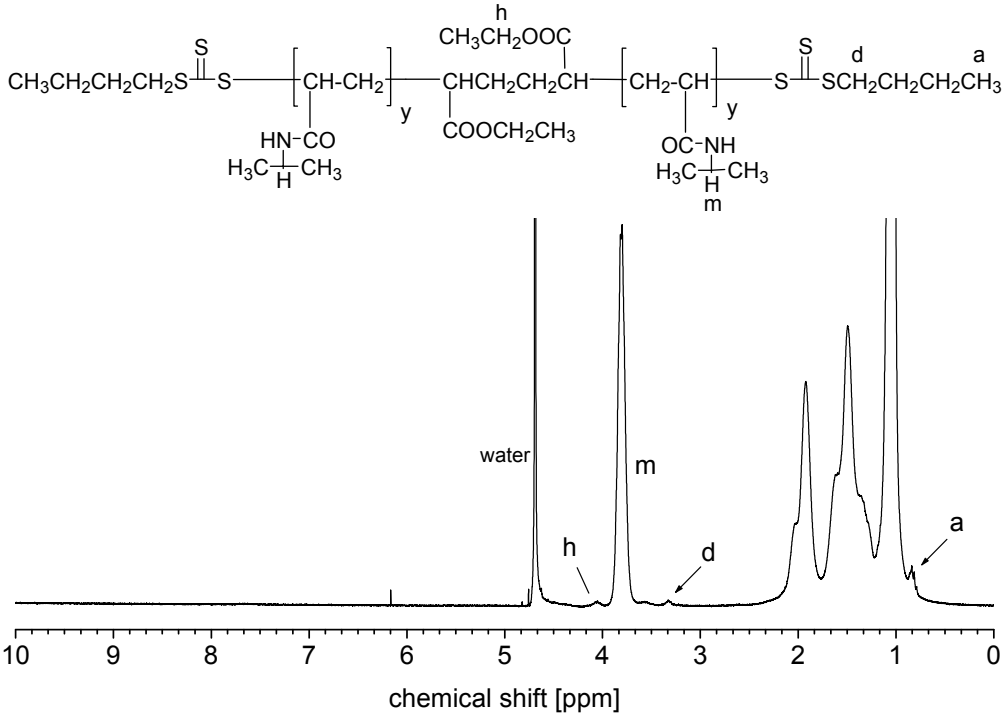


**Figure A9 $^{1}$H-NMR spectrum of PNIPAM-macroRAFT2 in $D_2O$.**

# PNIPAM-macroRAFT3

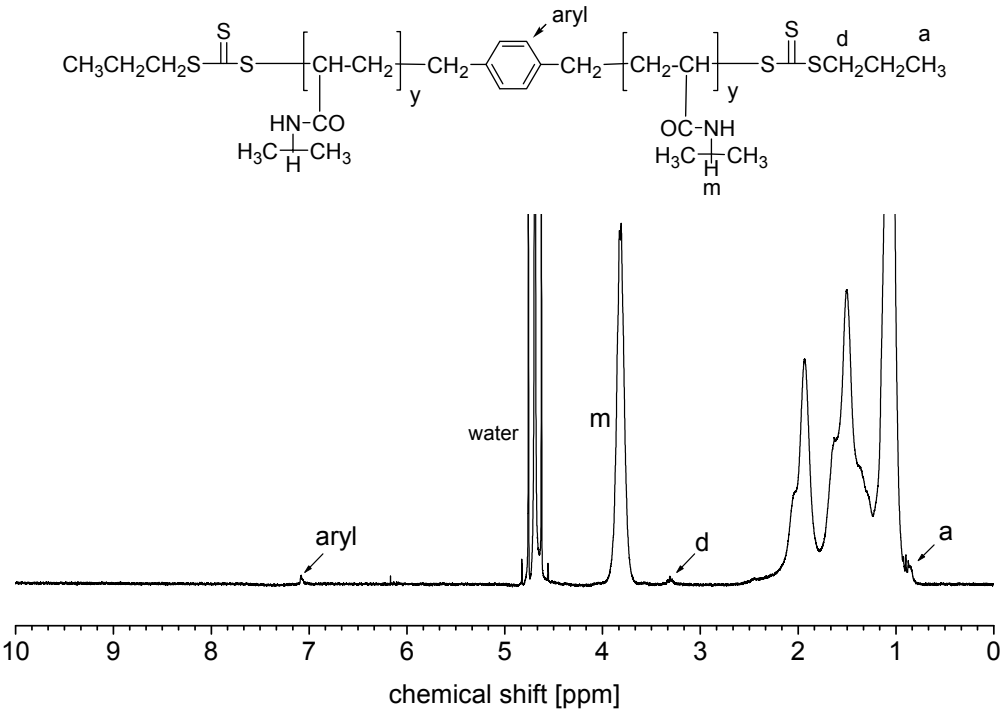


**Figure A10 $^{1}$H-NMR spectrum of PNIPAM-macroRAFT3 in $D_2O$.**

# p(M1)-macroRAFT CTA7

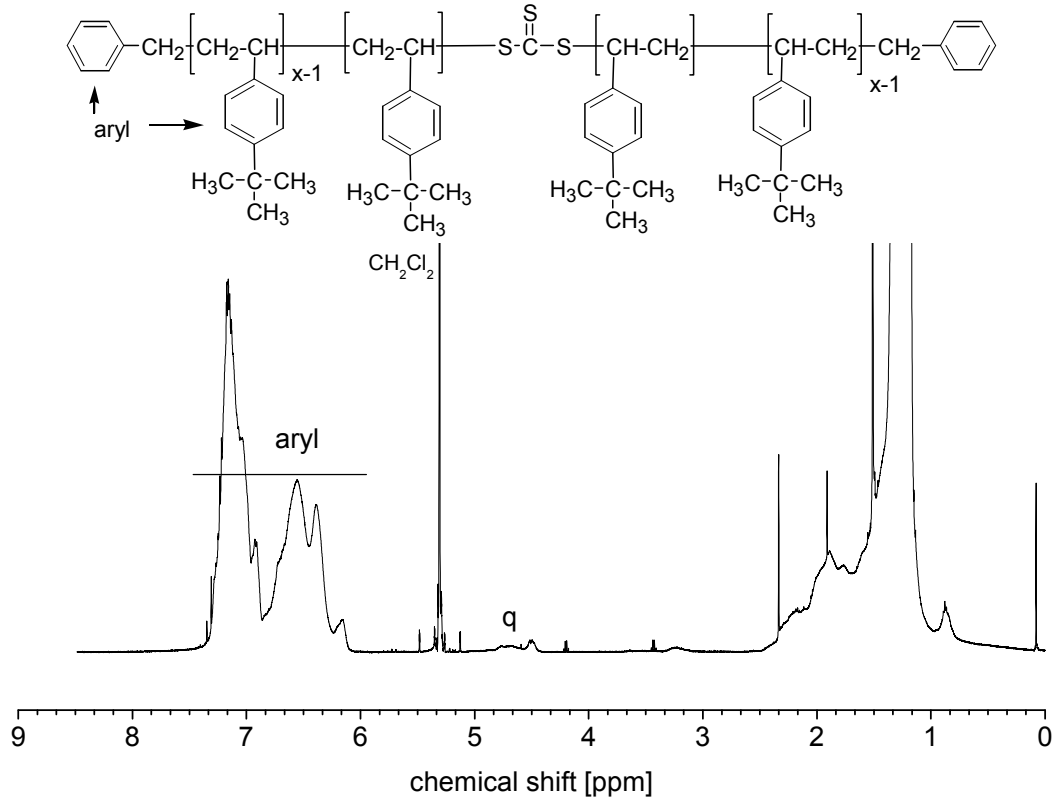


**Figure A11 $^1$H-NMR spectrum of p(M1)-macroRAFT CTA7 in $CD_2Cl_2$.**

# p(M2)-macroRAFT CTA4

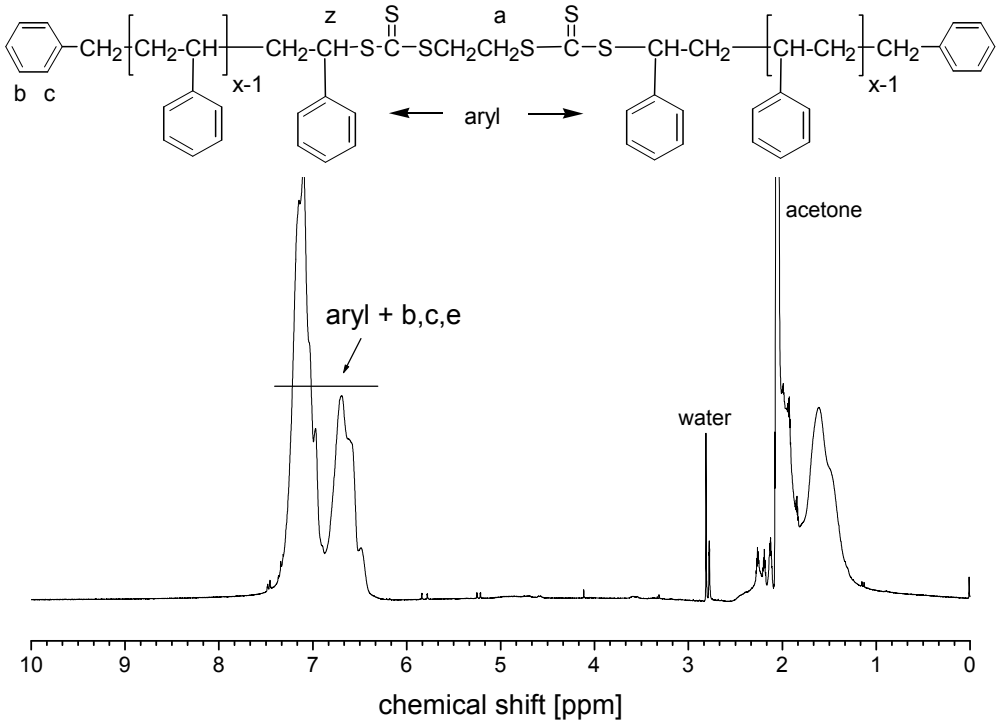


**Figure A12 $^1$H-NMR spectrum of p(M2)-macroRAFT CTA4 in $CD_2Cl_2$.**

# p(M5)-macroRAFT CTA7

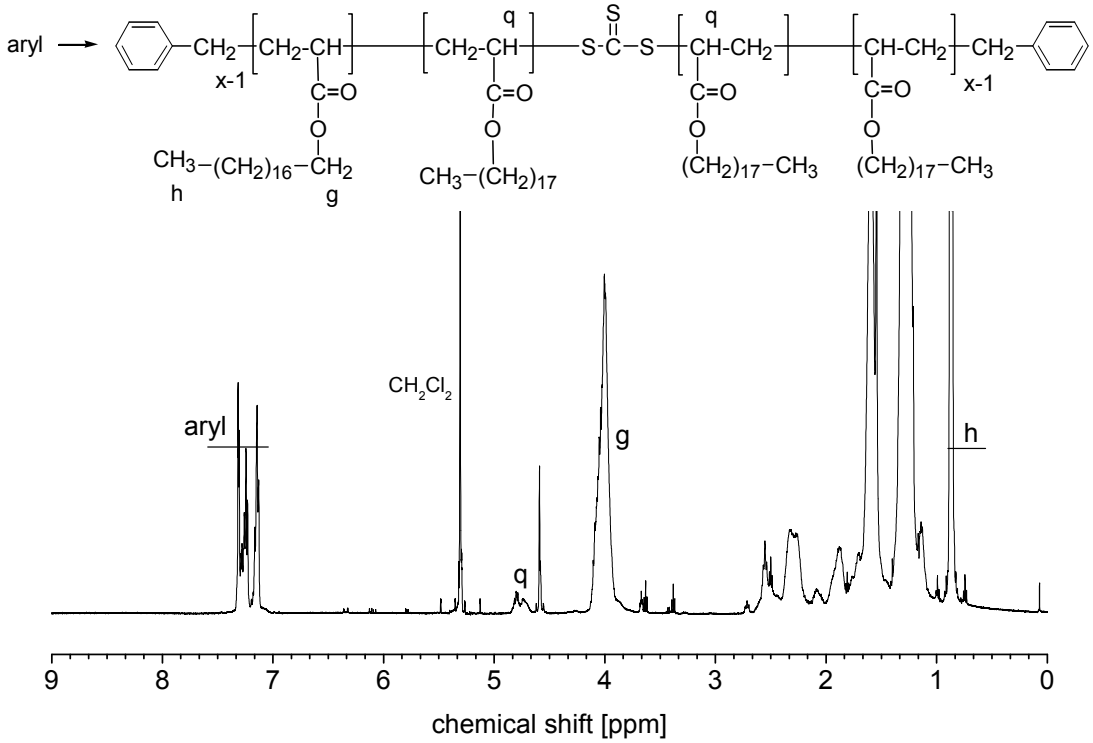


**Figure A13 $^1$H-NMR spectrum of p(M5)-macroRAFT CTA7 in $CD_2Cl_2$.**

# BAB: p(M1-M6-M1)

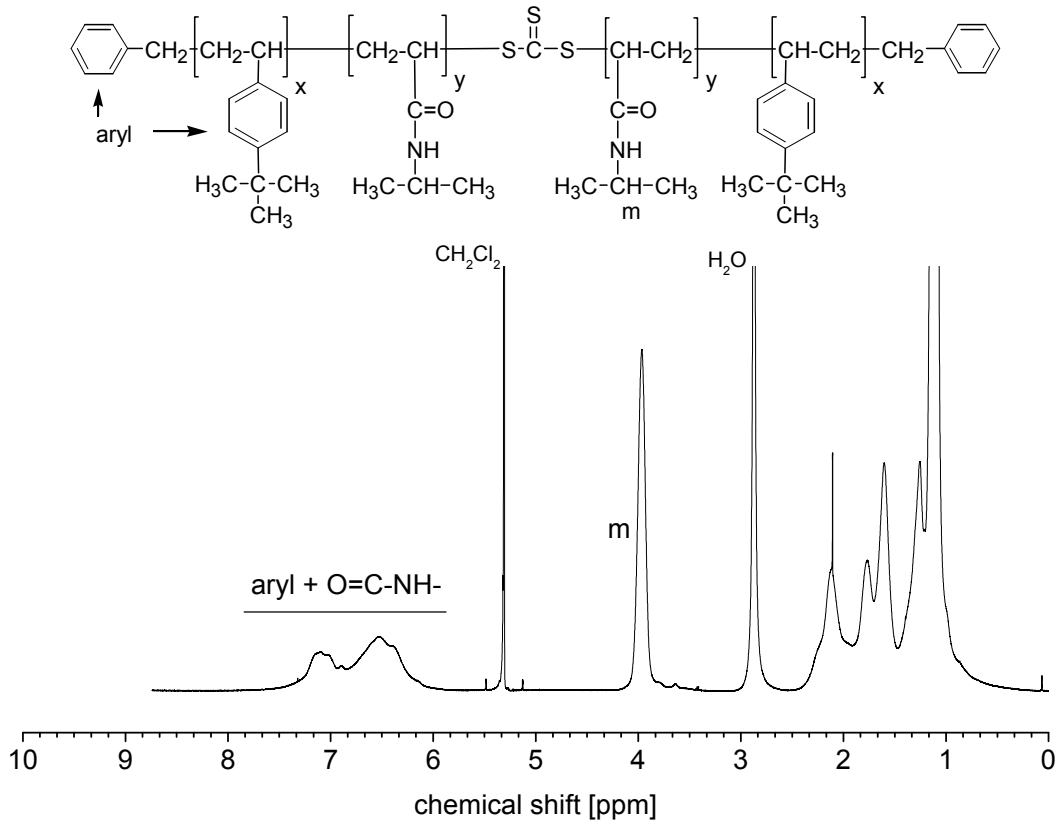


**Figure A14 $^{1}$H-NMR spectrum of triblock copolymer p(M1-M6-M1) in $CD_2Cl_2$**

# BAB: p(M2-M6-M2)

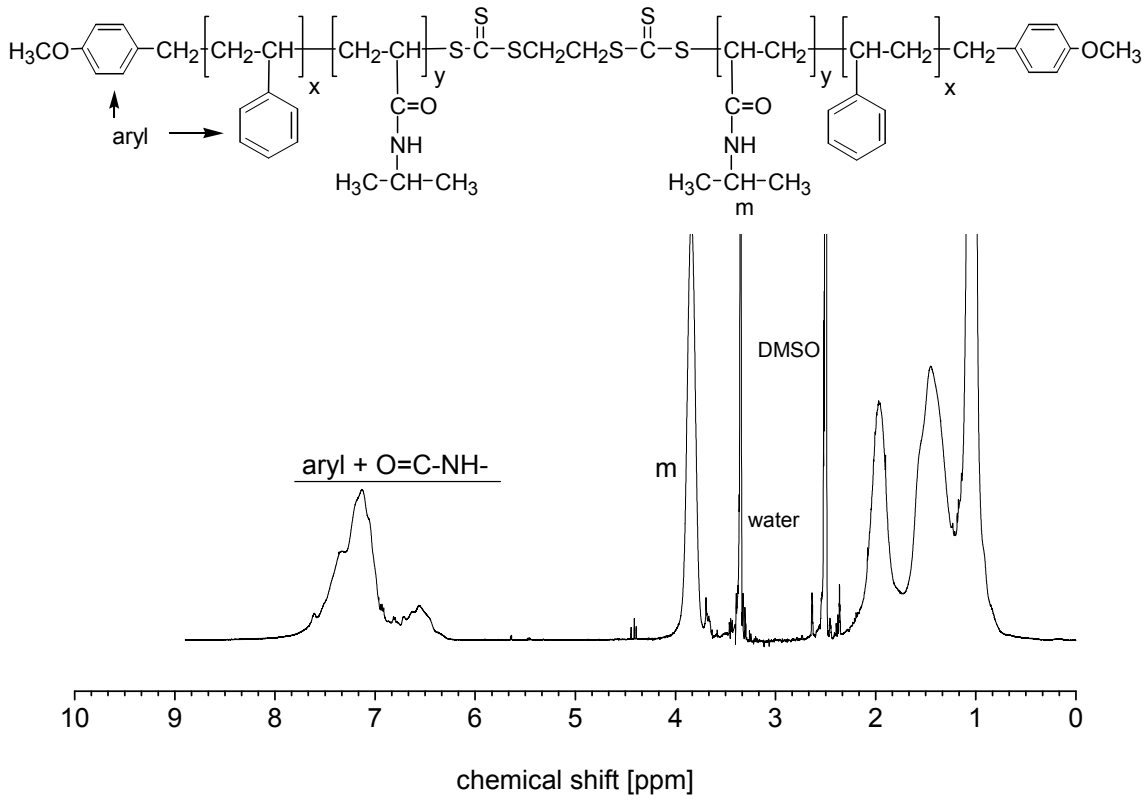


**Figure A15 $^{1}$H-NMR spectrum of triblock copolymer p(M2-M6-M2) in $CD_2Cl_2$**

*"Anyone who has never made a mistake has never tried anything new." Albert Einstein*

# *List of publications and posters*

# Publications

**Synthesis of Symmetrical Triblock Copolymers of Styrene and N-isopropylacrymide Using Bifunctional Bis(trithiocarbonate)s as RAFT Agents**

*Bivigou-Koumba, A. M.; Kristen, J.; Laschewsky, A.; Müller-Buschbaum, P.; Papadakis, C. M. Macromolecular Chemistry and Physics 2009, 210, 565-578.*

**Synthesis and Self-organization of Thermo-responsive Amphiphilic Symmetrical Triblock Copolymers Containing Poly(N-isopropylacrylamide) as Hydrophilic Middle Block, in Dilute and Concentrated Aqueous Solutions**

*Bivigou-Koumba, A. M.; Görnitz, E.; Laschewsky, A.; Müller-Buschbaum, P.; Papadakis, C. M. (accepted 2009).*

**Synthesis and Self-organization of Thermo-responsive Amphiphilic Symmetrical Triblock Copolymers Containing Poly(methoxydiethylene glycol acrylate) as Hydrophilic Middle Block, in Dilute and Concentrated Aqueous Solutions**

*Bivigou-Koumba, A. M.; Görnitz, E.; Laschewsky, A.; Müller-Buschbaum, P.; Papadakis, C. M. (to be submitted 2009).*

**The Collapse Transition of Poly(styrene-(N-isopropylacrymide) Diblock Copolymers in Aqueous Solution and in Thin Films.**

*Troll, K.; Kulkarni, A.; Wang, W.; Darko, C.; Bivigou-Koumba, A. M.; Laschewsky, A.; Müller-Buschbaum, P.; Papadakis, C. M. Colloid Polym. Sci. 2008, 286, 1079–1092.*

**Micellar Solutions from Symmetrical Amphiphilic Triblock Copolymers having a Temperature-Responsive Shell**

*Jain, A.; Kulkarni, A.; Bivigou-Koumba, A. M.; Wang, W.; Busch, P.; Laschewsky, A.; Müller-Buschbaum, P.; Papadakis, C. M. Macromol symposia 2009.*

**Aggregation behavior and segmental dynamics of triblock copolymers having a responsive middle block and hydrophobic end blocks**

*Joseph Adelsberger, Amit Kulkarni, Abhinav Jain, Achille M. Bivigou Koumba, Peter Busch, Vitaliy Pipich, Olaf Holderer, Thomas Hellweg, André Laschewsky, Peter Müller-Buschbaum, Christine M. Papadakis (submitted 2009).*

**Swelling and switching kinetics of gold coated end-capped poly(N-isopropylacrylamide) thin films**

*W. Wang, G. Kaune, J. Perlich, C. M. Papadakis, A. M. Bivigou Koumba, A. Laschewsky, K.Schlage, R. Röhlsberger, S. V. Roth, R. Cubitt, P. Müller-Buschbaum (submitted 2009).*

## Talk

**Mechanical Properties of Synthetic Thermo-responsive Hydrogels**

*Bivigou-Koumba, A. M.; Laschewsky, A.; Müller-Buschbaum, P.; Papadakis, C. M. 5.Zsigmondy Colloquium Bayreuth, 16.-17.03.2009.*

## Posters

**Novel RAFT agents for Synthesizing Amphiphilic Block Copolymers.**

*Bivigou-Koumba, A. M.; Zehm, D.; Laschewsky, A. Dept. of Chemistry, University of Potsdam, Germany (Sfb448), 11-13 October 2007, Van der Valk Resort in Linstow, Germany.*

**Synthesis, Aqueous Self-Organization and "smart" behaviour of Amphiphilic Triblock Copolymers.**

*Bivigou-Koumba, A. M.; Laschewsky, A.; Kulkarni, A.; Müller-Buschbaum, P.; Papadakis, C. M. 1-2 October 2008, FU Berlin, Germany.*

**"Missing" End-Group Peak occurring in bulk Polymerization of Styrene via the RAFT Process.**

*Bivigou-Koumba, A. M.; Kristen, J.; Laschewsky, A. University of Potsdam, Germany 5-8 October 2008, TU Clausthal, Germany.*

**Micellar Aggregation, hydrogel formation and "Smart" Behaviour of Amphiphilic ABA triblock Copolymers.**

*Bivigou-Koumba, A. M.; Kristen, J.; Laschewsky, A. 15-17 October 2008, Congress Centrum Würzburg, Germany.*

**Amphiphilic Binary and Ternary triblock Copolymers as Novel Stimulus-Responsive "Smart Surfactants"**.

*Laschewsky, A.; Bivigou-Koumba, A. M.; Kristen, J.; Li, W.; Skrabania, K.; Storsberg, J; Presented on the 21st Conference of the European Colloid and Interface society, 10-14 September 2007, Geneva, Switzerland.*

**Deswelling kinetics of micellar solutions and hydrogels from temperature-sensitive amphiphilic block copolymers**

*A. Meier-Koll, A.; Golosova1,A.; Jain, A.; Bivigou Koumba, A. M.; Laschewsky, A.; Busch, P.; Pipich, V.; Wiedersich, J.; Müller-Buschbaum, P.; Papadakis, C.M. Deutsche Neutronenstreutagung, 15-17 September 2008, Garching, Germany.*

**Smart Polymeric Hydrogels in Bulk Phase and in Thin Films**

*Wischerhoff, E.; Lutz, J.-F.; Bivigou-Koumba, A. M.; Laschewsky, A.; Kulkarni, A.; Müller-Buschbaum, P.; Papadakis, C. M.; Lankenau, A.; Uhlig, K.; Makromolekulare Chemie, Freiburg, 26-27 February 2009.*